AKADEMIE DER WISSENSCHAFTEN DER DDR
Forschungsbereich Geo- und Kosmoswissenschaften
ZENTRALINSTITUT FUR PHYSIK DER ERDE

Veröffentlichungen des Zentralinstituts für Physik der Erde
Nr. 63 Teil II

4th International Symposium
Geodesy and Physics of the Earth
G.D.R. Karl-Marx-Stadt, May 12th-17th, 1980

PROCEEDINGS

Part II

Editor: The Director of the Central Earth Physics Institute Potsdam

Als Manuskript gedruckt Potsdam 1981

F 102 / 82

Contents

Inhaltsverzeichnis

Part 2

Teil 2

ÜBER ANWENDUNG VON ERGEBNISSEN DER LASERENTFERNUNGSMESSUNGEN ZUM MONDE BEI AUFLÖSUNG EINIGER PROBLEME DER ASTRONOMIE UND GEODYNAMIK

V. K. Abalakin*), V. N. Bojko*), M. A. Fursenko*), O. M. Gromowa*), J. L. Kokurin**), W. F. Lobanow**), L. I. Rumjanzewa*), A. A. Schirjajew*), S. W. Sserowa*), A. N. Ssuchanowskij**)

A b s t r a c t - The present paper deals with some problems related to applications of lunar laser ranging results to improvement of parameters of the theories of the Moon's orbital motion and rotation (the Moon's physical librations) and to determination of the polar motion, the Earth's rotation variations and the continental drift effects. The principles of the numerical approach to the LLR ephemerides computation have been exposed in general features. Some examples of astronomical interest, i.e. the UT0 and GE determinations, are given.

Р е з ю м е - В статье рассмотрены некоторые проблемы, связанные с приложением результатов лазерной светолокации Луны к уточнению параметров теорий орбитального движения и вращения Луны (теория физической либрации Луны) и к определению движения земных полюсов, вариаций в угловой скорости вращения Земли и эффектов, обусловленных смещениями континентальных блоков. Излагаются основы численного подхода к вычислению эфемерид для лазерной светолокации Луны. Приводятся некоторые примеры, имеющие астрономическое значение - определение всемирного времени UT0 и геоцентрической гравитационной постоянной GE .

---

*) Institut für theoretische Astronomia der Akademie der Wissenschaften der UdSSR

**) Peter-Lebedew-Institut für Physik der Akademie der Wissenschaften der UdSSR

Im Wesentlichen ist die Methode der Laserentfernungsmessungen zum Monde (weiterhin als LEM-Methode bezeichnet) dem Radarverfahren ähnlich und besteht in der Bestimmung der möglichst genauen Fortpflanzungszeit der Lichtimpuls-Signale von der Erde zu dem Monde und zurück (der sogenannten Zeitverzögerung).

Die LEM-Experimente bis an die Mitte von 1979 waren an 9 Beobachtungsstationen zu verschiedenen Zeiten erfolgreich durchgeführt und nämlich, an dem Lick Observatory (Kalifornien, USA), dem MacDonald Observatory (Texas, USA), der Catalina Station (Arizona, USA), der Observatoire Pic-du-Midi (Frankreich), dem Krimer Astrophysikalischen Observatorium der Akademie der Wissenschaften der UdSSR, der Dodaira Station (Japan), der Agassiz Station des Smithsonian Astrophysical Observatory (Massachusetts, USA), dem Mount Haleakala Observatory (Hawaii, USA) und an der Orroral Valley Station (Australien), zur Zeit auch die Orroral Station kurz genannt.

Das heutige zu weitläufiger wissenschaftlicher Verwendung zugängliche Beobachtungsmaterial besteht vorwiegenderweise aus den an dem MacDonald Observatory gemachten Laserbeobachtungen (mehr als 2600 Normalpunkte umfassend), welche auf das Zeitintervall von März 1970 bis März 1979 verteilt sind. Man kann diese Beobachtungsangaben durch Vermittelung des U. S. National Space Science Data Center (das COSPAR World Data Center - A) erhalten. Der grösste Teil der bisher gewonnenen wissenschaftlichen Ergebnisse ist ausschliesslich auf diesen Daten gegründet.

Früher waren es verschiedenartige Abschätzungen von möglichen Verwendungsperspektiven der LEM-Ergebnisse zur Auflösung von den zu verschiedenen wissenschaftlichen Untersuchungsgebieten gehörenden Problemen durchgeführt, welche gezeigt haben, dass es möglich ist, einige Parameter der orbitalen Erde- bzw. Mondbewegung wesentlich verbessern zu können, auch die Lagen der Mondretroreflektoren und die Parameter der physischen Libration des Mondes zu bestimmen. Als andere Anwendungsziele kann man auch Bestimmungen von Positionen der Beobachtungsstationen auf der Erdoberfläche, die Untersuchungen der Erdrotation und der Bewegung der Erdpole sowie der Änderungen, die in der gegenseitigen Lage der geotektonischen Schollen vorkommen, und die Experimentalprüfungen verschiedener Gravitationstheorien erwähnen.

Es ist selbstverständlich, dass für die erfolgreiche Auflösung aller diesen wissenschaftlichen Probleme die Mondephemeri-

den von hoher Genauigkeit notwendig sind. Die Lösung dieses fundamentalen Problems wird zur Zeit hier im Institut für theoretische Astronomie folgenderweise durchgeführt:

Es werden zur adäquaten Beschreibung der Bahn- und Drehbewegungen des Mondes in womöglichst vollständiger Übereinstimmung mit den LEM-Ergebnissen und mit den optischen Mondbeobachtungen die numerischen Theorien konstruiert. Diese Theorien dienen als eine Grundlage für die Ephemeridenrechnung der topozentrischen Mondentfernungen D, die für Durchführung der LEM-Experimente am Krimer Astrophysikalischen Observatorium nötig sind. Diese Experimente werden da von der von Dr J L Kokurin geleiteten wissenschaftlichen Gruppe des Peter-Lebedew-Instituts für Physik mit dem 2.6 Meter Reflektor durchgeführt. Die Bezeichnung "Numerische Theorien" bedeutet, dass es sich um das Verfahren handelt, bei welchem die geozentrischen Mondkoordinaten durch die numerische Integration der die Mondbewegung beschreibenden Differentialgleichungen unmittelbar berechnet werden. Dabei wird es eine sehr effektive Methode benutzt, die von Bulirsch und Stoer ausgearbeitet und in der "Numerischen Mathematik" beschrieben wurde. In dem dynamischen gravitationellen Modell werden es die Störungseinflüsse von der Sonne und den sechs grossen Planeten des Sonnensystems (Merkur, Venus, Mars, Jupiter, Saturn, Uran) sowie die von den nicht-sphärischen Gestalten der Erde und des Mondes verursachten Störungen berücksichtigt, d.h. die zonalen Harmoniken in den Reihenentwicklungen von betreffenden Gravitationspotentialen werden bis zu der zweiten und der dritten Ordnung ins Acht genommen. Falls die Anfangsbedingungen des Integrationsverfahrens genügend genau sind, ist es möglich, die Mondephemeride auf Grund der Bulirsch-Stoerschen Methode mit dem maximalen Fehler von $\pm$ 0.5 Meter in der geozentrischen Mondentfernung zu berechnen. Die gegenseitige Vergleichung von den in dem ITA berechneten numerischen Mondephemeriden mit der Mondephemeride, die mit LURE 2A bezeichnet ist, hat die Abweichungen in der Mondentfernung von $\pm$ 60 Meter gezeigt.

Was die numerische Theorie der physischen Mondlibration betrifft, so ist sie auf der gleichzeitigen numerischen Integration des gesamten Systems von den die Mondbewegung in der geozentrischen Bahn beschreibenden Differentialgleichungen und den die Mondbewegung um den Mondmassenmittelpunkt beschreibenden Eulerschen dynamischen Gleichungen gegründet. Der Mond wird dabei als ein absolut starrer Körper betrachtet. Es werden in der Reihenentwicklung des Mondgravita-

tionspotentials die sphärischen Harmoniken bis zu der vierten Ordnung einschliesslich berücksichtigt. Die Anfangsbedingungen für die numerische Integration der Differentialgleichungen der Drehung des Mondes werden auf Grund von den von Dr Eckhardt sowie von Dr Kaula und Dr Baxa ausgearbeiteten analytischen Theorien der physischen Mondlibration ermittelt.

Hier wollen wir eine Bemerkung machen, die den Unterschied zwischen dem traditionellen selenographischen Bezugssystem und dem selenodätischen Koordinatensystem, dessen Achsen mit den Hauptträgheitsachsen des Mondes zusammenfallen, betrifft. Dieser Unterschied wurde von Dr Williams aus dem Jet Propulsion Laboratory entdeckt und abgeschätzt. Nämlich ist die Achse des kleinsten Hauptträgheitsmomentes ca. um 270 Bogensekunden in Länge ostwärts von Richtung des Ersten Radius, d.h. der fundamentalen Richtung des selenographischen Koordinatensystems, und um 75 Bogensekunden in Breite südwärts verschoben.

Um die Nominalzahlenwerte der Parameter zu verbessern, wird die Methode der Differentialkorrektion angewandt, die auf der Auflösung von Bedingungsgleichungen für Parameterverbesserungen mit verschiedenen Ausgleichungsmethoden gegründet ist. Als solche werden, z. B., die Methode der kleinsten Quadrate, die Kollokationsmethode u. a. auserwählt. Als Beispiel wird das Ergebnis der einmaligen Verbesserung der Anfangsdaten der Integration, die der numerischen Theorie der Mondbewegung LURE 2A und der von Dr Eckhardt in 1971 ausgearbeiteten Theorie der physischen Mondlibration entsprechen ($f = 0{,}63982$, d.h. $\beta = 6.3126 \times 10^{-4}$, $\gamma = 2.2737 \times 10^{-4}$, $J = 5552''.721$), angegeben. Es lauten nämlich die Verbesserungen der Parameter der Erd- und Mondbahn wie folgt:

$$\Delta\mathfrak{C} = + 0''.032 \pm 0''.026, \quad \Delta e' = - 0.027 \pm 0.014,$$
$$\Delta\pi_{\mathfrak{C}} = + 0''.032 \pm 0''.029, \quad \Delta\gamma' = + 0.200 \pm 0.037,$$
$$\Delta\Gamma = + 2''.25 \pm 0''.86, \quad \Delta f = - 0.0009 \pm 0.0006,$$
$$\Delta e = - 0.006 \pm 0.001, \quad \Delta J = - 0''.6 \pm 0''.3;$$
$$\Delta r_0 = + 36 \pm 9 \text{ (Meter)};$$

dabei beträgt der Gewichtseinheitfehler ε_0 $\pm$ 30 Meter. Hier wurde es von 1109 Normalpunkten Gebrauch gemacht, welche aus den am MacDonald Observatory ausgeführten Entfernungsmessungen zu Mondreflektoren "Apollo 11", "Apollo 14" und "Apollo 15" abgeleitet wurden. Als Anhang werden einige Arbeitsformeln und -ansätze gegeben, welche das zum Auflösen der gestellten Aufgabe dienende Algorithmenapparat

illustriert. Hier werden einige Aspekte der Berechnung der topozentrischen Mondentfernungen **D** und der Koeffizienten der Bedingungsgleichungen erläutert und Ergebnisse der Benutzung der Laserentfernungsmessungen in den Untersuchungen der Erdrotation (die von Dr Peter Bender ermittelten Differenzen von der Form UTO - UTO (BIH)) sowie bei der Verbesserung der fundamentalen astronomischen Konstanten (der von Dr Jim Williams berechnete Wert der geozentrischen Gravitationskonstante **GE**).

Zum Schluss sei es uns erlaubt, die wichtige Rolle von solchen internationalen kooperativen Unternehmungen wie EROLD und MERIT zu unterstreichen, welche sehr viel zu erfolgreichen geodynamischen Untersuchungen beitragen.

Es ist eine sehr angenehme Pflicht, unseren Kollegen vom Zentralinstitut für Physik der Erde der Akademie der Wissenschaften der DDR für ihre liebenswürdige Einladung und die herrlichsten Aufenthalts- und Arbeitsbedingungen während des 4. Internationalen Symposiums "Geodäsie und Physik der Erde" unseren innigsten Dank hier auszusprechen.

Unsere Danksagungen sind auch an Prof. Dr Jean Kovalevsky, Prof. Dr Milan Burša, Prof. Dr Carrol O. Alley, Prof. Dr William M. Kaula, Dr Odile Calame, Dr Barbara Kolaczek, Dr J. Derral Mulholland Dr Peter Shelus, Dr Peter Bender, Dr Jim Williams für ihre Unterstützung und Mitarbeit gerichtet.

B I B L I O G R A P H I E

Абалакин, В. К., В. Н. Бойко, Ю. Л. Кокурин, В. Ф. Лобанов, М. А. Фурсенко. 1975. О перспективах использования светолокационных (лазерных) наблюдений Луны. - Астрон. журн., 52, с. 387

Абалакин, В. К. 1978. Использование лазерных светолокационных наблюдений Луны для решения некоторых задач небесной механики и геодинамики. - Труды ИТА АН СССР, выпуск XVII, с. 82

Кокурин, Ю. Л, В. В. Курбасов, В. Ф. Лобанов, В. М. Можерин, А. Н. Сухановский, Н. С. Черных. 1966. Измерения расстояний до Луны посредством оптической локации. - Письма ЖЭТФ, 3, с. 139

Румянцева, Л. И. 1974. Численное интегрирование уравнений движения Луны с последующим улучшением начальных условий на БЭСМ-6 . - Бюллетень ИТА АН СССР, 13, с. 507

Abalakin, V. K, O. Calame, Yu. L. Kokurin, J. D. Mulholland, A. Ország, E. C. Silverberg. 1973. Analyse des premiers échos laser obtenus par le reflecteur de Lune 21. - C. R. Acad. Sci. Paris, 276 B, p. 673

Abalakin, V. K., M. A. Fursenko, Yu. L. Kokurin, V. F. Lobanov, A. N. Sukhanovsky, A. A. Gurstein. 1973. On Some Aspects of Utilizing Lunar Laser Ranging Results. - Phys. Earth a. Planet. Int., 7, p. 491

Bulirsch, R., J. Stoer. 1966. Numerical Treatment of Ordinary Differential Equations by Extrapolation Methods. - Num. Math., 8, p. 1

Eckhardt, D. H. 1967. Lunar Physical Libration Theory. - In: Measure of the Moon, p. 40. D. Reidel Publ. Comp., Dordrecht

Kaula, W. M. 1973. Potentialities of Lunar Laser Ranging for Measuring Tectonic Motions. - Phil. Trans. Roy. Soc. London, A 274, p. 185

Kaula, W. M., P. A. Baxa. 1973. The Physical Librations of the Moon Including Higher Harmonics Effects. - The Moon, 8, p. 287

Kovalevsky, J. 1974. Que pourra-t-il déduire des mesures de distance Terre - Lune par laser ? - In: New Problems in Astrometry, p. 269 D. Reidel Publ. Comp., Dordrecht

Luck, J. McK, M. J. Miller, B. J. Morgan. 1973. The National Mapping Astro-Geodetic Complex. - Proc. Astron. Soc. Australia, 2, p. 203

Mulholland, J. D. (Ed.). 1977. Scientific Applications of Lunar Laser Ranging (SALUR). D. Reidel Publ. Comp,, Dordrecht

Mulholland, J. D., P. J. Shelus, E. C. Silverberg. 1973. Laser Observations of the Moon: Normal Points for 1973. - Astron. Journ., 80, p. 1087

A N H A N G

Die Konfigurationsgeometrie in dem oben gestellten Problem der Laserentfernungsmessungen zum Monde kann man mit der folgenden Abbildung illustrieren, wo mit den Symbolen B und R eine terrestrische Beobachtungsstation und ein Mondreflektor bezeichnet sind, r_C und D sind die geozentrische Distanz des Mondmassenmittelpunktes bzw. die topozentrische Entfernung des Mondreflektors, ϱ_B , λ_E , Φ' sind die geozentrischen Koordinaten der Beobachtungsstation, R_C, l , b sind die selenographischen Koordinaten des Mondreflektors.

Die topozentrische Entfernung D wird aus der Formel

$$D = \left(X^2 + Y^2 + Z^2\right)^{1/2} \qquad (1.A)$$

berechnet, wo

$$\begin{bmatrix} X \\ Y \\ Z \end{bmatrix} = \begin{bmatrix} x_{\mathbb{C}} + x - x_B \\ y_{\mathbb{C}} + y - y_B \\ z_{\mathbb{C}} + z - z_B \end{bmatrix} \tag{2.A}$$

und die rechtwinkligen geozentrischen Mondkoordinaten $x_{\mathbb{C}}$, $y_{\mathbb{C}}$, $z_{\mathbb{C}}$ durch die Formel

$$\begin{bmatrix} x_{\mathbb{C}} \\ y_{\mathbb{C}} \\ z_{\mathbb{C}} \end{bmatrix} = \frac{1}{\sin \pi_{\mathbb{C}}} \begin{bmatrix} \cos\delta_{\mathbb{C}} \cos\alpha_{\mathbb{C}} \\ \cos\delta_{\mathbb{C}} \sin\alpha_{\mathbb{C}} \\ \sin\delta_{\mathbb{C}} \end{bmatrix} \tag{3.A}$$

mit den geozentrischen äquatorialen Mondkoordinaten $\alpha_{\mathbb{C}}$, $\delta_{\mathbb{C}}$ und der horizontalen Mondparallaxe $\pi_{\mathbb{C}}$ verbunden sind.

Sind x, y, z die rechtwinkligen geozentrischen äquatorialen Mondreflektorkoordinaten, so werden sie mit der Formel

$$\begin{bmatrix} x \\ y \\ z \end{bmatrix} = \mathcal{R}_{\mathbb{C}}\, \bar{p}(-\varepsilon)\, \bar{r}\left[-(\Omega + \sigma + \Delta\psi)\right] \bar{p}\,(J+\rho) \times$$
$$\times\, \bar{r}\left[180^\circ - (\mathbb{C} + \tau) + \Omega + \sigma + \Delta\psi\right] \cdot \begin{bmatrix} \cos b \cos l \\ \cos b \sin l \\ \sin b \end{bmatrix} \tag{4.A}$$

durch die selenographischen Reflektorkoordinaten $\mathcal{R}_{\mathbb{C}}$, l, b ausgedrückt, wobei $\mathbb{C}$ und Ω mittlere Längen des Mondes und des aufsteigenden Mondbahnknotens auf der Ekliptik bezeichnen, ε ist die Schiefe der Ekliptik, J ist die Neigung des Mondäquators gegen die Ekliptik, ρ, σ, τ bezeichnen hier die Komponenten der physischen Mondlibration und $\Delta\psi$ ist die Nutation in Länge. Den ähnlichen Ansatz bekommt man auch für die rechtwinkligen äquatorialen Koordinaten der Beobachtungsstation B:

$$\begin{bmatrix} x_B \\ y_B \\ z_B \end{bmatrix} = \rho_B\, \bar{r}(-S)\, \bar{p}(y_p)\, \bar{q}(x_p) \begin{bmatrix} \cos\varphi' \cos\lambda_E \\ \cos\varphi' \sin\lambda_E \\ \sin\varphi' \end{bmatrix} \tag{5.A}$$

wo mit S die wahre Greenwicher Sternzeit, mit x_p , y_p die auf das CIO bezogenen Polkoordinaten bezeichnet sind.

Bezeichnet man mit p_L und p_S beliebige mit dem Mond bzw. mit der Sonne verbundene Parameter, so lauten die Bedingungsgleichungen für die Parameterverbesserungen Δp wie folgt

$$D_{OBS} - D_{CALC} = \sum_{p_L,S} \left(\frac{\partial D}{\partial p_L} \Delta p_L + \frac{\partial D}{\partial p_S} \Delta p_S \right), \qquad (6.A)$$

in welchen bei der Analyse von Laserentfernungsmessungen zum Mond

$$p_L = \left\{ \mathbb{C}, \pi_{\mathbb{C}}, e, \gamma' = \sin\frac{i}{2}, r_0, f, J \right\} \qquad (7.A)$$

$$p_S = \left\{ T, e' \right\}$$

als Parameter p_L und p_S auserwählt werden können.

Die Koeffizienten, d. h. die Differentialquotienten $\frac{\partial D}{\partial p}$, die in den Bedingungsgleichungen (6.A) auftreten, kann man auf Grund von bestimmten mathematischen Modellen berechnen, die entweder die Dynamik des betreffenden Himmelskörpers oder die betrachtete geophysikalische Erscheinung beschreiben. Stellt man, z. B., die Greenwicher Sternzeit als

$$S = UTC\,(1 + Red^r) + \Delta\psi \cos\varepsilon + \delta S \qquad (8.A)$$

dar, wo die Erdwinkelgeschwindigkeitsvariation δS den folgenden Ausdruck

$$\delta S = c_1 \cos(2\pi \cdot 36525\,T) + s_1 \sin(2\pi \cdot 36525\,T) + \qquad (9.A)$$
$$+ c_2 \cos(2\pi \cdot 100\,T) + s_2 \sin(2\pi \cdot 100\,T) +$$
$$+ c_3 \cos(2\pi \cdot 86\,T) + s_3 \sin(2\pi \cdot 86\,T)$$

hat, so berechnet man den Differentialkoeffizient $\frac{\partial D}{\partial c_1}$, der bei der Parameterverbesserung Δc_1 steht, indem man die folgende Formel benutzt

$$\frac{\partial D}{\partial c_1} = \frac{\partial D}{\partial S} \cdot \frac{\partial S}{\partial c_1} = \bar{p}(\varepsilon_0)\,\bar{P}\bar{N}\bar{L}_{\bar{r}}\,\bar{r}(-S) \times$$

$$\times\ \bar{p}(y_p)\,\bar{q}(x_p) \begin{bmatrix} u \\ v \\ w \end{bmatrix} \cos\left(2\pi \cdot 36525\, T\right) \tag{10.A}$$

wo mit $[u \quad v \quad w]^T$ der geodätische Ortsvektor der Beobachtungsstation bezeichnet wird.

Das einfachste mathematische Modell, das die Verschiebung der die Beobachtungsstation B tragenden Kontinentalscholle beschreibt, kann man durch den folgenden Ansatz

$$\begin{bmatrix} u \\ v \\ w \end{bmatrix} = \begin{bmatrix} u_0 \\ v_0 \\ w_0 \end{bmatrix} + \begin{bmatrix} u_1 \\ v_1 \\ w_1 \end{bmatrix} (T - T_0) \tag{11.A}$$

darstellen, sodass der Differentialkoeffizient $\frac{\partial D}{\partial u_1}$ bei der Verbesserung Δu_1 kann man auf Grund der Formel

$$\frac{\partial D}{\partial u_1} = -\bar{p}(\varepsilon_0)\,\bar{P}\bar{N}\,\bar{r}(-S)\,\bar{p}(y_p)\,\bar{q}(x_p) \begin{bmatrix} T - T_0 \\ 0 \\ 0 \end{bmatrix} \tag{12.A}$$

berechnen.

Die Symbole $\bar{P}$ und $\bar{N}$ dienen in den Formeln (10.A) und (12.A) zur Bezeichnung der Präzessions- bzw. der Nutationsmatrix, mit $\bar{L}_{\bar{r}}$ wird die mit der Ableitung der Rotationsmatrix $\bar{r}$ verbundene Matrix von Lucas bezeichnet, so dass

$$\frac{d}{d\alpha}(\bar{r}) = \bar{L}_F \cdot \bar{r}(\alpha)\ ,$$

wo α ein gegebener Rotationswinkel ist.

Wie es oben schon erwähnt wurde, waren die am MacDonald Observatory gemachten Laserentfernungsmessungen zum Mond von mehre-

ren wissenschaftlichen Untersuchungsgruppen an verschiedenen Anstalten für astrometrische und geodynamische Analyse benutzt. Insbesondere gelang es Herrn Dr Peter Bender aus dem Joint Institute for Laboratory Astrophysics zu Boulder, Colorado, die zwischen den von dem BIH veröffentlichten Werten der Weltzeit UT0 und den aus den Laserentfernungsmessungen zum Monde bestimmten UT0-Werten bestehende Differenz in folgender Form

$$UT0 - UT0\,(BIH) = -0\overset{''}{.}007 \sin \odot - 0\overset{''}{.}023 \cos \odot + 0\overset{''}{.}011\,(t - t_0)$$

darstellen, wo $\odot$ die Sonnenlänge zur Zeit t bezeichnet und $t_0 = 1973$ ist.

Herr Dr Jim Williams aus dem Jet Propulsion Laboratory zu Pasadena, Kalifornien, hat auf Grund derselben Laserentfernungsmessungen zum Monde den Wert der geozentrischen Gravitationskonstante GE, und nämlich, $GE = 398600.49\ km^3\ s^{-1}$, ermittelt, indem er in seinen Rechnungen den Massenwert vom Erde-Mond-System $E + M$ gleich 1/ 328 900.53 und die Mondmasse μ gleich 1/81.3007 gesetzt und für die Lichtgeschwindigkeit C den Wert 299 792.458 km s^{-1} angenommen hatte.

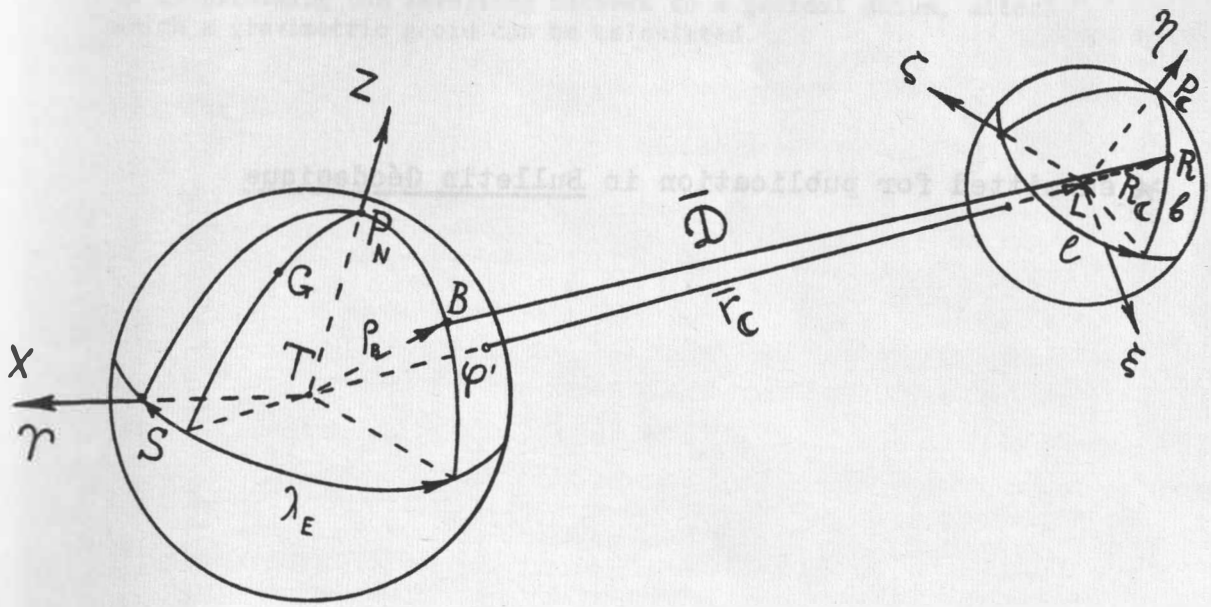

Abbildung 1 : Die Geometrie des Problems

LEAST-SQUARES ADJUSTMENT IN HILBERT SPACES*

J. ÁDÁM
Satellite Geodetic Observatory
H-1373 Budapest, Pf. 546.
Hungary

Abstract: The Hilbert spaces with their inner products are used to describe methods of least-squares adjustment as orthogonal projections on finite-dimensional subspaces. A unified Hilbert space approach of the least-squares adjustment methods A and B is suggested. Hence a new meaning to the intrinsic connections of adjustment groups, which can be derived from the geometry of Hilbert spaces is given. The interrelationships between adjustment groups make the accordance and the content congruency of the technically different solutions complete.

Finally, two examples are given, which demonstrate the correctness of our treatment. We are convinced that Hilbert space techniques in least-squares adjustment is an elegant and powerful geodetic method.

* submitted for publication in Bulletin Géodesique

THE NEED FOR A HIGH ACCURACY GEOID ON LAND AND SEA

P.V. Angus-Leppan and C. Rizos,
Department of Geodesy, School of Surveying,
University of New South Wales,
Sydney, 2033, Australia.

ABSTRACT

Data of new types and of higher accuracy hold out the prospect of determining the geoid to a higher accuracy. Over ocean areas the geoid has uses in its relationship to tectonic features, in the study of oceanographic features, in checking the accuracy of assumptions made in oceanographic techniques, and in determining the datum level for geodetic surveys.

On land, the uses of the geoid include investigations of tectonic features, relating satellite observing stations to terrestrial points, and providing the transformation between terrestrial surveys and positions fixed by satellite techniques. With increasing use of Doppler and, later, GPS systems, this last application will assume great practical importance in the future.

Techniques for determining the geoid to an accuracy of 10-20 cm depend on availability of suitable data. Over sea areas, a representation of the long wavelength geoid features can be obtained from satellite geopotential models. A relative geoid for regional areas is obtainable from gravity. For the continents, the major problem is transforming the levelling network to a geoidal datum, after which a gravimetric geoid can be calculated.

1. INTRODUCTION

The data available for geoid determination over ocean areas has always differed from that on land. Previously the data at sea was sparse and inaccurate, but now these areas have satellite altimetry coverage, which is not available on land. In recent times, also, geopotential solutions from satellite tracking have become available, giving a global coverage of data for the first time.

The improved extent and precision of data provide the possibility of determining a higher accuracy geoid. Current solutions have an accuracy approaching ±1-2 m (e.g. LERCH et al, 1978A;RAPP, 1979). The present paper looks at the need for a geoid one order of accuracy higher, ±0.1-0.2 m, and the possible methods for realising this accuracy in calculating it. For convenience this geoid will be referred to as the "10 cm geoid".

Many additional problems arise when trying to increase the accuracy of the geoid determination. The presence of sea surface topography complicates the solution in many ways.

Geodesy in general is in a transition between the 1 part in 10^6 precision of the early satellite era, to 1 in 10^8 (ANGUS-LEPPAN, 1973). An improvement in geoid determination is in line with this development.

2. THE NEED FOR A 10 cm GEOID

2.1 Over the Oceans

The stimulus provided by the availability of satellite altimetry has had a double effect. Initially it gave extra data on the geoid. In detail, however, the measurement refers to the sea level surface which is displaced from the geoid by a variable amount, the sea surface topography (SST), which may amount to ±2 m. It is of great value in oceanography and geodesy to know the magnitude of SST and its variations over the ocean surface and with time. As a result, the satellite altimetry has given rise to a need for an accurate, independently determined ocean geoid.

Uses of the ocean geoid include:

- Geodynamics. The geoid and its undulations can provide data which is important in investigations of tectonic structural features such as plate boundaries, ocean trenches, subduction zones, sea-mounts, etc.

- Oceanographic Features. In order to determine SST the three sets of data required are the satellite orbit, satellite altimetry and geoid height. (see e.g. MATHER, 1975). The SST is related directly to parameters such as temperature, density and motion of the water, and can thus show up features such as ocean currents and eddies. Time-varying components of these features as well as tides and seasonal variations can be monitored. It can also be noted that for deducing the short-term differential changes with time, e.g. tides, determination of the geoid is not essential.

- Oceanographic Methods. The independent determination of SST by geodetic methods, can provide a valuable check on the assumptions made and the degree to which the theory fits practice in oceanographic methods such as steric and geostrophic levelling.

- Height Datum for Geodetic Surveys. The magnitude of SST at the tide gauge which defines the levelling datum can be applied so as to relate the geodetic levelling net to the geoid, rather than the mean sea level at a particular station. At the same time this makes it possible to relate the levelling nets for different countries and continents.

2.2 On Land

The use of satellite altimetry and the many new oceanographic applications have diverted attention away from the geoid on land. Any inference that the geoid is less important on land would be wrong. There are both scientific and practical functions for which the geoid is needed, and the practical application in particular is growing.

- Geodynamics. As for sea areas, the relationship between the geoid and tectonic features is important in various investigations.

- Relating satellite stations to ground surveys. A further scientific use is in relating observing stations to ground surveys. These can serve to monitor their stability, to give the relative positions of different stations and provide ground truth for space experiments (e.g. WENZEL, 1979).

- Doppler and GPS. A practical use, which will undergo significant growth in the next ten years, is in relating satellite-determined positions on an ellipsoidal system to ground surveys, the heights in which are based on the geoid. For this application the geoid-ellipsoid separation is needed, to an accuracy related to that of the satellite position determination.

3. THE DEFINITION OF THE GEOID

In aiming at the higher accuracy of 1 in 10^8 geodesy, a number of factors have to be reassessed. These include the fundamental definitions, the basis and constants of the reference system, and the definition, accuracy and limitations of the data. In making these assessments it becomes apparent that SST is a factor which needs to be taken into account in many aspects.

When the geoid is determined to say ±6 m it is satisfactory to assume that it coincides with the mean sea level. The displacement between the two surfaces reaches ±2 m at most. For the higher order geodesy (1 in 10^8), a more precise definition of the geoid is needed. Clearly the geoid should be a level surface - a geopotential - and it should give the best mean fit to the sea surface. The various surfaces proposed by the definition differ only in the data used and the method of sampling in deriving the mean fit (MATHER, 1975B; LELGEMANN, 1976).

Further requirements are that the surface chosen should still be suitable for the operations in the traditional, lower precision geodesy (1 in 10^6), and that it should be acceptable to both oceanographers and geodesists. It should be possible to monitor, accurately, changes in the position of the geoid with time.

Each definition proposed refers to a level surface, at a selected epoch for which SST sampled has an average of zero.

- For the *geodetic* geoid, the SST is sampled at all the world's levelling datums.
- For the *oceanic* geoid, SST is sampled globally over the oceans, on an equal area basis.
- For the *oceanic/geodetic* geoid, SST is sampled globally over the oceans on an equal basis, *and* at continental tide gauges. Only these continental areas containing a tide gauge are included in the averaging process.
- For the *"geodetic boundary value solution"* geoid the level is chosen so that SST has no zero degree harmonic. In practice this differs from the previous definition only in using, for the whole land area serviced by a levelling datum, the value of SST at that datum.

All definitions except the oceanic geoid depend upon the set of tide gauges at levelling datums, and the geoid could vary with changes in that set. For this reason, and because it is arguably better to omit continental areas, where there is no physical surface to define SST, the *oceanic* definition is recommended. This is acceptable to geodesists provided the SST is determined from satellite altimetry.

A set of satellite altimetry data suitable for this task does not exist yet. The requirements are that the altimetry should be global and near-simultaneous, but repeated at intervals throughout the year so that seasonal influences can be eliminated.

With these geoids, it is necessary, after defining the surface, to determine the value of the geopotential on the geoid. It is possible to approach the problem from the other end, initially defining the geoid in terms of its geopotential (see e.g. RAPP, 1980).

4. DATA FOR GEOID DETERMINATION

Types of data which may be used for determining the geoid, include:

- surface gravity.
- geopotential models derived from analysis of satellite tracking.
- satellite altimetry.
- astro-geodetic positions.
- ground positions from satellites.

Characteristics of the data which are significant for geoid determination are their accuracy, distribution over the globe, resolution and the nature of the errors, their wavelengths and correlations.

5. DATA FOR THE GEOID IN OCEAN AREAS

The advent of satellite altimetry has stimulated investigations into the determination of the geoid in ocean areas. The investigations include, for example, those of MATHER (1974), CHRISTODOULIDIS (1976) and RAPP (1979). The review which follows is based mainly on a detailed investigation made by RIZOS (1980A).

5.1 Surface Gravity

The basic equation for the determination of the geoid from gravity is Stokes' Integral, which states that the geoid height, or geoid-ellipsoid separation, N, at a point P, is given by (HEISKANEN & MORITZ, 1967, 94):

$$N = \frac{R}{4\pi\gamma} \iint f(\psi)\ \Delta g\ d\sigma \qquad (5.1)$$

Here, ψ is the angle between the two geocentric radii, one to the computation point P, and the other to the element of surface $d\sigma$,

R is the geocentric radius,

Δg is the gravity anomaly,

$f(\psi)$ is Stokes' function, given by:

$$f(\psi) = \operatorname{cosec}(\psi/2) - 6\sin(\psi/2) + 1 - 5\cos\psi - 3\cos\psi\ \ell n\{\sin(\psi/2) + \sin^2(\psi/2)\} \qquad (5.2)$$

The integration in (5.1) is over the whole globe, requiring values of Δg to be known at every point on the geoid.

The solution using (5.1) is complicated by several factors: it is assumed that Δg represents values on the geoid, and that the geoid is spherical, of radius R. Also, there must be no mass outside the geoid. The procedure for taking these factors into account is complex and will not be detailed in this paper. In the Molodenskii approach (HEISKANEN & MORITZ, 1967, Section 8.3) the gravity anomaly on the geoid is replaced by the anomaly on the earth's surface and the geoid height is made up of two components, the Stokesian term N_s, which is predominant, and the non-Stokesian correction term ζ_c. For a particular point P_i, the Stokes' integral is evaluated by a system of quadratures:

$$N_{si} = \frac{\pi^2 R}{3.24\times10^4\,(4\pi\alpha)} \sum_{j=1}^{M} (n \times m)_j\ \mu_{ij}\ f(\psi_{ij})\ \Delta g_j \quad \text{(mgal)} \qquad (5.3)$$

where M is total number of gravity anomalies,

Δg_j is the representative gravity anomaly for an ($n^o \times m^o$) area

μ_{ij} is either a) $\cos\phi_j$ for the equiangular surface element ($n^o \times m^o$) defined by lines of latitude and longitude, or b) $\sin\psi_{ij}$, where the surface elements are based on templates, the subdivision being defined by concentric circles around P_i, and

ψ_{ij} is the angular distance from P_i to the element of surface area.

The requirements of the gravity anomalies used for computation are:

- error of representation less than ±3 mgal. (Requires 10 km spacing of stations in non-mountainous country.)
- gravity based on a standardisation network with stations spaced on a 1000 km grid, and errors less than ±0.1 mgal.
- systematic errors of gravity anomalies diminishing as wavelength increases (for wavelength 4000 km, error below ±0.05 mgal).
- normal gravity computed from geocentric coordinates.
- atmospheric attraction correction applied in determining gravity anomalies (RUMMEL & RAPP, 1976; ANDERSON, 1976).

A further requirement is that the height of the gravity measurement be referred not to sea level but to the geoid. The convenient assumption that sea level is the geoid involves an error in height of up to 2 m. It has been shown that, by modifying the geometry of the Telluroid in the Molodenskii approach to the boundary value problem, the necessity to know the SST at the observation point itself is avoided (RIZOS, 1980A, pp. 48-49). However the indirect effect of SST through the evaluation of the quadratures leads to an error in the geoid height estimated to be in the range ±0.15-0.60 m.

Global coverage of gravity observations is incomplete. A few continental areas, such as Australia, Europe and North America, have good coverage, which also extends over their continental shelves. The oceans in the northern hemisphere have a fair coverage, but in the southern hemisphere it is poor, particularly south of 40°S where observations are very sparse.

The quality of surface gravity data is not yet of the standard required. WENZEL (1979) has made an investigation in an area in which, comparatively, the observations are of very good quality and coverage is dense. The area extends between 31° and 78°N and 25°W - 42°E, covering Europe, the Mediterranean Sea and part of the North Atlantic Ocean. Two sets of data were supplied, one by the Defense Mapping Agency and the other by the International Gravity Bureau. Each set was in the form of 1° x 1° mean anomalies. When compared, the r.m.s. difference was ±12 mgal, with discrepancies of up to 87 mgal. There was evidence of differences being systematically distributed in parts of the area.

5.2 Geopotential Models

Geoid determination through the geopotential model makes use of the relationship expressed by Brun's equation (HEISKANEN & MORITZ, 1967, 85):

$$N = T/\gamma \qquad (5.4)$$

where N is the geoid height,

T is the disturbing potential, and

γ is the normal gravity.

The disturbing potential, T, is the difference between the gravitational potential, W, and the normal gravitational potential of the reference ellipsoid, U_G (HEISKANEN & MORITZ, 1967, Sections 1.9, 1.10). At a point P:

$$W_p = \frac{GM}{R_p} \sum_{n=0}^{n'} \left(\frac{a}{R_p}\right)^n \sum_{m=0}^{n} \sum_{\alpha=1}^{2} C_{\alpha nm} S_{\alpha nm} \qquad (5.5)$$

Here: GM is the product of the gravitational constant and the mass of the earth,

R_p is the geocentric distance to P,

a is the radius of some arbitrary sphere,

n' is the highest degree to which coefficients $C_{\alpha nm}$ are known,

$C_{\alpha nm}$ are spherical harmonic coefficients which can be determined from the analysis of orbital perturbation of satellites, and

$S_{\alpha nm}$ are harmonic functions defined by:

$$S_{1nm} = P_{nm}(\sin\phi) \cos m\lambda \quad ; \quad S_{3nm} = P_{nm}(\sin\phi) \sin m\lambda \qquad (5.6)$$

where $P_{nm}(\sin\phi)$ is the Legendre function of degree n and order m.

Making use of (5.5) and (5.4) the geoid height can be expressed as:

$$N = \frac{GM}{R_p \gamma p} \sum_{n=0}^{n'} \left(\frac{a}{R_p}\right)^n \sum_{m=0}^{n} \sum_{\alpha=1}^{2} \bar{C}_{\alpha nm} S_{\alpha nm} \qquad (5.7)$$

where $\bar{C}_{\alpha nm}$ are the residual coefficients obtained after correcting $C_{\alpha nm}$ for the harmonic representation of the normal gravitational potential U_G.

This brief summary glosses over a number of factors and does not take into account the effects of the atmosphere, though in practice this is essential in determining the 10 cm geoid.

There are many examples of the use of a geopotential field model to calculate geoid heights.

The odd-numbered Goddard Earth Models (GEM 9, GEM 7 etc.) use this form of data (LERCH et al, 1977). Accuracies are approaching the one metre level and further improvements can be expected as more laser tracking observations become available. Substantial volumes of additional observations from the latest generation of lasers will improve the positions of the tracking stations as well as providing improved values for the harmonic coefficients. The most serious defect in the current program is the globally uneven distribution of satellite laser ranging stations, particularly the lack of sufficient stations in southern latitudes.

Satellite observations for geopotential, unlike other data for geoid determination, are free from any relationship with the geometry of the sea surface. They only provide low resolution, and cannot represent features of wavelengths less than about 1000 km. The geopotential model needs to be downward continued to the geoid, taking into account the mass of the atmosphere. The theoretical development for this process requires care (RIZOS, 1980A, pp. 139-142).

The main limitation of geopotential models from satellite observations for geoid determination is their limited resolution. Various methods have been proposed to improve resolution, including a low level, drag-free satellite, satellite-to-satellite ranging, and use of gravity gradiometer. Of these, the satellite-to-satellite ranging approach appears to offer the most promise. Limited test observations have actually been carried out between the GEOS-3 and ATS-6 Satellites (MARSH et al, 1977). For further details see also HAJELA (1977), RUMMEL (1975) and RUMMEL (1976).

5.3 Satellite Altimetry in Combined Solutions

GEOS-3 satellite altimetry has also been used to improve geoid models, for example GEM 10B and GEM 10C (LERCH et al, 1978c). The GEM 10C solution combines three sets of data, the satellite tracking data used in GEM 9, surface gravity (38400 1^{o}x 1^{o} mean gravity anomalies) and GEOS-3 altimetry (28000 1^{o}x 1^{o} block means derived from 2300 passes). The accuracy appears to have reached the sub-metre level.

The geoid height N is related to geoid and ellipsoid as follows:

$$R_S = N + SST + A \qquad (5.8)$$

where R_S is the height of the satellite above the ellipsoid, a quantity determined from data on the satellite orbit, and

A is the corrected satellite altimeter reading.

In using satellite altimeter data for the geoid, the assumption is made that SST = 0, so that the geoid height is merely the difference between satellite height and altimeter reading.

Further progress in geoid determination will need to take into account the different relationships of the data types with SST. The data from satellite tracking is unaffected by the sea surface. However, surface gravity data is affected by the sea surface and the geoid in an indirect manner, the indirect effect being estimated at 0.15-0.6 m. Satellite altimetry data refers directly to the sea surface rather than the geoid, this direct effect being 1-2 m.

6. DETERMINATION OF THE OCEAN GEOID

Calculating SST from satellite altimetry is one of the most exacting tasks of geodesy. For each point it involves the calculation, to a high accuracy, of the radial position of the satellite in orbit, the corrected altimeter height above the surface, and the geoid height. The satellite altimetry is needed for differencing, and can make no contribution to the geoid height determination.

A procedure for the solution of the ocean geoid is to compute the SST first using the geoid as derived from the geopotential model (RIZOS, 1980A, pp. 37-51; 131-142; 259-260). Since this geoid includes only long wavelength features, the SST derived by differencing from it will include correct long wave information and, in addition, short wave SST superimposed on short wave geoid information. If necessary the short wave signal can be eliminated by appropriate filtering.

For regional SST studies, and where it is essential to separate the short wavelength geoid and SST undulations, high precision relative ocean geoids can be computed, provided there are gravity observations of sufficient accuracy and density. This is possible because the effect of SST on the computed geoid height is not direct, but comes in indirectly through the quadratures. This effect is of long wavelength, so it will displace the regional geoid by an amount which will be nearly constant over the region.

8. DATA FOR THE CONTINENTAL GEOID

The mean sea level determined at a tide gauge station will differ from the geoid by the amount of the SST. If this mean sea level is adopted as datum for a levelling network, all orthometric heights, including those of gravimetric stations, will be affected by the error, of magnitude equal to the SST.

Two additional sources of data are available on land: astro-geodetic positions and satellite-geodetic positions.

8.1 Astro-Geodetic Positions

Deviations of the vertical with respect to the ellipsoidal normal are generally accepted to have an accuracy of approximately ±0.5 arcsec. They yield geoid height differences which can be used to supplement data from other sources. An example where such data have been successfully used is in the land areas of the North Sea Region (MONKA et al, 1979; WENZEL, 1979) where it was estimated to give geoid height differences with an accuracy of $\pm 0.02\sqrt{S}$ to $\pm 0.04\sqrt{S}$ m, where S is in km. In this case data already existed for a large number of stations, forming a high density network. The astro-geodetic geoid determination was carried out using least squares collocation, in order to avoid several disadvantages of the conventional techniques of astronomic levelling in profiles or networks.

The basic relationship for the geoid from astro-geodetic position is:

$$dN = \varepsilon \, dS \qquad (8.1)$$

where N is the geoid-ellipsoid separation,

ε is the deflection of the vertical at the geoid, that is the deflection at the surface, corrected for curvature of the vertical between the surface and the geoid, and

S is the distance.

In practice, where a limited number of astro-geodetic stations are to be used, a linear variation of ε between stations can be assumed. For the difference of geoid-spheroid separation at two stations A and B, equation (8.1) becomes:

$$\Delta N_{AB} = \varepsilon \, \Delta S \qquad (8.2)$$

where ε is the mean deflection $\frac{1}{2}(\varepsilon_A + \varepsilon_B)$, and ΔS is the distance AB.

Because the determinations are tedious and expensive, even with new automated instruments, it is unlikely that this method would be the first choice in a new survey for geoid determination.

8.2 Satellite-Geodetic Positions

Systems which determine three-dimensional positions on a reference ellipsoid, from satellite observations, can be used to deduce the geoid height N, which is simply the difference between the ellipsoidal height and the height derived from levelling:

$$N = h - H \qquad (8.3)$$

where h is the ellipsoidal height,

H is the orthometric height, and

N is, as before, the height of the geoid above the ellipsoid.

An example of this principle in the determination of N is given by LACHAPELLE (1979).

At present, using commercial receivers in the Doppler-Transit system, the observations at a single station take several days, and unless extra-special techniques are used, the precision of a position is approximately ±1.5 m. The results are of value in determining the relationship between the reference frames of the geodetic survey and the satellite systems. However the method would not be economical for large scale determinations of geoid height, at present.

Geodesists are watching with interest the development of the Global Positioning System (GPS) designed to supersede the Doppler before 1990 (PARKINSON, 1979). Although designed for navigation there are possible modes of use for precise position fixing which are being investigated (ANDERLE, 1979). It has been reported that it will be possible to design convenient receivers, to fix positions to a precision of a few centimetres, and in a very short time. If these specifications are achieved, the surveyor will have a powerful new tool for position fixing in every day surveys and the geodesist a precise and economical method for geoid determination.

Using such an instrument for geodesy, a field traverse would be comparable in effort to a gravimeter survey. Station spacings on a 10 km grid would be feasible wherever the density of geodetic survey positions was sufficiently high.

For each point fixed using the instrument, for which the geodetic position was known, a geoid height would be known from equation (8.3). This could lead to a very detailed and precise geoid. The conventional methods for determining the geoid would not, however, be superseded as it is likely that the GPS receiver will only yield very precise *relative* positions. The most useful form of the GPS data for geoid determination would then be as differences of geoid-ellipsoidal separation ΔN.

The changes brought about in practical surveying through widespread day-to-day use of a system like the GPS, will also have their effect on geoid determination. The rapid determination of positions in a geocentric-ellipsoidal reference system will be very convenient and economical, but in order to relate the positions to all the pre-existing ground survey points and to current levelling results, geoid-ellipsoid separation N will be essential. So this will lead to an additional call for a detailed geoid, at an accuracy related to the precision of the best GPS position determinations.

9. GEODETIC LEVELLING DATUM

The geodetic levelling network for a continental area usually has one tide gauge adopted as the fundamental station for height datum, but for practical purposes the network may be deformed so as to fit mean sea level at a number of tide stations. (See for example the Australian case described in ROELSE et al, 1971.) Scientists prefer a free net adjustment, connected to only one tide station. Although mean sea level at that station will differ from the geoid by the amount of the SST, it can be assumed that the whole height network is displaced by a constant amount.

In the case of Australia, the free network has been calculated (MITCHELL, 1972) and the SST at the fundamental tide station, Jervis Bay, calculated by geodetic methods as (RIZOS, 1980A, p. 243):

SST at Jervis Bay: 0.2 ± 0.4 m

This compares with 0.3 ± 0.2 m extrapolated from oceanographic values of SST in the adjacent oceans.

The fact that the datum adopted for levelling is mean sea level and not the geoid causes an error in orthometric heights of 1-2 metres and a corresponding error in the gravity network of 0.3-0.6 milligals. It is a zero degree effect which can be interpreted as the gravity datum being in error by an absolute amount and the magnitude in terms of an absolute geoid height error is given by:

$$\frac{R}{\gamma} M\{\ell_{\Delta g}\} \qquad (9.1)$$

where R is the earth's mean radius,

γ is the normal gravity,

$M\{\ }$ denotes the mean value, and

$\ell_{\Delta g}$ is the effect, in milligals, of the SST at each levelling datum for the country or continent.

Alternatively, this zero degree effect can be used to adjust the surface chosen in the definition of the geoid. For example, rather than the "oceanic" definition based on satellite altimetry, the geopotential surface through the tide gauge zero can be adopted. If the displacement between tide gauge mean sea level and the geoid is unknown, the geoid definition can, in principle, be modified to take this into account.

It is now accepted that geodetic levelling is subject to systematic error, which may amount to a few decimetres per 1000 km (ANGUS-LEPPAN, 1979). In the north-south direction this is estimated at (0.3 S)mm where S is the length of the line in km. The systematic error in the east-west direction is smaller, but not negligible. Taking these errors into account, it is not justifiable to assume that a levelling network of dimensions 500 km square or larger, has a constant datum error with respect to the geoid. Away from the fundamental datum, the freely adjusted network will gradually warp.

In order to transform the levelling network to a datum surface which is consistently on the geoid to within 10 cm, it is necessary to go one step beyond the procedure described by RIZOS (1980A). SST must be determined at tide gauges, at intervals along the coastline, to which the levelling is connected. In order to maintain a precision of ±10 cm, a suitable spacing of the set of tide gauges is approximately 500 km. A levelling network adjusted to this set of gauges, where the mean sea level has been corrected by SST to give geoid height, should give heights accurately based on the geoid, which in turn are the appropriate levels for gravity stations.

10. DETERMINING THE GEOID ON LAND

A major problem in geoid determination on land, the effect of SST on the height datum, has been discussed in Section 9. This clears the way for the calculation of the geoid by the gravimetric method, taking into account the factors listed in Section 6.1. For a description of a careful determination of the geoid in the North Sea Area, which could well be a model for future operations see: MONKA et al, 1979, WENZEL, 1979. For the central area, mean gravity anomalies were prepared for areas 6'x 10'.

The gravimetric data can be supplemented by astro-geodetic geoid height differences where available. Similarly, the results of comparisons of Doppler and geodetic positions provide supplementary data. The role of GPS data when it becomes freely available, is discussed in Section 8.2.

Because satellite geopotential models provide smoothed,low-resolution geoids, this data does not have a major role in geoid determination on land. However it is valuable as an independent check on the geoid as determined by other methods.

11. CONCLUSIONS

Researchers in geodesy, already used to handling large volumes of data, will have to be prepared to deal with even larger volumes, if the 10 cm geoid is to be realised. For this, the data needs to be also of the appropriate precision.

The data requirements include:

- Altimetry data for definition of the geoid. Assuming that the

oceanic geoid is adopted, data will be all of the same type. The ideal data would be from a satellite fitted with an altimeter of the precision of SEASAT, in polar orbit and with period such that a global coverage could be achieved in a short time span. At least two global sets, but ideally about six, would be required, evenly spaced through the year so that seasonal variations could be eliminated. For this reason (and others) geodesists should be pressing for a successor to SEASAT, with appropriate orbital parameters for a global coverage.

- Surface Gravity. This is the only means of obtaining an accurate, detailed geoid at sea. The high cost of obtaining the data is a deterrent, but for regions of special interest it is worthwhile. Other areas where efforts should be concentrated are in improving the accuracy, by completing the standard gravity networks, and filling in the blank areas of the southern oceans.

  On land, efforts should be continued to bring the coverage, universally, up to the levels achieved in Australia, Europe and North America, basically a 10 km spacing of stations in low topography and denser coverage in mountains.

- Geoid Heights. The operation described in Section 8.2 to bring levelling networks onto the geoid datum, is an essential part of the program to improve the accuracy of gravity data, and hence the geoid. The requirement is the determination of SST at a selected set of tide gauges, which are connected to the levelling network.

- Geopotential Models. High accuracy ranging to satellites for improving the geopotential model appear to be a most effective means of improving the geoid. Extensive programs of laser ranging, with an accuracy of 10 cm or better, are required.

- GPS. When the new system is implemented fully, and if the specifications promised for the receiving instruments are achieved, a method of great economy and accuracy will be in the hands of the geodesist. This will provide the means of determining the geoid to unprecedented accuracy and detail on land. It will, at the same time, create a demand for the determination of a detailed, high accuracy representation of the geoid-ellipsoid separation.

ANDERLE, R.J. 1979. Accuracy of geodetic solutions based on Doppler measurements of the NAVSTAR global positioning system satellites. *Bull. Geodes.* Vol. 53, (2), 109-116.

ANDERSON, E.G. 1976. The Effect of Topography on Solutions of Stokes' Problem. *Unisurv* S14, Univ. of New South Wales, Australia, 223 pp + App.

ANGUS-LEPPAN, P.V. 1973. A System of Observations for Four-Dimensional Geodesy. In *Proc. Symp. Earth's Grav. Field & Secular Variations in Position*, Univ. of New South Wales, Australia, 702-709.

ANGUS-LEPPAN, P.V. 1979. Refraction in Levelling - Its Variation with Ground Slope and Meteorological Conditions. Paper pres. at *National & Regional Networks Session XVII Gen. Assemb. of Int. Assoc. of Geodesy*, Canberra, Australia, December 1979. Also *Aust. J. Geod. Photo & Surv.*, No. 31(1979), 27-42.

CHRISTODOULIDIS, D.C. 1976. On the Realisation of a 10 cm Relative Ocean Geoid. *Rep. No. 247, Dept. of Geodetic Science*, Ohio State University.

HAJELA, D.P. 1977. Recovery of 5° Mean Gravity Anomalies in Local Areas from ATS-6/GEOS-3 Satellite to Satellite Range Rate Observations. *Rep. No. 259, Dept. of Geodetic Science*, Ohio State University.

HEISKANAN, W.A. & MORITZ, H. 1967. *Physical Geodesy*, W.H. Freeman & Co., San Francisco, 364 pp.

LACHAPELLE, G. 1979. Comparison of Doppler-Derived and Gravimetric Geoid Undulations in North America. *Proc. 2nd Symp. Satellite Doppler Positioning*, Univ. of Texas, Austin, Jan. 1979, Vol.1, 653-670.

LELGEMANN, D. 1976. On the Definitions of the Listing Geoid Taking into Consideration Different Height Systems. *Proc. 3rd Int. Symp. Geodesy & Physics of the Earth*, Potsdam, 419-439, Oct. 1977.

LERCH, F.J., KLOSKO, S.M., LAUBSCHER, R.E. & WAGNER, C.A. 1977. Gravity Model Improvement Using GEOS-3 (GEM 9 & 10). *Spring Annual Meeting, Am. Geophys. Union*, Washington, D.C., June 1977. Goddard Space Flight Center Document X-921-77-246, Sept. 1977.

LERCH, F.J., WAGNER, C.A., KLOSKO, S.M., BELOTT, R.P., LAUBSCHER, R.E. & TAYLOR, W.A. 1978A. Gravity Model Improvement Using GEOS-3 Altimetry (GEM 10A & 10B). *1978 Spring Annual Meeting, Am. Geophys. Union*, Miami Beach, Fla., G.S.F.C., April 1978.

LERCH, F.J., BELOTT, R.P., KLOSKO, S.M. & LITKOWSKI, E.M. 1978B. Laser Reference Orbits and Altimeter Validation for GEOS-3. *Marine Geodesy Symp.*, Univ. of Miami, Florida, G.S.F.C. Sept. 1978.

LERCH, F.J., WAGNER, C.A., KLOSKO, S.M. & BELOTT, R.P. 1978C. Goddard Earth Model Development for Oceanographic Applications. *Marine Geodesy Symp.* Florida, G.S.F.C. Sept. 1978.

MARSH, J.G. et al. 1977. Gravity Anomalies Near the East Pacific Rise with Wavelengths Shorter than 3 300 km Recovered from GEOS-3/ATS-6 Satellite to Satellite Doppler Tracking Data. *NASA Technical Memorandum 79553.*

MATHER, R.S. 1974. On the Solution of the Geodetic Boundary Value Problem for the Definition of Sea Surface Topography. *Geophys. J. Roy. Astron. Soc.*, 39, 87-109.

MATHER, R.S. 1975A. On the Evaluation of Stationary Sea Surface Topography Using Geodetic Techniques. *Bull. Geodes.* 115, 65-82.

MATHER, R.S. 1975B. Mean Sea Level and the Definition of the Geoid. *XVIth Gen. Assemb. of IUGG*, Grenoble, 1975. Also *Unisurv* G23, Univ. of New South Wales, Australia, 68-79.

MATHER, R.S. 1977. Some Possibilities of Recovering Oceanographic Information from the SEASAT Missions. *Proc. 3rd Int. Symp. Geodesy and Physics of the Earth*, Oct. 1977, Potsdam, 59-82.

MITCHELL, H.L. 1972. An Australian Geopotential Network based on Observed Gravity. *Unisurv*. G18, Univ. of New South Wales, Australia, 35-50.

MONKA, F.M., TORGE, W., WEBER, G. & WENZEL, H.G. 1979. Improved Vertical Deflection and Geoid Determination in the North Sea Region. *Wiss. Arb. d. Fachrichtung Vermessungswesen*, Nr. 94, Univ. of Hannover.

PARKINSON, B.W. 1979. The global positioning system (NAVSTAR). *Bull. Geodes.* Vol. 53(2), 89-108.

PELLINEN, L.P. 1976. Recent Possibilities for the Determination of the Geopotential from Terrestrial and Satellite Data. *Proc. 3rd Int. Symp. Geodesy and Physics of the Earth*, Oct. 1977, Potsdam, 145-168.

RAPP, R.H. 1977. Potential Coefficient Determinations from 5° Terrestrial Gravity Data. *Rep. No. 251, Dept. of Geodetic Science*, Ohio State Univ., 51 pp + App.

RAPP, R.H. 1979. The Oceanic Geoid. Paper pres. at *XVII Gen. Assemb. of Int. Assoc. of Geodesy*, Canberra, Australia, Dec. 1979.

RAPP, R.H. 1980. Precise definition of the geoid and its realization for vertical datum applications. *2nd Int. Symp. on Problems Related to the Redefinition of North American Vertical Geodetic Networks*, Ottawa, May 1980.

RIZOS, C. 1980A. The Role of the Gravity Field in Sea Surface Topography Studies. *Unisurv* S17, Univ. of New South Wales, Australia, 286 pp.

RIZOS, C. 1980B. On Estimating the Global Ocean Surface Circulation from Satellite Altimetry. *Int.Symp.Oceanography from Space*,Venice,May 1980.

ROELSE, A., GRAINGER, H.W. & GRAHAM, J.W. 1971. The Adjustment of the Australian Levelling Survey 1970-71. *Tech. Rep.*12, Division of National Mapping, Canberra.

RUMMEL, R. 1975. Downward Continuation of Gravity Information from Satellite to Satellite Tracking or Satellite Gradiometry in Local Areas. *Dept. of Geodetic Science*, Ohio State University, Rep. No. 221.

RUMMEL, R., HALEJA, D.P. & RAPP, R.H. 1976. Recovery of Mean Gravity Anomalies from Satellite-Satellite Range Rate Date Using Least Squares Collocation. *Dept. of Geodetic Science*, Ohio State University, Report No. 248.

RUMMEL, R. & RAPP, R.H. 1976. The Influence of the Atmosphere on Geoid and Potential Coefficient Determinations from Gravity Data. *Jour. Geophys. Res.* 81, 5639-5642.

WENZEL, H.G. 1979. Recent Results of Geoid Determination by Combination Techniques in the North Sea Test Area. Paper pres. at *XVII Gen. Assemb. of IUGG*, Canberra, Australia, Dec. 1979.

A contribution to the mixed boundary value problem

by

K. Arnold[1)]

Summary

The dates given beforehand are the geoid undulations on the oceans and the gravity anomalies on the continents. There is derived a series development into certain functions X_n for the N-values on the Earth's surface the coefficients of which are determined by integrating over the N-values on the oceans and the Δg_F-values on the continents. This development is analog to the spherical harmonics development for the potential in case the gravity values are given all over the Earth.

The functions X_n depend on the spherical harmonics by a successive procedure. This is a solution of the mixed boundary value problem.

Further, an iterative procedure is developed to determine discrete values of N on the continents from N-values on the oceans and Δg_F-values on the continents, according to the mixed boundary value problem.

In the satellite altimetry and gravimetry, known quantities are the disturbing potential, T, on the oceans and the gravity anomalies, Δg_F, on the continents. From these heterogeneous data, the expansion by spherical harmonics shall be determined for the disturbing potential on the Earth's surface and in the external space.

$$(1) \quad T = \sum_n T_n S_n(\varphi,\lambda) \quad .$$

In view of

$$(2) \quad \Delta g_F = -\frac{\partial T}{\partial r} - \frac{2}{R} T$$

it follows that

$$(3) \quad \Delta g_F = \frac{1}{R} \sum_n (n-1)\, T_n S_n(\varphi,\lambda) \quad ,$$

where R denotes the radius of the Earth, $S_n(\varphi,\lambda)$ are the spherical harmonics, and r, φ, λ are the geocentric polar coordinates. Extending the expansion up to the order $n = \nu$, according to Brillouin one has

$$(4) \quad \Gamma = \iint_{\sigma_1} \Big[T - \sum_n^{\nu} T_n S_n \Big]^2 d\sigma + \iint_{\sigma_2} \Big[\Delta g_F - \frac{1}{R} \sum_n^{\nu} (n-1)\, T_n S_n \Big]^2 Q^2 \, d\sigma$$

$$(5) \quad \Gamma \longrightarrow \text{minimum}$$

1) AdW der DDR, Zentralinstitut für Physik der Erde,
DDR-15 Potsdam, Telegrafenberg A 17

$\mathfrak{a}_1$ denotes the area of the oceans, while $\mathfrak{a}_2$ means that of the continents.

$$(6) \quad Q = \frac{\mu_T^2}{\mu_g^2} .$$

μ_T is the residual root mean square deviation for the disturbing potential on the oceans, μ_g being the corresponding value for the gravity anomalies on the continents. The conditions for the minimum are

$$(7) \quad \frac{\partial T}{\partial T_q} = 0, \qquad (q = 0, 1, 2, \ldots) .$$

Instead of the spherical harmonics $S_n(\varphi,\lambda)$, the functions $X_n(\varphi,\lambda)$ are introduced by setting

$$(8) \quad T = \sum_n \xi_n X_n(\varphi,\lambda,r) .$$

X_n is obtained successively from X_{n-1},

$$(9),(10) \quad X_n = u_k \left[\sum_{p=0}^{k-1} c_{k.p} X_p + L_k \right], \qquad k = 0, 1, 2, \ldots,$$

$$(11) \quad L_k = S_k \left(\frac{R}{r}\right)^{k+1} .$$

Now one has for the gravity anomalies

$$(12) \quad \Delta g_F = - \sum_{n=0}^{\nu} \xi_n \frac{\partial X_n}{\partial r} - \frac{2}{R} \sum_{n=0}^{\nu} \xi_n X_n .$$

The function Γ to be minimized then becomes

$$(13) \quad \Gamma = \iint_{\mathfrak{a}_1} \left[T - \sum_{n=0}^{\nu} \xi_n X_n \right]^2 d\mathfrak{a} + \iint_{\mathfrak{a}_2} \left[\Delta g_F + \sum_{n=0}^{\nu} \xi_n \left\{ \frac{\partial X_n}{\partial r} + \frac{2}{R} X_n \right\} \right]^2 Q^2 \, d\mathfrak{a} .$$

The minimum conditions

$$(14) \quad \frac{\partial \Gamma}{\partial \xi_q} = 0 , \qquad (q = 0, 1, 2, \ldots)$$

yield the coefficients ξ_n ;

$$(15) \quad \sum_{n=0}^{\nu} \xi_n \delta_{n.q} = \iint_{\mathfrak{a}_2} T X_q \, d\mathfrak{a} - \iint_{\mathfrak{a}_2} \Delta g_F \, \psi(X_q) \, Q^2 \, d\mathfrak{a}$$

$\delta_{n.q}$ is the Kronecker symbol,

$$(16) \quad \delta_{n.q} = \begin{cases} 1 \\ 0 \end{cases} \quad \begin{cases} n = q \\ n \neq q \end{cases} .$$

According to (13) and (15), the functions X_n satisfy the following condition.

$$(17)\quad \iint_{\mathcal{A}_1} X_n X_q \, d\mathcal{A} + \iint_{\mathcal{A}_2} \psi(X_n)\, \psi(X_q)\, Q^2 \, d\mathcal{A} = \delta_{n,q}$$

where

$$(18)\quad \psi(X_n) = \frac{\partial X_n}{\partial r} + \frac{2}{R} X_n \,.$$

The coefficients

$$(19)\quad c_{i,k}\,,\quad u_k$$

for calculating the functions X_n from the spherical harmonics S_n are successively derived from the following equations.

$$(20)\quad c_{i,k} = -\iint_{\mathcal{A}_1} L_k X_i \, d\mathcal{A} - \iint_{\mathcal{A}_2} \psi(L_k)\, \psi(X_i)\, Q^2 \, d\mathcal{A}\,,$$

$$(21)\quad \left(\frac{1}{u_k}\right)^2 = -\sum_{i=0}^{k-1} c_{k,i}^2 + \iint_{\mathcal{A}_1} L_k^2 \, d\mathcal{A} + \iint_{\mathcal{A}_2} \psi^2(L_k)\, Q^2 \, d\mathcal{A}\,,$$

$$(22)\quad \begin{array}{l} k \succ i \\ i = 0, 1, 2, \ldots, (k-1) \\ k = 0, 1, 2, \ldots, \end{array} \,.$$

The coefficients ξ_n of the expansion of the disturbing potential T by the functions X_n are found by the relation

$$(23)\quad \xi_n = \iint_{\mathcal{A}_1} T X_n \, d\mathcal{A} - \iint_{\mathcal{A}_2} \Delta g_F\, \psi(X_n)\, Q^2 \, d\mathcal{A}\,.$$

If required, the spherical harmonics may again be substituted for the functions X_n.

For an infinite extension, ($\nu \dashrightarrow \infty$), Q is the corresponding quotient of the random errors of measurement. Then Q does no longer depend on ν and the functions X_n can a priori be determined once and for all.

If, on the basis of the desired boundary value problem, the T-values shall be determined at discrete points on the continents, then Molodensky's formula does good service for the inversion of the Stokes formula. Let N be the geoid undulation, then it follows that

$$(24)\quad (\Delta g_F)_0 + \frac{G}{R}(N)_0 + \frac{GR^2}{2\pi} \iint_{\mathcal{A}} \frac{N - N_0}{e^3} \, d\mathcal{A} = 0\,,$$

$$(25)\quad e = 2R \sin\frac{\psi}{2}\,.$$

For the singularity in the nearest neighbourhood of the test point one has

$$(26)\quad \iint_{\varrho} \frac{N-N_0}{e^3} \sin\psi \, d\psi \, d\alpha = \frac{1}{R^2} \pi\varrho \left[\nu_{2.1} + \nu_{2.3}\right] + \dots$$

$$(27)\quad N-N_0 = \nu_{1.1}\, e \cos\alpha + \nu_{1.2}\, e \sin\alpha + \nu_{2.1}\, e^2 \cos^2\alpha + \nu_{2.2}\, e^2 \sin\alpha \cos\alpha + \nu_{2.3}\, e^2 \sin^2\alpha + \dots .$$

If the radius ϱ is chosen small enough, the integral (26) becomes zero. Then, if σ is the remaining part of the spherical surface $\mathfrak{a}$, after the exclusion of the nearer neighbourhood of the test point within the radius ϱ, one obtains the following equation.

$$(28)\quad \left[\frac{G}{R} - \frac{GR^2}{2\pi} \iint_{\sigma} \frac{1}{e^3} \, d\mathfrak{a}\right] (N)_0 + \frac{GR^2}{2\pi} \iint_{\sigma} \frac{N}{e^3} \, d\mathfrak{a} + (\Delta g_F)_0 = 0 .$$

A substitution of sums for the integrals gives

$$(29)\quad c_0 N_0 + \sum_k c_{0.k} N_k + (\Delta g_F)_0 = 0 , \qquad k \neq 0 .$$

By separating, in the sum in (29), those areas where the N-values are known and unknown, respectively, one obtains

$$(30)\quad \sum_p a_{n.p} N_p + \sum_q a_{n.q} N_q + (\Delta g_F)_n = 0 ,$$

$$(31)\quad n,p = 0, 1, 2, \dots, F,$$

$$(32)\quad q = F+1, F+2, \dots, K .$$

Setting

$$(33)\quad b_n = \sum_q a_{n.q} N_q + (\Delta g_F)_n$$

for the known part, one obtains a linear set of equations for the determination of the unknown N-values,

$$(34)\quad \sum_p a_{n.p} N_p + b_n = 0 ,$$

$$(35)\quad n,p = 0, 1, 2, \dots, F .$$

This set of equations can be solved by the Gauss-Seidel iteration method. The convergence of the method is ensured because it can be shown that

(36) $|a_{n.n}| > \sum_{p} |a_{n.p}| \quad , \qquad p \neq n \; .$

References

[1] Brillouin, M.: La méthode des moindres carrés et les équations aux dérivées partielles de la physique mathématique.
Annales de Physique, 9. Série, Paris 6 (1916) S. 137-223.

[2] Hein, G.; Groten, E.: On the use of bandwidth and profile reduction in combination solutions of satellite altimetry.
Acta Geod. Geophys. et Montanistica, Acad. Sci. Hung., Budapest, 14, 1-2 (1979) S. 59-69.

[3] Rapp, R.H.: Global anomaly and undulation recovery using GEOS - 3 altimetry data.
Reports of the Dep. of Geodetic Science, Ohio State Univ. Nr. 285 (1979) 49 S.

The spacelike Molodenski problem including the rotational term of the gravity potential

A. Bode and E. Grafarend [1]

0. Introduction

The spacelike Molodenski or geodetic boundary value problem has gained new interest for a statement of the degree of approximation by an adjustment of threedimensional networks through collocation. The classical Molodenski problem is defined by a functional linearization of abservables of type gravity and potential through an *isotropic* normal field, e.g. gm/r where gm is the product of the gravitational constant and the mass of the earth, and r the distance of a telluroid point from the mass centre. Typically an isotropic boundary operator appears in such a linearization process, e.g. only a derivative of order zero and order one with respect to r. There has been the unsolved problem how to construct an unique solution for the more realistic case that the normal potential includes the centrifugal term, that is a normal potential of type $gm/r + \omega^2 r^2 \cos^2\varphi/2$. This *anisotropic* normal potential will be our starting point, here: At first we rigorously construct the *linearized* boundary operator for such a normal potential und prove that zero and first order derivatives appear with respect to radius r and latitude φ, a generalization of the classical Stokes boundary operator.
Secondly the geodetic boundary value problem based on such a linearized boundary operator is rigorously solved in the Hilbert space of spherical harmonics, mainly by applying the technique of base representation by *Wigner 3j-coefficients*. Finally the infinite dimensional system of equations is rigorously solved by the technique of Neumann series, set up around the Stokes solution. A *convergency proof* is given.

The problem we have solved here has attracted many geodesists; for instance, it was mentioned as an *unsolved* problem by F. Sanso (1977, 1978). Similar technology to construct a solution was used by K. Arnold (1980) who even used a more general normal field representation than ours.

This contribution is part of another one solely on *telluroid mappings* based on the above normal gravity field.

[1] Geodätisches Institut der Universität Stuttgart

1. Representation of the boundary operator of the geodetic boundary value problem

Geodesy will be based on Euclidean vector space structure. Topological notions are given by mass-free and mass-filled regions, e.g. the external space R_e of the earth and the internal space $R_i = R^3/R_e$ separated by the boundary ∂R, the surface. A boundary value problem will be called a *geodetic* one, if for a given gravity vector $\underset{\sim}{\Gamma}\{\underset{\sim}{x},W(\underset{\sim}{x})\}, \underset{\sim}{x}\in\partial R$, *the observational functional*, we can find (i) $\underset{\sim}{x}$ or the geometry space of the boundary, (ii) $W(\underset{\sim}{x})$, $\underset{\sim}{x}\in R_e$, or the gravity space of the external region, subject to the Poisson equation $\operatorname{div} \underset{\sim}{\Gamma}(\underset{\sim}{x}) = \operatorname{div}\operatorname{grad} W(\underset{\sim}{x}) = -4\pi G\rho(\underset{\sim}{x}) + 2\Omega^2$, $\underset{\sim}{x}\in R_i$ of a uniformly rotating body of velocity Ω and mass density $\rho(\underset{\sim}{x})$ multiplied bei G, the gravitational constant, especially $\lim_{r\to\infty} W(\underset{\sim}{x}) = 0$, $r = \|\underset{\sim}{x}\|$. We refer to (i) as the geometric part of the gbvp, whereas to (ii) as the physical part of the gbvp. Both, (i) and (ii) make the gbvp a free, nonlinear boundary value problem.

In order to *linearize* the gbvp we *decompose* $W = w + \delta w$, where w is called the normal potential, δw its disturbing counter part. Namely we choose $w := gmr^{-1} + \omega^2(x^2 + y^2)/2$ such that $G = g + \delta g$, $\omega = \Omega$ leading to $LW(\underset{\sim}{x}) = 2\Omega^2 = Lw(\underset{\sim}{x})$, $\underset{\sim}{x}\in\partial R$, $L := \operatorname{div}\operatorname{grad}$, the threedimensional Laplace operator, especially $L\delta w(\underset{\sim}{x}) = 0$, $\underset{\sim}{x}\in\partial R$!

Due to fact that the geometry of the 'real boundary' is unknown, *but* some approximate information 'where we are' is known, we introduce the *bijective* telluroid mapping $T : P\mapsto p$, $p = T(P)$. (T maps a point P of the 'real' boundary onto a point p of the approximate boundary, the telluroid, one-to-one.) The *inverse* telluroid mapping will be written $P = T^{-1}(p)$.

The known boundary data $\underset{\sim}{\Gamma}(\underset{\sim}{x}, W)$, $W(\underset{\sim}{x})$, $\underset{\sim}{x}\in\partial R$, will be approximated by linear series of B. Taylor 'around a known point p', namely

$$\underset{\sim}{\Gamma}(P) = \underset{\sim}{\gamma}(P) + \delta\underset{\sim}{\gamma}(P) = \underset{\sim}{\gamma}(p) + (\operatorname{grad}\underset{\sim}{\gamma})(p)\,\Delta\underset{\sim}{x} + \delta\underset{\sim}{\gamma}(P) \qquad (1.1i)$$

$$W(P) = w(P) + \delta w(P) = w(p) + (\operatorname{grad} w)(p)\,\Delta\underset{\sim}{x} + \delta w(P) \qquad (1.1ii)$$

or

$$\begin{bmatrix}\Delta\gamma_1\\ \Delta\gamma_2\\ \Delta\gamma_3\\ \Delta w\end{bmatrix} = \begin{bmatrix}\partial_{11}w & \partial_{12}w & \partial_{13}w\\ \partial_{21}w & \partial_{22}w & \partial_{23}w\\ \partial_{31}w & \partial_{32}w & \partial_{33}w\\ \partial_1 w & \partial_2 w & \partial_3 w\end{bmatrix}_P \cdot \begin{bmatrix}\Delta x_1\\ \Delta x_2\\ \Delta x_3\end{bmatrix} + \begin{bmatrix}\partial_1\delta w\\ \partial_2\delta w\\ \partial_3\delta w\\ \delta w\end{bmatrix}_P \qquad (1.2)$$

represented in an orthonormal (Cartesian) frame such that $\Delta\gamma_i := \Gamma_i(P) - \gamma_i(p)$ are the coordinates of the gravity anomaly vector $\underset{\sim}{\Delta\gamma}(P,p)$, $\Delta W := W(P) - w(p)$ the potential anomaly, $\partial_i = \partial/\partial x_i$, $\partial_{ij} = \partial_i \partial_j$. We will refer to (1.2) as the *mixed form* of the linearized nonlinear boundary operator : $\Delta\underset{\sim}{x} = \underset{\sim}{x}(P) - \underset{\sim}{x}(p)$ is unknown in geometry space, $\delta\gamma$ = grad δw and δw are unknowns in gravity space. A version with unknowns only in gravity space can be constructed in the following way: The matrix containing $\partial_i w$ and $\partial_{ij} w$ is partitioned according to

$$\begin{bmatrix} \Delta x_1 \\ \Delta x_2 \\ \Delta x_3 \end{bmatrix} = \begin{bmatrix} \partial_{11}w & \partial_{12}w & \partial_{13}w \\ \partial_{21}w & \partial_{22}w & \partial_{23}w \\ \partial_{31}w & \partial_{32}w & \partial_{33}w \end{bmatrix}_p^{-1} \cdot \begin{bmatrix} \Delta\gamma_1 - \partial_1\delta w \\ \Delta\gamma_2 - \partial_2\delta w \\ \Delta\gamma_3 - \partial_3\delta w \end{bmatrix} \tag{1.3}$$

$$\delta w(P) - \partial_i w(p)\partial^{ij}w(p)\partial_j\delta w(P) = \Delta w(P,p) - \partial_i w(p)\delta^{ij}w(p)\Delta\gamma_j(P,p) \tag{1.4}$$

where $\partial^{ij}w$ indicates the regular inverse of $\partial_{ij}w$. The summation convention over repeated indices is applied. Actually the first three equations of (1.2) have been used to determine Δx, in return this result was put into the fourth equation of (1.2) leading finally to (1.4) to which we refer as the *gravimetric form* of the linearized nonlinear boundary operator: It contains only δw and grad δw as unknowns in gravity space. In addition a shorter version of (1.4) is

$$\delta w - \gamma_i \partial\delta w/\partial\gamma_i = \Delta w - \partial w/\partial\gamma_i \Delta\gamma_i \tag{1.5}$$

In order to be more precise we must state the application of the telluroid mapping to make (1.4), (1.5) *computable*, e.g. we have to transform anomalies as being two-point functions into one-point functions, for instance $\Delta\gamma := \Gamma(P) - \gamma(p) = \Gamma(T^{-1}(p)) - \gamma(p) =: \tilde{\Gamma}(p) - \gamma(p)$, and similarly $L\delta w(P) = \partial x_i/\partial x_I \partial x_j/\partial x_I \partial_i\partial_j\delta w(T^{-1}(p)) = 0$, $\underset{\sim}{x} \in \partial R$. An example for a telluroid mapping is $\underset{\sim}{\Gamma}(P)/\|\Gamma(P)\| = \gamma(p)/\|\gamma(p)\|, W(P) = w(p)$ leading to a special form of (1.5), namely

$$\delta w - \gamma_i \partial\delta w/\partial\gamma_i = -\gamma_i \partial w/\partial\gamma_i \gamma^{-1}\Delta\gamma \tag{1.6}$$

In terms of gravimetrical spherical coordinates the telluroid mapping of this type can be written $\Lambda(P) = \lambda_\gamma(p)$, $\Phi(P) = \varphi_\gamma(p)$, $W(P) = w(p)$. For the detailed computation of the linearized boundary operator (1.4), (1.5), (1.6) we take adventage of the fact that, in geometrical spherical coordinates, the normal potential $w := gmr^{-1} + \omega^2(x^2 + y^2)/2 = gmr^{-1} + \omega^2 r^2 \cos^2\varphi/2 = w(\varphi, r)$ depends *only* on two coordinates φ, r instead of three, x, y, z:

Lemma 1.1 :

Let (1.4), (1.5), (1.6) be the linearized geodetic boundary operator on a harmonic disturbing potential δw. Assume a telluroid mapping of type $\Lambda(P) = \lambda(p)$, $\Phi(P) = \varphi(p)$, $W(P) = w(p)$. If $w = w(\varphi, r) = gmr^{-1} + \omega^2 r^2 \cos^2\varphi/2$ is a choice of a normal potential, then (1.6) can be rigorously represented in terms of geometrical spherical coordinates by

$$-[2 + \beta(1 - 3\sin^2\varphi)]\delta w + 3\beta \sin\varphi \cos\varphi\, \partial\delta w/\partial\varphi - (1 - \beta) r \partial\delta w/\partial r =$$

$$r \frac{(1 - \beta)^2 + \beta(1 + 2\beta)\sin^2 p - 3\beta^2 \sin^4\varphi}{(1 - \varepsilon)^{1/2}\,(1 + \frac{\varepsilon}{1 - \varepsilon}\sin^2\varphi)^{1/2}} \Delta\gamma \qquad (1.7)$$

where

$$\beta := \omega^2/gmr^{-3}\,, \quad \varepsilon := \beta(2 - \beta)$$

Corollary 1.1 :

If $\omega^2 = 0$, then the linearized geodetic boundary operator (1.7) reduces to

$$-2r^{-1}\delta w - \partial\delta w/\partial r = \Delta\gamma \qquad (1.8)$$

known as the geodetic boundary operator of G.G. Stokes (1848).

Proof:

For the proof we acknowledge the fact that for the normal potential

$w = gmr^{-1} + \omega^2(x^2 + y^2)/2 = gmr^{-1} + \omega^2 r^2\cos^2\varphi/2$ the normal gravity coordinates

$$\gamma_1 = \partial w/\partial x = (-\,gmr^{-3} + \omega^2)x = (-\,gmr^{-3} + \omega^2)r\cos\varphi\cos\lambda \qquad (1.9i)$$

$$=: \gamma_4\cos\lambda$$

$$\gamma_2 = \partial w/\partial y = (-\,gmr^{-3} + \omega^2)y = (-\,gmr^{-3} + \omega^2)r\cos\varphi\sin\lambda \qquad (1.9ii)$$

$$=: \gamma_4\sin\lambda$$

$$\gamma_3 = \partial w/\partial z = -\,gmr^{-3}z = -\,gmr^{-2}\sin\varphi \qquad (1.9iii)$$

can be written in terms of *two* independent functions, namely γ_3 and $\gamma_4 := (-\,gmr^{-3} + \omega^2)r\cos\varphi$ such that

$$\cos\lambda = \partial\gamma_1/\partial\gamma_4\ ,\ \sin\lambda = \partial\gamma_2/\partial\gamma_4\ ,\ 0 = \partial\gamma_3/\partial\gamma_4 \qquad (1.10)$$

$$0 = \partial\gamma_1/\partial\gamma_3\ ,\quad 0 = \partial\gamma_2/\partial\gamma_3$$

$$\gamma_i = \partial\gamma_i/\partial\gamma_\alpha\,\gamma_\alpha\ ,\ \alpha\in\{3,4\} \qquad (1.11)$$

$$\gamma_i\partial/\partial\gamma_i = \partial\gamma_i/\partial\gamma_\alpha\,\gamma_\alpha\,\partial/\partial\gamma_i = \gamma_\alpha\partial/\partial\gamma_\alpha\ . \qquad (1.12)$$

Let us introduce geometrical spherical coordinates by

$$y_1 := \lambda,\ y_2 := \varphi,\ y_3 := r\ . \qquad (1.13)$$

$$\partial/\partial\gamma_\alpha = \partial y_\beta/\partial\gamma_\alpha\ \partial/\partial y_\beta\ ,\ \alpha\in\{3,4\}\ ,\ \beta\in\{2,3\} \qquad (1.14)$$

$$\partial y_\beta/\partial\gamma_\alpha = (\partial\gamma_\alpha/\partial y_\beta)^{-1}\ \text{(2 x 2 matrix!)} \qquad (1.15)$$

$$\partial\gamma_\alpha/\partial y_\beta = \begin{bmatrix} (gmr^{-3} - \omega^2)r\sin\varphi & (2gmr^{-3} + \omega^2)\cos\varphi \\ -\,gmr^{-2}\cos\varphi & 2\,gmr^{-3}\sin\varphi \end{bmatrix} \qquad (1.16)$$

$$(\partial\gamma_\alpha/\partial y_\beta)^{-1} = \begin{bmatrix} r^{-1}\alpha^{-1}\sin\varphi & (2gmr^{-3} + \omega^2)\cos\varphi/(-2gmr^{-2}\alpha) \\ 2^{-1}\alpha^{-1}\cos\varphi & (-gmr^{-3} + \omega^2)r\sin\varphi/(-2gmr^{-2}\alpha) \end{bmatrix} \qquad (1.17)$$

$$\alpha := [gm\, r^{-3} - \omega^2(1 - \tfrac{3}{2}\cos^2\varphi)] \qquad (1.18)$$

In (1.18) α is *not* an index. If we combine (1.12), (1.14) and (1.17) for (1.6) we arrive at (1.7), q.e.d.

2. Solution of the geodetic boundary value problem by the Hilbert-space-method

The geodetic boundary value problem has already been solved by integral equation methods. However the practical realization of the results has been proven to be very problematic.
Therefore we want to find the solution with an other method, which we call *Hilbert-space-method* for the following reasons.

δw and $\Delta\gamma$ will be represented by *harmonic series*, that is as elements of a *Hilbert space* with the *solid spherical harmonics*, or the *surface spherical harmonics*, respectively as *basis* (subbasis). The *coordinates* (coefficients) of $\Delta\gamma$ are assumed as known. Substitution of the harmonic series for δw and $\Delta\gamma$ into the boundary operator, recombination of the two sides of the boundary operator with respect to the basis and comparison of the coordinates of the recombinated left and right hand side yields the systems of equations for determining the coordinates of δw. This is similar to the comparison of the coefficients of two polynomials.

Harmonic expansion for δw and $\Delta\gamma$

Because the disturbing potential δw should satisfy the *untransformed Laplace differential equation*, δw can assumed to be expanded in a *harmonic series*.

$$\delta w = \sum_{n=0}^{\infty} (R/r)^{n+1} \sum_{m=0}^{n} P_n^m(\sin\varphi)(a_n^m \cos m\lambda + b_n^m \sin m\lambda) \qquad (2.1)$$

$$P_n^m(\mu) := \frac{(-1)^m}{2^n n!} (1 - \mu^2)^{\frac{m}{2}} \frac{d}{d\mu}^{n+m} (\mu^2 - 1)^n$$

are the *Legendre polynomials*, see for instance E.W. Hobson (1931, p. 91, 56.).

The basis functions for δw are the (3-dimensional) *solid spherical harmonics*

$$\left(\frac{R}{r}\right)^{n+1} P_n^m(\sin\varphi) \cdot \begin{cases} \cos m\lambda \\ \sin m\lambda \end{cases}$$

After substituting (2.1) for δw into the boundary operator, which is defined on the telluroid, r also must be taken on the telluroid, or more exactly $r = r(\lambda,\varphi)$ would have to be substituted. A rearrangement of the boundary operator into a series of surface spherical harmonics would have to be performed.

However for *simplification purposes* we approximate the telluroid with a sphere of radius r = R. Hence let be R the radius of this sphere approximating the telluroid.

According to (2.1) we assume, that the gravity anomaly on the telluroid $\Delta\gamma = \tilde{T}(p) - \gamma(p)$ is developed into an approximating finite series of *surface spherical harmonics*, which will be written as an infinite series.

$$\Delta\gamma = \sum_{n=0}^{\infty} \sum_{m=0}^{n} P_n^m(\sin\varphi)\ (c_n^m \cos m\lambda + d_n^m \sin m\lambda), \qquad (2.2)$$

$$c_n^m := d_n^m := 0\ ,\ n > N.$$

The coordinates c_n^m , d_n^m of $\Delta\gamma$ are assumed to be known!

Because $\Delta\gamma$ has been developed only on a surface, the basis functions for $\Delta\gamma$ are the (2-dimensional) *surface spherical harmonics*

$$P_n^m(\sin\varphi) \cdot \begin{cases} \cos m\lambda \\ \sin m\lambda \end{cases}$$

Here the quotients $(R/r)^{n+1}$ are unity.

Otherwise we have to take $r = r(\lambda,\varphi)$ on the telluroid and $\Delta\gamma$ would not be completely developed into a series of surface spherical harmonics, which we assumed.

Substitution of the series for δw and $\Delta\gamma$ into the boundary operator. Basis representation of the boundary value operator

By multiplication with gm/r^3 and other simple transformations the boundary operator (1.7) takes the suitable form

$$[-(2\frac{gm}{r^3}+\omega^2)+3\omega^2\sin^2\varphi]\delta w+3\omega^2\sin\varphi\cos\varphi\frac{\partial\delta w}{\partial\varphi}+(-\frac{gm}{r^3}+\omega^2)r\frac{\partial\delta w}{\partial r}=$$

$$=\frac{gm}{r^2}\frac{\beta_o+\beta_1\sin^2\varphi+\beta_2\sin^4\varphi}{(1-\varepsilon)^{1/2}(1-\tilde{\varepsilon}\sin^2\varphi)^{1/2}}\Delta\gamma\,, \quad (2.3)$$

$$\beta_o := (1-\beta)^2\,,\ \beta_1 := \beta(1+2\beta)\,,\ \beta_2 := -3\beta^2\,,$$

$$\varepsilon := \beta(2-\beta)\,,\ \tilde{\varepsilon} := \frac{-\varepsilon}{1-\varepsilon}\,;\ \beta := \omega^2/gm\,r^{-3}$$

The right hand side of (2.3) can be expanded by applying the binomial series on $(1-\tilde{\varepsilon}\sin^2\varphi)^{-1/2}$.

$$\text{r.h. side of (2.3)} = gm\,r^{-2}\Big(\sum_{j=0}^{\infty} f_j \sin^{2j}\varphi\Big)\Delta\gamma\,, \quad (2.4)$$

$$f_j := (1-\varepsilon)^{-1/2}\sum_{i=0}^{2}\beta_i\binom{-1/2}{j-i}\tilde{\varepsilon}^{j-i}\,;$$

$$\binom{\alpha}{n} := \frac{\alpha(\alpha-1)\cdot\ldots\cdot(\alpha-n+1)}{n!}\,,\ \binom{\alpha}{n} := 0 \text{ for } n<0$$

are the binomial coefficients.

2.1 Left hand side of the boundary operator (2.3)

Together with δw the following derivatives are to be substituted into (2.3).

$$\partial\delta w/\partial r = -\frac{1}{r}\sum_{n=0}^{\infty}(n+1)(R/r)^{n+1}\sum_{m=0}^{n}P_n^m(a_n^m\cos m\lambda + b_n^m\sin m\lambda) \quad (2.1.1)$$

$$\partial\delta w/\partial\varphi = \sum_{n=0}^{\infty}(R/r)^{n+1}\sum_{m=0}^{n}dP_n^m(\sin\varphi)/d\varphi(a_n^m\cos m\lambda + b_n^m\sin m\lambda)$$

Hence products of the following form arise.

$$\sin^2\varphi\, P_n^m(\sin\varphi)\ ,\ \sin\varphi\cos\varphi\, dP_n^m(\sin\varphi)/d\varphi$$

They are to be transformed into a basis representation of the form $\Sigma\alpha_j^m P_j^m$. We use two wellknown recurrence relations of the theory of harmonic functions:

$$(2n+1)\mu P_n^m(\mu) = (n+m)P_{n-1}^m(\mu) + (n-m+1)P_{n+1}^m(\mu)\ , \tag{2.1.2}$$

$$(1-\mu^2)dP_n^m(\mu)/d\mu = (n+m)P_{n-1}^m(\mu) - n\mu P_n^m(\mu)$$

See I.S. Gradshteyn, I.M. Ryzhik (1965, p. 1005), E.W. Hobson (1931, p. 108 (42)), W. Kertz (1973, p. 59), N.N. Lebedev (1973, p. 248 (7.12.11), (7.12.15))

Setting $\mu := \sin\varphi$ and repeated application of the formulas (2.1.2) yields

$$\sin^2\varphi\, P_n^m = \rho_{n-2}^m P_{n-2}^m + \sigma_n^m P_n^m + \tau_{n+2}^m P_{n+2}^m\ , \tag{2.1.3i}$$

$$\rho_{n-2}^m := \frac{(n+m-1)(n+m)}{(2n-1)(2n+1)}$$

$$\sigma_n^m := \frac{(n-m)(n+m)}{(2n-1)(2n+1)} + \frac{(n-m+1)(n+m+1)}{(2n+1)(2n+3)}$$

$$\tau_{n+2}^m := \frac{(n-m+1)(n-m+2)}{(2n+1)(2n+3)}$$

$$\sin\varphi\cos\varphi\, dP_n^m(\sin\varphi)/d\varphi = \alpha_{n-2}^m P_{n-2}^m + \beta_n^m P_n^m + \gamma_{n+2}^m P_{n+2}^m\ , \tag{2.1.3ii}$$

$$\alpha_{n-2}^m := \frac{(n+1)(n+m)(n+m-1)}{(2n-1)(2n+1)}$$

$$\beta_n^m := \frac{(n+1)(n-m)(n+m)}{(2n-1)(2n+1)} - \frac{n(n-m+1)(n+m+1)}{(2n+1)(2n+3)}$$

$$\gamma_{n+2}^m := -\frac{n(n-m+1)(n-m+2)}{(2n+1)(2n+3)}$$

Obviously the 'spectrum' becomes wider by multiplying δw with $\sin^2\varphi$ or $\partial\delta w/\partial\varphi$ with $\sin\varphi\cos\varphi$

The formulas (2.1.3i-ii) yield

$$\sin^2\varphi\ \delta w = \tag{2.1.4i}$$

$$= \sum_{n=0}^{\infty} (R/r)^{n+1} \sum_{m=0}^{n} \sin^2\varphi\ P_n^m(a_n^m \cos m\lambda + b_n^m \sin m\lambda) =$$

$$= \sum_{n=2}^{\infty} (R/r)^{n-1} \sum_{m=0}^{n} \tau_n^m\ P_n^m(a_{n-2}^m \cos m\lambda + b_{n-2}^m \sin m\lambda) +$$

$$+ \sum_{n=0}^{\infty} (R/r)^{n+1} \sum_{m=0}^{n} \sigma_n^m\ P_n^m(a_n^m \cos m\lambda + b_n^m \sin m\lambda) +$$

$$+ \sum_{n=0}^{\infty} (R/r)^{n+3} \sum_{m=0}^{n} \rho_n^m\ P_n^m(a_{n+2}^m \cos m\lambda + b_{n+2}^m \sin m\lambda)$$

$$\sin\varphi \cos\varphi\ \partial\delta w/\partial\varphi = \tag{2.1.4ii}$$

$$= \sum_{n=0}^{\infty} (R/r)^{n+1} \sum_{m=0}^{n} \sin\varphi \cos\varphi\, d P_n^m(\sin\varphi)/d\varphi(a_n^m \cos m\lambda + b_n^m \sin m\lambda) =$$

$$= \sum_{n=2}^{\infty} (R/r)^{n-1} \sum_{m=0}^{n} \gamma_n^m\ P_n^m(a_{n-2}^m \cos m\lambda + b_{n-2}^m \sin m\lambda) +$$

$$+ \sum_{n=0}^{\infty} (R/r)^{n+1} \sum_{m=0}^{n} \beta_n^m\ P_n^m(a_n^m \cos m\lambda + b_n^m \sin m\lambda) +$$

$$+ \sum_{n=0}^{\infty} (R/r)^{n+3} \sum_{m=0}^{n} \alpha_n^m\ P_n^m(a_{n+2}^m \cos m\lambda + b_{n+2}^m \sin m\lambda)$$

Because of $P_\nu^m \equiv 0$ for $m > \nu$, we observe that $a_\nu^m := b_\nu^m := 0$, $m > \nu$.

Substitution of (2.1.4i-ii) together with $\partial\delta w/\partial r$ in the form of (2.1.1) yields for the left hand side of (2.3):

$$\sum_{n=2}^{\infty} (R/r)^{n-1} \sum_{m=0}^{n} \omega^2 r_n^m\ P_n^m(a_{n-2}^m \cos m\lambda + b_{n-2}^m \sin m\lambda) +$$

$$+ \sum_{n=0}^{\infty} (R/r)^{n+1} \sum_{m=0}^{n} [(n-1) g m\, r^{-3} + \omega^2 s_n^m]\ P_n^m(a_n^m \cos m\lambda + b_n^m \sin m\lambda) +$$

$$+ \sum_{n=0}^{\infty} (R/r)^{n+3} \sum_{m=0}^{n} \omega^2 t_n^m\ P_n^m(a_{n+2}^m \cos m\lambda + b_{n+2}^m \sin m\lambda)\ , \tag{2.1.5}$$

$$r_n^m := 3(\alpha_n^m + \tau_n^m) = -3\,\frac{(n-3)(n-m-1)(n-m)}{(2n-1)(2n-3)}\ ,$$

$$s_n^m := 3(\beta_n^m + \sigma_n^m) - (n+2) = -\frac{(n-1)(n+1)(4n+3) + 15m^2}{(2n-1)(2n+3)} \qquad (2.1.5i)$$

$$t_n^m := 3(\alpha_n^m + \rho_n^m) = 3\,\frac{(n+4)(n+m+1)(n+m+2)}{(2n+3)(2n+5)} \ ,$$

$$a_\nu^m = b_\nu^m = 0 \ , \ m > \nu \ .$$

Hence the restriction of the left hand side of the boundary operator (3.3) onto the sphere with radius r = R, approximating the telluroid, has the *basis representation*

$$\sum_{n=0}^{\infty} \sum_{m=0}^{n} \{(\omega^2 r_n^m a_{n-2}^m + [(n-1)gmR^{-3} + \omega^2 s_n^m] a_n^m + \omega^2 t_n^m a_{n+2}^m)\, P_n^m \cos m\lambda +$$

$$+ (\omega^2 r_n^m b_{n-2}^m + [(n-1)gmR^{-3} + \omega^2 s_n^m] b_n^m + \omega^2 t_n^m b_{n+2}^m)\, P_n^m \sin m\lambda\} \qquad (2.1.6)$$

$$a_\nu^m = b_\nu^m = 0 \ , \ m > \nu \ ,$$

where the cases n=0,1 are also included (see the first sum of the preceding expansions).

2.2 Right hand side (2.4) of the boundary operator (2.3)

The following product must be transformed into a basis representation.

$$\Big(\sum_{j=0}^{\infty} f_j \mu^{2j}\Big)\, \Delta\gamma =$$

$$= \Big(\sum_{j=0}^{\infty} f_j \mu^{2j}\Big) \sum_{n=0}^{N} \sum_{m=0}^{n} P_n^m(\mu)(c_n^m \cos m\lambda + d_n^m \sin m\lambda) \ , \qquad (2.2.1)$$

$$\mu := \sin\varphi \ ; \ c_n^m = d_n^m = 0 \ , \ n > N \ .$$

It is <u>sufficient</u> to show how the transformation works for the term

$$\Big(\sum_{j=0}^{\infty} f_j \mu^{2j}\Big) \sum_{n=0}^{N} \sum_{m=0}^{n} c_n^m P_n^m(\mu) \cos m\lambda \qquad (2.2.2)$$

At first the powers μ^{2j} can be expressed by Legendre polynomials:

$$\mu^{2j} = \sum_{\kappa=0}^{j} \pi_{j,\kappa} \, P^{0}_{2\kappa}(\mu) \, , \tag{2.2.3}$$

$$\pi_{j,\kappa} := \begin{cases} \dfrac{1}{2j+1} & , \ \kappa = 0 \\ \dfrac{2\,(4\kappa+1)}{2j+1} \prod_{\lambda=1}^{\kappa} \dfrac{f-\lambda+1}{2j+2\lambda+1} & , \ \kappa > 0 \end{cases}$$

Π denotes the product. (E.W. Hobson (1931, p. 44 (43) and others)

Hence the products $\mu^{2j} \, P^{m}_{n}$ can be reduced to linearcombinations of products of the forms $P^{0}_{2\kappa} \, P^{m}_{n}$ which are again to be transformed into a basis representation. The coordinates of these basis representations are essentially the *Wigner 3j-coefficients*.
The following expressions for determining these coordinates are based on results taken from D.E. Winch, R.W. James (1973).

Between our definition according to E.W. Hobson (1931, p.91, 56.)

$$P^{m}_{n}(\mu) := \frac{(-1)^{m}}{2^{n} n!} (1-\mu^{2})^{\frac{m}{2}} \left(\frac{d}{d\mu}\right)^{n+m} (\mu^{2}-1)^{n}$$

and the definition with complex representation according to D.E. Winch, R.W. James (1973, (2.1), (2.5)) exists the correspondence

$$Y^{m}_{n}(\lambda,\mu) := \left[(2n+1) \frac{(n-m)!}{(n+m)!}\right]^{1/2} P^{m}_{n}(\mu) \, e^{im\lambda} \tag{2.2.4}$$

For products of surface spherical harmonics we take from D.E. Winch, R.W. James (1973, (5.7), (5.8), (5.12), (5.18)) the representation

$$Y^{u}_{l} \, Y^{v}_{m} = \sum_{n} \left[(2l+1)(2m+1)(2n+1)\right]^{1/2} \overline{Y^{w}_{n}} \begin{pmatrix} l & m & n \\ u & v & w \end{pmatrix} \begin{pmatrix} l & m & n \\ 0 & 0 & 0 \end{pmatrix} \, , \tag{2.2.5}$$

valid: if $u + v + w = 0$,

$\sum_n \ldots$: 1, m, n must satisfy a triangle rule, which we will specify only for our application,

$\overline{Y_n^w}$: the complex conjugate of Y_n^w .

And the *Wigner 3j-coefficients:*

$$\begin{pmatrix} l & m & n \\ u & v & w \end{pmatrix} := $$

$$-1^{l-m-w}\Delta(l,m,n)[(l-n)!(l+n)!(m-v)!(m+v)!(n-w)!(n+w)!]^{1/2} \cdot$$

$$\cdot\sum_t (-1)^t [(l-u-t)!(n-m+u+t)!(m+v-t)!(n-l-v+t)!t!$$
$$(l+m-n-t)!]^{-1} ,$$

$\sum_t \ldots$: t runs as long as positive factorials occur (must here not be specified more precisely).

$$\begin{pmatrix} l & m & n \\ 0 & 0 & 0 \end{pmatrix} := \begin{cases} (-1)^s \dfrac{\Delta(l,m,n)\, s!}{(s-l)!(s-m)!(s-n)!} , & l+m+n \text{ even} \\ & (2s := l+m+n) \\ 0 , & l+m+n \text{ odd} \end{cases}$$

$$\Delta(l,m,n) := \left[\frac{(l+m-n)!(m+n-l)!(n+m-l)!}{(l+m+n+1)!}\right]^{1/2}$$

Taking (2.2.4) into account one obtains from (2.2.5)

$$P_l^u e^{iu\lambda} \cdot P_m^v e^{iv\lambda} = \left[\frac{(l+n)!(m+v)!}{(l-n)!(m-v)!}\right]^{1/2} \cdot$$

$$\cdot\sum_n (2n+1) \left[\frac{(n-w)!}{(n+w)!}\right]^{1/2} P_n^w e^{-iw\lambda} \begin{pmatrix} l & m & n \\ u & v & w \end{pmatrix} \begin{pmatrix} l & m & n \\ 0 & 0 & 0 \end{pmatrix}$$

For u: = 0 the condition u + v + w = 0 yields w = - v. Hence we obtain according to E.W. Hobson (1931, p. 99 (23))

$$P_n^w = P_n^{-v} = (-1)^v \frac{(n-v)!}{(n+v)!} P_n^v$$

It follows

$$P_1^0 P_m^v = (-1)^v \left[\frac{(m+v)!}{(m-v)!}\right]^{1/2} \cdot \sum_{(n \geq \max\{m-1,\, v\}) \wedge (1+m+n \text{ even})}^{n \leq m+1}$$

$$\{(2n+1)\left[\frac{(n-v)!}{(n+v)!}\right]^{1/2} P_n^v \begin{pmatrix} 1 & m & n \\ 0 & v & -v \end{pmatrix} \begin{pmatrix} 1 & m & n \\ 0 & 0 & 0 \end{pmatrix}\} \qquad (2.2.6)$$

From (2.2.6) results

$$P_{2\kappa}^0 P_n^m = \sum_{\nu \geq \max\{-\kappa,\, -\frac{1}{2}(n-m)\}}^{\nu \leq \kappa} w_{\kappa,n,\nu}^m P_{n+2\nu}^m \,, \qquad (2.2.7)$$

$$w_{\kappa,n,\nu}^m := (-1)^m \left[\frac{(n+m)!}{(n-m)!}\right]^{1/2} (n+2\nu+1) \frac{(n+2\nu-m)!}{(n+2\nu+m)!} \cdot$$

$$\cdot \begin{pmatrix} 2\kappa & n & n+2\nu \\ 0 & m & -m \end{pmatrix} \begin{pmatrix} 2\kappa & n & n+2\nu \\ 0 & 0 & 0 \end{pmatrix}$$

The basis representation of the right hand side (2.4) of the boundary value operator now is obtained from (2.2.3), (2.2.7) in the following steps.

$$\sum_{j=0}^{\infty} f_j \mu^{2j} \Big(\sum_{n=0}^{N} \sum_{m=0}^{n} c_n^m P_n^m \cos m\lambda \Big) =$$

$$= \sum_{n=0}^{N} \sum_{m=0}^{n} c_n^m \Big(\sum_{j=0}^{\infty} f_j \mu^{2j} P_n^m \Big) \cos m\lambda =$$

$$= \sum_{n=0}^{N} \sum_{m=0}^{n} c_n^m \Big(\sum_{j=0}^{\infty} f_j \sum_{\kappa=0}^{j} \pi_{j,\kappa} P_{2\kappa}^0 P_n^m \Big) \cos m\lambda =$$

$$= \sum_{n=0}^{N} \sum_{m=0}^{n} c_n^m \Big(\sum_{j=0}^{\infty} f_j \sum_{\kappa=0}^{j} \pi_{j,\kappa} \cdot \sum_{\nu \geq \max\{-\kappa,\, -\frac{1}{2}(n-m)\}}^{\nu \leq \kappa} w_{\kappa,n,\nu}^m P_{n+2\nu}^m \Big) \cos m\lambda =$$

$$= \sum_{n=0}^{N} \sum_{m=0}^{n} c_n^m \sum_{\kappa_o \geq -\frac{1}{2}(n-m)} v_{n,\kappa_o}^m P_{n+2\kappa_o}^m \cos m\lambda =$$

$$= \sum_{k=0}^{\infty} \sum_{m=0}^{\min\{k,N\}} \sum_{\kappa_o \geq \frac{1}{2}(m-k)}^{\kappa_o \leq \frac{1}{2}(N-k)} c_{k+2\kappa_o}^m v_{k+2\kappa_o,\kappa_o}^m P_k^m \cos m\lambda =$$

$$= \sum_{k=0}^{\infty} \sum_{m=0}^{k} c'^{m}_{k} P^{m}_{k} \cos m\lambda \quad , \tag{2.2.8}$$

$$v^{m}_{n,\kappa_o} := \sum_{j=|\kappa_o|}^{\infty} f_j \sum_{\kappa=|\kappa_o|}^{j} \pi_{j,\kappa} w^{m}_{\kappa,n,\kappa_o} \quad (-\tfrac{1}{2}(n-m) \le \kappa_o < \infty)$$

$$c'^{m}_{k} := \sum_{\kappa_o \ge \frac{1}{2}(m-k)}^{\kappa_o \le \frac{1}{2}(N-k)} c^{m}_{k+2\kappa_o} \sum_{j=|\kappa_o|}^{\infty} f_j \sum_{\kappa=|\kappa_o|}^{j} \pi_{j,\kappa} w^{m}_{\kappa,k+2\kappa_o,\kappa_o} \tag{2.2.8i}$$

$$c'^{m}_{k} := 0 \ , \ m > N \quad . \tag{2.2.8ii}$$

Analogously the transformation of the d^{m}_{n} is obtained:

$$d'^{m}_{k} := \sum_{\kappa_o \ge \frac{1}{2}(m-k)}^{\kappa_o \le \frac{1}{2}(N-k)} d^{m}_{k+2\kappa_o} \sum_{j=|\kappa_o|}^{\infty} f_j \sum_{\kappa=|\kappa_o|}^{j} \pi_{j,\kappa} w^{m}_{\kappa,k+2\kappa_o,\kappa_o} \tag{2.2.9i}$$

$$d'^{m}_{k} := 0 \ , \ m > N \tag{2.2.9ii}$$

Hence the right hand side (2.4) of the boundary operator (2.3) has on the sphere with radius r = R, approximating the telluroid, the *basis representation*

$$gm\, R^{-2} \sum_{n=0}^{\infty} \sum_{m=0}^{n} P^{m}_{n} (c'^{m}_{n} \cos m\lambda + d'^{m}_{n} \sin m\lambda) \ , \tag{2.2.10}$$

c'^{m}_{n} , d'^{m}_{n} according to (2.2.8i - 2.2.9ii).

For $\omega := 0$ we must have

$$c'^{m}_{n}(\omega := 0) = c^{m}_{n} \ , \ d'^{m}_{n}(\omega := 0) = d^{m}_{n} \tag{2.2.11}$$

Hence the coordinates of the right hand side can be expressed by the coordinates of $\Delta\gamma$ in the following form.

$$c'^{m}_{n} = c^{m}_{n} + \omega^2 \delta c^{m}_{n} \ , \quad d'^{m}_{n} = d^{m}_{n} + \omega^2 \delta d^{m}_{n} \tag{2.2.12}$$

From (2.1.6) and (2.2.10) we obtain

Lemma 2.1 :

The boundary operator in the form (2.3) has on the sphere with radius $r = R$, approximating the telluroid, the basis representation

$$\sum_{n=0}^{\infty}\sum_{m=0}^{n}\{$$

$$(\omega^2 r_n^m\, a_{n-2}^m + [(n-1)gmR^{-3}+\omega^2 s_n^m]\, a_n^m + \omega^2 t_n^m\, a_{n+2}^m)\, P_n^m \cos m\lambda +$$

$$+ (\omega^2 r_n^m\, b_{n-2}^m + [(n-1)gmR^{-3}+\omega^2 s_n^m]\, b_n^m + \omega^2 t_n^m\, b_{n+2}^m)\, P_n^m \sin m\lambda \} =$$

$$= gmR^{-2}\sum_{n=0}^{\infty}\sum_{m=0}^{n} P_n^m\,(c'^m_n \cos m\lambda + d'^m_n \sin m\lambda)\,, \qquad (2.5)$$

$$a_\nu^m = b_\nu^m = 0\,,\ m > \nu\,; \qquad (2.5i)$$

c'^m_n, d'^m_n *according to (2.2.8i - 2.2.9ii), where*

$$c'^m_n = d'^m_n = 0\,,\ m > N\,.$$

3. The systems of equations for determining the coordinates of the disturbing potential δw and their solutions.

From Lemma 2.1 follows immediately, that a *comparison of coordinates* with respect to the base functions $P_n^m \cos m\lambda$ and $P_n^m \sin m\lambda$ leads to

Lemma 3.1 :

The equations for determining the coordinates a_n^m, b_n^m of the disturbing potential δw are given by

$$\omega^2 r_n^m\, a_{n-2}^m + [(n-1)gmR^{-3}+\omega^2 s_n^m]\, a_n^m + \omega^2 t_n^m\, a_{n+2}^m =$$

$$= gmR^{-2}\, c'^m_n\,, \qquad (3.1i)$$

$$a_{n-2}^m := 0\,,\ n-2 < m \qquad (3.1ii)$$

$$\omega^2 r_n^m\, b_{n-2}^m + [(n-1)gmR^{-3} + \omega^2 s_n^m]\, b_n^m + \omega^2 t_n^m\, b_{n+2}^m =$$

$$= gmR^{-2}\, d'^m_n \quad , \tag{3.2.i}$$

$$b_{n-2}^m := 0 \quad , \quad n-2 < m \tag{3.2ii}$$

Because the equations (3.1i - ii) are mathematically the same as (3.2i - ii) we can restrict us in the following to treating only the equations (3.1i - ii) and we will obtain analogous results for the equations (3.2i - ii).

The equations (3.1i - ii) contain for every fixed $m \in \{0, 1, 2, \ldots\}$ two systems of equations, depending on the fact whether n is *even* or *odd*. The *range* n_i^m of the index n of the equations (3.1i), which are contained in one of these systems, is uniquely determined by the *index pair* $' \begin{smallmatrix} m \\ i \end{smallmatrix} '$, $i \in \{1, 2\}$, e.g. 1 for n odd, 2 for n even. This is essentially a result of the condition (3.1ii).

Definition 3.1 :

$$m \text{ even} : i = 1 : \quad n_i^m := \{m+1, m+3, \ldots\} \quad (a_{m-1}^m = 0) \tag{3.3i}$$

$$i = 2 : \quad n_i^m := \{m, m+2, \ldots\} \quad (a_{m-2}^m = 0) \tag{3.3ii}$$

$$m \text{ odd} : i = 1 : \quad n_i^m := \{m, m+2, \ldots\} \quad (a_{m-2}^m = 0) \tag{3.3iii}$$

$$i = 2 : \quad n_i^m := \{m+1, m+3, \ldots\} \quad (a_{m-1}^m = 0) \tag{3.3iv}$$

Now the *characteristic* systems of equations can be typified by

$$G_i^m : \equiv M_i^m\, \underset{\sim}{a}_i^m = \underset{\sim}{c}'^m_i \tag{3.4}$$

where the index pair $' \begin{smallmatrix} m \\ i \end{smallmatrix} '$ indicates, that the rows of the matrix M_i^m contain the coefficients of the equations (3.1i) with $n \in n_i^m$. In analogy the unknown vector $\underset{\sim}{a}_i^m$ and the right hand side $\underset{\sim}{c}'^m_i$ are defined. Every further application of the index pair $' \begin{smallmatrix} m \\ i \end{smallmatrix} '$ runs analogously.

For $\omega := 0$ we arrive at the *classical* solution of G.G. Stokes (1848):

$$c'^m_n\,(\omega:=0) = c_n^m \Rightarrow (n-1)gmR^{-3}\, a_n^m = gmR^{-2}\, c_n^m \Rightarrow a_n^m = \frac{R}{n-1}\, c_n^m \tag{3.5i}$$

Taking the above formalism into account the Stokes solution can be written in the form

$$\underset{\sim}{a}_i^m = \text{diag}\,(\frac{R}{n-1})_i^m\, \underset{\sim}{c}_i^m \quad , \tag{3.5ii}$$

where diag (...) denotes a *diagonal* matrix.

Example 3.1:
A *nondegenerate* system of equations, $m = 0$, $i = 2$:

$$\begin{bmatrix} (-\frac{gm}{R^3} + \omega^2 s_0^0) & \omega^2 t_0^0 & 0 & \cdot & \cdot & \cdot \\ \omega^2 r_2^0 & (+\frac{gm}{R^3} + \omega^2 s_2^0) & \omega^2 t_2^0 & \cdot & \cdot & \cdot \\ 0 & \omega^2 r_4^0 & (3\frac{gm}{R^3} + \omega^2 s_4^0) & \omega^2 t_4^0 & \cdot & \cdot \\ \cdot & \cdot & \cdot & \cdot & \cdot & \cdot \\ \cdot & \cdot & \cdot & \cdot & \cdot & \cdot \end{bmatrix} \begin{bmatrix} a_0^0 \\ a_2^0 \\ a_4^0 \\ \vdots \end{bmatrix} = \frac{gm}{R^2} \begin{bmatrix} c'^0_0 \\ c'^0_2 \\ c'^0_4 \\ \vdots \end{bmatrix} \tag{3.6}$$

$s_0^0 = -1$, $t_0^0 = 8/5$,

$r_2^0 = 2$, $s_0^0 = -11/7$, $t_2^0 = 24/7$

a_0^0 leads to a refinement of the term $u_0 := gm\, r^{-1}$ in the potential or of gm, respectively.

All the matrices of the other systems of equations have the same structure.

Nearly all matrices M_i^m (incl. M_2^0) allow a *regular splitting* of type $(D_i^m)^{-1} M_i^m = I_i^m - A_i^m$, whre D_i^m is a diagonal matrix, I_i^m the corresponding *unit matrix*, A_i^m a *'regular' tridiagonal* matrix. What we call a 'regular' matrix will be defined in the following chapter 3.1.

We then call the corresponding systems of equations G_i^m also *regular*.

In these cases one succeeds in proving the existence and computability of unique solutions, which will be done in chapter 3.1. Obviously the regularity of the A_i^m can be interpreted as a generalized *'diagonal dominance'* of the M_i^m

There are two exceptions of *nonregular* systems of equations, for the cases $m = 0,\ i = 1$ and $m = 1,\ i = 1$. These cases will be discussed in chapter 3.2.

3.1 Solution of the regular systems of equations G_i^m .

In the case $n \neq 1$ one receives after division of the equations (3.1i) by the factor $(n-1)gmR^{-3}$ the equivalent equations:

$$a_n^m - \beta_n (-r_n^m a_{n-2}^m - s_n^m a_n^m - t_n^m a_{n+2}^m) = c''^m_n \quad , \; n \neq 1 \; ! \tag{3.1.1}$$

$$\beta_n := \frac{\omega^2}{gmR^{-3}(n-1)} \quad , \quad c''^m_n := \frac{R}{n-1} c'^m_n \quad ,$$

$$a_{n-2}^m := 0 \quad , \; n-2 < m \quad \text{(see (3.1ii))}.$$

By this transformation the equations G_i^m have been changed into the equivalent systems

$$\tilde{G}_i^m := \equiv (I_i^m - A_i^m) \tilde{a}_i^m = c''^m_i \tag{3.1.2}$$

with the *split* matrices

$$(I_i^m - A_i^m) := (D_i^m)^{-1} M_i^m \quad , \; D_i^m := \text{diag } ((n-1)gmR^{-3})_i^m \tag{3.1.2i}$$

(without the cases $m = 0$, $i = 1$ and $m = 1$, $i = 1$, where in the first row of the corresponding matrices gmR^{-3} is multiplied by $(n-1) = 0$) and the right hand sides

$$\tilde{c}''^m_i := \text{diag } (R(n-1)^{-1})_i^m \tilde{c}'^m_i \tag{3.1.2ii}$$

The A_i^m are again tridiagonal matrices. Their rows result from the row vectors

$$[-\beta_n r_n^m \; , \; -\beta_n s_n^m \; , \; -\beta_n t_n^m] \quad , \quad n \in n_i^m \quad . \tag{3.1.2iii}$$

In the following we also will use the respresentation

$$A_i^m = : \omega^2 B_i^m \quad , \tag{3.1.3}$$

when we want to point out, that the β_n contain the factor ω^2.

We show that all the matrices A_i^m are regular.

Definition 3.1.1 :

A (not necessarily finite) matrix $A = [a_{ij}]$ will be called regular, if the sums of the absolutes of the row elements are bounded by some $\alpha < 1$:

$$\sum_{j=1}^{\infty} |a_{ij}| \leq \alpha \ , \quad i = 1, 2, \ldots \quad . \tag{3.1.4i}$$

A (not necessarily finite) vector $\underline{y} = y_1, y_2, \ldots$ *will be called bounded, if the absolutes of its coordinates are bounded by some* β*:*

$$|y_i| \leq \beta \ , \quad i = 1, 2, \ldots \quad . \tag{3.1.4ii}$$

(see L. Collatz (1964, p. 192, 14.4))

Lemma 3.1.1 :

The matrices A_i^m *are regular and* $\alpha := 0.9 \cdot 10^{-1}$ *can be taken.*

Proof:

For the r_n^m, s_n^m, t_n^m in (2.1.5i) the estimates are valid:

$$\left|\frac{r_n^m}{n-1}\right| < 2 \ , \ \left|\frac{s_n^m}{n-1}\right| < 5 \ , \ \left|\frac{t_n^m}{n-1}\right| < 18 \qquad (n \neq 1) \tag{3.1.5i}$$

Taking

$\omega := 7.292\,115 \cdot 10^{-5}$ [rad sec^{-1}], $gm := 3.986\,030 \cdot 10^5$[km^3 sec^{-2}] ,
$R := 6\,400$ [km] ,

we obtain for the sums of the absolutes of row elements (3.1.2iii) of the A_i^m the estimation:

$$|\beta_n r_n^m| + |\beta_n s_n^m| + |\beta_n t_n^m| = \omega^2/\frac{gm}{R^3} \left|\frac{r_n^m}{n-1}\right| + \left|\frac{s_n^m}{n-1}\right| + \left|\frac{t_n^m}{n-1}\right| <$$

$$< 3.497 \cdot 10^{-3} \cdot 25 \cong 8.74 \cdot 10^{-2} \qquad (n \neq 1) \tag{3.1.5ii}$$

Hence $\alpha := 0.9 \cdot 10^{-1}$ can be taken and the A_i^m are regular matrices according to definition 3.1.1, q.e.d.

The systems of equations $\tilde{G}_i^m$ can be written in the form

$$\underline{a}_i^m = A_i^m \underline{a}_i^m + \underline{c}''^m_i =: T_i^m \underline{a}_i^m$$

Hence we will have to search for the *fixpoints* of the *operators* T_i^m . Statements about solvability and representation of the solutions are obtained from the following theorem of the mathematical fix point theory.

Theorem 3.1.2 :

Assume the matrix A to be regular and the vector $\underline{y}$ to be bounded.

Then the equation $\underline{x} = A\underline{x} + \underline{y} =: T\underline{x}$ has a unique solution x .

The total step iteration $\underline{x}_{n+1} := T\underline{x}_n$ converges for every bounded starting vector $\underline{x}_0$ to the unique solution $\underline{x}$.

Corollary 3.1.2i :

The unique solution $\underline{x}$ can be represented by a Neumann series, that is

$$\underline{x} = (I - A)^{-1}\,\underline{y} = (I + A + A^2 + \ldots)\,\underline{y} \quad ,$$

where I is the corresponding unit matrix and $(I + A + A^2 + \ldots)$ is a Neumann series.

Proof:

For the proof of Theorem 3.1.2 we must refer to the mathematical literature, for instance L. Collatz (1964, p. 192, 14.4).

Starting with $\underline{x}_0 := \underline{y}$ the total step iteration yields

$$\underline{x}_n = T\underline{x}_{n-1} = (A^n + A^{n-1} + \ldots + A + I)\,\underline{y} \quad .$$

Hence it follows

$$\underline{x} = \lim_{n\to\infty} \underline{x}_n = (I + A + A^2 + \ldots)\,\underline{y} = (I - A)^{-1}\,\underline{y} \quad , \quad \text{q.e.d.} \quad .$$

Supplement 3.1.2ii :

From the proof of theorem (3.1.1) in L. Collatz (1964) it becomes obvious, that $\underline{x}$ is the unique solution in the complete space of all bounded vectors $\underline{\xi} = [\xi_1, \xi_2, \ldots]$. Starting with a bounded vector $\underline{x}_0$, the total step iteration remains in this complete space.

The consequence is, that a solution, which is different from the unique bounded solution $\underline{x}$, cannot be bounded. This is important for one of the two nonregular systems G_i^m in chapter 3.2.

The application of Lemma 3.1.1, Theorem 3.1.2 and Corollary 3.1.2i to the systems of equations $\tilde{G}_i^m$ leads to the solutions of the equivalent systems G_i^m .

Theorem 3.1.4 :

Let the right hand sides $\underset{\sim}{\zeta}''^m_i$ of the systems of equations $\tilde{G}_i^m$ be bounded. Then the equivalent systems of equations G_i^m have unique bounded solutions $\underset{\sim}{a}^m_i$, which can be represented by a Neumann series in the following way.

$$\underset{\sim}{a}^m_i = (I^m_i - A^m_i)^{-1}\ \underset{\sim}{\zeta}''^m_i = (I^m_i + A^m_i + (A^m_i)^2 + \ldots)\ \mathrm{diag}\ (R(n-1)^{-1})^m_i\ \underset{\sim}{\zeta}'^m_i = \tag{3.1.6i}$$

$$= \mathrm{diag}\ (R(n-1)^{-1})^m_i\ \underset{\sim}{\zeta}^m_i +$$

$$+ \omega^2\ \{\mathrm{diag}\ (R(n-1)^{-1})^m_i\ \delta\underset{\sim}{\zeta}^m_i + B^m_i\ (I^m_i - A^m_i)^{-1}\ \mathrm{diag}\ (R(n-1)^{-1})^m_i\ \underset{\sim}{\zeta}^m_i\ \} +$$

$$+ \omega^4\ B^m_i\ (I^m_i - A^m_i)^{-1}\ \mathrm{diag}\ (R(n-1)^{-1})^m_i\ \delta\underset{\sim}{\zeta}^m_i \quad , \tag{3.1.6ii}$$

where $\delta\underset{\sim}{\zeta}^m_i$ is defined by the representation $\underset{\sim}{\zeta}'^m_i = \underset{\sim}{\zeta}^m_i + \omega^2\ \delta\underset{\sim}{\zeta}^m_i$ according to (2.2.12), for B^m_i see (3.1.3).

Corollary 3.1.4i :

Breaking off of the series (3.1.6i) with the first order term $A^m_i\ \mathrm{diag}\ (R(n-1)^{-1})\ \underset{\sim}{\zeta}'^m_i$ yields for the coordinates of the solutions $\underset{\sim}{a}^m_i$ the representation

$$a^m_n = \frac{R}{n-1}\ \{c'^m_n - (\omega^2/R^3)(\frac{r^m_n}{n-3}\ c'^m_{n-2} + \frac{s^m_n}{n-1}\ c'^m_n + \frac{t^m_n}{n+1}\ c'^m_{n+2}) + \ldots\}\ ,\ n \in n^m_i\ , \tag{3.1.7}$$

where $$r^m_m := r^m_{m+1} := 0 \tag{3.1.7i}$$

for the first coordinates a^m_m or a^m_{m+1} , respectively.

Proof:

Up to (3.1.6i) all is clear because of Lemma 3.1.1, Theorem 3.1.2, Corollary 3.1.2i and Supplement 3.1.2ii.

Substitution of $\underset{\sim}{\zeta}'^m_i = \underset{\sim}{\zeta}^m_i + \omega^2\ \delta\underset{\sim}{\zeta}^m_i$ into (3.1.6i) and rearrangement with respect to the powers $\omega^0 = 1$, ω^2, ω^4 leads straightforward to (3.1.6ii).

Taking into account the structure of A^m_i given in (3.1.2iii) we obtain (3.1.7) and (3.1.7i), q.e.d. .

It is obvious that the first term in (3.1.7)

$$\frac{R}{n-1}\, c'^{m}_{n} = \frac{R}{n-1}\,(c^{m}_{n} + \omega^2\, \delta c^{m}_{n}) \qquad \text{(see (2.2.12))}$$

contains the solution of Stokes $R(n-1)^{-1}c^{m}_{n}$ (see (3.5i)).

Hence, as expected, the solution of the problem under consideration results from Stokes' solution by adding some terms of the order $O(\omega^2)$. More precisely the difference to Stokes' solution is given by (3.1.6ii).

The first term diag $(R(n-1)^{-1})^{m}_{i}\, c^{m}_{i} \equiv$ (3.5ii) represents the solution of Stokes.

In the second term, which is of order $O(\omega^2)$, the first (second) part is due to the change on the left (right) hand side of the boundary operator.

The third term, which is of order $O(\omega^4)$, can be explained by the mutual effect of the changes on the left and right hand side of the boundary operator.

3.2 Solution of the nonregular systems of equations.

In the first row of the corresponding matrices gmR^{-3} is multiplied by $(n-1) = 0$ (see (3.1i)).

3.2.1 A not essentially degenerate system of equations, $m = 1$, $i = 1$:

$$\begin{bmatrix} (0 \cdot \frac{gm}{R^3} + \omega^2 s^1_1) & \omega^2 t^1_1 & 0 & \cdots \\ \omega^2 r^1_3 & (2\frac{gm}{R^3} + \omega^2 s^1_3) & \omega^2 t^1_3 & 0 \;\vdots \\ 0 \;\vdots & \omega^2 r^1_5 & (4\frac{gm}{R^3} + \omega^2 s^1_5) & \omega^2 t^1_5 \\ & 0 \;\vdots & & \end{bmatrix} \cdot \begin{bmatrix} a^1_1 \\ a^1_3 \\ a^1_5 \\ \vdots \end{bmatrix} = \frac{gm}{R^2} \begin{bmatrix} c'^1_1 \\ c'^1_3 \\ c'^1_5 \\ \vdots \end{bmatrix} \qquad (3.2.2)$$

$s_1^1 = -3$, $t_1^1 = 36/7$,

$r_3^1 = 0$, $s_3^1 = -3$, $t_3^1 = 70/11$

Because of $r_3^1 = 0$ the system of equations G_1^1 is (partially) *decomposed* into the first equation with the index $n = 1$

$$\omega^2 s_1^1 a_1^1 + \omega^2 t_1^1 a_3^1 = c'^1_1 \qquad (3.2.3)$$

and into the system of equations $\tilde{G}_1^1$, which in (3.2.2) is located in the lower right corner (dotted lines).

The matrix $\tilde{M}_1^1$ corresponding to $\tilde{G}_1^1$ is again a tridiagonal matrix. Its row indices n are different from 1. Hence in analogy to the matrices treated in chapter 3.1, there exists a splitting $(\tilde{D}_1^1)^{-1} \tilde{M}_1^1 = (\tilde{I}_1^1 - \tilde{A}_1^1)$ with a tridiagonal matrix $\tilde{A}_1^1$. Because the rows of $\tilde{A}_1^1$ also satisfy the estimation (3.1.5ii), lemma 3.1.1 is valid, that is $\tilde{A}_1^1$ is regular. Hence the case $m = 1$, $i = 1$ is reduced to the regular case discussed in chapter 3.1.
It follows from Theorem 3.1.4 and Corollary 3.1.4i, that the system $\tilde{G}_1^1$ has a unique bounded solution, which can be represented by (3.1.6i-ii) or (3.1.7).

If the coordinate a_3^1 is known from the solution $\tilde{a}_1^1$ of $\tilde{G}_1^1$, then a_1^1 is uniquely determined by (3.2.3). Hence G_1^1 has a unique bounded solution $\underset{\sim}{a}_1^1$.

For a_1^1 cannot be chosen just any value in contrast to what is the case in the solution of Stokes' problem. This is caused by the rotational term in the normal potential, by which the boundary operator is no longer *isotropic*.

3.2.2 An essentially degenerate system of equations, $m = 0$, $i = 1$:

$$\left[\begin{array}{c|ccc} (0 \cdot \frac{gm}{R^3} + \omega^2 s_1^0) & \omega^2 t_1^0 & 0 \ \ldots & \\ \hline \omega^2 r_3^0 & (2\frac{gm}{R^3} + \omega^2 s_3^0) & \omega^2 t_3^0 & 0 \ \ldots \\ 0 & \omega^2 r_5^0 & (4\frac{gm}{R^3} + \omega^2 s_5^0) & \omega^2 t_5^0 \\ \vdots & 0 & \ddots & \ddots \\ & \vdots & & \end{array}\right] \cdot \left[\begin{array}{c} a_1^0 \\ \hline a_3^0 \\ a_5^0 \\ \vdots \end{array}\right] = \frac{gm}{R^2} \left[\begin{array}{c} c'^0_1 \\ \hline c'^0_3 \\ c'^0_5 \\ \vdots \end{array}\right] \qquad (3.2.4)$$

$s_1^0 = 0$, $t_1^0 = -\ 18/7$,

$r_3^0 = 0$, $s_3^0 = -\ 8/3$, $t_3^0 = 140/33$

Because the first column of the corresponding matrix M_1^0 is the zero vector, any value can be taken for a_1^0, as in the solution of Stokes' problem. Hence the first column is not essential for the system of equations G_1^0.
The omitting of the first column of M_1^0 leads to the systems of equations

$$\bar{G}_1^0 : \equiv \bar{M}_1^0 \, \underset{\sim}{\bar{a}}_1^0 = \underset{\sim}{\bar{c}}_1^0 \quad , \tag{3.2.5}$$

where in $\underset{\sim}{a}_1^0$ the first coordinate is a_3^0 .
$\bar{M}_1^0$ is a *lower triangle matrix*, so that the following recurrence relation leads to a unique solution of (3.2.5).

$$a_3^0 := \frac{1}{\omega^2 t_1^0} \frac{gm}{R^2} c'^0_1 \ , \quad a_5^0 := \frac{1}{\omega^2 t_3^0} \{\frac{gm}{R^2} c'^0_3 - (2\frac{gm}{R^3} + \omega^2 s_3^0)\, a_3^0\},$$

$$a_{n+2}^0 := \frac{1}{\omega^2 t_n^0} \{\frac{gm}{R^2} c'^0_n - \omega^2 r_n^0 \, a_{n-2}^0 - ((n-1)\frac{gm}{R^3} + \omega^2 s_n^0)\, a_n^0\} \ . \tag{3.2.6}$$

However without an additional condition for c'^0_1 the solution (3.2.6) is not usable, because for any c'^0_1 the solution (3.2.6) is in general not bounded, that is, it cannot lead to a convergent series for $\delta\omega$. The unique bounded solution of G_1^0 is obtained, if c'^0_1 satisfies a certain condition.

Lemma 3.2.1 :

Let $\tilde{G}_1^0$ be the system of equations that is obtained from $\bar{G}_1^0$ by omitting the first equation (in (3.2.4) in the lower right corner given by the dotted lines).
A solution $\underset{\sim}{\bar{a}}_1^0$ of $\bar{G}_1^0$ is bounded if and only if c'^0_1 or c_1^0, respectively, satisfies the condition

$$c'^0_1 = \omega^2 t_1^0 \, a_3^0 \quad . \tag{3.2.7}$$

Then $\bar{a}_1^0$ is equal to the unique bounded solution $\tilde{a}_1^0$ of $\tilde{G}_1^0$, which is determined by (3.1.6i-ii), (3.1.7) or the recurrence relation (3.2.6).

a_3^0 in (3.2.7) is the first coordinate of $\tilde{a}_1^0$ and it can be represented according to (3.1.7) by

$$a_3^0 = \frac{R}{2}\{c'^0_3 - (\omega^2/\frac{gm}{R^3})(\frac{s_3^0}{2}c'^0_3 + \frac{t_3^0}{4}c'^0_5) + \ldots\} \quad . \tag{3.2.8}$$

Proof:

Let the system $\bar{G}_1^0$ be separated into the first equation

$$\omega^2 t_1^0 a_3^0 = c'^0_1 \tag{3.2.9}$$

and into the system $\tilde{G}_1^0$.

The matrix $\tilde{M}_1^0$, corresponding to $\tilde{G}_1^0$, is exactly as the matrices M_i^m, treated in chapter 3.1, a tridiagonal matrix with row indices different from 1. Hence a splitting $(\tilde{D}_1^0)^{-1}\tilde{M}_1^0 = (\tilde{I}_1^0 - \tilde{A}_1^0)$ exists with a tridiagonal matrix $\tilde{A}_1^0$, which is regular, because its rows satisfy the estimation (3.1.5ii), so that Lemma 3.1.1 is valid. It follows from Theorem 3.1.4 and Corollary 3.1.4i that exactly one bounded solution $\tilde{\underset{\sim}{a}}_1^0$ of $\tilde{G}_1^0$ exists, which can be represented by (3.1.6i-ii) or (3.1.7).

Now let $\bar{\underset{\sim}{a}}_1^0$ be a bounded solution of $\bar{G}_1^0$. $\bar{\underset{\sim}{a}}_1^0$ is also a bounded solution of $\tilde{G}_1^0$, which is unique according to the preceding statements. This means that the coordinate a_3^0 is already uniquely determined by the system $\tilde{G}_1^0$. According to (3.1.7) we have (3.2.8) for a_3^0.
But a_3^0 must also satisfy equation (3.2.9). Substituting (3.2.8) for a_3^0 into (3.2.9) yields condition (3.2.7).

Conversely, let $\bar{\underset{\sim}{a}}_1^0$ be a solution of $\bar{G}_1^0$ for a c'^0_1, which satisfies condition (3.2.7).
This solution must satisfy the recurrence relation (3.2.6), which leads to a unique solution, so that $\bar{\underset{\sim}{a}}_1^0$ is uniquely determined. Therefore $\bar{\underset{\sim}{a}}_1^0$ must coincide with the unique bounded solution (which necessarily satisfies condition (3.2.7)), q.e.d. .

Solutions $\bar{\underset{\sim}{a}}_1^0$ of $\bar{G}_1^0$ from another c'^0_1, which does not satisfy condition (3.2.7), cannot be bounded, because the bounded solution of $\bar{G}_1^0$ is unique, as is proved in Lemma 3.2.1. These solutions are of no significance, because they cannot lead to converging series for the disturbing potential $\delta\omega$.

For the coordinates b_n^m corresponding to the basis functions $P_n^m \sin m\lambda$ the same statements as for the a_n^m are obtained, because the equations (3.2i-ii) to determine the b_n^m are mathematically the same as the equations (3.1i-ii) to determine the a_n^m. In the preceding only the letter ' a ' must be replaced by the letter ' b ' and the letter ' c ' by ' d '.

Literature

Arnold, K. : Die Eindeutigkeit des Randwertproblems der physikalischen Geodäsie. Vermessungstechnik, Berlin 28 (1980)2, S. 44 - 46

Collatz, L. : Funktionalanalysis und Numerische Mathematik. Springer, Berlin, 1964

Gradshteyn, I.S., Ryzhik, I.M. : Table of Integrals, Series and Products. Academie Press, 1965

Grafarend, E. and W. Niemeier : The free, nonlinear boundary value problem of physical geodesy. Bulletin Geodesique 101 (1971) 243 - 262

Heiskanen, W.A., Moritz, H. : Physical Geodesy. Freeman, San Francisco, 1967 (Reprint, Technical University Graz, Austria, 1979)

Hobson, E.W. : The Theory of Spherical and Ellipsoidal Harmonics. Second Reprint of the edition 1931 (Cambridge University Press), Chelsea Publ. Co., 1965

Kertz, W. : Potentialtheorie in der Geophysik. Skriptum, Technische Universität Braunschweig, 1973

Lebedev, N.N. : Spezielle Funktionen und ihre Anwendung. B.I.-Wissenschaftsverlag, Mannheim, 1973

Moritz, H. : Recent Developments in the Geodetic Boundary-Value-Problem. Reports of the Department of Geodetic Science, No. 266, Ohio State University, Columbus, Ohio, 1977

Sanso, F. : The geodetic boundary value problem in gravity space.
Atti della Accademia Nazionale dei Lincei, Serie VIII, vol. XIV, fasc. 3, Roma (1977) 39 - 97

Sanso, F. : The local solvability of Molodensky's problem in gravity space.
manuscripta geodaetica 3 (1978) 157 - 227

Wigner, E. : Gruppentheorie und ihre Anwendung auf die Quantenmechanik der Atomspektren.
Nachdruck der Ausgabe Braunschweig 1931, Vieweg, Braunschweig 1977

Winch, D.E., James, R.W. : Computations with Spherical Harmonics and Fourier Series in Geomagnetism.
Methods in Computational Physics, Vol. 13, Academic Press, 1973

Summary

The linearized boundary operator of the geodetic boundary value Problem is derived for a normal potential including a term of the centrifugal potential. The linearized boundary operator is rigorously computed leading beside a derivative with respect to the spherical coordinate radius r to an additional derivative with respect to the spherical coardinate latitude φ. The linearized geodetic boundary value problem is rigorously solved by the Hilbert space method, e.g. a spherical harmonic representation of the unknown disturbing potential and the known gravity anomaly! A base representation of the infinite dimensional system of equations is achieved by using recurrence relations of spherical harmonics and Wigner 3j-coefficients. The solution of the system of equations is constructed by a Neumann series whose convergency is proved by a theorem of the mathematical fix point theory. It becomes obvious that the solution can be represented by a generalized Stokes function which beside the spherical distance depends upon the azimuth of a great circle connecting two points projected onto the unit sphere.

Ju.D.Boulanger [1)]

SOME RESULTS OF MEASUREMENTS OF NON-TIDAL GRAVITY CHANGES

In the USSR, first researches on secular cr, in other terms, non-tidal gravity changes commenced in 1935. They were stimulated a great deal by large discrepancy (of several tens of mgal) in repeated gravity measurements within the Caucasus and Middle Asia [1].

With this purpose, Drs. Boulanger and Pariisky performed repeated pendular measurements within the Central Caucasus. As a result of the analysis made by Dr. Pariisky [2] it was deduced that great gravity changes result from accumulation of measurement errors. In case we do assume gravity variations in time, they cannot exceed several tenths of mgal per year.

The pendulum installation, which existed at the time, did not have sufficient accuracy capable of registering gravity variations of such value. There arises, therefore, a necessity to work out new means of measurement and techniques which could allow to raise the acouracy of gravity definition. The Second World War interfered with this work and interrupted it for a long time. Only in the fifties it became possible to resume this research. By that time, there was constructed a highly accurate wide-range gravimeter "GAE-3" and, a bit later, - "GAG-2".

Many times repeated gravimetric connections between Moscow and Potsdam and repeated measurements performed through Potsdam-Riga-Moscow-Kazan-Sverdlovsk-Chita-Takhtamygda-Petropavlovsk Kamchatsky and also through Tbilissi-Ashkhabad-Balkhash-Alma-Ata -Dushanbe show that the obtained gravity variations are much less than the errors of their definition and do not exceed ± 0.02 mgal per year [3].

1) Inst. Fiziki Zemli AN SSSR, Moskva, Bolschaja Grusinskaja 10

Later, repeated measurements made in 1968 and 1974 by International Gravimetric Expedition, sponsored by KAPG (Commission set up by the Academies of Socialist countries on "Planetary Geophysical Research program) and the geodetic services of Socialist countries show that non-tidal gravity changes at sites Tallin, Vilnius, Warsaw, Krakow, Prague, Budapest, Bucharest and Sofia are insignificant relative to Potsdam and cannot exceed 2-3 μgal per year [5].

World literature has many examples of significant gravity changes revealed by repeated measurements. Lack of sufficient metrological facilities for these measurements in the majority of cases does not allow to compare the results of these measurements. At the same time, many authors regard these discrepancies as related to the changes of the Earth's gravity field. Such experimental measurements of gravity field changes in time often differ by two orders or more.

Theoretical estimations of possible gravity changes, based on comparison of various Earth models and on the influence on them of endogenic and exogenic effects, also differ by several orders.

Thus, the problem of variability in time of the Earth's gravity field is considerably complex. Its solution, no doubt, has great significance for the whole complex of geosciences and for many other branches of it: physics, metrology, geodesy, astronomy, etc. Therefore, each new result showing gravity changes in time should be carefully analysed. Besides, it should be noted that up to the most recent time all measurements of gravity changes have been performed by relative methods which principally could not reveal <u>global</u> changes.

At the end of the sixties, in the field of instrumental gravimetry great progress was achieved. New instruments were constructed-absolute ballistic gravimetres which have greater accuracy of measurements than the relative instruments. Professor Sakuma (Sèvres, France) constructed the stationary absolute gravimeter, Professor Faller (USA) - portable absolute gravimeter. The analogue instrument was created in the USSR in the Institute of Automatics and Electrometry of the Siberian Department, USSR Academy of Sciences. A bit later, a portable instrument was built in Italy.

The Faller and Sakuma instruments were used to establish a reference mark and scale of the new International Gravimetric Standardisation Net in 1971 (IGSN-71) [4]. From 1967 to 1973, the Sakuma instrument was used to perform systematic measurements of absolute gravity changes in Sèvres.

The Soviet absolute gravimeter called GABL (absolute ballistic laser gravimeter) was first used in research in 1972. Later, the instrument was modernized and, at present, it is possible to take measurements of gravity with the accuracy of about $\pm 6\text{-}8 \times 10^{-9}$ g [6].

GABL instrument was utilized to perform numerous repeated measurements of gravity in Novosibirsk, at the International gravimetric site Ledovo (Moscow) and in Potsdam, in 1976 and 1978. In 1977, in Sèvres, GABL was calibrated with the Italian instrument and the instrument of Dr. Sakuma.

Table 1 presents comparison of gravity measurements at sites of IGSN-71 which were obtained in 1969-1970 during the construction of this system with gravity measurements performed by GABL in 1976-1978. These results show that for this period gravity has increased, in average, at 45 ± 2.7 μgal at all four sites:

Sèvres, Potsdam, Ledovo, and Helsinki. It is remarkable that all obtained results are in good agreement.

These changes first of all could be the result of the shift of the IGSN-71 reference mark or, secondly, of real gravity changes at these sites. The most probable is the first cause. Data by Prof. Sakuma show that in Sèvres, during the construction of the IGSN-71 (1969), the gravity value was minimal. In 1972 it increased by 45 μgal. Later on, there were no considerable gravity changes. During the construction of IGSN-71 g value in Sèvres acquired great significance and the value obtained in 1969 was in fact considered as the reference mark, which caused lower gravity value at sites of IGSN-71.

The reason for gravity changes in Sèvres is not established. It can be of global scale, of regional or of local one. In any case, however, the increase in gravity in Sèvres by $+54\pm14$ μgal for 1969-1977 [5] is apparent.

Fig. 1 shows results of repeated gravity measurements performed by GABL at sites: Novosibirsk, Ledovo and Potsdam. For better clarity all results are adjusted to Ledovo. The scheme indicates that for 1973-1978 practically the same gravity changes were recorded at all three sites. In Moscow, the rate was $9.1\pm$ ±2.0 μgal/year, in Novosibirsk - 10.7 ± 0.9 μgal/year, and in Potsdam - 9.9 ± 9.1 μgal/year. In total, measurements show that this reduction had the rate of 9.9 ± 1.3 μgal/year.

In the first approximation, these changes could be considered as quasi-periodical with the 5-year period and 20 μgal amplitude. Reliability of these measurements is supported statistically. If we consider the totality of changes as random distribution of errors, the error for weight unit will be ±11.7 μgal. This error will be less by half, i.e. ±5.7 μgal, if it is calculated by

diverge from the approximated curve. Such reduction of the error cannot be attributed to random distribution of errors.

Similar tendency was registered by Prof. Sakuma in Sèvres during 1967-1973. There were recorded the quasi-periodical gravity changes with about the same period but rather greater amplitude - about 25 μgal. It was considered as a local phenomenon. Observations of gravity changes taken by us were performed along the line over 5000 km. It allows, for the first time, to conclude on global character of the observed gravity changes or, at least, consider this phenomenon covering the significant part of Eurasia.

It is obvious, that performed observations are not sufficient either to define the period or the amplitude of the revealed phenomenon. Thus, in future it is necessary to continue measurements at the old sites and to add at least two new sites located east of Novosibirsk: within the Baikal rift and in Kamchatka. It is necessary to define the latitudinal effect of these changes. For this purpose observations should be made at considerably different latitudes.

In conclusion, the author expresses his gratitude to all the participants of the work with the absolute gravimeter: to Drs. Arnautov, Scheglov, Kalish, Stus, and Tarasjuk, without whose assistance the results described in the paper could not be obtained.

J.D.Boulanger

Moscow, April, 1980

Table 1

Comparison of new absolute gravity measurements*/ with IGSN-71 results.

NN	Site	g in IGSN-71	Type of measurements	g new results	Discrepancy
		μgal		μgal	μgal
1.	Potsdam S-13	981 261 371 ± 17	transmission from Ledovo by relative methods	981 261 421±12	+50 ± 21
2.	Potsdam S-13	981 261 371 ± 17	by GABL instrument	981 261 416±9	+45 ± 19
3.	Helsinki	981 900 590 ± 19	transmission from Potsdam by relative methods	981 900 632 ± 20	+42 ± 28
4.	Sèvres A_3	980 925 880 ± 14	by GABL instrument	980 925 929±16	+49 ± 21
				Average:	+46 ± 1.8

*/ Corrected according to results of the third g measurement in Potsdam (September, 1980).

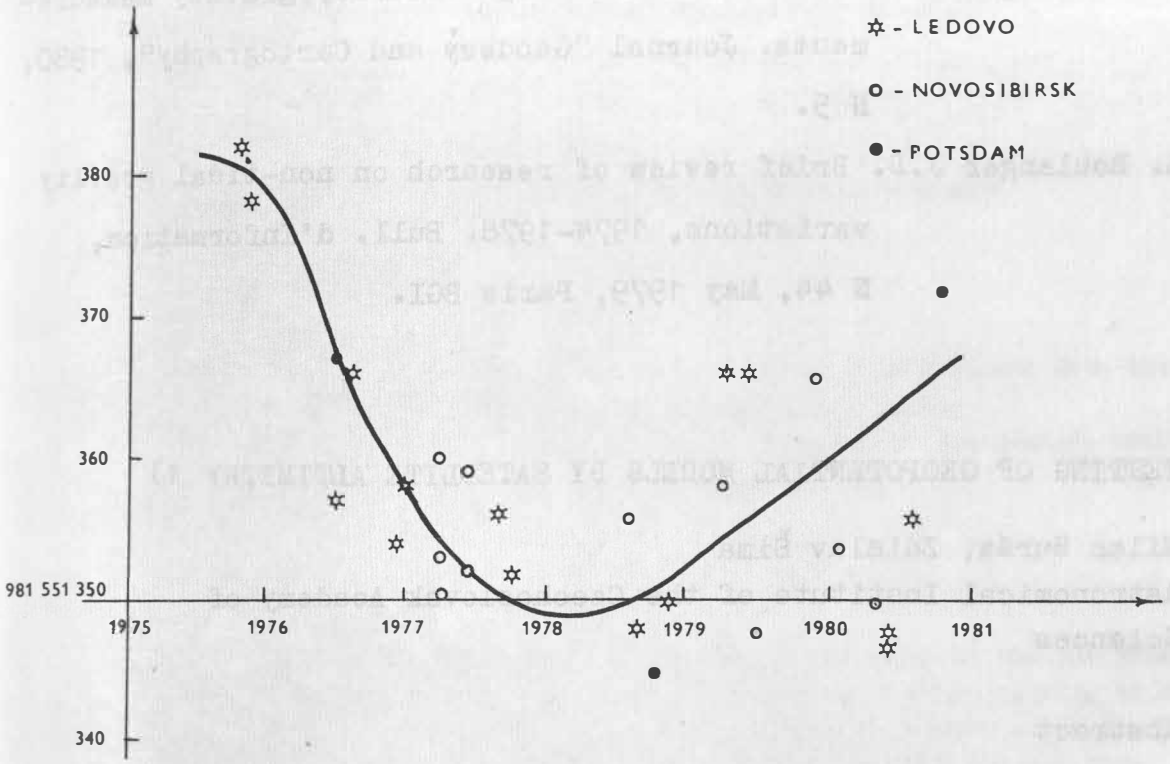

References

1. Abakelia M.S. On gravity changes in time as the result of geotectonic movements in the Caucasus. Problems of Soviet Geology, VI, N 2, 1936.

2. Pariisky N.N. Investigation of gravity changes in time in the Caucasus. International Geological Congress, XVII Session. Abstracts of Reports. M.-L.,1937, p. 189-190.

3. Boulanger J.D. Secular gravity changes. Physics of the Earth, N 10, 1974, p.25-32.

4. Morelli C., Gantar C., Honkasalo T., McConnel R., et al. The International gravity standardisation net 1971, International Association of Geodesy, Paris, Special Publication 4.

5. Boulanger J.D. Some results on high-accuracy gravity measurements. Journal "Geodesy and Cartography", 1980, N 5.

6. Boulanger J.D. Brief review of research on non-tidal gravity variations, 1974-1978. Bull. d'Information, N 44, May 1979, Paris BGI.

TESTING OF GEOPOTENTIAL MODELS BY SATELLITE ALTIMETRY [1)]

Milan Burša, Zdislav Šima
Astronomical Institute of the Czechoslovak Academy of Sciences

Abstract

An attempt has been made for testing geopotential models SE II, SE III, SE IV.3, SE V, GEM 6, GEM 7, GEM 8, GEM 10B, GRIM 2 using new altimetry data (Rapp 1979, OSU rep. No. 285). On the basis of the altimetry geoid heights, an assumed geocentric ellipsoid and the tested model the geopotential, scale factor $R_o = GM/W_o$ has been calculated for each $\sim 5^o$ x 5^o block. Assuming errors in the altimetry data as negligible, the scatter of values R_o is due only to errors of geopoential models. In this case the standard deviation in R_o (for $\sim 5^o$ x 5^o block) indicates the tested model accuracy as a whole. The possibility of detecting the differences in the mean sea-level heights on the basis of satellite altimetry has been discussed.

---

1) Erschienen in: Bull. Astron. Inst. Czechosl. 32(1981)2, S. 65 - 67

Laser Satellite Ranging Using the Automated SBG Camera

by

Harald Fischer[1], Reinhart Neubert[1] and Ludwig Grunwaldt[1]

Abstract

Daylight and Earth shadow laser ranging of satellites has been obtained with the aid of a computer controlled step motor drive for the Potsdam SBG-Camera.
SAO orbital elements are used as input information for the controlling desktop computer. No detailed predictions from a large computer are necessary.

1. Introduction

The Potsdam Laser Ranging Station has been operating since 1974. At the 3rd Symposium in Weimar 1976 we reported on first experiments to change from visual tracking to absolute pointing. After having checked that the mechanical stability of the SBG mount is sufficient for that purpose, an automatic tracking system was constructed and put into experimental operation in 1978. Punched tape input was used at first converting later to on-line computer control. The purpose of this paper is to summarize the present state of the equipment, associated software and experience obtained.

2. Description of the Equipment

2.1. Mount and Optical System

The Potsdam laser ranging system uses a modified SBG camera mount. The 4 axis mount of this camera is used even in the automatic tracking mode which simplifies the mount control because only small accelerations of the drives are necessary. Step motors are used as drives at the 3rd and 4th axis and in addition the axes are equipped with digital encoders. These encoders are used only for presetting the mount and for calibration measurements (star observations). During the pass no back information is sent from the encoders to the computer. The mount is preset before each pass in such a way, that the 3rd axis drive acts approximately along track, with small cross track corrections

1 Akademie der Wissenschaften der DDR, Zentralinstitut für Physik der Erde, DDR - 1500 Potsdam, Telegrafenberg A 17

applied by the 4th axis drive.

The precise presetting of the mount bears some problems, however, which could be solved with the help of additional inclination measuring equipment and taking into account the bending of the 3rd, i. e. the main tracking axis. Frequent checks of the mount base orientation are necessary using observations of the polar star.

The transmitter is a two-stage passive Q-switched ruby laser giving approx. 20 ns duration pulses at a rate of 10 pulses per minute in normal mode.

Table 1. Main Technical Data

Laser	
Type:	Ruby
Pulse Energy:	1 J
Pulse Duration:	20 ns
Repetition Rate:	10 per min.
Mount:	
Type:	4-Axis
Tracking Mode:	Automatic, Step Motors
Tracking Accuracy:	1 min of arc
Epoch Counter Resolution:	10 microsec
Range Counter Resolution:	0.1 nanosec
Range Noise:	0.4...1.5 m
Ranging Capabilities:	All Laser Satellites

The receiver system, placed near the cassegrainian focus of the main telescope, now uses a gated RCA 31034 A photomultiplier with high quantum efficiency at ruby laser wavelength.

To gate the PMT, total voltage is switched from half the end value to full voltage immediately before the expected arrival of the echo signal.

By help of a dichroic mirror, the receiver telescope may be used as a guide in the case of weak satellites, which has proved to be very helpful for the aquisition of STARLETTE and LAGEOS and in some cases for GEOS A, too.

2.2 Ranging and Control Electronics

A simplified block scheme of the electronical system is given in Fig. 1.

In comparison to the earlier configuration /1/, /2/, the automatic control block and the computer have been added and the counters for epoch and range have been replaced by instruments with higher resolution (10 μs and 0.1 ns, respectively).

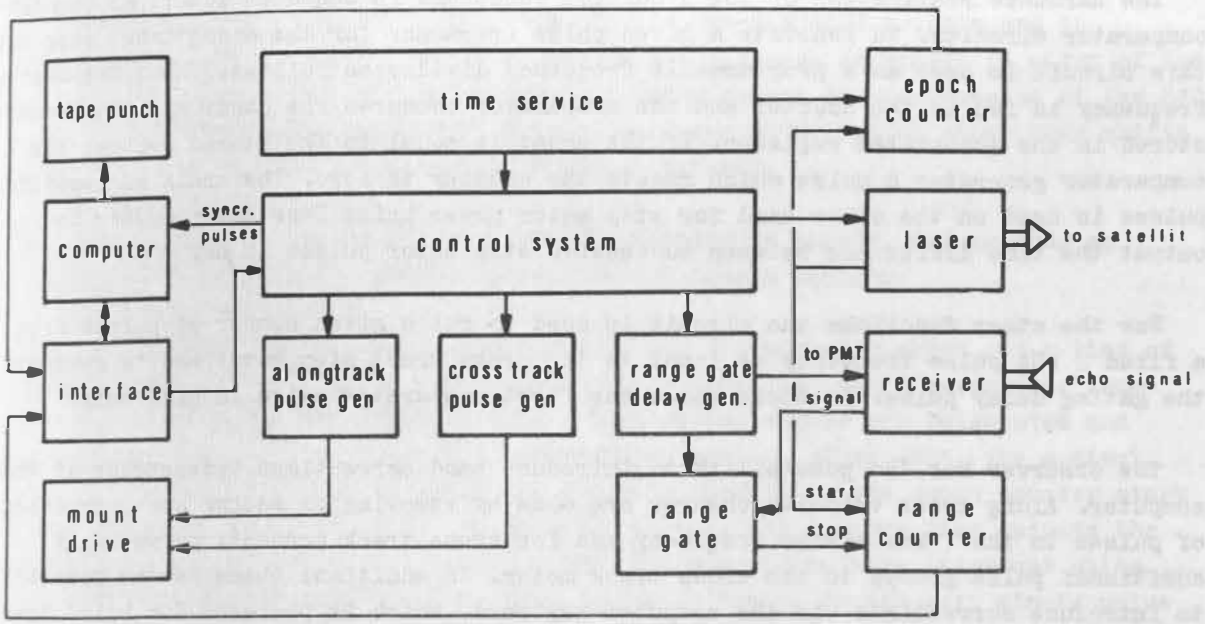

Fig. 1. Simplified Block Scheme of the Laser Ranging System

Central part is the HP 9825 desktop computer interfaced via the bus system to the control block, epoch counter, range counter and to a tape punch for output of the results.

For timing, we take advantage of the cèsium clock-based time service located at our institute. Via cable we receive a 1 MHz reference frequency and in addition pulses for marking each minute and second. So the mount control and epoch counter are easily synchronized to UTC. Only for the range counter the internal reference generator is used. During a pass, the computer is forced by interrupt pulses each 2nd second to calculate and output a control information. These numbers represent the angular velocity along track, the cross track angular correction and the expected range. After these 3 values are output, a new cycle starts. The control unit has built in registers and accepts the information, calculated before by the computer, in an exact 2 sec sequence. After acception, the new value is valid for control. So any change in computing time has no influence.

Immediately after acception of the expected ranges, that means each 6th second, the laser is fired and measurement starts. A small part of the laser power is led to a photodiode which generates start pulses. These start pulses trigger the epoch counter to output the epoch, start the range counter and the digital gate time generator. The latter generates delayed pulses according to the predicted range which are used to switch on the PMT power supply and 225 µs later to open the range gate for the signal pulses.

The hardware realization of the 3 control functions is based on identical counter-comparator circuits. To generate a given pulse frequency for the along track step motor, this circuit is used as a programmable frequency divider as follows. The 1 MHz master frequency is fed to the counter and the comparator compares the count with the number stored in the associated register. If the count is equal to the stored number, the comparator generates a pulse which resets the counter to zero. The train of resetting pulses is used on the other hand for step motor power unit. Thus the computer has to output the time difference between successive step motor pulses in μs.

For the other functions the circuit is used to cut a given number of pulses from a fixed 2 kHz pulse frequency as input to the cross track step motor, and to generate the gating delay pulse. In these cases the first comparator pulse is used only.

The observer has the possibility to introduce hand corrections independent of the computer. Along track velocity changes are made by removing or adding some percentage of pulses to the 1 MHz master frequency, and for cross track corrections we apply additional pulse groups to the cross track motor. In addition, there is the possibility to introduce corrections via the computer keyboard, which is prefered for blind tracking. Only time shift corrections are used at present.

3. Software and Operating Procedure

The system software may be divided into three parts: the prediction and real time control system, the reduction and analysis system and some auxiliary programs. All subroutines for the first part are present in parallel in the memory to simplify the use by the observer. The HP 9825 desktop computer has proved to be very well suited for our purpose, because all necessary subroutines may be called simply via special function keys and time corrections may be input during program execution via the keyboard without complications. The measurements are recorded after the satellite pass on the second track of the same tape cartridge which contains the program. This cartridge also contains a library of SAO orbital elements.

The analysis program system is used to compare the measurements with updated predictions to reduce instrumental influences and to do some filtering. The reduced measurements are collected on a separate cartridge.

Auxiliary programs are available for data handling and formatting and for mount orientation calculation from polar star observation.

3.1. Prediction and Control System

Main parts of the software are subroutines for satellite orbit prediction based on SAO orbital elements. We use the polynomial terms, the most important long periodic perturbation terms and in addition short periodic perturbation terms according to J_2. Neglecting short periodic perturbations according to tesseral harmonics and to lunar

interaction, we have some loss in accuracy but a strong simplification of the program. From comparisions to calculations using the well known AIMLASER program and to measurements we found, that the contribution of the tesseral harmonics is often of the same order of magnitude or even lower than the error caused by inaccuracies of the SAO elements itself. The latter is especially the case for GEOS C which shows time shifts of up to 1 sec 10 days after the reference epoch already.

The time required to calculate a satellite position is approx. 0.7 seconds so that computing time is not a great problem for the simple program.

At first the observer has the possibility to let the computer print out a list of culmination times of the useful passes for a given satellite and time period. Immediately before the selected pass, the mount orientation angles are calculated and printed out including corrections for instrumental errors. After that, the control program may be started. Input information for this program is the epoch counter start time and the wanted receiver gate time (usally 50 µs). The program then outputs the first angular velocity value and waits for the first synchronizing interrupt pulse. The interrupt pulses are blocked by a gate, which is opened by the next minute pulse from the time base after pressing the start key. The computer delivers at first only velocity information raising up the velocity step by step in such a way, that the satellite velocity is reached when it passes the center of the field of view. After that, the program calls each 6th second the satellite position routine "SAPOS" and outputs cyclic the three necessary components as described earlier. No precalculation of satellite positions and associated interpolation are used. After the "SAPOS" call and output of the new velocity to the interface there is sufficient time to read the last measurement. This measurement is then compared with the prediction and an acoustic signal is generated by the computer if the deviation is smaller than 1 km indicating an echo signal.
After each pass a set of usually 10 target calibration measurements is taken and the average is included together with meteorological data in the data set recorded on magnetic tape.

3.2. Data Analysis

The data analysis program reads the measurements from magnetic tape and compares them to predictions. Some time shift may be input for improved matching. There is a subroutine to calculate this time shift in such a way, that the difference between predicted and measured range becomes equal for two selected points. Using the so determined time shift the range deviations are usually well below 1 km. The operator may input a limit to the computer so that points, the deviation of which exceeds the limit, are automatically omitted. During the process of comparison the calibration correction and mount centering correction are carried out. The atmospheric refraction is not corrected according to international practice, but the zenith distance angle of each point is calculated from matched predictions and included in the data set for later use.

To detect very small errors and to check the range noise level, the operator may call a polynomial subroutine to fit the differences between predicted and measured range. The polynomial degree should be chosen as low as possible. The computer prints out the residuals of the polynomial fit, the rms error and an optional histogram of the residuals. From this information "runaway" points or possible instrumental errors, for instance missing bits in the measured data, are easily found. Points with residuals greater than three times the standard deviation are usually omitted. After completion of data inspection the reduced set is stored on a separate tape cartridge. The procedure of data analysis takes a few minutes. So the observer may quickly check the data quality between observations. In addition, he may easily calculate time corrections to be used for the next passes.

3.3. Auxiliary Programs

To take advantage of the dialogue capability of the desktop computer, we installed further programs. Among this is a program for the determination of the mount orientation bias angles from polar star observations. Main part of this program is a subroutine for the calculation of the apparent place at given MJD (precession, nutation, aberration). If completed with a catalogue of well distributed stars on tape, this program may be used in future for a more refined mount orientation method.

A second group which is not complete yet, is for management of the growing number of measurements. Among these there is a program for transfer of the data into special formates.

4. Results

After introduction of the new control system the tracking has become more reliable and the amount of measurements could be increased. This is the case especially for STARLETTE and LAGEOS. The results obtained using the new configuration are summarized in table 2. The hardware changes were introduced step by step during the whole period

Table 2. Ranging Results
(Given numbers are number of passes and, in brackets, number of points)

Period	GEOS A	GEOS C	STARL.	LAGEOS	Sum
Sept.-Dec. 78	25(689)	12(181)	12(209)		49(1079)
Febr.-Mar. 79	3(81)	3(50)	2(82)	2(50)	10(263)
Apr.-June 79	38(1250)	44(1486)	3(47)		85(2783)
Sept.-Oct. 79	33(1500)	14(490)	4(73)	10(385)	61(2448)
Mar.-Apr. 80	12(553)	9(296)	5(87)	4(118)	30(1054)
Sum	111(4073)	82(2503)	26(498)	16(553)	235(7627)

and therefore the output was limited somewhat by instrumental difficulties.

Whereas the majority of passes is observed catching the satellite visually at the beginning of the observation, some passes using fully blind tracking (Earth shadow, daylight) have been obtained for all satellites except for LAGEOS. We did not try to observe LAGEOS at daytime yet because of the very high noise background at single photoelectron level. For the other satellites we reduce the PMT voltage to prevent damage of the sensitive GaAs-photocathode.

Improving the optical background suppression we hope to be able to observe LAGEOS under twilight conditions in future.

As an example that the system may detect echo signals out of very strong background noise we show in Fig. 2 the analysis of a LAGEOS measurement taken at a very

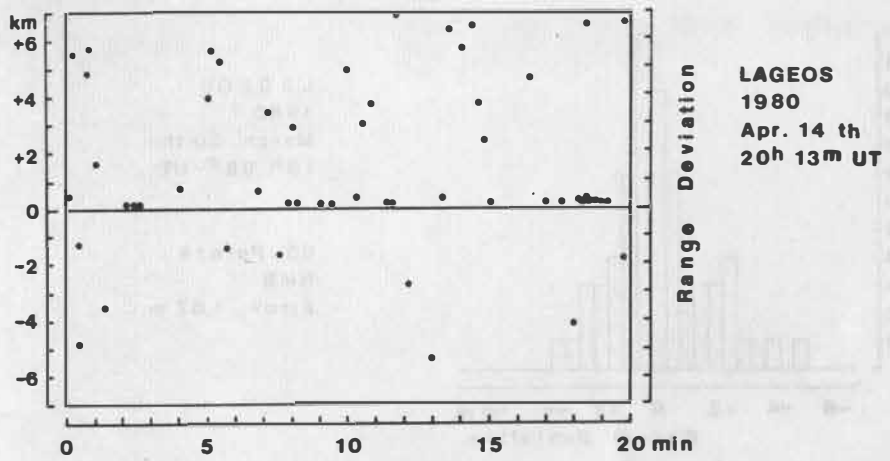

Fig. 2. Range - Time - Diagram

low detection threshold. In Fig. 2 the differences between predicted and measured range are plotted in dependence of time. In Fig. 3 the corresponding histogram is given. It

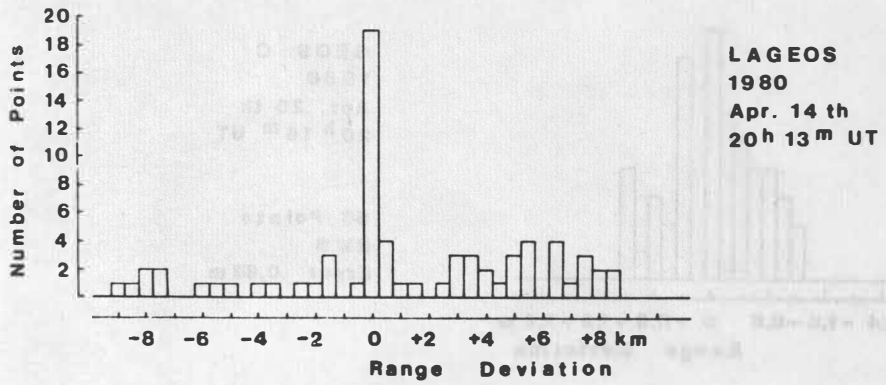

Fig. 3. Histogram of Range Deviations

clearly shows the signal peak at small deviations. The detection conditions in this case are not far from the moon ranging, but usually (at night) we work under conditions of much lower background noise and stronger signals giving about 30 % detection probability for LAGEOS. The typical rms value of the range scattering is for LAGEOS about 1.5 m according to the laser pulse width of 20 ns. As an example the distribution of range residuals were plotted in Fig. 4 for a LAGEOS pass with 63 signal points.

For strong signals we have a somewhat lower range noise between 0.4 und 1.0 m rms for GEOS satellites and STARLETTE. In Fig. 5 the distribution for a GEOS C pass with 56 points is given. No points have been removed in both cases. In the last example the rms noise may be somewhat overestimated because of unsufficient fitting of the polynomial. The lowest range noise (0.1...0.5 m rms) has been observed for calibration target measurements. This would have been expected because of the lower signal fluctuations from the terrestrial target in comparison to satellite signals.

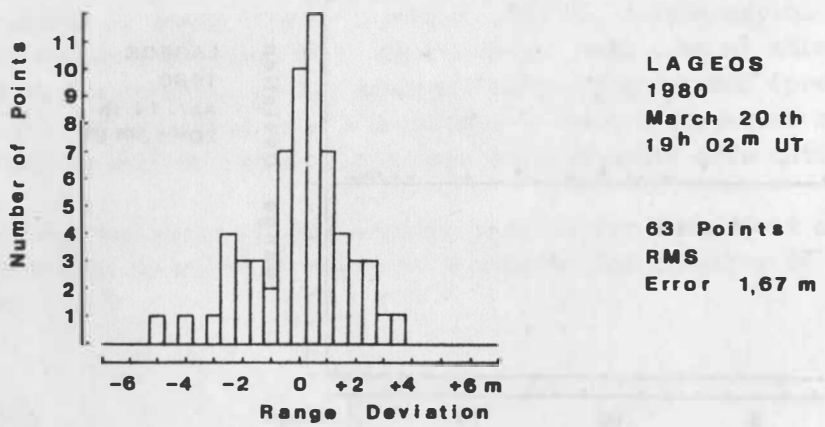

Fig. 4. Histogram of Range Resdiduals

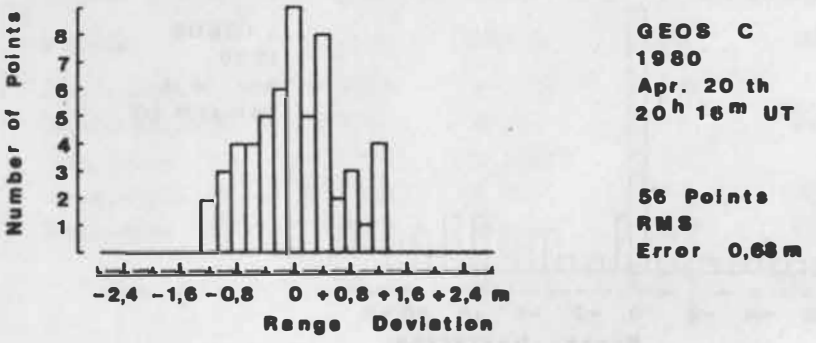

Fig. 5. Histogram of Range Residuals

Acknowledgements

The authors are indebted to Dipl.-Ing. Ch. Selke for expert help with electronics and construction of the interface.

Further we thank I. Prochazka (Technical University Prague) for supplying AIMLASER predictions using the Delft version, made available by Dr. K.F. Wakker (Delft University of Technology).

References

/1/ Fischer, H.; Neubert, R. : Veröffentl. des Zentralinst. für Physik der Erde Nr. 40, Potsdam 1976, S. 77-95

/2/ Neubert, R.; Fischer, H.: Proceedings, 3rd Intern. Symp. Geodesy and Physics of the Earth, Weimar 1976, Part 3, p. 795-801

GEODÄTISCHE DATUMTRANSFORMATIONEN

E. W. Grafarend, Stuttgart, E. H. Knickmeyer, Stuttgart,
B. Schaffrin, Bonn

Summary:

A systematic approach of geodetic datum transformations including geometric and physical terms and refering to a linear Gauß - Markov model is presented. Observational equations can be characterized by a typical rank deficiency with respect to injectivity which can be excluded by a sufficient number of constraints. Reference is made to the geometry of null space of the observational equations (functionals). Two examples prove the power of the method:
(i) adjustment of a distance network in geometry space;
(ii) adjustment of observational functionals in geometry and gravity space (physical geodesy).

Zusammenfassung:

Geodätische Datumtransformationen werden in systematischer Weise für ein lineares Gauß - Markov Modell vorgestellt, welches sowohl geometrische als auch physikalische Parameter im Unbekanntenvektor umfaßt. Der injektive Rangdefekt (Spaltendefekt) der Designmatrix erster Ordnung in den Beobachtungsgleichungen steuert das Datumproblem und die Anzahl der Bedingungsgleichungen, die zu einer Inversion eines Normalgleichungssystems notwendig sind. Die Rolle des Nullraumes der Beobachtungsgleichungen (Funktionale) wird herausgearbeitet. Zwei Beispiele belegen die Kraft des hier präsentierten Konzeptes der Datumtransformationen:
(i) Ausgleichung eines Streckennetzes im Geometrieraum
(ii) Ausgleichung von Beobachtungsfunktionalen im Geometrie- und Schwereraum (physikalische Geodäsie)

0. Einleitung

Um aus geodätischen Beobachtungen Koordinaten ableiten zu können, bedarf es der Festlegung eines Bezugssystems, speziell eines Datums. Den verschiedenen geodätischen Aufgabenstellungen angepaßt, gibt es nicht nur eine Wahl eines Datums, sondern eine Folge von verschiedenartigen Festsetzungen, beispielsweise im lokalen, regionalen, kontinentalen und interkontinentalen oder globalen Bereich. Vor allem in der Navigation und geometrischen Geodäsie begegnet man deshalb der Aufgabe, Koordinaten von einem Bezugssystem in ein anderes umrechnen zu müssen. Wir nennen hier nur die Arbeiten von S.Heitz (1969), E.J. Krakiwski und D. B. Thompson (1974), C. L. Merry und P. Vanicek (1974), R. Sigl (1978) und W. Torge (1980). Aufgabe unserer nachfolgenden Untersuchungen ist es deshalb, eine Systematik von Datumtransformationen allgemeiner Art zu entwickeln. Als steuerndes Element einer Datumtransformation wird sich der injektive Rangdefekt (Spaltendefekt) der Koeffizientenmatrix eines linearen Modells der Beobachtungsgleichungen und das zugeordnete System von Bedingungsgleichungen erweisen, welches das lineare Modell invertierbar macht.

Im ersten Abschnitt über Datumtransformationen innerhalb eines linearen Ausgleichungsmodells mit injektivem und surjektivem Rangdefekt geben wir zunächst die zwei entscheidenden Eigenschaften eines Systems von Bedingungsgleichungen an, die zur Behebung eines Datumdefektes erfüllt sein müssen: Unabhängigkeit der Bedingungsgleichungen, Unabhängigkeit der Spaltenräume von A' und B', den transponierten Matrizen des Designs erster Ordnung (Konfiguration) und nullter Ordnung (Datum). Die Lösungstheorie spaltendefekter Gleichungssysteme mit dem Hilfsmittel von Bedingungsgleichungen wird anschließend in den Zusammenhang mit der Minimierung der Euklidischen Norm des Unbekanntenvektors gestellt. Verschiedene Matrizen B_1, B_2, und Vektoren c_1, c_2 in den linearen Bedingungsgleichungen $Bx = c$ determinieren die Datumtransformationen (1.10). Ein erstes Beispiel der Theorie von Datumtransformationen wird im zweiten Abschnitt über dreidimensionale Netze im Geometrieraum gegeben. Der dritte Abschnitt ist dem allgemeinen Zusammenhang zwischen der Datumtransformation und den gewählten Restriktionen gewidmet, insbesondere der Frage nach der geometrischen - physikalischen Interpretierbarkeit von restriktiv gesteuerten Datumtransformationen. Ein zweites Beispiel der Theorie von Datumtransformationen wird im vierten Abschnitt über dreidimensionale Netze im Geometrie- und Schwereraum vorgestellt.

1. Datumtransformationen innerhalb eines linearen Ausgleichungsmodells mit injektivem und surjektivem Rangdefekt

Ein lineares Modell sei mit seinen ersten beiden Momenten des nx1 dimensionalen Beobachtungsvektors y vorgegeben, namentlich

(1.1a) $E(y) = Ax$

(1.1b) $D(y) = E\{[y-E(y)]\,[y-E(y)]'\} = \Sigma$,

wobei A nxm dimensionale Designmatrix erster Ordnung vom Rang $r = r(A) < \min\{n,m\}$ und Σ nxn dimensionale Designmatrix zweiter Ordnung, Varianz - Kovarianz - Matrix des Beobachtungsvektors, und x mx1 dimensionaler Unbekanntenvektor ist. Die Dispersionsmatrix Σ habe vollen Rang, jedoch die Designmatrix A den Spaltendefekt $d := m-r \neq 0$. Der Spaltendefekt der Designmatrix bewirkt, daß die kleinste - Quadrate - Lösung nur bis auf die Freiheitsgrade festgelegt ist, über die mit Hilfe von Bedingungsgleichungen

(1.2) $Bx = c$

verfügt werden kann. Dadurch wird das Datum eindeutig festgelegt, sofern etwa gilt

(1.3a) $o(B) = dxm$, $r(B) = d$

(Unabhängigkeit der Bedingungsgleichungen)

und

(1.3b) $S(A') \cap S(B') = \{0\}$

(Unabhängigkeit der Spaltenräume von A' und B').

Eine Ausgleichung im Modell (1.1) mit den Bedingungen (1.2) führt auf eine eindeutige Lösung der Parameter, namentlich

(1.4) $\hat{x} = (A'\Sigma^{-1}A+B'B)^{-1}\,(A'\Sigma^{-1}y+B'c)$.

Eine Herleitung von (1.4) ist in E. Grafarend et al (1979 p.189-192) gegeben, kann aber auch nach K. R. Koch (1980 p. 57-60, 170-172) erfolgen. Üblicherweise wird der Datumdefekt behoben,

(i)

indem einzelnen Komponenten des Parametervektors bestimmte Werte zugewiesen werden;

(ii)
indem der ganze Parametervektor in der euklidischen Norm minimiert wird;

(iii)
indem ein Teil des Parametervektors in der euklidischen Norm minimiert wird;

natürlich können auch Mischformen, z.B. von (i) und (iii), auftreten. Die dazugehörigen Matrizen B für die Bedingungsgleichungen (1.2) lassen sich ohne Schwierigkeiten angeben.

zu (i)
B besteht aus den d verschiedenen dx1 Einheitsvektoren und dazu m-d dx1 Nullvektoren, z.B.

(1.5a) $B = [I_d, 0]$;

(1.6a) c beliebig, aber fest

c enthält die zugewiesenen Werte.

zu (ii)
Der Spaltenraum von B' steht orthogonal auf dem Spaltenraum von A', also $S(A') \perp S(B')$ bzw.

(1.5b) $AB' = 0$, $r(B) = d$

(1.6b) $c = 0$.

zu (iii)
Der Spaltenraum von B' muß orthogonal auf dem Spaltenraum von A' stehen, wobei A durch Streichen gewisser Spalten von A entsteht, z.B. durch

(1.7) $\underset{\sim}{A} := A \begin{bmatrix} 0 & 0 \\ 0 & I_s \end{bmatrix}$ $\qquad (r(\underset{\sim}{A}) = s-d \geq 0$

so daß $S(\underset{\sim}{A}') \perp S(B')$ bzw.

(1.5c) $\underset{\sim}{A}B' = A \begin{bmatrix} 0 & 0 \\ 0 & I_s \end{bmatrix} B' = 0$, $r(B) = d \leq s$

(1.6c) $c = 0$

gilt.

In den beiden letzten Fällen sollte beachtet werden, daß die Spalten von B' keineswegs selbst zueinander orthogonal, sondern nur linear unabhängig sein müssen; außerdem ist B nicht eindeutig.

Auf Grund dieser Ausführungen wird deutlich, daß jede beliebige Datum - Transformation durch eine Änderung der Matrix B und des Vektors c erklärt werden kann. Dabei sollen im folgenden die Parametervektoren x_1, x_2 gegenübergestellt werden, die mit unterschiedlichen Matrizen B_1, B_2 und Vektoren c_1, c_2 geschätzt worden sind. Offensichtlich ist

(1.8) $A'\Sigma^{-1}y = (A'\Sigma^{-1}A+B_1'B_1)\hat{x}_1-B_1'c_1 = (A'\Sigma^{-1}A+B_2'B_2)\hat{x}_2-B_2'c_2$

und daraus

(1.9) $\hat{x}_2 = (A'\Sigma^{-1}A+B_2'B_2)^{-1}\left[(A'\Sigma^{-1}A+B_1'B_1)\hat{x}_1+B_2'c_2-B_1'c_1\right]$

andererseits durch Subtraktion

(1.10a) $\hat{x}_2 = \hat{x}_1+\left[(A'\Sigma^{-1}A+B_2'B_2)^{-1}-(A'\Sigma^{-1}A+B_1'B_1)^{-1}\right]A'\Sigma^{-1}y$
$+ (A'\Sigma^{-1}A+B_2'B_2)^{-1}B_2'c_2-(A'\Sigma^{-1}A+B_1'B_1)^{-1}B_1'c_1$

(1.10b) $\hat{x}_2 = \{I+\left[(A'\Sigma^{-1}A+B_2'B_2)^{-1}-(A'\Sigma^{-1}A+B_1'B_1)^{-1}\right]A'\Sigma^{-1}A\}\hat{x}_1$
$+(A'\Sigma^{-1}A+B_2'B_2)^{-1}B_2'c_2-(A'\Sigma^{-1}A+B_1'B_1)^{-1}B_1'c_1$

unter Verwendung der Normalgleichungen .

(1.11) $A'\Sigma^{-1}A\hat{x}_1 = A'\Sigma^{-1}A\hat{x}_2 = A'\Sigma^{-1}y$.

Eine Transformation T: $R^m \longrightarrow R^m$ mit

(1.12a) $\hat{x}_2 = T(\hat{x}_1)$

folgt hier der Darstellung

(1.12b) $\hat{x}_2 = M\hat{x}_1 + l$

mit einer gewissen mxm Matrix M und einem gewissen mx1 Vektor l, die beide keineswegs eindeutig bestimmt sind, wie ein Vergleich von (1.9) und (1.10b) deutlich macht. $\hat{x}_i$ (i=1,2) durchläuft bei Variation des Beobachtungsvektors y nicht den gesamten R^m, sondern nur den (m-d)-dimensionalen Unterraum

(1.13) $S_i := S\{(A'\Sigma^{-1}A+B_i'B_i)^{-1}A'\Sigma^{-1}\}$ $(i=1,2)$

der um den Translationsvektor

(1.14) $s_i := (A'\Sigma^{-1}A+B_i'B_i)^{-1}B_i'c_i$ $(i=1,2)$

verschoben ist. Nur für $\hat{x}_1$ mit

(1.15) $\hat{x}_1 - s_1 \in S_1$

müssen die verschiedenen Darstellungen gemäß (1.12b) auf denselben Vektor $\hat{x}_2$ mit

(1.16) $\hat{x}_2 - s_2 \in S_2$

führen.

Es bleibt uns freigestellt, nach einer solchen Matrix M und einem solchen Vektor l zu suchen, die zwar (1.12b) erfüllen, jedoch zusätzlich eine bestimmte Struktur aufweisen, die den geometrischen und physikalischen Vorstellungen entspricht, die wir uns von einem bestimmten Problem machen. Dazu möge das nachfolgende Beispiel dienen.

2. Ein erstes Beispiel: Dreidimensionale Netze im Geometrie-Raum

Der Parametervektor x möge ausschließlich Zuschläge von näherungsweisen Punktkoordinaten enthalten und zwar je drei Koordinaten $\Delta x_j := X_j - x_j$, $\Delta y_j := Y_j - y_j$, $\Delta z_j := Z_j - z_j$ für jeden Punkt P_j $(j = 1,\ldots, k)$. Werden beispielsweise ausschließlich Winkel in einem Netz beobachtet, so kann (1.12a) aus einer dreidimensionalen Ähnlichkeitstransformation herrühren, z. B.

$$(2.1)\quad \begin{bmatrix} x_j + \Delta x_j \\ y_j + \Delta y_j \\ z_j + \Delta z_j \end{bmatrix}_2 = (1+\lambda)\, R_3 \begin{bmatrix} x_j + \Delta x_j \\ y_j + \Delta y_j \\ z_j + \Delta z_j \end{bmatrix}_1 + t$$

für alle $j = 1,\ldots, k$,

$$(2.2)\quad t := \begin{bmatrix} t_x \\ t_y \\ t_z \end{bmatrix}, \quad R_3 = \begin{bmatrix} 1 & \gamma & -\beta \\ -\gamma & 1 & \alpha \\ \beta & -\alpha & 1 \end{bmatrix}, \quad \lambda \in R,$$

worin λ einen kleinen Maßstabfaktor, t einen Translationsvektor und α,β,γ kleine Drehwinkel in einer dreidimensionalen Drehmatrix R_3 bezeichnen. Mit diesem Ansatz bekommt (1.12b) die Form (m = 3k)

$$(2.3)\quad \hat{x}_2 = (1+\lambda)\begin{bmatrix} R_3 & 0\ldots 0 \\ 0 & R_3 \ldots 0 \\ \ldots & \\ 0 & 0 \quad R_3 \end{bmatrix}(x_0 + \hat{x}_1) + \left(\begin{bmatrix} t \\ t \\ \ldots \\ t \end{bmatrix} - x_0\right)$$

$$= (1+\lambda)\,(I_k \boxtimes R_3)\,(x_0 + \hat{x}_1) + (e_k \boxtimes t - x_0)$$

Dabei bezeichnet I_k die k-dimensionale Einheitsmatrix, $e_k := [1,\ldots,1]'$ den kx1 Summationsvektor, $x_0 := [x_1,y_1,z_1,x_2,y_2,z_2,\ldots,x_k,y_k,z_k]'$ den Vektor der Näherungskoordinaten und "$\boxtimes$" das Kroneckerprodukt, definiert durch

$$(2.4)\quad A \boxtimes B := [a_{ij}\,B].$$

Betrachtet man beispielsweise die 3xk Matrizen

$$(2.5)\quad \hat{X}_i := \begin{bmatrix} \Delta x_1 & \ldots & \Delta x_k \\ \Delta y_1 & \ldots & \Delta y_k \\ \Delta z_1 & \ldots & \Delta z_k \end{bmatrix}_i \quad (i = 1,2), \qquad X_0 := \begin{bmatrix} x_1 & \ldots x_k \\ y_1 & \ldots y_k \\ z_1 & \ldots z_k \end{bmatrix}$$

so gilt gerade

$$(2.6)\quad \hat{x}_i = \operatorname{vec} \hat{X}_i \ (i = 1,2),\ x_0 = \operatorname{vec} X_0$$

Somit entspricht (2.3) der vektoriellen Form des Gleichungssystems

$$(2.7)\quad \hat{X}_2 = (1+\lambda)\,R_3\,(X_0 + \hat{X}_1) + (te_k' - X_0)$$

Die zentrale Frage lautet nun:

Wie lassen sich aus der Kenntnis von B_i und c_i für i = 1,2 die Parameter der Ähnlichkeitstransformation (2.1) gewinnen, die in dem 7x1 Vektor

$$(2.8)\quad p := [\lambda,\alpha,\beta,\gamma,t_x,t_y,t_z]'$$

gesammelt sein mögen?

Dazu schreiben wir (2.1) unter Vernachlässigung von Produkten kleiner Größen

$$(2.9)\quad \begin{bmatrix} \Delta\hat{x}_j \\ \Delta\hat{y}_j \\ \Delta\hat{z}_j \end{bmatrix}_2 = \begin{bmatrix} \Delta\hat{x}_j \\ \Delta\hat{y}_j \\ \Delta\hat{z}_j \end{bmatrix}_1 + F_j'\,p$$

für alle j = 1,...,k, mit

$$(2.10)\quad F_j' := \begin{bmatrix} x_j & 0 & -z_j & y_j & 1 & 0 & 0 \\ y_j & z_j & 0 & -x_j & 0 & 1 & 0 \\ z_j & -y_j & x_j & 0 & 0 & 0 & 1 \end{bmatrix},$$

worin die Näherungskoordinaten (x_j,y_j,z_j) der Punkte P_j (j = 1,...,k) eingehen. Insgesamt verbleibt anstelle von (2.3)

(2.11) $\hat{x}_2 = \hat{x}_1 + F'p$

mit

(2.12) $F' := [F_1,\ldots,F_k]'$, $o(F') = 3kx7$

Vergleiche hier insbesondere E. Grafarend et al (1979 p.192-195) und K. R. Koch (1980 p.173-175). Wie dort angegeben, überzeugt man sich leicht, daß für das Beispiel des Winkelnetzes

(2.13) $AF' = 0$

(2.14) $r(F) = 7$

falls $k \geq 3$, gilt. In anderen Netztypen sind gewisse Modifikationen vorzunehmen; so ist z.B. in Streckennetzen die erste Spalte von F; sowie die Komponente λ im Vektor p zu streichen.

Damit läßt sich das Gleichungssystem (2.11), das wegen (1.11) und (2.13) konsistent sein muß, eindeutig lösen nach (1.10a) und (2.14) durch

(2.15) $$p = (FF')^{-1} F(\hat{x}_2-\hat{x}_1) =$$
$$= (FF')^{-1}F[(A'\Sigma^{-1}A+B_2'B_2)^{-1} (A'\Sigma^{-1}y+B_2'c_2)$$
$$- (A'\Sigma^{-1}A+B_1'B_1)^{-1} (A'\Sigma^{-1}y+B_1'c_1)].$$

Selbstverständlich würde es auch genügen, 7 linear unabhängige Zeilen von F' zur Matrix $\underset{\sim}{F}'$, z.B.

(2.16) $\underset{\sim}{F}' := [I_7,0]\, F'$

zusammenzufassen und dann

(2.17) $p = (\underset{\sim}{F}')^{-1} (\hat{x}_2-\hat{x}_1)$

zu rechnen; zur Kontrolle muß danach (2.11) erfüllt sein.

Ein numerisches Beispiel sei das folgende eines ebenen Streckennetzes, bestehend aus drei Punkten. Tab. 2.1 gibt die einzelnen Streckenmessungen mit den Werten "beobachtet minus berechnet" an. Die berechneten Distanzen entstammen den Koordinatennäherungswerten der Tab. 2.2. Die Designmatrix erster Ordnung A unseres linearen Modells $E(y) = Ax$ ist in Tab. 2.3 für Näherungsstrecken der Länge Eins zusammengestellt. Tab. 2.4 enthält zwei Versionen von Bedingungsgleichungen, endlich Tab. 2.5 die zugehörigen nach (1.4) oder (1.9),(1.10) berechneten Lösungen $\hat{x}_1$ und $\hat{x}_2$. Sei $F = B_2$, so ergibt sich (2.15) $p = [\gamma,t_x,t_y]'$ zu $\gamma = 0{,}00029$ (Drehwinkel) und $t_x = -0{,}01018$, $t_y = -0{,}02008$ (Translationen). Lösung 2 ($B_2x_2 = 0$) kann mit diesen Werten entsprechend (2.3) verprobt werden.

Tab. 2.1 : Streckenmessungen

$S_{12} = 1{,}0001$, $y_1 = \Delta s_{12} = S_{12} - s_{12} = 0{,}0001$

$S_{13} = 1{,}0005$, $y_2 = \Delta s_{13} = S_{13} - s_{13} = 0{,}0005$

$S_{23} = 0{,}9996$, $y_3 = \Delta s_{23} = S_{23} - s_{23} = -0{,}0004$

Tab. 2.2 : Koordinatennäherungswerte

$x_1 = \sqrt{3}/2$, $y_1 = 1/2$

$x_2 = \sqrt{3}$, $y_2 = 1$

$x_3 = \sqrt{3}/2$, $y_3 = 3/2$

Tab. 2.3 : Designmatrix erster Ordnung A

$$A = \begin{bmatrix} (x_1-x_2)s_{12}^{-1} & (y_1-y_2)s_{12}^{-1} & -(x_1-x_2)s_{12}^{-1} & -(y_1-y_2)s_{12}^{-1} & 0 & 0 \\ (x_1-x_3)S_{13}^{-1} & (y_1-y_3)s_{13}^{-1} & 0 & 0 & -(x_1-x_3)s_{13}^{-1} & -(y_1-y_3)s_{13}^{-1} \\ 0 & 0 & (x_2-x_3)s_{23}^{-1} & (y_2-y_3)s_{23}^{-1} & -(x_2-x_3)s_{23}^{-1} & -(y_2-y_3)s_{23}^{-1} \end{bmatrix}$$

$$A = \begin{bmatrix} -\sqrt{3}/2 & -1/2 & \sqrt{3}/2 & 1/2 & .0 & 0 \\ 0 & -1 & 0 & 0 & 0 & 1 \\ 0 & 0 & \sqrt{3}/2 & -1/2 & -\sqrt{3}/2 & 1/2 \end{bmatrix}$$

Tab. 2.4 : Bedingungsgleichungen

$$B_1 = \begin{bmatrix} 1 & 0 & 0 & 0 & 0 & 0 \\ 0 & 1 & 0 & 0 & 0 & 0 \\ 0 & 0 & 0 & 0 & 1 & 0 \end{bmatrix}, \quad c_1 = \begin{bmatrix} 0{,}01 \\ 0{,}02 \\ 0.01 \end{bmatrix}$$

$$B_2 = \begin{bmatrix} 1/2 & -\sqrt{3}/2 & 1 & -\sqrt{3} & 3/2 & -\sqrt{3}/2 \\ 1 & 0 & 1 & 0 & 1 & 0 \\ 0 & 1 & 0 & 1 & 0 & 1 \end{bmatrix}, \quad c_2 = \begin{bmatrix} 0 \\ 0 \\ 0 \end{bmatrix}$$

Tab. 2.5 : Lösungen $\Delta\hat{x}$, $\hat{X} = x+\Delta\hat{x}$, $\Delta\hat{y}$, $\hat{Y} = y+\Delta\hat{y}$

Lösung 1		Lösung 2	
$\Delta x_1 = 0{,}01$	$X_1 = 0{,}87602$	$\Delta x_1 = -0{,}00004$	$X_1 = 0{,}86599$
$\Delta y_1 = 0{,}02$	$Y_1 = 0{,}52000$	$\Delta y_1 = -0{,}00033$	$Y_1 = 0{,}49967$
$\Delta x_2 = 0{,}00968$	$X_2 = 1{,}74173$	$\Delta x_2 = -0{,}00021$	$X_2 = 1{,}73184$
$\Delta y_2 = 0{,}02075$	$Y_2 = 1{,}02075$	$\Delta y_2 = +0{,}00017$	$Y_2 = 1{,}00017$
$\Delta x_3 = 0{,}01$	$X_3 = 0{,}87602$	$\Delta x_3 = +0{,}00025$	$X_3 = 0{,}86628$
$\Delta y_3 = 0{,}02050$	$Y_3 = 1{,}52050$	$\Delta y_3 = +0{,}00017$	$Y_3 = 1{,}50017$

3. Der allgemeine Zusammenhang zwischen der Datum-Transformation und den gewählten Restriktionen

Entsprechend der im vorigen Abschnitt geschilderten Vorgehensweise kann auch dann verfahren werden, falls keine genauen Vorstellungen über die Parameter des Vektors p wie in (2.8) bestehen.
Ausgehend von (1.11) gilt stets

(3.1) $A'\Sigma^{-1}A(\hat{x}_2-\hat{x}_1) = 0$

und daher

(3.2) $\hat{x}_2-\hat{x}_1 \in N(A'\Sigma^{-1}A) = N(A)$

da Σ als regulär vorausgesetzt wurde; N(A) bezeichnet den Nullraum von A. Zur nxm Matrix A mit dem Spaltendefekt d läßt sich eine mxd Matrix G' konstruieren mit den Eigenschaften

(3.3) $AG' = 0$

(3.4) $r(G) = d$

so daß gilt

(3.5) $S(A') \perp S(G')$.

Beachte die Korrespondenz dieser Bedingungen zu (1.5b). Beispielsweise nach K. R. Koch (1980 p.33-34) gilt stets

(3.6) $S(A') \perp N(A)$

und daher

(3.7) $N(A) = S(G')$

wegen

(3.8) $\dim N(A) = d = \dim S(G')$.

Nach (3.2) gilt deshalb

(3.9) $\hat{x}_2 - \hat{x}_1 \in S(G')$

für jede Wahl einer Matrix G, die den Bedingungen (3.3) und (3.4) genügt. Folglich ist das Gleichungssystem

(3.10) $\hat{x}_2 - \hat{x}_1 = G'p$

konsistent und läßt sich wegen (3.4) eindeutig auflösen zu

$$(3.11)\quad p = (GG')^{-1}G(\hat{x}_2 - \hat{x}_1) =$$
$$= (GG')^{-1}G[(A'\Sigma^{-1}A+B_2'B_2)^{-1}\ (A'\Sigma^{-1}y+B_2'c_2)$$
$$- (A'\Sigma^{-1}A+B_1'B_1)^{-1}\ (A'\Sigma^{-1}y+B_1'c_1)],$$

worin (1.10a) berücksichtigt worden ist.

Mit dem dx1 Parametervektor p aus (3.11), in den nur die gegebenen Größen A, Σ, y sowie die unterschiedlichen B_i und c_i (i = 1,2) eingehen, läßt sich somit eine Umrechnung von $\hat{x}_1$ in $\hat{x}_2$ und umgekehrt nach (3.10) vornehmen; p enthält dabei die zugehörigen Datum-Parameter. Andererseits führt (3.10) auf

(3.12) $(I-G'(GG')^{-1}G)\ (\hat{x}_2 - \hat{x}_1) = 0$

so daß der mx1 Vektor

(3.13) $g := (I-G'(GG')^{-1}G)\hat{x}_i \qquad (i = 1,2)$

unabhängig von der Wahl der Matrizen B_i und der Vektoren c_i (i = 1,2) ist; g hängt also nur von A, Σ und y ab. Beispielsweise nach K. R. Koch (1980 p.60) gilt explizit

(3.14) $(I-G'(GG')^{-1}G) = (A'\Sigma^{-1}A)^{+}A'\Sigma^{-1}A$

so daß sich mit (1.11)

(3.15) $g = (A'\Sigma^{-1}A)^{+}A'\Sigma^{-1}y$

gleichzeitig als kleinste-Quadrate-Lösung kleinster Norm im Modell (1.1) erweist: Dies entspricht dem Fall (1.5b) und (1.6b), wonach gemäß (1.4) sofort

(3.16) $g = (A'\Sigma^{-1}A+G'G)^{-1}A'\Sigma^{-1}y$

gefolgert werden kann. Geht man mit (3.16) in die Formeln (3.10) und (3.11) ein und berücksichtigt

(3.17) $Gg = 0$

auf Grund von (3.13), so erhalten wir für irgendeine kleinste-Quadrate-Lösung (1.4), die bestimmten Bedingungen (1.2) genügen soll, gerade den Effekt

(3.18) $\hat{x}-g = G'(GG')^{-1}G[(A'\Sigma^{-1}A+B'B)^{-1}(A'\Sigma^{-1}y+B'c)]$

gegenüber der kleinste-Quadrate-Lösung kleinster Norm nach (3.16). Der zugehörige dx1 Parametervektor

(3.19) $p = (GG')^{-1}G[(A'\Sigma^{-1}A+B'B)^{-1}(A'\Sigma^{-1}y+B'c)]$

enthält dann die speziellen Datum-Parameter bezüglich der Lösung g nach (3.16).

Gleichzeitig wird deutlich, daß die Datum-Parameter einer beliebigen Transformation nach (3.11) als Differenz der speziellen Datum-Parameter zweier Transformationen auf g gemäß (3.18) resultieren. Beachte, daß (3.18) und (3.19) unabhängig von der speziellen Wahl der Matrix G sind. Jedoch wird man G in der Regel so wählen, daß der Vektor p der Datum-Parameter gerade solche Komponenten beinhaltet, welche die Wirkung der Bedingungsgleichungen (1.2) geometrisch oder physikalisch veranschaulichen, wie es im zweiten Abschnitt vorgeführt worden ist.

4. Ein zweites Beispiel: Dreidimensionale Netze im Geometrie- und Schwereraum

In Punkten P der Erdoberfläche seien Größen im Schwere- und Geometrieraum gemessen, mit denen im Sinne der integrierten Geodäsie nach (1.2) unbekannte Parameter bestimmt werden sollen. Als Messungen oder aus Messungen abgeleitete Größen mögen Strecken, Azimute, Horizontalrichtungen, Vertikalrichtungen (Komplemente zu "Zenitdistanzen"), astronomische Längen, astronomische Breiten, absolute Schwerewerte, Potentialdifferenzen vorliegen. Unbekannt sind die cartesischen Koordinaten der Punkte P, oder besser gesagt, Korrekturwerte auf Näherungswerte, Störungen von astronomischer Länge, astronomischer Breite (Lotabweichungen), von Schwerewerten und Potentialen relativ zu einem normalen Schwerefeld und zusätzlich normale Feldparameter, z.B. (gm, J_2, a, ω) - Produkt aus Gravitationskonstante g und Masse m der Modellerde, zonaler Kugelfunktionskoeffizient J_2, große Halbachse a eines rotationssymmetrischen Niveauellipsoides, ω seine Drehgeschwindigkeit - und Parameter, welche die Transformation des normalen Feldes in einem System festlegen, in dem die Punkte P koordiniert sind.

In unserem numerischen Beispiel legen wir ein einfaches kugelsymmetrisches Normalfeld zugrunde, dessen Mittelpunkt M gegen den Koordinatenursprung 0 verschoben ist, so daß gilt

$$w = (gm) \; / \sqrt{(X-X_M)^2+(Y-Y_M)^2+(Z-Z_M)^2}.$$

Die linearisierten Beobachtungsgleichungen können als solche in einem Somigliana - Pizetti - Normalschwerefeld angesehen werden - sie sind vollständig in E. Grafarend und B. Richter (1978) angegeben - in dem die Exzentrizität auf Null gesetzt wird. Wir verzichten hier auf überschüssige Beobachtungen: In einem dreidimensionalen Dreiecksnetz seien die Strecken S_{12}, S_{13}, S_{23}, das Azimut A_{12}, die Vertikalrichtungen B_{12}, B_{13} (Komplemente zu "Zenitdistanzen", Schwerewerte Γ_1, Γ_2, Γ_3 beobachtet, astronomische Längen Λ_1, Λ_2, Λ_3, und astronomische Breiten Φ_1, Φ_2, Φ_3 aus astronomischen Beobachtungen abgeleitet. Unbekannt sind die car-

tesischen Koordinaten X_1, Y_1, Z_1, X_2, Y_2, Z_2, X_3, Y_3, Z_3, Störungen der astronomischen Länge $\delta\lambda_1$, $\delta\lambda_2$, $\delta\lambda_3$ und der astronomischen Breiten $\delta\phi_1$, $\delta\phi_2$, $\delta\phi_3$, Störungen der Schwere $\delta\gamma_1$, $\delta\gamma_2$, $\delta\gamma_3$ sowie Normalfeldparameter gm, X_M, Y_M, Z_M. Entsprechend E. Grafarend und B. Richter (1977) ist die lineare Abhängigkeit der Störungen des Azimutes $\delta\alpha$ und der Vertikalrichtung $\delta\beta$ von den Störungen der astr. Länge $\delta\lambda$ und der astr. Breite $\delta\phi$ direkt in die Beobachtungsgleichungen eingearbeitet worden, um zusätzliche Rangdefekte zu vermeiden. Das Format der Matrix A ist durch die Anzahl n = 15 der Beobachtungen in der Reihenfolge Strecken, Azimut, Vertikalrichtungen, astr. Längen, astr. Breiten, Schwerewerte und durch die Anzahl m = 22 der Unbekannten in der Reihenfolge cartesische Koordinaten, Störungen von astr. Längen, astr. Breiten, Schwerenund Normalfeldparameter bestimmt. Der Spaltendefekt d der Matrix A beträgt d(A) = m - r(A) = 7 und kann wie folgt interpretiert werden: ein Translationsdefekt der Netzkonfiguration von drei, ein Defekt auf Grund des nicht festgelegten Wertes gm und ein Translationsdefekt von drei wegen der Struktur des normalen Schwerefeldes. Der Spaltendefekt d = 7 fixiert die Anzahl der Zeilen der Matrix B. In der ersten Datumfestlegung werden die Korrekturwerte $\Delta x_1 = 0$, $\Delta y_1 = 0$, $\Delta z_1 = 0$, $\delta(gm) = 0$, $X_M = 0$, $Y_M = 0$, $Z_M = 0$ gesetzt. Dagegen ist eine zweite oder alternative Datumfestlegung

$\Delta x_1+\Delta x_2+\Delta x_3 = 0$, $\Delta y_1+\Delta y_2+\Delta y_3 = 0$, $\Delta z_1+\Delta z_2+\Delta z_3 = 0$

(Auffelderung der Koordinatenzuschläge auf den geometrischen Mittelpunkt), $\delta(gm) = -1{,}7 \cdot 10^{-9}$, $X_M = Y_M = -Z_M = -30{,}000$. Um die Dimensionen in den Formeln (1.4), (1.9), (1.10) vergleichbar zu halten, sind die Bedingungsgleichungen so anzuschreiben, daß c dimensionslos ist.

Während die Abb. 4.1, 4.2 und 4.3 die Struktur der Matrizen A, B_1, B_2 und Vektoren c_1, c_2 illustriert - nur Elemente ungleich Null wurden gekennzeichnet - enthalten Tab. 4.1 die heterogenen Beobachtungen,

Tab. 4.2 Näherungswerte der Koordinaten und (gm), Tab. 4.3 die Lösungen Δx, X, Δy, Y, Δz, Z, $\delta\lambda$, $\delta\phi$, $\delta\gamma$, δ(gm), X_M, Y_M, Z_M für die obigen Datumfestlegungen. Die numerischen Ergebnisse lassen folgende Interpretation zu. Die Schnittstelle der bisher üblichen stufenweisen Auswertung (1. Stufe: Ausgleichung nach unbekannten Koordinaten, 2. Stufe: Ausgleichung auf der Basis eines speziellen normalen Schwerefeldes mit Störungen als Unbekannten) wird durch die integrierte Bearbeitungsweise bestätigt. Im Rahmen der Meßgenauigkeit sind die Beobachtungsanomalien nahezu identisch mit den Störungen. Insbesondere sind die Störungen recht empfindlich gegenüber der Datumfestlegung. Von besonderer Bedeutung ist deshalb die Formulierung der Bedingungsgleichungen.

Zusammenfassend möchten wir die Vorteile der hier aufgezeigten Behandlung des Datumproblems aufzeigen: Beliebig viele Datumparameter können eingeführt werden, ein besonderer Wert im Rahmen der integrierten Geodäsie. Datumtransformationen ergeben sich in natürlicher Art und Weise anhand der Bedingungsgleichungen, mit denen injektive Rangdefekte "geheilt" werden.

Abb. 4.1 : Struktur der Designmatrix erster Ordnung A

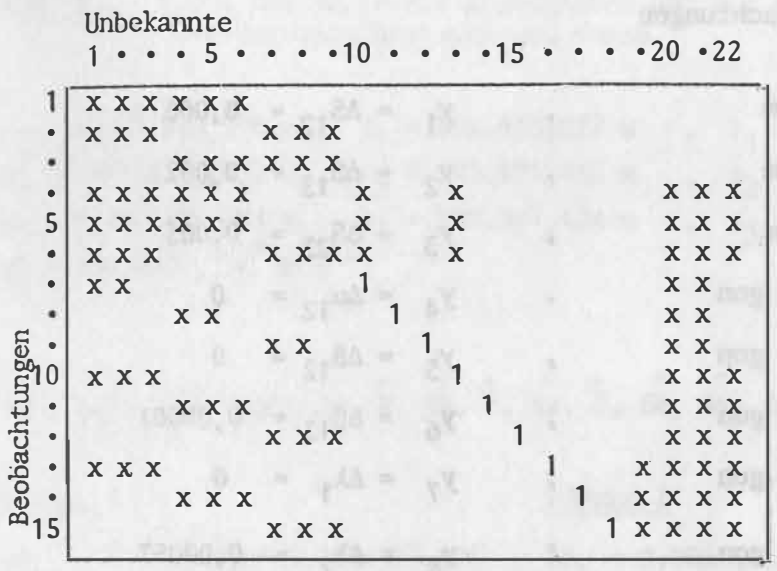

Abb. 4.2 : Struktur der Matrix B_1 und des Vektors c_1

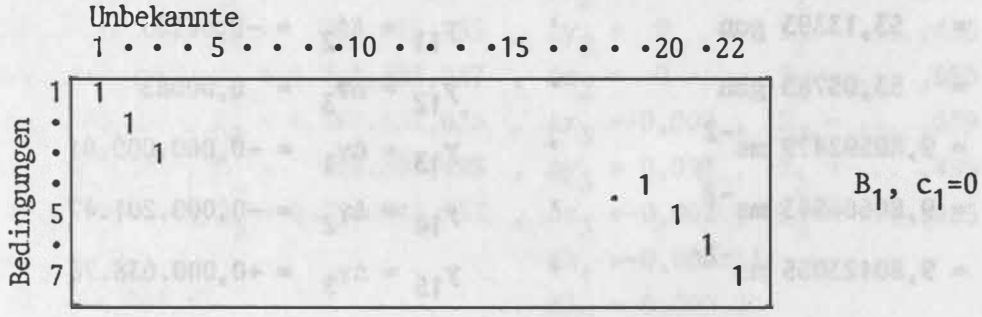

Abb. 4.3 : Struktur der Matrix B_2 und des Vektors c_2

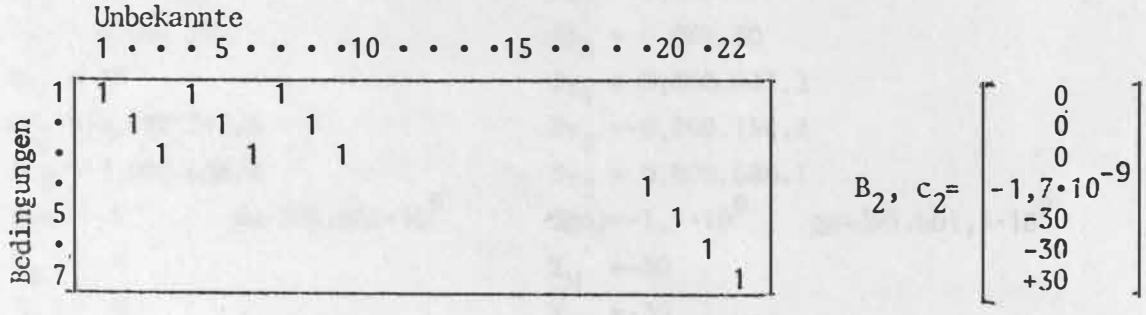

Tab. 4.1 : Beobachtungen

S_{12} = 4.457,014 m	,	$y_1 = \Delta S_{12}$ =	0,006
S_{13} = 5.302,758 m	,	$y_2 = \Delta S_{13}$ =	0,002
S_{23} = 9.047,544 m	,	$y_3 = \Delta S_{23}$ =	0,005
A_{12} = -193,81328 gon	,	$y_4 = \Delta\alpha_{12}$ =	0
B_{12} = -4,4000 gon	,	$y_5 = \Delta\beta_{12}$ =	0
B_{13} = 9,1131 gon	,	$y_6 = \Delta\beta_{13}$ =	0,00001
Λ_1 = 13,54765 gon	,	$y_7 = \Delta\lambda_1$ =	0
Λ_2 = 13,54180 gon	,	$y_8 = \Delta\lambda_2$ =	0,00057
Λ_3 = 13,60574 gon	,	$y_9 = \Delta\lambda_3$ =	-0,00149
Φ_1 = 53,09079 gon	,	$y_{10} = \Delta\phi_1$ =	0
Φ_2 = 53,13393 gon	,	$y_{11} = \Delta\phi_2$ =	-0,00105
Φ_3 = 53,05783 gon	,	$y_{12} = \Delta\phi_3$ =	0,00083
Γ_1 = 9,80592479 ms^{-2}	,	$y_{13} = \Delta\gamma_1$ =	-0,000.000.01
Γ_2 = 9,80666543 ms^{-2}	,	$y_{14} = \Delta\gamma_2$ =	-0,000.201.47
Γ_3 = 9,80423035 ms^{-2}	,	$y_{15} = \Delta\gamma_3$ =	+0,000.638.78

Tab. 4.2 : Näherungswerte der Koordinaten und des Produktes Gravitationskonstante und Masse

$x_1 = 4.187.535{,}996$ m , $y_1 = 904.833{,}027$ m , $z_1 = 4.721.760{,}231$ m
$x_2 = 4.184.221{,}479$ m , $y_2 = 903.675{,}455$ m , $z_2 = 4.724.505{,}950$ m
$x_3 = 4.189.634{,}641$ m , $y_3 = 909.391{,}494$ m , $z_3 = 4.720.046{,}957$ m
$gm = 398.603 \cdot 10^9\ m^3 s^{-2}$

Tab. 4.3 : Lösungen $\hat{\Delta x}$, $\hat{X}$, $\hat{\Delta y}$, $\hat{Y}$, $\hat{\Delta z}$, $\hat{Z}$, $\hat{\delta\lambda}$, $\hat{\delta\phi}$, $\hat{\delta\gamma}$, $\hat{\delta(gm)}$

Lösung 1		Lösung 2	
$\Delta x_1 = 0$	$X_1 = 4.187.535{,}996$	$\Delta x_1 = 0{,}003$	$X_1 = \ldots{,}999$
$\Delta y_1 = 0$	$Y_1 = 904.833{,}027$	$\Delta y_1 = 0$	$Y_1 = \ldots{,}027$
$\Delta z_1 = 0$	$Z_1 = 4.721.760{,}231$	$\Delta z_1 = 0{,}003$	$Z_1 = \ldots{,}234$
$\Delta x_2 = -0{,}003$	$X_2 = 4.184.221{,}476$	$\Delta x_2 = 0$	$X_2 = \ldots{,}479$
$\Delta y_2 = 0$	$Y_2 = 903.675{,}455$	$\Delta y_2 = 0$	$Y_2 = \ldots{,}455$
$\Delta z_2 = -0{,}003$	$Z_2 = 4.724.505{,}947$	$\Delta z_2 = 0$	$Z_2 = \ldots{,}950$
$\Delta x_3 = -0{,}005$	$X_3 = 4.189.634{,}636$	$\Delta x_3 = -0{,}002$	$X_3 = \ldots{,}639$
$\Delta y_3 = 0{,}001$	$Y_3 = 909.391{,}495$	$\Delta y_3 = 0{,}001$	$Y_3 = \ldots{,}495$
$\Delta z_3 = -0{,}005$	$Z_3 = 4.720.046{,}952$	$\Delta z_3 = -0{,}002$	$Z_3 = \ldots{,}955$
$\delta\lambda_1 = 0$		$\delta\lambda_1 = -0{,}000.34$	
$\delta\lambda_2 = 0{,}000.57$		$\delta\lambda_2 = 0{,}000.22$	
$\delta\lambda_3 = -0{,}001.49$		$\delta\lambda_3 = -0{,}001.83$	
$\delta\phi_1 = 0$		$\delta\phi_1 = 0{,}000.46$	
$\delta\phi_2 = -0{,}001.05$		$\delta\phi_2 = -0{,}000.59$	
$\delta\phi_3 = 0{,}000.83$		$\delta\phi_3 = 0{,}001.30$	
$\delta\gamma_1 = 0$		$\delta\gamma_1 = 0{,}000.047.2$	
$\delta\gamma_2 = -0{,}000.201.5$		$\delta\gamma_2 = -0{,}000.154.4$	
$\delta\gamma_3 = 0{,}000.638.8$		$\delta\gamma_3 = 0{,}000.686.1$	
$\delta(gm) = 0$	$gm = 398.603 \cdot 10^9$	$\delta(gm) = -1{,}7 \cdot 10^9$	$gm = 398.601{,}3 \cdot 10^9$
$X_M = 0$		$X_M = -30$	
$Y_M = 0$		$Y_M = -30$	
$Z_M = 0$		$Z_M = +30$	

Literatur

Grafarend, E., H. Heister, R. Kelm, H. Kropff und B. Schaffrin (1979) : Optimierung geodätischer Meßoperationen, H. Wichmann Verlag, Karlsruhe 1979

Grafarend, E. und B. Richter (1977) : The generalized Laplace condition, Bulletin Geodesique 51 (1977) 287-293

Grafarend, E. und B. Richter (1978) : Threedimensional geodesy - the datum problem - Zeitschrift für Vermessungswesen 1o3 (1978) 44-59

Heitz, S. (1969): Transformationen zwischen ellipsoidischen Koordinatensystemen, Deutsche Geodätische Kommission, Bayerische Akademie der Wissenschaften, Report A 64, München 1969

Koch, K.R. (198o) : Parameterschätzung und Hypothesentests in linearen Modellen, Dümmler-Verlag, Bonn 198o

Krakiwski, E.J. and D.B. Thompson (1974) : Mathematical models for the combination of terrestrial and satellite networks, The Canadian Surveyor 28 (1974) 6o6-615

Merry, C.L. and P. Vanicek (1974) : The geoid and datum translation components, The Canadian Surveyor 28 (1974) 56-62

Sigl, R. (1978) : Zur Transformation von Datumskoordinaten, in : Festschrift für Walter Höpcke, Wissenschaftliche Arbeiten der Lehrst.f. Geod., Phot. u. Kart. , Technische Universität Hannover, Nr. 83, S. 148-154, Hannover 1978

Torge, W. (198o) : Geodätisches Datum und Datumtransformationen, in : H. Pelzer (Her.) : Geodätische Netze in Landes- und Ingenieurvermessung, S. 131-14o, K. Wittwer Verlag, Stuttgart 198o

Direct Methods for Geodetic Boundary Problems[1)]

by

Petr Holota[2)]

Contents

1. Introduction

Great progress has been made in the solution of the geodetic boundary problem during the past 5 to 6 years (see HÖRMANDER [2] , SANSÒ [14] , [15] , [16]).

---

1) This paper was presented by the author at the 4th International Symposium "Geodesy and Physics of the Earth", GDR, Karl-Marx-Stadt, May 12th-17th, 1980 (to appear in the proceedings of this Symposium).

2) Research Institute of Geodesy, Topography and Cartography, 250 66 Zdiby 98/Prague, Czechoslovakia

The function spaces principally used for studying the problem represent a significant advance as compared with previous techniques sometimes replacing the exactness by intuition. Consistent work with function spaces makes it possible to profit from the whole wealth of abstract results of the functional analysis. The geodetic boundary problem could thus for the first time be successfully solved as a non-linear one. Necessary and sufficient conditions for the existence and the uniqueness of the local solution of the problem were specified and the stability of the solution was possible to study.

However, HÖRMANDER s and SANSÒ´s results require a certain degree of regularity of both the input boundary data and the boundary itself. These requirements are sometimes considered rather mild but there is also a reasonably motivated tendency to generalize them. It seems therefore appropriate to study the problem in terms of the weak solution in the usual Sobolev spaces, see NEČAS [11] , REKTORYS [12] , LIONS-MAGENES [8] , MIKHLIN [9] , WHITEMAN [19] .

Another reasons for using direct variational methods to solve the linearized geodetic boundary problem, i.e. an oblique derivative problem for the Laplace equation, issue from a numerical implementation aspect. The traditional method of integral equations, if used to solve the given problem, leads to the singular equation containing an integral convergent in the sense of Cauchy´s principal value only. It is thus impossible to apply the Riesz theory on the compact operator and problems could emerge in connection with the boundedness (continuity) of the respective inverse operator, that is with the stability of the method used. On the other hand, it is

well known that direct variational methods are stable as related to small variations in input data.

In addition, direct variational methods enable us to formulate a comparatively broad class of problems for various boundary conditions and for rather general simply as well as multiply connected domains. This is very important when taking into account the gravitational interaction with other celestial bodies and, consequently, formulating time-dependent problems.

The linearized geodetic boundary problem is formulated for an unbounded domain and the use of a direct variational method for an investigation of the weak solution would necessarily imply work in spaces with weight. This approach will be avoided by using the Kelvin transformation as a useful means of formulating an equivalent problem for a bounded domain. At the same time, however, we will arrange the transformation so as to relatively magnify in the image that part of the boundary which is of particular interest to us. In respect of the numerical solution requiring a limited number of basic functions, the approach just mentioned has some advantages. An appropriate choice of the Kelvin transformation could also be an efficient tool, if used under real conditions, in suppressing in the image those parts of the boundary which are not covered by the input boundary data. A similar remark was also made by KRARUP in [6] .

Let it be mentioned at the end of this introductory part that attempts have already been made to use variational methods for the solution of the geodetic boundary problem. In these papers, however, the linearized geodetic boundary problem is dealt with only in its more or less simplified form, mostly in spherical approximation, e.g.

in NAKIBOGLU [10] . When taking into account the oblique derivative as an essential feature of the problem, it is necessary to find, in the first place, an appropriate decomposition of the Laplace operator. The problem becomes, of course, more complex but approaches reality in a more accurate way.

Let us recall finally that the weak solution concept has an important advantage consisting in the fact that the existence of the weak solution can be established relatively easily by some of the methods of functional analysis (Lax-Milgram theorem). Natural function spaces corresponding to this concept are the Sobolev spaces.

As usual, general existence theorems do not answer the question concerning the quality of the weak solution (differentiability, etc.). Nevertheless, it is important for us to know what quality of the boundary (its smoothness) and all those data that define the problem in question is sufficient for the weak solution to be the classical solution (satisfying the differential equation and the boundary condition pointwise).

Problems like this are topics of the theory of the regularity of weak solutions which in general is rather hard but assuming that the boundary and all input data belong to the class, say, C^∞ , we hope that all results can be expected to hold in the classical sense.

2. Linearized geodetic boundary problem

To solve the linearized geodetic boundary problem means to find such a function $\dot{w}$ that

$$\Delta \dot{w} = 0 \quad in \quad ext\, \Gamma \,, \tag{2.1}$$

$$\dot{v} + \langle k , \operatorname{grad} \dot{v} \rangle = F \quad \text{on} \quad \Gamma , \tag{2.2}$$

$$\dot{v}(y) = c/|y| + O(|y|^{-3}) , \quad y \longrightarrow \infty , \tag{2.3}$$

where $\langle \ , \ \rangle$ denotes the scalar product and

$$\begin{aligned} k &= -g'^{-1} g \quad , \\ g &= \operatorname{grad} w \quad , \\ g' &= [\partial^2 w / \partial y_i \, \partial y_j] \quad . \end{aligned} \tag{2.4}$$

Recall that w in the above equations denotes the gravity potential of the earth's model body, e.g. of the reference ellipsoid; g' is so-called Marussi tensor; and k thus indicates the isozenithal vector field which on Γ is close to $y/2$. The surface Γ represents a model shape of the earth's body, telluroid, the construction of which is connected with the structure of the right hand side F of equation (2.2) and will not be specified here. This and all the other important details concerning the formulation of the linearized geodetic boundary problem can be found in HÖRANDER [2] .

As mentioned in the introductory part, our aim is to obtain a direct variational solution of the problem (2.1)-(2.3). In the following section we will deal with the Kelvin transformation, see KELLOGG [4] , p. 231, the use of which enables us to formulate an equivalent problem for a bounded domain. However, an attempt is made to arrange the transformation so as to relatively enlarge that part of the boundary Γ and its neighbouring space which is particularly interesting when solving the problem. For this reason we will situate the centre of the sphere of inversion S_R (with the radius R) at a

point which in general does not coincide with the origin of the system of coordinates (y_1, y_2, y_3).

Introducing a new system of coordinates (x_1, x_2, x_3) with the origin at point z such that the translative relation

$$y = x + z \tag{2.5}$$

is valid, the function

$$\tilde{u}(x) = \dot{v}(x + z) \tag{2.6}$$

will have to be a solution of the following problem

$$\Delta \tilde{u} = 0 \quad \text{in} \quad ext\, \Gamma \,, \tag{2.1'}$$

$$\tilde{u} + \langle h, grad\, \tilde{u} \rangle = F \quad on \quad \Gamma \,, \tag{2.2'}$$

$$\tilde{u}(x) = c/|x + z| + O(|x + z|^{-3}), \; x \longrightarrow \infty \,. \tag{2.3'}$$

However, in regard of the asymptotic behaviour of the potential in infinity, see KELLOGG [4], p. 144; SMIRNOV [18], Chap. VI, Sec. 137, the last condition can be rewritten as follows

$$\tilde{u}(x) = c(1/|x| - \langle x,z \rangle/|x|^{-3}) + \tag{2.3''}$$

$$+ O(|x|^{-3}) \,, \; x \longrightarrow \infty \,.$$

3. Kelvin transformation

By Kelvin transformation, in our case the inversion in the sphere S_R, any point x is carried into its image x' and it holds

$$(3.7) \qquad x' = x\,\frac{R^2}{|x|^2}\,, \quad x = x'\,\frac{R^2}{|x'|^2}\,, \quad |x|\cdot|x'| = R^2\,.$$

Further, if $\tilde{u}$ is harmonic function in a domain $ext\ \Gamma$, then

$$(3.8) \qquad u(x') = \frac{R}{|x'|}\ \tilde{u}(x) = \frac{R}{|x'|}\ \tilde{u}\left(x'\,\frac{R^2}{|x'|^2}\right)$$

is harmonic in the domain $\Omega = int\ \Gamma'$ into which $ext\ \Gamma$ is carried by the inversion.

From (3.8) it also follows that

$$(3.9) \qquad \tilde{u}(x) = \frac{R}{|x|}\ u(x') = \frac{R}{|x|}\left(x\,\frac{R^2}{|x|^2}\right)$$

and we can calculate

$$\frac{\partial \tilde{u}}{\partial x_i}(x) = -\frac{R x_i}{|x|^3}\ u(x') + \frac{R}{|x|}\sum_{j=1}^{3}\frac{\partial u}{\partial x_j'}(x')\,\frac{\partial x_j'}{\partial x_i}(x)\,.$$

But

$$\frac{\partial x_j'}{\partial x_i}(x) = \frac{R^2}{|x|^2}\left(\delta_{ij} - 2\,\frac{x_i x_j}{|x|^2}\right)$$

and thus

$$\frac{\partial \tilde{u}}{\partial x_i}(x) = -\frac{R x_i}{|x|^3}\ u(x') + \frac{R^3}{|x|^3}\left(\frac{\partial u}{\partial x_i'}(x') - 2\,\frac{x_i}{|x|^2}\sum_{j=1}^{3} x_j\,\frac{\partial u}{\partial x_j'}(x')\right)$$

Hence, it is simple to conclude that

$$\langle h, \operatorname{grad} \tilde{u} \rangle = -\frac{R}{|x|^3} \langle x, h \rangle u + \frac{R^3}{|x|^3} \langle h - 2\frac{x}{|x|^2}\langle x, h \rangle, \operatorname{grad} u \rangle$$

and

$$\tilde{u} + \langle h, \operatorname{grad} \tilde{u} \rangle = \frac{R}{|x|}\left(1 - \frac{1}{|x|^2}\langle x, h \rangle\right) u + \frac{R^3}{|x|^3}\langle h - 2\frac{x}{|x|^2}\langle x, h \rangle, \operatorname{grad} u \rangle .$$

Passing to coordinates x_1', x_2', x_3', we denote

$$\rho(x') = 1 - \frac{1}{R^2}\left\langle \cdot, h\left(x'\frac{R^2}{|x'|^2} + z\right)\right\rangle , \tag{3.10}$$

$$s(x') = h\left(x'\frac{R^2}{|x'|^2} + z\right) - 2\frac{x'}{|x'|^2}\left\langle x', h\left(x'\frac{R^2}{|x'|^2} + z\right)\right\rangle , \tag{3.11}$$

$$H(x') = \frac{R}{|x'|} F\left(x'\frac{R^2}{|x'|^2} + z\right) . \tag{3.12}$$

Now the problem equivalent to (2.1)-(2.3), i.e. the boundary problem for the function u, can be written in the form

$$\Delta u = 0 \quad \text{in} \quad \operatorname{int} \Gamma' , \tag{3.13}$$

$$\rho u + \frac{|x'|^2}{R^2}\langle s, \operatorname{grad} u \rangle = H \quad \text{on} \quad \Gamma' , \tag{3.14}$$

$$u(x') = \frac{c}{R}\left(1 - \frac{1}{R^2}\langle x', z \rangle\right) + O(|x'|^2), \; x' \to 0 , \tag{3.15}$$

where the asymptotic development (2.3") has been used in (3.15). Comparing the coefficients of the Taylor expansion of the function u at point 0 with the coefficients of the development (3.15), it is obvious that the condition (3.15) is equivalent to equations

$$u(0) = \frac{c}{R} \quad , \tag{3.16}$$

$$\frac{\partial u}{\partial x_i'}(0) = -\frac{c}{R^3} x_i \quad , \quad i = 1,2,3 \quad . \tag{3.17}$$

A simple calculation can verify that

$$|s(x')| = |h(y)| \quad , \quad \langle x', s(x') \rangle = -\langle x', h(y) \rangle \quad . \tag{3.18}$$

As regards the coefficient $p(x')$, it can be stated that, for the time being, it depends on the vector h . If given in a special form, its properties become more apparent in the following section. However, $p(x')$ may attain, in general, positive as well as negative values.

4. The simple Molodensky problem

The title of this section corresponds to KRARUP'S terminology from [5] and to the situation when $h = y/2$. Hence,

$$p = \frac{1}{2}\left(1 - \frac{1}{R^2}\langle x', z \rangle\right) \quad , \tag{4.1}$$

$$s = -\frac{R^2}{2|x'|^2} x' \left(1 + \frac{2}{R^2}\langle x', z \rangle\right) + \frac{1}{2} z \quad . \tag{4.2}$$

Example 4.1. For $z = (0,0,0)$ we have $\rho = \frac{1}{2}$,

$$s = -\frac{R^2}{2|x'|^2}\, x'$$

and the boundary condition (3.14) is of the form

$$\frac{1}{2}\, u - \frac{1}{2} \langle x', \operatorname{grad} u \rangle = H \quad \text{on} \quad \Gamma' . \tag{4.3}$$

Introducing new coordinates r_1 , r_2 , r_3 by the relation

$$x' = r + d\,\frac{z}{|z|} \quad , \tag{4.4}$$

we obtain

$$\rho = \frac{1}{2} - \frac{1}{2R^2}\left(\langle r, z\rangle + d|z|\right) . \tag{4.5}$$

Next, we will calculate

$$\frac{|x'|^2}{R^2} = \frac{d}{|z|}\left[1 + \frac{2}{R^2}\left(\langle r, z\rangle + d|z|\right) - \right.$$
$$\left. - \frac{|z|}{dR^2}\left(d^2 + d\,\frac{R}{|z|} - |r|^2\right)\right] , \tag{4.6}$$

$$x'\left(1 + \frac{2}{R^2}\langle x', z\rangle\right) - \frac{|x'|^2}{R^2}\, z =$$
$$= r\left[1 + \frac{2}{R^2}\left(\langle r, z\rangle + d|z|\right)\right] -$$
$$+ \frac{1}{R^2}\, z\left(d^2 + d\,\frac{R^2}{|z|} - |r|^2\right) .$$

Thus

$$s = -\frac{|z|}{2d}\left[r + \frac{x'}{|x'|^2}\left(d^2 + d\,\frac{R^2}{|z|} - |r|^2\right)\right] . \tag{4.7}$$

Example 4.2. If Γ is a sphere then, owing to conformity of the Kelvin transformation, Γ' also is a sphere. If ϱ is the radius of the sphere Γ (let be denoted S_ϱ) then the position of points A, D in Fig. 1 is given by the vectors

$$x_A = -(\varrho + |z|)\frac{z}{|z|}, \quad x_D = (\varrho - |z|)\frac{z}{|z|}.$$

Points A, D are carried by the inversion into points

$$x_A' = -\frac{z}{|z|}\frac{R^2}{\varrho + |z|}, \quad x_D' = \frac{z}{|z|}\frac{R^2}{\varrho - |z|}$$

lying on the diameter of Γ'. It can easily be concluded that

$$\varrho' = \frac{1}{2}|x_D' - x_A'| = \frac{R^2\varrho}{|\varrho^2 - |z|^2|} \tag{4.8}$$

is the radius of the sphere Γ' (denoted by S_ϱ' in Fig.1). According to our figure the point

$$x_s' = (\varrho' - |x_A'|)\frac{z}{|z|} = \frac{R^2}{\varrho^2 - |z|^2}\, z \tag{4.9}$$

is the centre of the sphere S_ϱ'.

The equation

$$d^2 + d\frac{R^2}{|z|} - \varrho'^2 = 0 \tag{4.10}$$

is satisfied by

$$d_{1,2} = -\frac{R^2}{2|z|} \pm \left(\frac{R^4}{4|z|^2} + \varrho'^2 \right)^{1/2}$$

which in view of (4.8) yields

$$(4.11) \qquad d_1 = R^2 \frac{|z|}{\varrho^2 - |z|^2} = \operatorname{sign}(\varrho^2 - |z|^2) \frac{\varrho'}{\varrho} |z| \,,$$

$$(4.12) \qquad d_2 = -R^2 \frac{1}{\varrho^2 - |z|^2} \frac{\varrho^2}{|z|} = -\operatorname{sign}(\varrho^2 - |z|^2) \varrho\varrho' \frac{1}{|z|} \,.$$

Taking now into consideration equations (4.4), (4.9) and (4.11), it is not difficult to see that for $d = d_1$ (the root d_2 is, for the present, not discussed) the origin of the coordinate system (r_1, r_2, r_3) is identical with the point

$$x_S' = d_1 \frac{z}{|z|} \,,$$

i.e. with the centre of the sphere S_ϱ'. At the same time, however,

$$(4.6') \qquad \frac{|x'|}{R^2} = \frac{d_1}{|z|} \left[1 + \frac{2}{R^2} \left(\langle r, z \rangle + d_1 |z| \right) \right] =$$

$$= \left(\frac{R}{\varrho^2 - |z|^2} \right)^2 \left(\varrho^2 + |z|^2 + 2\varrho |z| \cos(r, z) \right) \,,$$

$$(4.7') \qquad s = -\frac{|z|}{2d_1} r = -\frac{\varrho^2 - |z|^2}{2R^2} r =$$

$$= -\operatorname{sign}(\varrho^2 - |z|^2) \frac{\varrho}{2\varrho'} r = -\operatorname{sign}(\varrho^2 - |z|^2) \frac{\varrho r}{2|r|}$$

and it may be noted that, in view of the first equation (3.18), the last result could be expected. Thus, the

vector s is normal to the sphere S_ϱ' - in agreement with the conformity of the Kelvin transformation. It is also possible to verify for the example just quoted that

$$(4.13) \qquad p = \frac{1}{2} - \frac{\varrho\,|z|\cos(r,z) + |z|^2}{2(\varrho^2 - |z|^2)}$$

and that for p the following inequality holds

$$(4.14) \qquad \frac{\varrho - 2|z|}{2(\varrho - |z|)} \leqslant p \leqslant \frac{\varrho + 2|z|}{2(\varrho + |z|)}$$

Summing up, if Γ is a sphere with the radius ϱ, and if we use the coordinate system (r_1, r_2, r_3) with the origin x_s', then the solution of the simple Molodensky problem requires to find such a function u that

$$(4.15) \qquad \Delta u = 0 \quad \text{in} \quad \text{int}\,\Gamma' \equiv \text{int}\,S_\varrho' \,,$$

$$(4.16) \qquad \frac{1}{2}\left[1 - \frac{1}{R^2}(\langle r,z\rangle + d_1|z|)\right]u -$$

$$- \frac{1}{2}\left[1 + \frac{2}{R^2}(\langle r,z\rangle + d_1|z|)\right]\langle r, \text{grad}\,u\rangle = H \quad \text{on} \quad \Gamma',$$

$$(4.17) \qquad u\left(-d_1\frac{z}{|z|}\right) = \frac{c}{R} \,,$$

$$(4.18) \qquad \frac{\partial u}{\partial \zeta_i}\left(-d_1\frac{z}{|z|}\right) = -\frac{c}{R^3}z_i \,, \quad i = 1,2,3 \,.$$

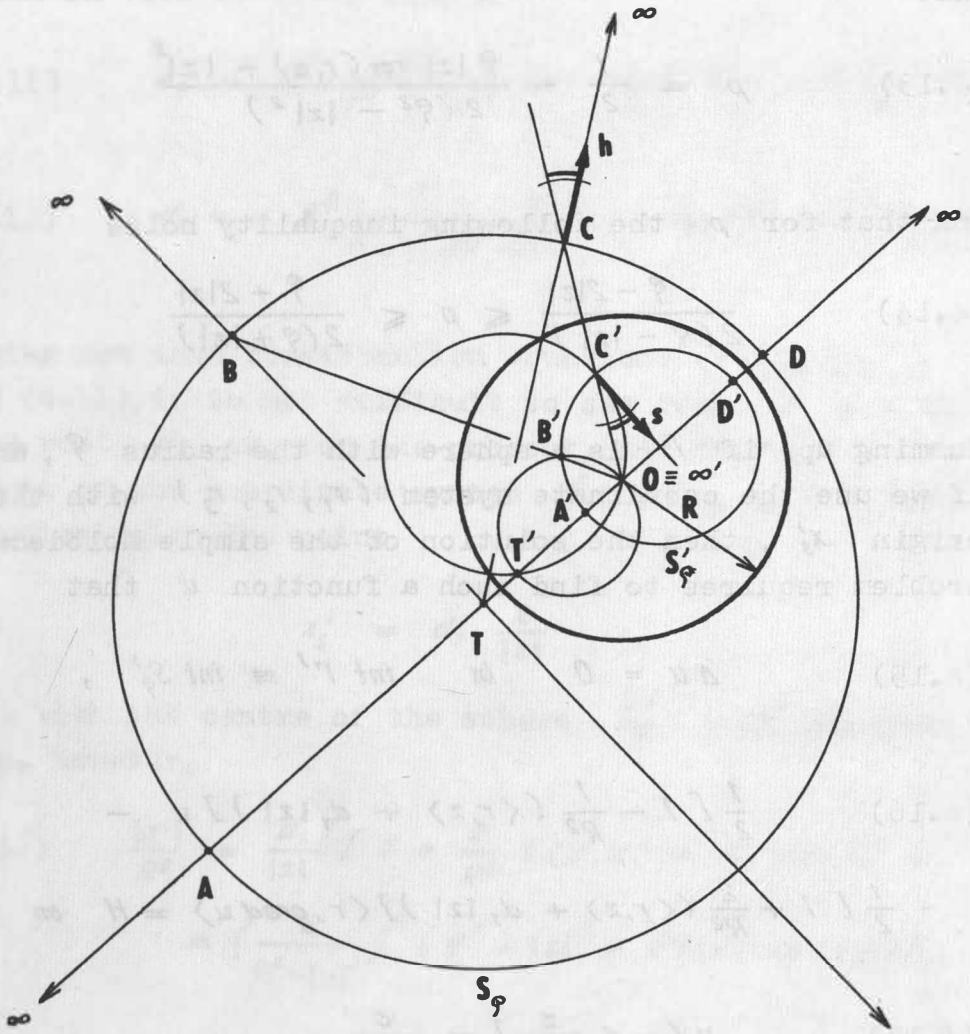

fig. 1

5. Direct metods - elementary notions

As was already mentioned, we will be engaged in a weak solution of the problem (3.13)-(3.15). Our approach will be conformable particularly to that of NEČAS in [11] , or REKTORYS in [12] , but our aim is not to give here a systematic exposition of the whole concept of the weak solution of boundary problems for elliptic equations. In order not to omit some characteristic features of such an approach but to retain its integrity, we will give here at least an elementary explanation of some basic notions. The reader is also referred to the pertinent information given by KUFNER, JOHN, FUČÍK [7] .

5.1. The space $W_2^{(1)}(\Omega)$

Recall, first, that the use of the Kelvin transformation made it possible to work with the bounded domain Ω ($= int\, \Gamma'$).

Let us denote by $\mathcal{E}(\bar{\Omega})$ a set of all functions infinitely differentiable in Ω and together with all their derivatives continuously prolongable on the closure $\bar{\Omega}$ of the domain Ω , i.e. up to its boundary $\partial\Omega$. Let it be noted explicitly that in this paper we restrict ourselves to real functions only.

By $L_2(\Omega)$ we will denote the Hilbert space of square integrable functions on Ω . $L_2(\Omega)$ is provided by the scalar product

$$(5.1.1) \qquad (v, u) = \int_\Omega v(x)\, u(x)\, dx$$

where $dx = dx_1 dx_2 dx_3$. The integrals are taken in the Lebesgue sense. Instead of $L_2(\Omega)$ we will simply write only L_2 .

On $\mathcal{E}(\bar{\Omega})$ we introduce the scalar product

$$(5.1.2) \qquad (v,u)_{W_2^{(1)}(\Omega)} \equiv (v,u)_1 \equiv$$
$$\equiv \int_\Omega v\cdot u\, dx + \sum_{i=1}^{3} \int_\Omega \frac{\partial v}{\partial x_i}\frac{\partial u}{\partial x_i}\, dx \ .$$

The space $W_2^{(1)}(\Omega)$ is defined as a closure of the set $\mathcal{E}(\Omega)$ produced as a completion of $\mathcal{E}(\bar{\Omega})$ with respect to the norm

$$(5.1.3) \qquad \|v\|_1 = (v,v)_1^{1/2} \ .$$

For sake of brevity we will write simply $W_2^{(1)}$.

Remark 5.1.1. The notion of completion is explained in REKTORYS [12] , Chap. 29, in general in RUDIN [13] , p. 71 or in some other books on mathematical analysis.

If $f \in W_2^{(1)}$, $\partial f/\partial x_i$, $i = 1,2,3$, is defined as a function from L_2 . In fact, in view of the definition of $W_2^{(1)}$, we have $f = \lim_{n\to\infty} f_n$ in $W_2^{(1)}$ where

$$f_n \in \mathcal{E}(\bar{\Omega}) \quad \text{thus} \quad \partial f_n/\partial x_i \ , \ n = 1,2,\dots,$$

is a Cauchy fundamental sequence in L_2 . We denote its limit in L_2 by $\partial f/\partial x_i$ and we will call it a generalized derivative. It can be shown that in this way $\partial f/\partial x_i$ is uniquely defined, see NEČAS [11] , §1, Sec. 1.1.

The space $W_2^{(1)}$ is, of course, equipped by the scalar product (5.1.2) and is often called an energetic

space or a space of functions with "finite energy". In this connection, the scalar product (5.1.2) is often referred to as an energetic product and the norm (5.1.3), an energetic norm.

5.2. Lipschitzian boundary and notion of trace

Intuitively, the existence and properties of the boundary values of a function defined on Ω are influenced not only by the function itself but also by the smoothness of the boundary $\partial\Omega$.

We say that the boundary $\partial\Omega$ is continuous if there exist $\alpha > 0$, $\beta > 0$, a finite number of Cartesian coordinate system (x_{r1}, x_{r2}, x_{r3}) , in brief (x'_r, x_{r3}) , $r = 1, 2, \ldots, m$, and continuous functions $a_r(x'_r)$ defined on the open sets

$$\Delta_r = \{ x'_r ; |x_{ri}| < \alpha , i = 1,2 \}$$

such that

(i) each point $x \in \partial\Omega$ can be expressed at least in one of the m coordinate systems in the form $x = (x'_r, a(x'_r))$,

(ii) the points $x = (x'_r, x_{r3})$ for which $x'_r \in \Delta_r$, $a(x'_r) < x_{r3} < a_r(x'_r) + \beta$ belong to Ω and those for which $x'_r \in \Delta_r$, $a_r(x'_r) - \beta < x_{r3} < a_r(x'_r)$ belong to the exterior of $\bar{\Omega}$ (i.e. to $E_3 - \bar{\Omega}$), see Fig. 2.

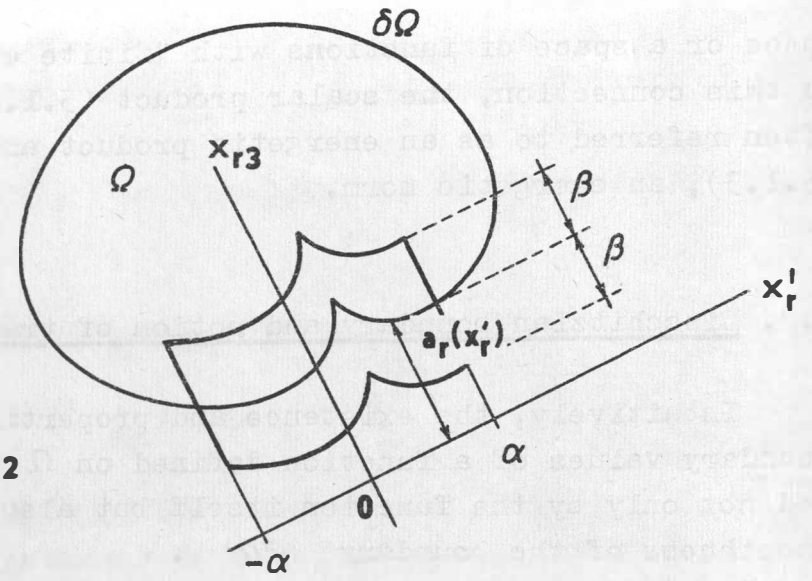

fig. 2

We say that $\partial\Omega$ is a lipschitzian boundary if all functions a_r are locally lipschitzian in Δ_r, this means that

$$x_r', y_r' \in K \Rightarrow |a_r(x_r') - a(y_r')| \leq const. |x_r' - y_r'|$$

is valid for each closed set $K \subset \Delta_r$; thus a_r is lipschitzian on each compact $K \subset \Delta_r$.

The bounded domain Ω we are concerned with is understood in the following text to be the domain with the lipschitzian boundary. It can be stated that such a type of domain is already general enough to cover, with a small degree of idealization, also those domains with boundaries whose regularity corresponds to the smoothness of real topography. Domains with the lipschitzian boundary are, e.g., the sphere, ellipsoid, cube, and polyhedron as well as substantially more general domains with smooth, or piecewise smooth, boundaries, etc. Let us note, however, that among domains with the lipschitzian boundary cannot be ranged, for instance, those domains having singularities analogous to highly sharp vertices in two dimensional case.

It can be shown, see NEČAS [11] , Chap. 2, §4, lemma 4.2; KUFNER, JOHN, FUČÍK [7] , Chap. 6, Sec. 6.2, Theorem 6.2.14 or FUČÍK, KUFNER [1] , Chap. II, Sec. 8.3, that each of the functions a_r describing the lipschitzian boundary of the domain Ω , has a total differential almost everywhere in Δ_r , i.e. except a zero subset of Δ_r (with respect to Lebesgue measure). Hence, the lipschitzian boundary $\partial\Omega$ has an outer (inner) normal almost everywhere.

As will be shown on the following pages, it is possible to speak in a certain precise sense about boundary values on $\partial\Omega$ of functions from $W_2^{(1)}$.

By $L_2(\partial\Omega)$ we will denote the space of square integrable function on $\partial\Omega$.

In the preceding section the space $W_2^{(1)}$ was produced by functions of the set $\mathcal{E}(\bar{\Omega})$ and by their "cover" in metric (5.1.3), i.e., roughly speaking, by those functions from $L_2(\Omega)$ for which it is still possible to speak in a certain generalized sense about their derivatives of the first order.

• For every continuous function on $\bar{\Omega}$, and obviously for every function $v \in \mathcal{E}(\bar{\Omega})$, its values on the boundary $\partial\Omega$ are uniquely defined. The function $v(x)$, $x \in \partial\Omega$ will be called a trace of the function $v \in \mathcal{E}(\bar{\Omega})$ on $\partial\Omega$. The trace of the function v is evidently continuous on the boundary $\partial\Omega$ and hence, obviously, square integrable on $\partial\Omega$.

The possibility of extending the notion of the trace to all functions from $W_2^{(1)}(\Omega)$, and accordingly also to those which do not belong to $\mathcal{E}(\bar{\Omega})$ or are not even continuously prolongable up to the boundary,

is demonstrated in the following theorem (for proof see NEČAS [11] , Chap. 1. §1, Theorem 1.2).

Theorem 5.2.1. Let Ω be a bounded domain with the lipschitzian boundary. Then there exists a uniquely determined continuous linear mapping from $W_2^{(1)}(\Omega)$ into $L_2(\partial\Omega)$ such that for all $x \in \partial\Omega$ and $v \in \mathcal{E}(\Omega)$ it is $T(v)(x) \quad v(x)$.

According to theorem 5.2.1, each function $v \in W_2^{(1)}(\Omega)$ is given a function Tv , its trace. On the contrary, the question arises as to whether each function from $L_2(\partial\Omega)$ is a trace of some function from $W_2^{(1)}(\Omega)$. The reply is negative, see NEČAS [11] , Chap. 1, §2, Remark 1.2. Several comments on the question of traces can be found in REKTORYS [12] , Chap. 30. Let us also mention that theorem 5.2.1 is not correct if $\partial\Omega$ is not the lipschitzian boundary. To see it, it suffices to consider a plane domain with a sufficiently sharp point on its boundary, e.g. the Lebesgue edge, see NEČAS [11] , Chap. 1, §2, Exercise 1.7.

In the following pages we will denote the trace on $\partial\Omega$ of a function v from $W_2^{(1)}(\Omega)$ simply by v .

Recall that the space $L_2(\partial\Omega)$ was introduced here in a very intuitive way. Exact formulations defining this normed Banach space can be found in NEČAS [11] , Chap. 2, §4.1. The corresponding notion of the surface integral is defined by the lemma on the partition of unity in the same book, i.e. in [11] , Chap. 3, §1.1.

Let us have now in E_3 a fixed Cartesian coordinate system and let us formulate - at the end of this section (also without proof) - the Green theorem which is very useful in the sequel.

Theorem 5.2.2. Let Ω be a bounded domain with the lipschitzian boundary. Let u, v be two arbitrary

functions from $W_2^{(1)}(\Omega)$, then

$$(5.2.1)\qquad \int_\Omega \frac{\partial u}{\partial x_i}(x)\, v(x)\,dx = \int_{\partial\Omega} u(x)v(x)n_i(x)\,dS - \int_\Omega u(x)\frac{\partial v}{\partial x_i}(x)\,dx$$

where $i = 1,2,3$ and $n(x) = (n_1(x), n_2(x), n_3(x))$ is the unit vector of the external normal at point x .

Proof of this theorem can be found in general form in NEČAS [11] , Chap. 3, §1.2. The existence of the two outer integrals in (5.2.1) is obvious. The existence of the surface integral is a consequence of the theorem on traces and of the fact, see p. 18 , that the normal of the lipschitzian boundary exists almost everywhere .

6. Generalized oblique derivative problem

Let us mention that in the following text Ω is still understood to be a bounded domain with the lipschitzian boundary.

Let $a_{ij}(x)$, $b_i(x)$; $i,j = 1,2,3$ be bounded Lebesgue-measurable functions in Ω and let it hold that

$$(6.1)\qquad \sum_{i,j=1}^{3} a_{ij}(x)\xi_i\xi_j \geq \text{const.}\ |\xi|^2 , \quad \text{const.} > 0 ,$$

for almost all $x \in \partial\Omega$ and all vectors

$\xi = (\xi_1, \xi_2, \xi_3)$, $\xi \neq 0$.

By

$$A(v,u) = \int_\Omega \sum_{i,j=1}^{3} a_{ij} \frac{\partial v}{\partial x_i} \frac{\partial u}{\partial x_j} \, dx + \int_\Omega \sum_{i=1}^{3} b_i v \frac{\partial u}{\partial x_i} \, dx \tag{6.2}$$

we define a bilinear form on $W_2^{(1)}(\Omega) \times W_2^{(1)}(\Omega)$.

It can be seen immediately that $A(v,u)$ is continuous on $W_2^{(1)}(\Omega) \times W_2^{(1)}(\Omega)$, i.e. there exists a constant $M > 0$ such that for all $v, u \in W_2^{(1)}(\Omega)$ it is $A(v,u) \leq M \|v\|_1 \cdot \|u\|_1$.

Further, let us define on $W_2^{(1)}(\Omega) \times W_2^{(1)}(\Omega)$ the boundary bilinear form

$$a(v,u) = \int_{\partial\Omega} \alpha \, Tv \, Tu \, dS \tag{6.3}$$

where $\alpha(x)$ is a bounded Lebesgue-measurable function on $\partial\Omega$ and T is the operator of traces, see theorem 5.2.1.

From theorem 5.2.1 it is quite evident that the form $a(v,u)$ is continuous on $W_2^{(1)}(\Omega) \times W_2^{(1)}(\Omega)$.

In conformity with our earlier remark in Sec. 5.2, we will denote in the following text the trace on $\partial\Omega$ of a function v simply as v.

Finally, let $f \in L_2(\partial\Omega)$.

The function $u \in W_2^{(1)}(\Omega)$ is called the weak solution of the boundary problem with an oblique derivative if

$$A(v,u) + a(v,u) = \int_{\partial\Omega} v f \, dS \tag{6.4}$$

holds for all $v \in W_2^{(1)}(\Omega)$.

7. Relation to the classical solution

It will be shown that the definition of the weak solution from the preceding section actually presents a meaningful extension of the classical notion of the solution of an oblique derivative boundary problem. For this reason we will assume that u, the functions a_{ij}, b_i, α, f and the boundary $\partial\Omega$ of the domain Ω are sufficiently smooth. Using now the Green theorem we obtain

$$A(v,u) + a(v,u) = -\int_\Omega v\Big(\sum_{i,j=1}^{3}\frac{\partial}{\partial x_i}\Big(a_{ij}\frac{\partial u}{\partial x_j}\Big) - \sum_{i=1}^{3} b_i\frac{\partial u}{\partial x_i}\Big)dx + \int_{\partial\Omega} v\sum_{i,j=1}^{3} a_{ij}n_i\frac{\partial u}{\partial x_j}\,dS \tag{7.1}$$

where the vector $\sigma = (\sigma_1, \sigma_2, \sigma_3)$,

$$\sigma_j = \sum_{i=1}^{3} a_{ij}n_i \,, \tag{7.2}$$

defined on $\partial\Omega$, is oriented towards the exterior of the domain Ω and is never tangential to its boundary $\partial\Omega$. Indeed, in view of (6.1), we have

$$(\sigma, n) \geq \text{const.} > 0 \,. \tag{7.3}$$

By means of a usual reasoning concerned with an integral from a continuous function it is now possible to write

$$(7.4)\qquad \sum_{i=1}^{3} a_{ii}\frac{\partial^2 u}{\partial x_i} + \sum_{\substack{i,j=1\\ i\neq j}}^{3} (a_{ij} + a_{ji})\frac{\partial^2 u}{\partial x_i \partial x_j} +$$

$$+ \sum_{i=1}^{3} \Big(\sum_{j=1}^{3} \frac{\partial a_{ji}}{\partial x_j} - b_i \Big) \frac{\partial u}{\partial x_i} = 0 \quad \text{in} \quad \Omega \ ,$$

$$(7.5)\qquad \alpha u + \langle \sigma, \operatorname{grad} u \rangle = f \quad \text{on} \quad \partial\Omega$$

and our definition from the preceding section then actually results in a generalization of the classical oblique derivative boundary problem.

8. Oblique derivative problem for Laplace equation

The differential operator on the right hand side of (7.4) will be the Laplacian operator if and only if the coefficients a_{ij} , b_i will satisfy the following relations

$$(8.1)\qquad \begin{aligned} a_{ii} &= 1 \ , \\ a_{12}(x) &= -\, a_{21}(x) = a_3(x) \ , \\ a_{23}(x) &= -\, a_{32}(x) = a_1(x) \ , \\ a_{31}(x) &= -\, a_{13}(x) = a_2(x) \ , \end{aligned}$$

$$(8.2)\qquad \begin{aligned} -b_1 &= \frac{\partial a_3}{\partial x_2} - \frac{\partial a_2}{\partial x_3} \ , \\ -b_2 &= \frac{\partial a_1}{\partial x_3} - \frac{\partial a_3}{\partial x_1} \ , \\ -b_3 &= \frac{\partial a_2}{\partial x_1} - \frac{\partial a_1}{\partial x_2} \ . \end{aligned}$$

In a case like this, the boundary problem (7.4), (7.5) will be of the form

$$\Delta u = 0 \quad in \quad \Omega \,, \tag{8.3}$$

$$\alpha u + \langle \sigma, grad\, u \rangle = f \quad on \quad \partial\Omega \tag{8.4}$$

where

$$\begin{aligned} \sigma_1 &= n_1 + a_2 n_3 - a_3 n_2 \,, \\ \sigma_2 &= -a_1 n_3 + n_2 + a_3 n_1 \,, \\ \sigma_3 &= a_1 n_2 - a_2 n_1 + n_3 \end{aligned} \tag{8.5}$$

and

$$\langle \sigma, n \rangle = 1 \,. \tag{8.6}$$

It is easy to arrive at some additional relations between vectors $a = (a_1, a_2, a_3)$, σ, n which hold on the boundary $\partial\Omega$ and result from equation (8.5). By direct calculation it is simple to verify that

$$\langle \sigma - n, a \rangle = 0 \,, \tag{8.7}$$

$$n \times \sigma = a - \langle n, a \rangle n \,, \tag{8.8}$$

$$a \times n = \sigma - n \,, \tag{8.9}$$

$$\sigma \times a = |a|^2 n - \langle n, a \rangle a - (\sigma - n) \,, \tag{8.10}$$

$$\begin{aligned} |n \times \sigma|^2 = |\sigma - n|^2 = |\sigma|^2 - 1 = tg^2(n,\sigma) = \\ = |a|^2 - \langle n, a \rangle^2 = \langle n \times \sigma, a \rangle \,, \end{aligned} \tag{8.11}$$

$$(8.12)\qquad |a \times n|^2 = |\sigma - n|^2 = |\sigma|^2 - 1 = \\ = |a|^2 \sin(n,a) \ ,$$

$$(8.13)\qquad |\sigma \times a|^2 = (|\sigma|^2 - 1)(1 + |a|^2) \ .$$

where $\times$ means the vector product.

9. Bilinear form

Our introduction of functions $a_i(x)$ has as yet been quite formal. We have also shown that the weak solution is, in fact, an extension of the respective classical notion.

Our aim is now to construct the functions $a_i(x)$ for the given vector σ satisfying (8.6) so as to meet equations (8.5) on the boundary. Recall that, according to the assumption, they together with the components of the vector

$$b = - \operatorname{curl} a$$

given by equation (8.2), should be bounded and Lebesgue-measurable in Ω .

It is obvious from (8.7) and (8.8) or (8.12) that the vector $a(x)$ is determined at point x of the boundary $\partial\Omega$ so as to be situated in the plane perpendicular to the vector $\sigma - n$, its modulus and position in this plane being interrelated by

$$(9.1)\qquad |\sigma|^2 - 1 = |a|^2 - (n,a)^2 = \\ = |a|^2 \sin^2(n,a) \ .$$

This indeterminacy is a consequence of the singularity of the system (8.5). It is simple to verify that its determinant equals zero.

Let us now approach the determination of the vector $a(x)$ at points x of the domain Ω .

Example 9.1. Suppose that the vector a , continuous on the closure $\bar{\Omega}$ of the domain Ω , is determined in Ω so that $curl\, a = 0$. Then there exists a function P such that

$$a = grad\, P \quad on \quad \bar{\Omega} \,. \tag{9.2}$$

Hence, owing to the fact that

$$\int_{(l)} \langle grad\, P, dl \rangle = 0 \tag{9.3}$$

is valid for an arbitrary closed curve situated in $\bar{\Omega}$, equation

$$\int_{(l)} \langle n \times \sigma , dl \rangle = \int_{(l)} |\sigma - n| \cos(n \times \sigma, dl)\, |dl| = 0 \tag{9.4}$$

must also be true on an arbitrary closed circuit (l) with regard to (8.8). Imagine now, for the purpose of practical interpretation, that the shape of the boundary $\partial\Omega$ is given by a form of the earth surface topography (possibly somewhat idealized) and $\sigma = \langle n, g \rangle^{-1} g$, where g is the gradient of the earth gravity field. Let $(\tilde{l})$ be any contour line on the side of a conical hill. It is obvious that such a line is closed and at every point x its tangential vector is co-linear with the direction of the vector product $n(x) \times \sigma(x)$ (i.e.,

it runs in the direction of $n \times \sigma$). Thus $\cos(n \times \sigma, d\tilde{\ell}) = 1$ along such a line and hence

$$\int_{(\tilde{\ell})} |\sigma - n| \, |d\tilde{\ell}| = 0 \tag{9.5}$$

which necessarily implies that $\sigma = n$ at all points of the contour line $(\tilde{\ell})$. However, this cannot be generally true. By analogy, it is not difficult to see that a similar result can be obtained for any closed surve along which $\cos(n \times \sigma, d\ell) > 0$. This means that the vector σ cannot be arbitrarily given as its choice is a priori limited by the shape of the boundary $\partial\Omega$ Returning now to the beginning of this example, it is evident that it is necessary to leave the assumption $\operatorname{curl} a = 0$ which, as has been shown, does not allow us to solve an oblique derivative problem (for the Laplace equation) for an arbitrary vector σ satisfying (8.6) only. Hence, it is too restrictive, particularly, for the solution of the linearized geodetic boundary problem.

Example 9.2. Suppose now that the vector a , continuous on $\bar{\Omega}$, is determined in Ω so that $(a, \operatorname{curl} a) = 0$ and $\operatorname{curl} a \neq 0$ is valid for all $x \in \Omega$ belonging to a certain neighbourhood of the boundary $\partial\Omega$. As is known, see SMIRNOV [17] , Chap. III, Sec. 79; Chap. IV, Sec. 122, under these assumptions there exists a function P and an integral multiplier μ such that

$$\mu a = \operatorname{grad} P \quad \text{on} \quad \bar{\Omega} \tag{9.6}$$

and

$$\mu \operatorname{curl} a = a \times \operatorname{grad} \mu \quad \text{on} \quad \bar{\Omega} \, . \tag{9.7}$$

It can be shown, on the basis of a similar reasoning as in the preceding example, that

$$(9.8)\qquad \int_{(\ell)} \mu \langle n \times \sigma, d\ell \rangle = \int_{(\ell)} \mu \, |\sigma - n| \, \cos(n \times \sigma, d\ell) \, |d\ell| = 0$$

necessary holds along any closed curve $(\ell) \in \partial\Omega$. As has already been demonstrated by the preceding example, the case $\mu(x) = const.$, $x \in \partial\Omega$ should be avoided. Let us imagine now, similarly as in example 9.1, that we have the vector field $\sigma = \langle n, g \rangle^{-1} g$ and our conical hill (with a rounded top). Let $(\hat{\ell})$ be any closed curve on the side of our hill running from point A to point B along a contour line; consequently, $\cos(n \times \sigma, d\hat{\ell}) = 1$ in this part of the curve; from point B to top C and from C to point A along the slope line; consequently, $\cos(n \times \sigma, d\hat{\ell}) = 0$ in these parts of the curve. Hence

$$(9.9)\qquad 0 = \int_{(\hat{\ell})} \mu \, |\sigma - n| \, d\hat{\ell} = \int_{(\hat{\ell}_{AB})} \mu \, |\sigma - n| \, d\hat{\ell}.$$

and in view of an arbitrary choice of points A, B on the mentioned contour line and the inequality $|\sigma - n| > 0$, equation (9.9) necessarily implies $\mu = 0$ along the whole contour line. However, the contour line itself was also arbitrarily chosen and thus it can be shown that $\mu = 0$ on the whole conical hill side. By means of closed curves composed of two segments on neighbouring contour lines and two segments on slope lines connecting the former, it can be finally shown that $\mu = 0$ is valid on the whole boundary $\partial\Omega$. Considering now (9.6), one can conclude that the coefficients a_i, $i = 1, 2, 3$, cannot be represented by means of the function P and the integral multiplier μ on the boundary $\partial\Omega$. This result is a natural consequence of the fact that there is

neither a scalar nor quasi-scalar field whose lines of force would run on $\partial\Omega$ in the direction of contour lines.

Summing up, to solve linearized geodetic boundary problem one must necessarily assume that

$$b = -\operatorname{curl} a \neq 0 \quad . \tag{9.10}$$

Hence, the bilinear form $A(v,u)$ is not symmetric and

$$A(v,u) = \int_\Omega \langle \operatorname{grad} v, \operatorname{grad} u \rangle \, dx + \int_\Omega \langle a, \operatorname{grad} v \times \operatorname{grad} u \rangle \, dx - \int_\Omega \langle \operatorname{curl} a, \operatorname{grad} u \rangle v \, dx \tag{9.11}$$

In view of equations

$$\langle a, \operatorname{grad} v \times \operatorname{grad} u \rangle = \langle \operatorname{grad} u, a \times \operatorname{grad} v \rangle , \tag{9.12}$$

$$\operatorname{curl} va = v \operatorname{curl} a - a \times \operatorname{grad} v \quad ,$$

see SMIRNOV [17] , Chap. IV, Sec. 124, we have

$$\langle \operatorname{curl} a , \operatorname{grad} u \rangle v = \langle \operatorname{curl} va, \operatorname{grad} u \rangle + \langle \operatorname{grad} u , a \times \operatorname{grad} v \rangle ,$$

thus also

$$A(v,u) = \int_\Omega \langle \operatorname{grad} v , \operatorname{grad} u \rangle \, dx - \int_\Omega \langle \operatorname{curl} va , \operatorname{grad} u \rangle \, dx \quad . \tag{9.13}$$

Assuming now that v, u, a_i are sufficiently smooth, it is possible to arrive at an equivalent form of the bilinear form $A(v,u)$. Hence, with the use of the Green theorem and the fact that $div\, curl\, va = 0$, we obtain

$$A(v,u) = \int_\Omega \langle grad\, v, grad\, u \rangle\, dx - \int_{\partial\Omega} \langle curl\, va, n \rangle\, u\, dS \tag{9.14}$$

and note that

$$\int_{\partial\Omega} \langle curl\, va, n \rangle\, dS = 0 \tag{9.15}$$

as a general consequence of the Stokes theorem, see SMIRNOV [17], Chap. III, Sec. 73.

A similar manipulation as in (9.12) yields

$$\langle curl\, va, n \rangle\, u = \langle curl\, vua, n \rangle + \langle n \times a, grad\, u \rangle\, v$$

and taking into consideration equation (8.9), we can conclude that the equivalent form of $A(v,u)$ is as follows

$$A(v,u) = \int_\Omega \langle grad\, v, grad\, u \rangle\, dx + \int_{\partial\Omega} \langle \sigma - n, grad\, u \rangle\, v\, dS\,. \tag{9.16}$$

Remark 9.1. The form in (9.16) is very important for practical computation. In that case we usually work

with sufficiently smooth functions and, consequently, the forms in (9.11) and (9.16) are equivalent.

10. V-ellipticity

It was shown in the preceding section in the case of the linearized geodetic boundary problem the weak solution concept is necessarily connected with the asymmetry of the form $A(v,u)$. This means that the Ritz method which consists of minimising a certain functional of energy cannot be used for the numerical solution. On the other hand, the use of methods like the Galerkin and least squares methods is not restricted as it does not necessarily require the symmetry of the form $A(v,u)$. However, this will not be discussed in detail in this paper. We merely refer to NEČAS [11] , REKTORYS [12] , WHITEMAN [19] , MIKHLIN [9] . Principally, it is necessary to choose in the space $W_2^{(1)}(\Omega)$ an appropriate function base. In this respect the finite elements approach as discussed in JUNKINS and ENGELS [3] seems to be very promising. The problem to find the weak solution (more precisely its approximation) consists, subsequently, of solving a certain system of linear equations.

The existence and uniqueness, in connection with direct variational methods are usually studied by means of the so-called V-ellipticity of the bilinear form $A(v,u) + a(v,u)$, see NEČAS [11] , Chap. 1, §3; REKTORYS [12] , Chap. 33. Hence, in the case of the problem defined in Sec. 8., the study on the existence and uniqueness of the weak solution requires to clarify the question for which $v \in W_2^{(1)}(\Omega)$ the inequality

$$(10.1)\quad A(v,v) + a(v,v) = \int_\Omega (\operatorname{grad} v, \operatorname{grad} v)\, dx - \int_\Omega (\operatorname{curl} a, \operatorname{grad} v)\, v\, dx + \int_{\partial\Omega} \alpha v^2\, dS \geq c \|v\|_1^2 , \quad c > 0,$$

and, after a small manipulation, the inequality

$$(10.1') \quad \int_\Omega \langle \operatorname{grad} v, \operatorname{grad} v \rangle \, dx - \frac{1}{2} \int_{\partial\Omega} \langle \operatorname{curl} a, n \rangle v^2 \, dS + \int_{\partial\Omega} \alpha v^2 \, dS \geq c \, \|v\|_1^2 , \quad c > 0 ,$$

where $\int_{\partial\Omega} \langle \operatorname{curl} a, n \rangle \, dS = 0$, is valid.

Example 10.1. Changing the notation slightly, we have shown in example 4.1 that the boundary condition for the simple Molodensky problem is of the form

$$\frac{1}{2} u - \frac{1}{2} \langle x, \operatorname{grad} u \rangle = H \quad \text{on} \quad \partial\Omega .$$

Assuming now that $\langle x, n \rangle > 0$ (i.e., the domain Ω is starshaped at the origin), the boundary condition can be given an equivalent form:

$$(10.2) \quad -\langle x, n \rangle^{-1} u + \langle x \langle x, n \rangle^{-1}, \operatorname{grad} u \rangle = -2 \langle x, n \rangle^{-1} H$$

which, compared with (8.4), yields

$$(10.3) \quad \alpha = -\langle x, n \rangle^{-1} , \quad \sigma = x \langle x, n \rangle^{-1} , \quad f = -2 \langle x, n \rangle^{-1} H .$$

Let now $v = \text{const.}$, then

$$A(v, v) + a(v, v) = -(\text{const.})^2 \int_{\partial\Omega} \langle x, n \rangle^{-1} dS < 0$$

and the inequality (10.1) cannot hold for such a function. Let further $v = x_i$; then, considering (8.5) and (10.2),

$$A(v,v) + a(v,v) = \int_\Omega dx +$$

$$+ \int_{\partial\Omega} (\sigma_i - n_i)\, x_i\, dS - \int_{\partial\Omega} \sigma_i x_i\, dS = 0$$

and the ineqality (10.1) cannot be valid either. The reason why we have failed in proving the V-ellipticity of the form $A(v,u) + a(v,u)$ for $v = const.$, $v = x_i$, $i = 1,2,3$ is somewhat deeper. In fact, for $u = x_i$ and all $v \in W_2^{(1)}(\Omega)$ (considering (8.5) again) we have

$$A(v,u) + a(v,u) = \int_\Omega \frac{\partial v}{\partial x_i}\, dx +$$

$$+ \int_{\partial\Omega} (\sigma_i - n_i)\, v\, dS - \int_{\partial\Omega} (x,n)^{-1} v x_i\, dS = 0$$

thus the functions x_i, $i = 1,2,3$, are, as is known, obvious solutions of the homogeneous simple Holodensky problem. These are, of course, ruled out by the condition (3.15) or (3.17). Let now ε, $0 < \varepsilon \leq 1$, be a sufficiently large constant. Supposing $\varepsilon \leq \cos(x,n) \leq 1$, it is possible to state conclusively that the V-ellipticity of the bilinear form $A(v,u) + a(v,u)$ can be proved for all $v \in W_2^{(1)}(\Omega)$ such that

$$\int_\Omega v\, dx = \int_\Omega v x_i\, dx = 0, \quad i = 1,2,3,$$

which is in conformity with the HÖRMANDER existence and uniqueness theorem 1.5.1 from [2], valid for the classical solution.

References

[1] Fučík, S.; Kufner, A.: Nelineární diferenciální rovnice. SNTL, Praha 1978.

[2] Hörmander, L.: The Boundary Problems of Physical Geodesy. The Royal Inst. of Technology, Division of Geodesy, Stockholm 1975; also in : Archive for Rational Mechanics and Analysis 62 (1976), 1-52.

[3] Junkins, J.L.; Engels, R.C.: The Finite Elements Approach in Gravity Modelling. Manuscripta Geodaetica, Vol. 4 (1979), 185-206.

[4] Kellogg, O.D.: Foundations of Potential Theory. Dover Publications, Inc., New York 1953.

[5] Krarup, T.: Letters on Molodensky's Problem I: The Simple Molodenskiy Problem. Unpublished manuscript communicated to the members of I.A.G. Special Study Group 4.31.

[6] Krarup, T.: Some Remarks about Collocation. In : Approximation Methods in Geodesy, Lectures Delivered at the 2nd Int. Summer School in the Mountains on Math. Methods in Physical Geodesy. Ramsau, Austria, August 23 to September 2, 1977. Edited by H. Moritz and H. Sunkel. H. Wischmann Verlag, Karlsruhe 1978, pp. 193-209.

[7] Kufner, A.; John, O.; Fučík, S.: Function Spaces. Academia, Prague 1977.

[8] Lions, J.L.; Magenes, E.: Problèmes aux limites non homogenes et applications, Volume 1. Dunod, Paris 1968.

[9] **Михлин, С.Г.: Вариационные методы в математической физике. Гостехиздат, Москва 1957.**

[10] Nakiboglu, S.M.: Variational Formulation of Geodetic Boundary Value Problem. Bull. Geod. (1978), 93-100.

[11] Nečas, J.: Les méthodes directes en théorie des équations elliptiques. Academia, Prague 1967.

[12] Rektorys, K.: Variační metody v inženýrských problémech a v problémech matematické fyziky. SNTL, Praha 1974.

[13] Rudin, W.: Principles of Mathematical Analysis. McGraw-Hill Book Company, New York 1964.

[14] Sansò, F.: The Geodetic Boundary Value Problem in Gravity Space. Memorie della Academia Nazionale dei Lincei. S. VIII, vol. XIV, Sez. I, 3; Roma 1977; pp. 39-97.

[15] Sansò, F.: The Local Solvability of Lolodensky's Problem in Gravity Space. Manuscripta Geodaetica, Vol. 3 (1978), 157-227.

[16] Sansò, F.: The Gravity Space Approach to the Geodetic Boundary Value Problem Including Rotational Effects. Manuscripta Geodaetica, Vol. 4 (1979), 207-244.

[17] Смирнов, В.И.: Курс высшей математики, том II . Наука, Москва 1965.

[18] Смирнов, В.И.: Курс высшей математики, том III , часть 2. Гос. изд. физ.-мат. лит., Москва 1958.

[19] The Mathematics of Finite Elements and Applications. Proceedings of the Brunel University Conference of the Inst. of Math. and Its Applications held in April 1972. Edited by J.R. Whiteman. Academic Press, London and New York 1973.

Genauigkeitsuntersuchungen zu dem gravimetrischen Verfahren der Bestimmung absoluter Höhenanomalien und Lotabweichungen aus terrestrischem Schwerematerial

J. Ihde
VEB Kombinat Geodäsie und Kartographie, Forschungszentrum

Summary

Three main error influences of remote areas (distance from the station $> 9^{\circ}$) on height anomalies and deflections of the vertical are being regarded:

a) The prediction errors of mean terrestrial free air anomalies have the greatest influence and amount to about $\pm$ 0",2 in each component for deflections of the vertical and to $\pm$ 3 m for height anomalies (results from 1977).

b) The error of the compartment method, which originates from converting the integral formulas of Stokes and Vening-Meinesz into summation formulas, can be neglected if the anomalies for points and gravity profiles are compiled to $5^{\circ} \times 5^{\circ}$ mean values.

c) The influences of the mean gravimetric correction terms of Arnold - estimated for important mountains of the earth by means of an approximate formula - on height anomalies may amount to 1 - 2 m and on deflections of the vertical to 0",05 - 0",1 and, therefore, they have to be taken into account for exact calculations.

The computations of errors are carried out using a covariance function of global free air anomalies for points.
The influences of different global data series of mean free air anomalies differ up to 7 m and 1" respectively. The latest gravimetric data series deduced by means of satellite altimetry may result in accuracies of better than $\pm$ 1 m for absolute height anomalies.

1. Einführung

Mit den globalen satellitengeodätischen Verfahren werden absolute geodätische Koordinaten erhalten, die sich auf ein geozentrisch gelagertes Koordinatensystem beziehen.

Das gravimetrische Verfahren der Bestimmung absoluter Höhenanomalien und Lotabweichungen ergibt in Verbindung mit den gemessenen natürlichen Koordinaten, der Normalhöhe und der astronomischen Breite und Länge, ebenfalls absolute geozentrische Koordinaten.

Was von dem astronomisch-gravimetrischen Verfahren und den satellitengeodätischen Verfahren jeweils nicht selbstständig gelöst werden kann, ist die Bestimmung der stationären Meerestopographie, die einmal als Grundlage für ozeanologische Forschungen zum anderen für die Anlage eines einheitlichen Welthöhensystems von Bedeutung ist. Sie läßt sich nur durch Kombination beider Verfahren ableiten, aus absoluten gravimetrischen Geoidhöhen in Verbindung mit satellitengeodätischen Altimetermessungen.

Vergleiche zwischen satellitengeodätisch und gravimetrisch abgeleiteten absoluten geodätischen Koordinaten für ein und denselben Punkt ergaben Koordinatenunterschiede bis zu 100 m. Untersuchungen zeigten, daß ein Großteil der Differenzen aus der Ungenauigkeit des globalen Schwerematerials, also aus dem gravimetrischen Verfahren resultierten. Nachfolgende Betrachtungen sollen klären, welche Genauigkeit mit der gravimetrischen Methode mit aktuellem globalen terrestrischen Schwerematerial (für Aufpunktentfernungen größer 1000 km) erreicht werden kann.

2. Untersuchte Fehlereinflüsse

Die Berechnung absoluter gravimetrischer Höhenanomalien und Lotabweichungen mit den Integralformeln von Stokes und Vening-Meinesz

$$\left.\begin{matrix} \\ \zeta \end{matrix}\right\} = \frac{R}{4\pi\gamma} \int_{\sigma} \Delta g_F \, S(\psi) \, d\sigma \qquad (1)$$

$$\left.\begin{matrix} \xi \\ \eta \end{matrix}\right\} = \frac{\varrho}{4\pi\gamma} \int_{\sigma} \Delta g_F \, V(\psi) \left\{\begin{matrix} \cos\alpha \\ \sin\alpha \end{matrix}\right\} d\sigma$$

setzt die Kenntnis der kontinuierlichen Schwereverteilung über die gesamte Erdoberfläche voraus. Praktisch liegt die gemessene Schwerebeschleunigung nur in diskreten Punkten vor, wodurch eine bestimmte Messungsdichte realisiert ist. Die diskreten Punktschwerewerte werden zu Mittelwerten prädiziert, die einen Prädiktionsfehler als Funktion der Messungsdichte besitzen. Der Einfluß des Prädiktionsfehlers auf Höhenanomalien und Lotabweichungen ist der erste untersuchte Fehlereinfluß.

Die Integralformeln nach Stokes und Vening-Meinesz gehen bei Verwendung mittlerer Freiluftanomalien $\overline{\Delta g_F}$ in Summenformeln über. Der dabei entstehende Fehler der mittleren Anomalien als Funktion der Kompartimentgröße wird als Summationsfehler bezeichnet.

Die Oberflächenfreiluftanomalien Δg_F werden bei der Berechnung von Höhenanomalien und Lotabweichungen an der Erdoberfläche nach der Theorie von Molodenski durch gravimetrische Korrekturglieder berichtigt. Im allgemeinen benutzt man nur das lineare Glied der Reihenlösungen von Molodenski oder Arnold. In die geodätische Praxis hat die lineare Lösung nach Pellinen mit der ebenen Reliefkorrektion als Approximation der Reihenentwicklung von Molodenski Eingang gefunden, die auch für das Gebiet der DDR angewendet wird.

Die Berechnung der linearen Korrekturglieder ist sehr aufwendig, so daß sie nur für einige Gebiete der Erde vorliegen und bei der Berechnung absoluter Höhenanomalien und Lotabweichungen im allgemeinen nur in aufpunktnahen Gebieten ($\psi < 1000$ km) berücksichtigt werden.

Als dritte Fehlergröße wird untersucht, welcher Fehlereinfluß auf Grund der Vernachlässigung der linearen Korrekturglieder in der globalen Zone entsteht.

3. Ergebnisse der Fehleruntersuchungen

3.1. Prädiktionsfehler mittlerer terrestrischer Freiluftanomalien

Die Prädiktionsfehler verursachen von den hier untersuchten Fehlern den größten Einfluß auf Höhenanomalien und Lotabweichungen.

Für die 1977 von Rapp [8] veröffentlichten terrestrischen flächengleichen $5^\circ \times 5^\circ$ - Freiluftanomalien wurden mit bekannten Messungsdichten für jedes Kompartiment individuelle Repräsentationsfehler abgeleitet und ihre Fortpflanzung auf Höhenanomalien und Lotabweichungen berechnet (Tafel 1). Wegen der hohen Messungsdichte im mitteleuropäischen Raum werden die Prädiktionsfehlereinflüsse der nahen Zone $\psi < 9^\circ$ vernachlässigbar klein angenommen (s. a. [4], Tafel 7).

Tafel 1
Einfluß individueller Prädiktionsfehler (Repräsentationsfehler) mittlerer Anomalien auf Höhenanomalien und Lotabweichungen für einen in der DDR gelegenen Aufpunkt

ψ_u	ψ_o	m_ζ in m	m_ξ in "	m_η in "
50°	180°	$\pm 3{,}11$	$\pm 0{,}166$	$\pm 0{,}148$
20°	180°	3,16	0,206	0,165
9°	180°	3,22	0,221	0,182

Aus dem Vergleich der Ergebnisse der numerischen Integration verschiedener Datenserien lassen sich gewisse Rückschlüsse auf die Genauigkeit der Höhenanomalien und Lotabweichungen ziehen. In Tafel 2 sind die Einflüsse der globalen Zone $\psi > 9^\circ$, die aus drei Serien mittlerer Freiluftanomalien abgeleitet wurden, gegenübergestellt. Die Differenzen zwischen den Ergebnissen können zum Teil auf die Vervollständigung des Schwerematerials (Erhöhung der Messungsdichte) und die unterschiedliche Verarbeitung der Ausgangsdaten zu mittleren Anomalien zurückgeführt werden. Allerdings überschreiten die Differenzen zwischen den Datenserien bei der Lotabweichung in Breite die Fehler aus individuellen Prädiktionsfehlern der mittleren Anomalien beträchtlich (Tafel 1).

Tafel 2
Ergebnisse der numerischen Integration der Freiluftanomalien drei verschiedener Epochen der Zone $9^\circ < \psi < 180^\circ$ bezogen auf die Helmertsche Normalschwereformel 1901 im System Potsdam

Jahr der Veröffentlichung	Datenserie	Literatur	Anzahl der Kompartimente	ζ	ξ	η
1970	$20^\circ \times 20^\circ$-ZIPE	1970 [2]	86			
	$5^\circ \times 5^\circ$-OSU	1959 [3]	326	+10 m	+2,3"	+1,8"
	$1^\circ \times 1^\circ$-GIP	1964 [1]	915			
1975	$5^\circ \times 5^\circ$-SAO	1975 [9]	1654	+18 m	+1,2"	+2,5"
1977	$5^\circ \times 5^\circ$-OSU	1977 [8]	1654	+20 m	+0,3"	+2,5"

3.2. Der Summationsfehler

Der Summationsfehler ist der Verfahrensfehler der Kompartimentmethode, bei dem zwei Fehlerursachen unterschieden werden (Tafel 3).

Tafel 3
Summationsfehlereinfluß mittlerer flächengleicher $5^\circ \times 5^\circ$ - Freiluftanomalien auf Höhenanomalien und Lotabweichungen

ψ_u	ψ_o	wegen mittleren Anomalien		wegen Mittelpunktwerten der analytischen Funktionen		Gesamteinfluß $m_{J\Sigma}$	Gesamteinfluß $m_{\Theta\Sigma}$
		in m	in "	in m	in "	in m	in "
50°	180°	$\pm$0,087	$\pm$0,0048	$\pm$0,024	$\pm$0,0009	$\pm$0,090	$\pm$0,0049
20°	180°	0,17	0,013	0,062	0,0073	0,18	0,015
9°	180°	0,30	0,044	0,22	0,074	0,37	0,086
4°	180°	0,53	0,21	1,03	0,80	1,16	0,83

Erstens gehen in die Rechnung statt der von den Integralformeln (1) geforderten kontinuierlichen Schwereverteilung mittlere Freiluftanomalien, also ein geglättetes Schwerefeld ein. Mittlere $5^\circ \times 5^\circ$ - Freiluftanomalien im Bereich $9^\circ < \psi < 180^\circ$ führen zu Fehlereinflüssen auf Höhenanomalien und Lotabweichungen von ± 0,3 m bzw. ± 0,04"; $1^\circ \times 1^\circ$ - Anomalien von ± 0,015 m bzw. ± 0,002". Dieser Einfluß ist vergleichbar mit dem Abbruchfehler bei der Verwendung von Kugelfunktionskoeffizienten.

Zweitens werden die Argumente ψ, α der analytischen Funktionen $S(\psi)$, $V(\psi)$, $\sin\alpha$, $\cos\alpha$ auf die Kompartimentmittelpunkte bezogen, wodurch wegen nichtlinearen Verlaufs der analytischen Funktionen Abweichungen zu ihren integralen Mittelwerten entstehen. Diese Fehlerquelle kann durch numerische Integration über $S(\psi)$, $V(\psi) \cdot \cos\alpha$, $V(\psi) \cdot \sin\alpha$ über jedes Kompartiment ausgeschaltet werden. Bereits eine Unterteilung in 4 Teilkompartimente führt zu vernachlässigbaren Fehlereinflüssen.

3.3. Fehlereinflüsse bei Nichtberücksichtigung gravimetrischer Korrekturglieder

Für die Berechnung des linearen mittleren gravimetrischen Korrekturgliedes nach Arnold wurde eine Näherungsformel abgeleitet und in zwei Testgebieten (Mittelgebirge, Hochgebirge) geprüft. Es wurde eine für die Fehlerschätzung genügend genaue Übereinstimmung mit streng berechneten mittleren Korrekturgliedern gefunden. Mit der Näherungsformel wurden für 60 bedeutende Gebirge und Erhebungen der Erde mittlere Korrekturglieder geschätzt ($\psi > 9^\circ$) und ihr Einfluß auf einen in der DDR gelegenen Aufpunkt berechnet:

$$\Delta\zeta_{\overline{KG}} = -1{,}7 \text{ m}$$
$$\Delta\xi_{\overline{KG}} = +0{,}045''$$
$$\Delta\eta_{\overline{KG}} = -0{,}105'' .$$

Es zeigt sich, daß die Nichtberücksichtigung der linearen Glieder der Lösungen des Randwertproblems für aufpunktferne Gebiete Fehler von einigen Metern sowohl bei absoluten Höhenanomalien als auch bei absoluten Lotabweichungen hervorrufen kann.

4. Diskussion der Ergebnisse

Die derzeit (Stand 1977) erreichbare Genauigkeit gravimetrischer Höhenanomalien und Lotabweichungen wird durch die Messungsdichte globaler terrestrischer Schwereanomalien begrenzt. Sie liegt für $9^\circ < \psi < 180^\circ$ bei

$$m_\zeta = \pm 3{,}2 \text{ m}, \quad m_\varepsilon = \pm 0{,}2''.$$

Die hohe Messungsdichte (etwa 2 km) der Punktschwerewerte im mitteleuropäischen Bereich rechtfertigt die Annahme, daß die Prädiktionsfehler der nahen Zone $\psi < 9^\circ$ annähernd ohne Einfluß bleiben.

Bei Verwendung mittlerer $5^{\circ} \times 5^{\circ}$ - Freiluftanomalien entstehen Summationsfehlereinflüsse

$$m_{\zeta\Sigma} = \pm 0{,}37 \text{ m}, \qquad m_{\Theta\Sigma} = \pm 0{,}09'' ,$$

die auf alle Fälle vernachlässigbar sind, wenn der Summationsfehleranteil wegen Mittelpunktwerten der analytischen Funktionen ausgeschaltet wird

$$m_{\zeta\Sigma} = \pm 0{,}3 \text{ m}, \qquad m_{\Theta\Sigma} = \pm 0{,}04'' .$$

Für Höhenanomalien mit dm - Genauigkeit und Lotabweichungen mit Fehlern kleiner 0";01 müssen $1^{\circ} \times 1^{\circ}$ - Mittelwerte der Freiluftanomalien verwendet werden. Die Freiluftanomalien müssen weltweit mit mittleren gravimetrischen Korrekturgliedern reduziert werden.
Mit derzeit erreichbaren Genauigkeiten satellitenaltimetrisch abgeleiteter mittlerer Freiluftanomalien auf den Ozeanflächen in Kombination mit terrestrischen Anomalien läßt sich bereits jetzt die Genauigkeit der Höhenanomalien auf $\pm$ 1 m verbessern. Eine weitere Steigerung der Genauigkeit der Höhenanomalien bzw. Geoidhöhen ist insofern von Bedeutung, als daß sich aus satellitengeodätischen Altimetermessungen in Verbindung mit gravimetrischen Geoidhöhen die stationäre Meerestopographie bestimmen läßt, die in den Pegelpunkten für die Anlage eines einheitlichen Höhensystems und als Grundlage für ozeanologische Forschungen wichtig ist.

Gravimetrisch abgeleitete absolute geodätische Koordinaten können in der Genauigkeit nicht mit absoluten satellitengeodätischen Koordinaten konkurrieren. Jedoch ist die gravimetrische Methode zur satellitengeodätischen als unabhängiges Verfahren auch in Zukunft von Bedeutung.

Literatur

[1] Arnold, K.: Die Freiluftanomalien im Europäischen Bereich.
Veröff. Geod. Inst. Potsdam, Berlin 1964, Nr. 24.

[2] Arnold, K.; Franske, P.; Stange, L.: Zur Bestimmung der Schwereanomalien und Geoidundulationen aus aufeinanderfolgenden Satellitendurchgängen in den Jahren 1967, 1968 und 1969.
Vermessungstechnik, Berlin 18 (1970) 12, S. 444.

[3] Heiskanen, W.A.; Moritz, H.: Physical Geodesy.
San Francisco and London:
W.H. Freeman and Company, 1967.

[4] Ihde, J.: Die optimale Verteilung der Messungsdichte von Schwerewerten zur Ableitung absoluter gravimetrischer Lotabweichungen und Höhenanomalien.
Vermess.-Techn., Berlin 28 (1980) 1, S. 12-16.

[5] Magnizki; Browar; Schimbirew: Theorie der Figur der Erde.
Berlin: Verlag für Bauwesen, 1964.

[6] Molodenski, M.S.: Grundbegriffe der geodätischen Gravimetrie.
Berlin: VEB Verlag Technik, 1960.

[7] Molodenski, M.S.; Eremeev, V.F.; Jurkina, M.J.:
Metody izučenija vnešnego gravitacionnogo polja i figury zemli. Arbeiten des CNIIGAiK, Moskau 1960, Nr. 131.

[8] Rapp, R.H.: Potential coefficient determiniations from 5^{o} terrestrial gravity data.
Ohio State Univ., Rep. Dep.
Geod. Sci., Columbus 1977, Nr. 251.

[9] Williamson, M.R.; Gaposchkin, E.M.: The estimation of 550 km x 550 km mean gravity anomalies.
Smithson. Astrophys. Obs.,
Smithson. Inst., Spec. Rep.,
Cambridge/Mass. 1975, No. 363.

Technische Universität Dresden
Sektion Geodäsie und Kartographie
W. Keller, S. Meier

GEODÄTISCHE INTEGRALFORMELN UND VERALLGEMEINERTE FUNKTIONEN

In den letzten Jahren wurde für gravimetrische Arbeiten in starkem Maße die Kollokation nach kleinsten Quadraten benutzt. Die Anwendung des Kollokationsverfahrens setzt die Kenntnis der statistischen Eigenschaften der ersten und zweiten Ableitungen des Störpotentials voraus. Gewöhnlich sind jedoch nur die statistischen Eigenschaften der Schwereanomalien Δg in Form deren Kovarianzfunktion C bekannt. Es muß daher folgende Aufgabe gelöst werden:

Vorgelegt seien: - ein stationärer Prozeß Δg in R^2 mit der Kovarianzfunktion C sowie

- Gewichtsfunktionen

$$f_i: \begin{cases} R^2 \longrightarrow R^1 \\ x \longrightarrow -\frac{1}{2\pi\gamma_o} \frac{x_i}{|x|^3} \end{cases} \qquad (i = 1,2).$$

Gesucht seien die Auto- bzw. Kreuzkovarianzfunktionen C_{ij} der Prozesse

$$s_i := f_i * \Delta g = -\frac{1}{2\pi\gamma_o} \int_{R^2} \frac{x_i - y_i}{|x-y|^3} \Delta g\,(y)\, dy \qquad (i = 1,2). \qquad (1)$$

Deutet man Δg als den Prozeß der Schwereanomalien, so erkennt man in (1) unschwer die ebene VENING-MEINESZ Formel und in den s_i die Prozesse der Lotabweichungskomponenten, d. h. der ersten Ableitungen des Störpotentials.

Von GRAFAREND wurden als Lösung des Problems die Beziehungen

$$C_{ij} = f_i * f_j * C \qquad (i,j = 1,2) \qquad (2)$$

angegeben. Es wurden jedoch keine Ausführungen über die Existenz der Faltungsprodukte (1), (2) gemacht. Die aus der Literatur bekannten hinreichenden Existenzbedingungen sind hier verletzt, da die Funktionen f_i an der Stelle Null nichtintegrierbare algebraische Singularitäten besitzen. Es bleibt daher offen, in welchem Sinn die Faltungsprodukte (1), (2) zu verstehen sind.

Im folgenden soll eine Deutung von (1) und (2) gegeben werden, die sich auf eine Verallgemeinerung des Funktionenbegriffs stützt.

VERALLGEMEINERTE FUNKTIONEN;
VERALLGEMEINERTE STOCHASTISCHE PROZESSE

Die Menge aller unendlich oft differenzierbaren, finiten Funktionen werde mit $\mathcal{D}$ bezeichnet. Die Elemente von $\mathcal{D}$ heißen auch Testfunktionen.
Ein lineares, stetiges Funktional auf $\mathcal{D}$ heißt verallgemeinerte Funktion oder auch Distribution. Die Menge der Distributionen werde mit $\mathcal{D}'$ bezeichnet. Durch (f, φ) werde die Anwendung eines $f \in \mathcal{D}'$ auf ein $\varphi \in \mathcal{D}$ symbolisiert. Schließlich sei $[\Omega, \mathcal{A}, P]$ ein Wahrscheinlichkeitsraum. Eine schwach meßbare Abbildung $X: \Omega \to \mathcal{D}'$ heißt verallgemeinerter stochastischer Prozeß (VSP).

Beispiele: 1. Durch die Abbildungen

$$f_i: \begin{cases} \mathcal{D} \to R^1 \\ \varphi \to -\frac{1}{2\pi\gamma_0} \int_0^\infty r^{-1} \int_0^{2\pi} \begin{pmatrix}\cos\alpha \\ \sin\alpha\end{pmatrix} \varphi(r\cos\alpha, r\sin\alpha)\, dx\, dr \end{cases} \qquad (i = 1,2) \qquad (3)$$

$$C: \begin{cases} \mathcal{D} \to R^1 \\ \varphi \to \int_{R^2} \varphi(x)\, C(x)\, dx \end{cases} \qquad (4)$$

werden lineare Funktionale auf $\mathcal{D}$ definiert. Den "klassischen" Funktionen f_i und C werden auf diese Weise Distributionen zugeordnet. Die für Distributionen definierten Operationen können somit auch auf "klassische" Funktionen angewendet werden.

2. Die Abbildung

$$\Delta g: \begin{cases} \Omega \to \mathcal{D}' \\ \omega \to \Delta g(\omega): (\Delta g(\omega), \varphi) := \int_{R^2} \Delta g(x, \omega)\, \varphi(x)\, dx \end{cases} \qquad (5)$$

definiert einen VSP. Dieser VSP ist in natürlicher Weise dem Prozeß Δg der Schwereanomalien zugeordnet. Dieser Prozeß im klassischen Sinne kann daher gleichzeitig als VSP betrachtet werden.

VERALLGEMEINERTE FALTUNG

Für $f, g \in \mathcal{D}'$ wird durch

$$(f \circledast g, \varphi) := (f(x), (g(y), \varphi(x+y))) \quad (\varphi \in \mathcal{D})$$

ein verallgemeinertes Faltungsprodukt $f \circledast g$ in $\mathcal{D}'$ definiert.

Während die Existenz der Faltungen $s_i = f_i * \Delta g$ im klassischen Sinne ungesichert ist, kann man zeigen, daß die verallgemeinerten Faltungen

$$\sigma_i := f_i \circledast \Delta g \qquad (i = 1,2) \qquad (7)$$

existieren, wenn f_i als Distribution und Δg als VSP gemäß (3), (5) aufgefaßt werden. Das Faltungsprodukt σ_i ist wiederum ein VSP. Es gilt ferner für die Auto- und Kreuzkovarianzdistribution der VSP σ_i:

$$C_{ij} = f_i \circledast f_j \circledast C . \qquad (i,j = 1,2) \qquad (8)$$

Die Prozesse σ_i und deren Auto- bzw. Kreuzkovarianzdistributionen sind zunächst verallgemeinerte Prozesse bzw. verallgemeinerte Funktionen. Eine unmittelbare geometrische oder physikalische Deutung dieser Größen ist daher nicht möglich. Man kann aber klassische Funktionen $\bar{C}_{ij}$ und stochastische Prozesse $\bar{s}_i$ angeben, so daß

$$(\sigma_i, \varphi) = \int_{R^2} \bar{s}_i(x, \omega)\varphi(x)\,dx \qquad (i = 1,2) \quad (\varphi \in \mathcal{D}) \qquad (9)$$

$$(C_{ij}, \varphi) = \int_{R^2} \bar{C}_{ij}(x)\varphi(x)\,dx \qquad (i,j = 1,2) \quad (\varphi \in \mathcal{D}) \qquad (10)$$

gilt. Es bestehen daher auch die folgenden Beziehungen

$$\bar{s}_i = f_i \circledast \Delta g \qquad (i = 1,2) \qquad (11)$$

$$\bar{C}_{ij} = f_i \circledast f_j \circledast C \qquad (i,j = 1,2). \qquad (12)$$

Die Prozesse $\bar{s}_i$ sind also die verallgemeinerten Faltungen von f_i mit Δg, und die Funktionen $\bar{C}_{ij}$ sind deren Auto- bzw. Kreuzkovarianzfunktionen.

Die von GRAFAREND angegebenen Beziehungen (2) sind daher gesichert, wenn alle auftretenden Faltungsoperationen als verallgemeinerte Faltungen gedeutet werden.
Falls jedoch die Faltungen (1) und (2) auch im klassischen Sinn existieren, gilt:

$$f_i \circledast \Delta g = f_i * \Delta g \qquad (i = 1,2) \qquad (13)$$

$$f_i \circledast f_j \circledast C = f_i * f_j * C. \quad (i,j = 1,2) \qquad (14)$$

Es ergeben sich in diesem Fall bei klassischer Rechnung und bei Rechnung über den Umweg verallgemeinerter Funktionen die gleichen Resultate. Sollte aber die klassische Rechnung versagen, so ist mit den verallgemeinerten Funktionen ein Mittel gegeben. dennoch zu sinnvollen Ergebnissen zu gelangen.

Literatur

[1] GEL'FAND, I. M.; ŠILOV, G. E.: Obobščennye funcii, Vyp 1. Isd. 2
Moskva: Fizmatgiz 1959

[2] GEL'FAND I. M.; VILENKIN, N. Ja.: Nekotorye primenenije garmoničeskogo analiza. Osnaščennye gilbertovy prostranstva, Obobščennye funcii, vyp. 4
Moskva: Fizmatgiz 1961

[3] GRAFAREND, E.: Isotropietests von Lotabweichungsverteilungen in Westdeutschland. I/II.
Z. Geophys., Würzburg 37 (1971) 4, S 719 - 733,
38 (1972) 2, S 243 - 255

[4] KELLER, W; MEIER, S.: Kovarianzfunktionen der 1. und 2. Ableitungen des Schwerepotentials in der Ebene.
Veröff. Zentralinst. f. Physik d. Erde, Potsdam
(im Druck)

The Similarity Transformation of the Gravitational Potential

Alfred Kleusberg

Geodätisches Institut der Universität Stuttgart

Summary

The transformation properties of the gravitational potential represented by spherical harmonics due to variations of type translation, rotation and scale are investigated. The similarity transformation is used close to the identity. It is proved (i) that scale and rotation variations do not change the degree of the spherical harmonics, but (ii) that a translation transforms spherical harmonics of degree ℓ into spherical harmonics of degree ℓ and $\ell + 1$. Geodetic examples are given: Rotational variation due to diurnal polar motion, translational variation due to mass centre shift and scale variation of the underlying coordinate system.

1. Introduction

A familiar expansion of the earths gravitational field in a coordinate system $S'(O',x',y',z')$ is

$$U(r',\lambda',\varphi') = g\cdot M \sum_{\ell=0}^{\infty} \frac{a^{\ell}}{r'^{\ell+1}} \sum_{m=0}^{\ell} P_{\ell m}(\sin\varphi')\,(C'_{\ell m}\cos m\lambda' + S'_{\ell m}\sin m\lambda') \qquad (1.1)$$

where

$$P_{\ell m}(x) = \frac{(1-x^2)^{\frac{m}{2}}}{2^{\ell}\,\ell!}\,\frac{d^{\ell+m}}{dx^{\ell+m}}\,(x^2-1)^{\ell}$$

are the Associated Legendre Functions and

$$\left.\begin{matrix} C_{\ell m} \\ S_{\ell m} \end{matrix}\right\} = \frac{2-\delta_{0m}}{M\cdot a^{\ell}}\,\frac{(\ell-m)!}{(\ell+m)!}\int r^{\ell} P_{\ell m}(\sin\varphi)\left\{\begin{matrix}\cos m\lambda \\ \sin m\lambda\end{matrix}\right\} dm$$

are the unnormalized Potential coefficients.

Using the relation

$$C'_{\ell m}\cos m\lambda' + S'_{\ell m}\sin m\lambda' = \frac{1}{2}\left[(C'_{\ell m} - i\,S'_{\ell m})\exp im\lambda' + (C'_{\ell m} + i\,S'_{\ell m})\exp -im\lambda'\right]$$

where $i^2 = -1$

we get an expression equivalent to(1.1) which is more convenient for transformation purposes.

$$U(r', \lambda', \varphi') = gM \sum_{\ell=0}^{\infty} \frac{a^{\ell}}{r'^{\ell+1}} \sum_{m=0}^{\ell} P_{\ell m}(\sin\varphi') \frac{1}{2} [(C'_{\ell m} - i S'_{\ell m}) \exp im\lambda' + (C'_{\ell m} + i S'_{\ell m}) \exp -im\lambda'] \quad (1.2)$$

If we want to express the potential (1.2) in another coordinate system S (O,x,y,z)

$$U(r, \lambda, \varphi) = gM \sum_{\ell=0}^{\infty} \frac{a^{\ell}}{r^{\ell+1}} \sum_{m=0}^{\ell} P_{\ell m}(\sin\varphi) \frac{1}{2} [(C_{\ell m} - i S_{\ell m}) \exp im\lambda + (C_{\ell m} + i S_{\ell m}) \exp -im\lambda] \quad (1.3)$$

we have to perform a transformation of the potential coefficients

$C'_{\ell m}, S'_{\ell m} \longrightarrow C_{\ell m}, S_{\ell m}$.

Such a transformation may be necessary by reason of the following examples

(i) The expansion of the earths gravitational potential (1.1) would be sufficient timelike invariant if evaluated in the figur axis coordinate system of a rigid earth. But the figur axis varies from epoch to epoch with respect to an earth-fixed system due to non-rigidity. These variations can be described by physical models (*McClure* 1973). To express the gravitational potential in the earth-fixed system one has to perform a transformation with timelike varying transformation parameters α, β (Rotation about x,y axis, respectively) derived from the physical model.

(ii) There are many different earth models (e.g. Goddard Earth Models, SAO Standard Earths). To prove, whether there are different underlying coordinate systems used one has to investigate whether transformation parameters are derivable from the different potential expansions.

Many authors dealt with transformation of spherical harmonics (*Jeffreys* 1964,

Aardom 1969, *Winch and James* 1973, *Balmino and Borderies* 1977, *Sidlichovsky* 1978, 1979, *Ciaccaglia* 1980). They introduced transformation parameters of any largeness for rotation and translation. Thus the Wigner 3-j-coefficients appear in the transformation formulae.
In the above mentioned examples (i) and (ii) the transformation parameters can be assumed to be very small. Therefore we are going to derive more convenient formulae for the special case of a similarity transformation close to the identity.

2. The similarity transformation close to the identity

Suppose the transformation $S \rightarrow S'$ for any vector $\bar{x}$ is given by

$$\bar{x}' = (1+\delta k)\, R\,(\alpha,\beta,\gamma)\,(\bar{x} + \bar{t}) \qquad (2.1)$$

where $\delta k, \alpha, \beta, \gamma$ are scale variation, rotation angles about the x-axis, y-axis and z-axis, respectively and $\bar{t} = [tx,ty,tz]^T$ is the origin translation vector. Furthermore assume all transformation parameters to be small enough to neglect squares and products. Then (2.1) can be linear approximated by

$$\begin{bmatrix} x' \\ y' \\ z' \end{bmatrix} = \begin{bmatrix} x \\ y \\ z \end{bmatrix} + \begin{bmatrix} \delta k\cdot x + \gamma\cdot y - \beta\cdot z + tx \\ \delta k\cdot y - \gamma\cdot x + \alpha\cdot z + ty \\ \delta k\cdot z + \beta\cdot x - \alpha\cdot y + tz \end{bmatrix} = \begin{bmatrix} x \\ y \\ z \end{bmatrix} + \begin{bmatrix} \delta x \\ \delta y \\ \delta z \end{bmatrix} \qquad (2.2)$$

Using

$$r' = (x'^2+y'^2+z'^2)^{1/2} = ((x+\delta x)^2 + (y+\delta y)^2 + (z+\delta z)^2)^{1/2}$$

$$\lambda' = \arctan \frac{y'}{x'} = \arctan \frac{y+\delta y}{x+\delta x}$$

$$\varphi' = \arctan \frac{z'}{(x'^2+y'^2)^{1/2}} = \arctan \frac{z+\delta z}{((x+\delta x)^2+(y+\delta y)^2)^{1/2}}$$

and

$$\cos\lambda = \frac{1}{2}(\exp i\lambda + \exp -i\lambda)$$

$$\sin\lambda = \frac{i}{2}(\exp -i\lambda - \exp i\lambda)$$

we get the transformation $S \rightarrow S'$ in spherical coordinates in linear approximation

$$\begin{bmatrix} r' \\ \lambda' \\ \varphi' \end{bmatrix} = \begin{bmatrix} r \\ \lambda \\ \varphi \end{bmatrix} + \begin{bmatrix} \delta r \\ \delta\lambda \\ \delta\varphi \end{bmatrix}$$

where

$$\delta r = r\cdot\delta k + \frac{1}{2}\cos\varphi\,[(tx - ity)\exp i\lambda + (tx + ity)\exp -i\lambda] + tz\sin\varphi$$

$$\delta\lambda = -\gamma + \frac{1}{2}\tan\varphi\,[(\alpha + i\beta)\exp -i\lambda + (\alpha - i\beta)\exp i\lambda] -$$

$$- \frac{1}{2r\cos\varphi}\,[(ty + itx)\exp i\lambda + (ty - itx)\exp -i\lambda] \qquad (2.3)$$

$$\delta\varphi = \frac{1}{2}\,[(\beta + i\alpha)\exp i\lambda + (\beta - i\alpha)\exp -i\lambda] + \frac{tz}{r}\cos\varphi -$$

$$- \frac{\sin\varphi}{2r}\,[(tx + ity)\exp -i\lambda + (tx - ity)\exp i\lambda].$$

If the transformation parameters are small the expansion of the potential in S' can be expressed as a linear function of the potential representation in S,

$$U(r',\lambda',\varphi') = U(r,\lambda,\varphi) + \frac{\partial}{\partial r}U(r,\lambda,\varphi)\,\delta r + \frac{\partial}{\partial\lambda}U(r,\lambda,\varphi)\,\delta\lambda + \frac{\partial}{\partial\varphi}U(r,\lambda,\varphi)\,\delta\varphi \qquad (2.4)$$

where

$$\frac{\partial}{\partial r}U(r,\lambda,\varphi) = -gM\sum_{\ell=0}^{\infty}\frac{a^{\ell}(\ell+1)}{r^{\ell+2}}\sum_{m=0}^{\ell}P_{\ell m}(\sin\varphi)\,\frac{1}{2}\,[(C'_{\ell m} - iS'_{\ell m})\exp im\lambda +$$

$$+ (C'_{\ell m} + iS'_{\ell m})\exp -im\lambda]$$

$$\frac{\partial}{\partial\lambda}U(r,\lambda,\varphi) = gM\sum_{\ell=0}^{\infty}\frac{a^{\ell}}{r^{\ell+1}}\sum_{m=0}^{\ell}P_{\ell m}(\sin\varphi)\,\frac{m}{2}\,[(S'_{\ell m} + iC'_{\ell m})\exp im\lambda + \qquad (2.5)$$

$$+ (S'_{\ell m} - iC'_{\ell m})\exp -im\lambda]$$

$$\frac{\partial}{\partial\varphi}U(r,\lambda,\varphi) = gM\sum_{\ell=0}^{\infty}\frac{a^{\ell}}{r^{\ell+1}}\sum_{m=0}^{\ell}(-m\tan\varphi\,P_{\ell m}(\sin\varphi) + P_{\ell,m+1}(\sin\varphi))\cdot$$

$$\cdot\frac{1}{2}\,[(C'_{\ell m} - iS'_{\ell m})\exp im\lambda + (C'_{\ell m} + iS'_{\ell m})\exp -im\lambda]$$

and δr, $\delta\lambda$, $\delta\varphi$ are given in (2.3).

3. Transformation Formulae

If we insert (2.3) and (2.5) into Equ. (2.4) and use some recurrence formulae for Legendre's associated functions given by (*Kertz*, 1973) finally we get transformation formulae for potential coefficients under a similarity transformation close to the identity (for detailed computation see Appendix).

$$
\begin{aligned}
C_{\ell m} = {} & [1-\delta k\,(\ell+1)]\; C'_{\ell m} - [m\cdot\gamma]\; S'_{\ell m} \\
& + \left[\frac{1+\delta_{1m}}{2}\,\beta\right] C'_{\ell,m-1} + \left[\frac{1+\delta_{1m}}{2}\,\alpha\right] S'_{\ell,m-1} \\
& - \left[\frac{(\ell+m+1)\,(\ell-m)}{2}\,\beta\right] C'_{\ell,m+1} + \left[\frac{(\ell+m+1)\,(\ell-m)}{2}\,\alpha\right] S'_{\ell,m+1} \\
& - \left[(\ell-m)\,\frac{tz}{a}\right] C'_{\ell-1,m} \\
& - \left[\frac{1+\delta_{1m}}{2}\,\frac{tx}{a}\right] C'_{\ell-1,m-1} + \left[\frac{1+\delta_{1m}}{2}\,\frac{ty}{a}\right] S'_{\ell-1,m-1} \\
& + \left[\frac{(\ell-m-1)\,(\ell-m)}{2}\,\frac{tx}{a}\right] C'_{\ell-1,m+1} + \left[\frac{(\ell-m-1)\,(\ell-m)}{2}\,\frac{ty}{a}\right] S'_{\ell-1,m-1}
\end{aligned}
\tag{3.1}
$$

$$
\begin{aligned}
S_{\ell m} = {} & [1-\delta k\,(\ell+1)]\; S'_{\ell m} + [m\cdot\gamma]\; C'_{\ell m} \\
& + \left[\frac{1+\delta_{1m}}{2}\,\beta\right] S'_{\ell,m-1} - \left[\frac{1+\delta_{1m}}{2}\,\alpha\right] C'_{\ell,m-1} \\
& - \left[\frac{(\ell+m+1)\,(\ell-m)}{2}\,\beta\right] S'_{\ell,m+1} - \left[\frac{(\ell+m+1)\,(\ell-m)}{2}\,\alpha\right] C'_{\ell,m+1} \\
& - \left[(\ell-m)\,\frac{tz}{a}\right] S'_{\ell-1,m} \\
& - \left[\frac{1+\delta_{1m}}{2}\,\frac{tx}{a}\right] S'_{\ell-1,m-1} - \left[\frac{1+\delta_{1m}}{2}\,\frac{ty}{a}\right] C'_{\ell-1,m-1} \\
& + \left[\frac{(\ell-m-1)\,(\ell-m)}{2}\,\frac{tx}{a}\right] S'_{\ell-1,m+1} - \left[\frac{(\ell-m-1)\,(\ell-m)}{2}\,\frac{ty}{a}\right] C'_{\ell-1,m+1}
\end{aligned}
\tag{3.2}
$$

For most purposes the use of fully normalized spherical harmonics and potential coefficients is more convenient, i.e.:

$$
U = gM \sum_{\ell=0}^{\infty} \frac{a^{\ell}}{r^{\ell+1}} \sum_{m=0}^{\ell} \overline{P}_{\ell m}(\sin\varphi)\,(\overline{C}_{\ell m}\cos m\lambda + \overline{S}_{\ell m}\sin m\lambda)
$$

$$\bar{P}_{\ell m} = \sqrt{(2-\delta_{om})\ (2\ell+1)\ \frac{(\ell-m)!}{(\ell+m)!}}\ P_{\ell m}$$

$$\left.\begin{matrix}\bar{C}_{\ell m}\\ \bar{S}_{\ell m}\end{matrix}\right\} = \sqrt{\frac{1}{(2-\delta_{om})\ (2\ell+1)\ \frac{(\ell+m)!}{(\ell-m)!}}} \left\{\begin{matrix}C_{\ell m}\\ S_{\ell m}\end{matrix}\right.$$

Using these functions for the expansion of the gravitational potential we get the more symmetric transformation formulae

$$\begin{aligned}
\bar{C}_{\ell m} = {} & [1-\delta k(\ell+1)]\ \bar{C}'_{\ell m} - [m\cdot\gamma]\ \bar{S}'_{\ell m} \\
& + [(\ell-m+1)\ (\ell+m)\ (1+\delta_{1m})]^{1/2}\ [\tfrac{\beta}{2}\ \bar{C}'_{\ell,m-1} + \tfrac{\alpha}{2}\ \bar{S}'_{\ell,m-1}] \\
& - [(\ell+m+1)\ (\ell-m)]^{1/2}\ [\tfrac{\beta}{2}\ \bar{C}'_{\ell,m+1} - \tfrac{\alpha}{2}\ \bar{S}'_{\ell,m+1}] \\
& - [\tfrac{2\ell-1}{2\ell+1}\ (\ell+m)\ (\ell-m)]^{1/2}\ \tfrac{tz}{a}\ \bar{C}'_{\ell-1,m} \\
& - [\tfrac{2\ell-1}{2\ell+1}\ (\ell+m-1)\ (\ell+m)\ (1+\delta_{1m})]^{1/2}\ [\tfrac{tx}{2a}\ \bar{C}'_{\ell-1,m-1} - \tfrac{ty}{2a}\ \bar{S}'_{\ell-1,m-1}] \\
& + [\tfrac{2\ell-1}{2\ell+1}\ (\ell-m-1)\ (\ell-m)]^{1/2}\ [\tfrac{tx}{2a}\ \bar{C}'_{\ell-1,m+1} + \tfrac{ty}{2a}\ \bar{S}'_{\ell-1,m+1}]
\end{aligned} \tag{3.3}$$

$$\begin{aligned}
\bar{S}_{\ell m} = {} & [1-\delta k\ (\ell+1)]\ \bar{S}'_{\ell m} + [m\cdot\gamma]\ \bar{C}'_{\ell m} \\
& + [(\ell-m+1)\ (\ell+m)\ (1+\delta_{1m})]^{1/2}\ [\tfrac{\beta}{2}\bar{S}'_{\ell m-1} - \tfrac{\alpha}{2}\ \bar{C}'_{\ell,m-1}] \\
& - [(\ell+m+1)\ (\ell-m)]^{1/2}\ [\tfrac{\beta}{2}\bar{S}'_{\ell,m+1} + \tfrac{\alpha}{2}\ \bar{C}'_{\ell,m+1}] \\
& - [\tfrac{2\ell-1}{2\ell+1}\ (\ell+m)\ (\ell-m)]^{1/2}\ \tfrac{tz}{a}\ \bar{S}'_{\ell-1,m} \\
& - [\tfrac{2\ell-1}{2\ell+1}\ (\ell+m-1)\ (\ell+m)\ (1+\delta_{1m})]^{1/2}\ [\tfrac{tx}{2a}\bar{S}'_{\ell-1,m-1} + \tfrac{ty}{2a}\ \bar{C}'_{\ell-1,m-1}] \\
& + [\tfrac{2\ell-1}{2\ell+1}\ (\ell-m-1)\ (\ell-m)]^{1/2}\ [\tfrac{tx}{2a}\bar{S}'_{\ell-1,m+1} - \tfrac{ty}{2a}\ \bar{C}'_{\ell-1,m+1}]
\end{aligned} \tag{3.4}$$

4. Numerical examples

Example 1: Diurnal Polar Motion

Mc Clure (1973) states that the diurnal variation of the axis of principal moment of inertia with respect to the rotation axis may come up to an amount of ± 60m which corresponds to rotation angles of ± 2'' about the x-axis or y-axis. *Nagel* (1976) computes the corresponding addition term of the second degree potential coefficients from variations of the second order inertia tensor. This leads to

$$\begin{aligned} C_{21} &= C'_{21} + \beta \cdot C'_{20} \\ S_{21} &= S'_{21} - \alpha \cdot C'_{20} \end{aligned} \qquad (4.1)$$

Using the equations (3.1) and (3.2) we get

$$\begin{aligned} C_{21} &= C'_{21} + \beta \cdot C'_{20} - 2\beta C'_{22} + 2\alpha S'_{22} \\ S_{21} &= S'_{21} - \alpha \cdot C'_{20} - 2\beta S'_{22} - 2\alpha C'_{22}. \end{aligned} \qquad (4.2)$$

Both systems of formulae yield variations in C_{21} and S_{21} of $1 \cdot 10^{-8}$ at most. The differences between (4.1) and (4.2) are of order 10^{-10}. The variation of the potential coefficients of higher degree due to diurnal polar motion are still neglectable at present. Some examples:

$$\bar{C}_{3,0} = \bar{C}'_{3,0} \pm 5 \cdot 10^{-11}$$

$$\bar{C}_{13,1} = \bar{C}'_{13,1} \pm 7 \cdot 10^{-12}$$

$$\bar{C}_{28,0} = \bar{C}'_{28,0} \pm 3 \cdot 10^{-12}$$

Example 2: Datum Shift

Introducing an origin translation vector $t = (tx, ty, tz)^T$ yields the well known formulae for the variation of first degree coefficients:

$$\bar{C}_{11} = \bar{C}'_{11} - \bar{C}'_{00} \cdot \left(\frac{1}{3}\right)^{1/2} \cdot \frac{tx}{a}$$

$$\bar{S}_{11} = \bar{S}'_{11} - \bar{C}'_{00} \cdot \left(\frac{1}{3}\right)^{1/2} \cdot \frac{ty}{a}$$

$$\bar{C}_{10} = \bar{C}'_{10} - \bar{C}'_{00} \cdot \left(\frac{1}{3}\right)^{1/2} \cdot \frac{tz}{a}$$

For $t = (100m, 100m, 100m)$ and $\bar{C}'_{11} = \bar{S}'_{11} = \bar{C}'_{10} = 0$ we get $\bar{C}_{11} = \bar{S}_{11} = \bar{C}_{10} \approx$ $\approx -0.9 \cdot 10^{-5}$.

The variations of higher degree coefficients are of order $< 10^{-7}$.
Some examples:

$$\bar{C}_{3,1} = \bar{C}'_{3,1} \pm 10^{-8}$$

$$\bar{S}_{3,1} = \bar{S}'_{3,1} \pm 10^{-10}$$

$$\bar{C}_{13,1} = \bar{C}'_{13,1} \pm 10^{-11}$$

$$\bar{C}_{28,0} = \bar{C}'_{28,0} \pm 10^{-11}$$

Example 3: Scale variation

Scale variation δk of the underlying coordinate system results in

$$\left.\begin{matrix}\bar{C}_{\ell m} \\ \bar{S}_{\ell m}\end{matrix}\right\} = (1-(\ell+1)\delta k) \cdot \left\{\begin{matrix}\bar{C}'_{\ell m} \\ \bar{S}'_{\ell m}\end{matrix}\right.$$

The effect of scale variation increases linearly for increasing degree of the coefficients. For a realistic value $\delta k = \pm 1.10^{-6}$ this leads to variations of $\mp 3 \cdot 10^{-5}$ for coefficients of degree 30 which is below the threshold of significance.

Appendix

From Equations (2.3) - (2.5) we get

$$U = gM \sum_{\ell=0}^{\infty} \frac{a^{\ell}}{r^{\ell+1}} \sum_{m=0}^{\ell} P_{\ell m}(\sin\varphi)\frac{1}{2}[(C'_{\ell m}-iS'_{\ell m})\exp im\lambda+(C'_{\ell m}+iS'_{\ell m})\exp -im\lambda] \quad (A1)$$

$$- gM \sum_{\ell=0}^{\infty} \frac{a^{\ell}}{r^{\ell+1}} \sum_{m=0}^{\ell} P_{\ell m}(\sin\varphi)\frac{1}{2}[(C'_{\ell m}-iS'_{\ell m})\exp im\lambda+(C'_{\ell m}+iS'_{\ell m})\exp -im\lambda]\cdot(\ell+1)\delta k \quad (A2)$$

$$- gM \sum_{\ell=0}^{\infty} \frac{a^{\ell}}{r^{\ell+2}} \sum_{m=0}^{\ell} P_{\ell m}(\sin\varphi)\frac{1}{2}[(C'_{\ell m}-iS'_{\ell m})\exp im\lambda+(C'_{\ell m}+iS'_{\ell m})\exp -im\lambda]\cdot(\ell+1)\cdot$$

$$\cdot\frac{\cos\varphi}{2}[(tx-ity)\exp i\lambda+(tx+ity)\exp -i\lambda] \quad (A3)$$

$$- gM \sum_{\ell=0}^{\infty} \frac{a^{\ell}}{r^{\ell+2}} \sum_{m=0}^{\ell} P_{\ell m}(\sin\varphi)\frac{1}{2}[(C'_{\ell m}-iS'_{\ell m})\exp im\lambda+(C'_{\ell m}+iS'_{\ell m})\exp -im\lambda]\cdot$$

$$\cdot(\ell+1)\cdot tz\cdot\sin\varphi \quad (A4)$$

$$- gM \sum_{\ell=0}^{\infty} \frac{a^{\ell}}{r^{\ell+1}} \sum_{m=0}^{\ell} P_{\ell m}(\sin\varphi)\frac{1}{2}[(S'_{\ell m}+iC'_{\ell m})\exp im\lambda+(S'_{\ell m}-iC'_{\ell m})\exp -im\lambda]\cdot m\cdot\gamma \quad (A5)$$

$$+ gM \sum_{\ell=0}^{\infty} \frac{a^{\ell}}{r^{\ell+1}} \sum_{m=0}^{\ell} P_{\ell m}(\sin\varphi)\frac{1}{2}[(S'_{\ell m}+iC'_{\ell m})\exp im\lambda+(S'_{\ell m}-iC'_{\ell m})\exp -im\lambda]\cdot$$

$$\cdot m\cdot\frac{\tan\varphi}{2}[(\alpha-i\beta)\exp i\lambda+(\alpha+i\beta)\exp -i\lambda] \quad (A6)$$

$$+ gM \sum_{\ell=0}^{\infty} \frac{a^{\ell}}{r^{\ell+2}} \sum_{m=0}^{\ell} P_{\ell m}(\sin\varphi)\frac{1}{2}[(S'_{\ell m}+iC'_{\ell m})\exp im\lambda+(S'_{\ell m}-iC'_{\ell m})\exp -im\lambda]\cdot$$

$$\cdot m\cdot\frac{1}{2\cos\varphi}[(ty-itx)\exp -i\lambda+(ty+itx)\exp i\lambda] \quad (A7)$$

$$- gM \sum_{\ell=0}^{\infty} \frac{a^{\ell}}{r^{\ell+1}} \sum_{m=0}^{\ell} P_{\ell m}(\sin\varphi)\frac{1}{2}[(C'_{\ell m}-iS'_{\ell m})\exp im\lambda+(C'_{\ell m}+iS'_{\ell m})\exp -im\lambda]\cdot$$

$$\cdot m\cdot\frac{\tan\varphi}{2}[(\beta+i\alpha)\exp i\lambda+(\beta-i\alpha)\exp -i\lambda] \quad (A8)$$

$$- gM \sum_{\ell=0}^{\infty} \frac{a^{\ell}}{r^{\ell+2}} \sum_{m=0}^{\ell} P_{\ell m}(\sin\varphi)\frac{1}{2}[(C'_{\ell m}-iS'_{\ell m})\exp im\lambda+(C'_{\ell m}+iS'_{\ell m})\exp -im\lambda]\cdot$$

$$\cdot m\cdot\tan\varphi\cdot\cos\varphi\cdot tz \quad (A9)$$

$$+ gM \sum_{\ell=0}^{\infty} \frac{a^{\ell}}{r^{\ell+2}} \sum_{m=0}^{\ell} P_{\ell m}(\sin\varphi)\frac{1}{2}[(C'_{\ell m}-iS'_{\ell m})\exp im\lambda+(C'_{\ell m}+iS'_{\ell m})\exp -im\lambda]\cdot m\cdot\tan\varphi\cdot$$

$$\cdot\frac{\sin\varphi}{2}[tx-ity)\exp i\lambda+(tx+ity)\exp -i\lambda] \quad (A10)$$

$$+ gM \sum_{\ell=0}^{\infty} \frac{a^{\ell}}{r^{\ell+1}} \sum_{m=0}^{\ell} P_{\ell,m+1}(\sin\varphi)\frac{1}{2}[(C'_{\ell m}-iS'_{\ell m})\exp\, im\lambda+(C'_{\ell m}+iS'_{\ell m})\exp -im\lambda]\cdot$$

$$\cdot\frac{1}{2}[(\beta+i\alpha)\exp\, i\lambda+(\beta-i\alpha)\exp -i\lambda] \qquad (A11)$$

$$+ gM \sum_{\ell=0}^{\infty} \frac{a^{\ell}}{r^{\ell+2}} \sum_{m=0}^{\ell} P_{\ell,m+1}(\sin\varphi)\frac{1}{2}[(C'_{\ell m}-iS'_{\ell m})\exp\, im\lambda+(C'_{\ell m}+iS'_{\ell m})\exp -im\lambda]\cdot\cos\varphi\cdot tz \qquad (A12)$$

$$- gM \sum_{\ell=0}^{\infty} \frac{a^{\ell}}{r^{\ell+2}} \sum_{m=0}^{\ell} P_{\ell,m+1}(\sin\varphi)\frac{1}{2}[(C'_{\ell m}-iS'_{\ell m})\exp\, im\lambda+(C'_{\ell m}+iS'_{\ell m})\exp -im\lambda]\cdot$$

$$\cdot\frac{\sin\varphi}{2}[(tx-ity)\exp\, i\lambda+(tx+ity)\exp -i\lambda] \qquad (A13)$$

This Taylor expansion can be summarized in six terms depending on the transformation parameters (2.1)

$$U = U_o + U_1(\delta k) + U_2(\gamma) + U_3(\alpha,\beta) + U_4(tz) + U_5(tx,ty) \qquad (A14)$$

$$U_o = gM \sum_{\ell=0}^{\infty} \frac{a^{\ell}}{r^{\ell+1}} \sum_{m=0}^{\ell} P_{\ell m}(\sin\varphi)\frac{1}{2}[(C'_{\ell m}-iS'_{\ell m})\exp\, im\lambda+(C'_{\ell m}+iS'_{\ell m})\exp -im\lambda]$$

$$= gM \sum_{\ell=0}^{\infty} \frac{a^{\ell}}{r^{\ell+1}} \sum_{m=0}^{\ell} P_{\ell m}(\sin\varphi)\ (C'_{\ell m}\cos m\lambda+S'_{\ell m}\sin m\lambda)$$

$$U_1(\delta k) = gM \sum_{\ell=0}^{\infty} \frac{a^{\ell}}{r^{\ell+1}} \sum_{m=0}^{\ell} P_{\ell m}(\sin\varphi)\frac{1}{2}[(C'_{\ell m}-iS'_{\ell m})\exp\, im\lambda+(C'_{\ell m}+iS'_{\ell m})\exp -im\lambda](\ell+1)\delta k$$

$$= gM \sum_{\ell=0}^{\infty} \frac{a^{\ell}}{r^{\ell+1}} \sum_{m=0}^{\ell} P_{\ell m}(\sin\varphi)\ (C'_{\ell m}\cos m\lambda+S'_{\ell m}\sin m\lambda)\cdot(\ell+1)\delta k$$

$$U_2(\gamma) = gM \sum_{\ell=0}^{\infty} \frac{a^{\ell}}{r^{\ell+1}} \sum_{m=0}^{\ell} P_{\ell m}(\sin\varphi)\frac{1}{2}[(S'_{\ell m}+iC'_{\ell m})\exp\, im\lambda+(S'_{\ell m}-iC'_{\ell m})\exp -im\lambda]\cdot m\cdot\gamma$$

$$= -gM \sum_{\ell=0}^{\infty} \frac{a^{\ell}}{r^{\ell+1}} \sum_{m=0}^{\ell} P_{\ell m}(\sin\varphi)\cdot m\cdot\gamma(S'_{\ell m}\cos m\lambda - C'_{\ell m}\sin m\lambda)$$

To remodel $U_3(\alpha,\beta)$, $U_4(tz)$ and $U_5(tx,ty)$ in terms of spherical harmonics we have to introduce some recurrence formulae given by (*Kertz*, 1973):

$$\sin\varphi\, P_{\ell m}(\sin\varphi) = \frac{\ell+m}{2\ell+1} P_{\ell-1,m}(\sin\varphi) + \frac{(\ell-m+1)}{2\ell+1} P_{\ell+1,m}(\sin\varphi) \qquad (A15)$$

$$m\cdot\tan\varphi\, P_{\ell m}(\sin\varphi) = \frac{(\ell+m)(\ell-m+1)}{2} P_{\ell,m-1}(\sin\varphi) + \frac{1}{2} P_{\ell,m+1}(\sin\varphi) \qquad (A16)$$

$$\cos\varphi\, P_{\ell m}(\sin\varphi) = \frac{(\ell+m)(\ell+m-1)}{2\ell+1} P_{\ell-1,m-1}(\sin\varphi) - \frac{(\ell-m+1)(\ell-m+2)}{2\ell+1} P_{\ell+1,m-1}(\sin\varphi) \qquad (A17)$$

$$\cos\varphi\, P_{\ell m}(\sin\varphi) = -\frac{1}{2\ell+1} P_{\ell-1,m+1}(\sin\varphi) + \frac{1}{2\ell+1} P_{\ell+1,m+1}(\sin\varphi) \qquad (A18)$$

$$\frac{m}{\cos\varphi} P_{\ell m}(\sin\varphi) = \frac{(\ell+m)(\ell+m-1)}{2} P_{\ell-1,m-1}(\sin\varphi) + \frac{1}{2} P_{\ell-1,m+1}(\sin\varphi) \qquad (A19)$$

$$\frac{m}{\cos\varphi} P_{\ell m}(\sin\varphi) = \frac{(\ell-m+1)(\ell-m+2)}{2} P_{\ell+1,m-1}(\sin\varphi) + \frac{1}{2} P_{\ell+1,m+1}(\sin\varphi) \qquad (A20)$$

These recurrence formulae are valid if the second subskript is greater than or equal to zero. In addition, we have to use (*Kertz*, 1973)

$$\cos\varphi\, P_{\ell}(\sin\varphi) = -\frac{1}{2\ell+1} P_{\ell-1,1}(\sin\varphi) + \frac{1}{2\ell+1} P_{\ell+1,1}(\sin\varphi) \qquad (A21)$$

$$\sin\varphi\, P_{\ell}(\sin\varphi) = \frac{\ell}{2\ell+1} P_{\ell-1}(\sin\varphi) + \frac{\ell+1}{2\ell+1} P_{\ell+1}(\sin\varphi) \qquad (A22)$$

for the transformation of zonal terms (m=o). Furthermore we need (*Balmino and Borderies* 1977)

$$P_{\ell,-m}(\sin\varphi) = (-1)^m \frac{(\ell-m)!}{(\ell+m)!} P_{\ell m}(\sin\varphi) \qquad (A23)$$

From (A6), (A8) and (A11) we get:

$$\begin{aligned} U_3(\alpha,\beta) = gM \sum_{\ell=o}^{\infty} \frac{a^{\ell}}{r^{\ell+1}} \sum_{m=o}^{\ell} \Big\{ & \big(\tfrac{1}{4} P_{\ell,m+1}(\sin\varphi) - \tfrac{m}{4}\tan\varphi\, P_{\ell m}(\sin\varphi)\big)\big[(\beta+i\alpha)\exp i\lambda + \\ & + (\beta-i\alpha)\exp -i\lambda\big]\cdot\big[(C'_{\ell m} - iS'_{\ell m})\exp im\lambda + (C'_{\ell m} + iS'_{\ell m})\exp -im\lambda\big] \\ & + \tfrac{m}{4}\tan\varphi\, P_{\ell m}(\sin\varphi)\big[(\alpha-i\beta)\exp i\lambda + (\alpha+i\beta)\exp -i\lambda\big]\big[(S'_{\ell m} + iC'_{\ell m})\exp im\lambda + \\ & + (S'_{\ell m} - iC'_{\ell m})\exp -im\lambda\big]\Big\} \\ = gM \sum_{\ell=o}^{\infty} \frac{a^{\ell}}{r^{\ell+1}} \sum_{m=o}^{\ell} \Big\{ & \tfrac{1}{4} P_{\ell,m+1}(\sin\varphi)\big[\big[(C'_{\ell m} - iS'_{\ell m})\exp i(m+1)\lambda + \\ & + (C'_{\ell m} + iS'_{\ell m})\exp -i(m-1)\lambda\big](\alpha+i\beta) + \big[(C'_{\ell m} - iS'_{\ell m})\exp i(m-1)\lambda + \\ & + (C'_{\ell m} + iS'_{\ell m})\exp -i(m+1)\lambda\big](\beta-i\alpha)\big] - \tfrac{m}{2}\tan\varphi\, P_{\ell m}(\sin\lambda) \\ & \big[(C'_{\ell m} + iS'_{\ell m})\exp -i(m-1)\lambda\cdot(\beta+i\alpha) + (C'_{\ell m} - iS'_{\ell m})\exp i(m-1)\lambda\cdot(\beta-i\alpha)\big]\Big\} \end{aligned}$$

Using (A16) and (A23) leads to

$$U_3(\alpha,\beta) = gM \sum_{\ell=0}^{\infty} \frac{a^\ell}{r^{\ell+1}} \sum_{m=0}^{\ell} \Big\{ \frac{1}{4} P_{\ell,m+1}(\sin\varphi)[(C'_{\ell m}-iS'_{\ell m})\exp i(m+1)\lambda\cdot(\beta+i\alpha)+$$

$$+(C'_{\ell m}+iS'_{\ell m})\exp -i(m+1)\lambda\cdot(\beta-i\alpha)] - \frac{(\ell+m)(\ell-m+1)}{4} P_{\ell,m-1}(\sin\varphi)\cdot$$

$$\cdot[(C'_{\ell m}-iS'_{\ell m})\exp i(m-1)\lambda\cdot(\beta-i\alpha)+(C'_{\ell m}+iS'_{\ell m})\exp -i(m-1)\lambda\cdot(\beta+i\alpha)]\Big\}$$

$$U_3(\alpha,\beta) = gM \sum_{\ell=0}^{\infty} \frac{a^\ell}{r^{\ell+1}} \sum_{m=0}^{\ell} \frac{1}{2} P_{\ell,m+1}(\sin\varphi)[(\beta C'_{\ell m}+\alpha S'_{\ell m})\cos(m+1)\lambda+$$

$$+(\beta S'_{\ell m}-\alpha C'_{\ell m})\sin(m+1)\lambda]$$

$$-gM \sum_{\ell=0}^{\infty} \frac{a^\ell}{r^{\ell+1}} \sum_{m=0}^{\ell} \frac{(\ell+m)(\ell-m+1)}{2} P_{\ell,m-1}(\sin\varphi)\cdot$$

$$\cdot[(\beta C'_{\ell m}-\alpha S'_{\ell m})\cos(m-1)\lambda+(\beta S'_{\ell m}+\alpha C'_{\ell m})\sin(m-1)\lambda] \qquad \text{(A24)}$$

Summarizing (A4), (A9) and (A12) we get:

$$U_4(tz) = gM \sum_{\ell=0}^{\infty} \frac{a^\ell}{r^{\ell+2}} \sum_{m=0}^{\ell} [(-\frac{(\ell+1)}{2}\sin\varphi - \frac{m}{2}\tan\varphi\cos\varphi)P_{\ell m}(\sin\varphi)+$$

$$+\frac{1}{2}\cos\varphi P_{\ell,m+1}(\sin\varphi)]\cdot tz\cdot$$

$$\cdot[(C'_{\ell m}-iS'_{\ell m})\exp im\lambda+(C'_{\ell m}+iS'_{\ell m})\exp -im\lambda]$$

Making use of (A15), (A16), (A17) and (A18) one finds

$$U_4(tz) = gM \sum_{\ell=0}^{\infty} \frac{a^\ell}{r^{\ell+2}} \sum_{m=0}^{\ell} (-\frac{(\ell-m+1)(\ell+m+1)}{2(2\ell+1)} - \frac{(\ell-m)(\ell-m+1)}{2(2\ell+1)})P_{\ell+1,m}(\sin\varphi)\cdot tz\cdot$$

$$\cdot[(C'_{\ell m}-iS'_{\ell m})\exp im\lambda+(C'_{\ell m}+iS'_{\ell m})\exp -im\lambda]$$

$$U_4(tz) = gM \sum_{\ell=0}^{\infty} \frac{a^{\ell+1}}{r^{\ell+2}} \sum_{m=0}^{\ell} -(\ell-m+1)P_{\ell+1,m}(\sin\varphi)\cdot\frac{tz}{a}[C'_{\ell m}\cos m\lambda+S'_{\ell m}\sin m\lambda] \qquad \text{(A25)}$$

The sum of (A3), (A7), (A10) and (A13) results in

$$U_5(tx,ty)=gM \sum_{\ell=0}^{\infty} \frac{a^\ell}{r^{\ell+2}} \sum_{m=0}^{\ell} \Big\{ [(-\frac{(\ell+1)}{4}\cos\varphi+\frac{m}{4}\tan\varphi\sin\varphi)P_{\ell m}(\sin\varphi)-$$

$$-\frac{1}{4}\sin\varphi P_{\ell,m+1}(\sin\varphi)]\cdot$$

$$\cdot[(C'_{\ell m}-iS'_{\ell m})\exp im\lambda+(C'_{\ell m}+iS'_{\ell m})\exp -im\lambda][(tx-ity)\exp i\lambda+(tx+ity)\exp -i\lambda]$$

$$+\frac{m}{4\cos\varphi}P_{\ell m}(\sin\varphi)[(S'_{\ell m}+iC'_{\ell m})\exp im\lambda+(S'_{\ell m}-iC'_{\ell m})\exp -im\lambda]$$

$$[(ty-itx)\exp -i\lambda+(ty+tx)\exp i\lambda]\Big\}$$

Using (A15)-(A23) leads to

$$U_5(tx,ty)=gM\sum_{\ell=0}^{\infty}\frac{a^{\ell+1}}{r^{\ell+2}}\sum_{m=0}^{\ell}\frac{1}{2}P_{\ell+1,m+1}(\sin\varphi)[\frac{tx}{a}C'_{\ell m}-\frac{ty}{a}S'_{\ell m})\cos(m+1)\lambda+$$

$$+(\frac{tx}{a}S'_{\ell m}+\frac{ty}{a}C'_{\ell m})\sin(m+1)\lambda]+$$

$$+gM\sum\frac{a^{\ell+1}}{r^{\ell+2}}\sum\frac{(\ell-m+2)(\ell-m+1)}{2}P_{\ell+1,m-1}(\sin\varphi)$$

$$[(\frac{tx}{a}C'_{\ell m}+\frac{ty}{a}S'_{\ell m})\cos(m-1)\lambda+(\frac{tx}{a}S'_{\ell m}-\frac{ty}{a}C'_{\ell m})\sin(m-1)\lambda] \qquad (A26)$$

Changing the subscript in (A24)-(A26) yields

$$U = U_o + U_1(\delta k) + U_2(\gamma) + U_3(\alpha,\beta) + U_4(tz) + U_5(tx,ty)$$

$$= gM\sum_{\ell=0}^{\infty}\frac{a^{\ell}}{r^{\ell+1}}\sum_{m=0}^{\ell}P_{\ell m}(\sin\varphi)[(C'_{\ell m}(1-\delta k(\ell+1))-S'_{\ell m}\cdot m\cdot\gamma)\cos m\lambda+(S'_{\ell m}\cdot(1-\delta k(\ell+1))+$$

$$+C'_{\ell m}\cdot m\cdot\gamma)\sin m\lambda] \qquad (A27)$$

$$+gM\sum_{\ell=0}^{\infty}\frac{a^{\ell}}{r^{\ell+1}}\sum_{m=1}^{\ell+1}P_{\ell m}(\sin\varphi)\cdot\frac{1}{2}[(\beta C'_{\ell,m-1}+\alpha S'_{\ell,m-1})\cos m\lambda+(\beta S'_{\ell,m-1}-\alpha C'_{\ell,m-1})\sin m\lambda] \qquad (A28)$$

$$-gM\sum_{\ell=0}^{\infty}\frac{a^{\ell}}{r^{\ell+1}}\sum_{m=-1}^{\ell-1}P_{\ell m}(\sin\varphi)\frac{(\ell+m-1)(\ell-m)}{2}\cdot$$

$$\cdot[(\beta C'_{\ell,m+1}-\alpha S'_{\ell,m+1})\cos m\lambda+(\beta S'_{\ell,m+1}+\alpha C'_{\ell,m+1})\sin m\lambda] \qquad (A29)$$

$$-gM\sum_{\ell=1}^{\infty}\frac{a^{\ell}}{r^{\ell+1}}\sum_{m=0}^{\ell-1}P_{\ell m}(\sin\varphi)(\ell-m)\frac{tz}{a}[C'_{\ell-1,m}\cos m\lambda+S'_{\ell-1,m}\sin m\lambda] \qquad (A30)$$

$$-gM\sum_{\ell=1}^{\infty}\frac{a^{\ell}}{r^{\ell+1}}\sum_{m=1}^{\ell}P_{\ell m}(\sin\varphi)\cdot\frac{1}{2}[(\frac{tx}{a}C'_{\ell-1,m-1}-\frac{ty}{a}S'_{\ell-1,m-1})\cos m\lambda+$$

$$+(\frac{tx}{a}S'_{\ell-1,m-1}+\frac{ty}{a}C'_{\ell-1,m-1})\sin m\lambda] \qquad (A31)$$

$$+ gM \sum_{\ell=1}^{\infty} \frac{a^{\ell}}{r^{\ell+1}} \sum_{m=-1}^{\ell} P_{\ell m}(\sin\varphi) \frac{(\ell-m-1)(\ell-m)}{2} [(\frac{tx}{a} C'_{\ell-1,m+1} + \frac{ty}{a} S'_{\ell-1,m+1}) \cos m\lambda +$$

$$+ (\frac{tx}{a} S'_{\ell-1,m+1} - \frac{ty}{a} C'_{\ell-1,m+1}) \sin m\lambda] \qquad (A32)$$

In (A28) the second subscript can start at m = o and end at m = ℓ because of $C'_{\ell,-1} = S'_{\ell,-1} =$ o and $P_{\ell,\ell+1}$ = o. In (A29) the second index can end at m = ℓ since $C'_{\ell,\ell+1} = S'_{\ell,\ell+1}$ = o. Using (A23) and cos(-λ) = cosλ, sin(-λ) = -sinλ for the case of m = -1 we rewrite (A29)

$$- gM \sum_{\ell=o}^{\infty} \frac{a^{\ell}}{r^{\ell+1}} \sum_{m=o}^{\ell} P_{\ell m}(\sin\varphi) \frac{(\ell+m+1)(\ell-m)}{2} [(\beta C'_{\ell,m+1} - \alpha S'_{\ell,m+1}) \cos m\lambda +$$

$$+ (\beta S'_{\ell,m+1} + C'_{\ell,m+1}) \sin m\lambda] \qquad (A33)$$

$$+ gM \sum_{\ell=o}^{\infty} \frac{a^{\ell}}{r^{\ell+1}} \sum_{m=o}^{\ell} P_{\ell m}(\sin\varphi) \frac{\delta_{1m}}{2} [(\beta C'_{\ell,m-1} + \alpha S'_{\ell,m-1}) \cos m\lambda +$$

$$+ (\beta S'_{\ell,m-1} - \alpha C'_{\ell,m-1}) \sin m\lambda]$$

where δ_{1m} = 1 for m = 1 and zero otherwise. In (A30) the range of the second subscript can be extended to m = ℓ because of $C'_{\ell-1,\ell} = S'_{\ell-1,\ell}$ = o. The first index can start at ℓ = o since $C'_{-1,m} = S'_{-1,m}$ = o. The latter also is valid in (A31). Here the second subscript also can start at m = o for $C'_{\ell-1,-1} = S'_{\ell-1,-1}$ = o. In (A32) the first index can start at ℓ = o because of $C'_{-1,m+1} = S'_{-1,m+1}$ = o and the range of the second index can be extended to m = ℓ since $C'_{\ell-1,\ell}$ = $C'_{\ell-1,\ell+1} = S'_{\ell-1,\ell} = S'_{\ell-1,\ell+1}$ = o. Introducing (A23) and using cos(-λ) = cosλ, sin(-λ) = -sinλ (A32) can be rewritten as

$$+ gM \sum_{\ell=o}^{\infty} \frac{a^{\ell}}{r^{\ell+1}} \sum_{m=o}^{\ell} P_{\ell m}(\sin\varphi) \frac{(\ell-m-1)(\ell-m)}{2} [(\frac{tx}{a} C'_{\ell-1,m+1} + \frac{ty}{a} S'_{\ell-1,m+1}) \cos m\lambda +$$

$$+ (\frac{tx}{a} S'_{\ell-1,m+1} - \frac{ty}{a} C'_{\ell-1,m+1}) \sin m\lambda] \qquad (A34$$

$$- gM \sum_{\ell=o}^{\infty} \frac{a^{\ell}}{r^{\ell+1}} \sum_{m=o}^{\ell} P_{\ell m}(\sin\varphi) \frac{\delta_{1m}}{2} [(\frac{tx}{a} C'_{\ell-1,m-1} - \frac{ty}{a} S'_{\ell-1,m-1}) \cos m\lambda +$$

$$+ (\frac{tx}{a} S'_{\ell-1,m-1} + \frac{ty}{a} C'_{\ell-1,m-1}) \sin m\lambda]$$

In summarizing the terms (A27), (A28), (A30), (A31), (A33) and (A34) we get the following expression

$$U = gM \sum_{\ell=0}^{\infty} \frac{a^{\ell}}{r^{\ell+1}} \sum_{m=0}^{\ell} P_{\ell m}(\sin\varphi)(C_{\ell m}\cos m\lambda + S_{\ell m}\sin m\lambda)$$

where

$$\begin{aligned}
C_{\ell m} = {} & + [1-\delta k(\ell+1)]\, C'_{\ell m} && - [m\cdot\gamma]\, S'_{\ell m} \\
& + [\tfrac{1}{2}(1+\delta_{1m})\beta]\, C'_{\ell,m-1} && + [\tfrac{1}{2}(1+\delta_{1m})\alpha]\, S'_{\ell,m-1} \\
& - [\tfrac{1}{2}(\ell+m+1)(\ell-m)\beta]\, C'_{\ell,m+1} && + [\tfrac{1}{2}(\ell+m+1)(\ell-m)\alpha]\, S'_{\ell,m+1} \\
& - [(\ell-m)\tfrac{tz}{a}]\, C'_{\ell-1,m} && \\
& - [\tfrac{1}{2}(1+\delta_{1m})\tfrac{tx}{a}]\, C'_{\ell-1,m-1} && + [\tfrac{1}{2}(1+\delta_{1m})\tfrac{ty}{a}]\, S'_{\ell-1,m-1} \\
& + [\tfrac{1}{2}(\ell-m-1)(\ell-m)\tfrac{tx}{a}]\, C'_{\ell-1,m+1} && + [\tfrac{1}{2}(\ell-m-1)(\ell-m)\tfrac{ty}{a}]\, S'_{\ell-1,m+1}
\end{aligned}$$

and

$$\begin{aligned}
S_{\ell m} = {} & + [1-\delta k(\ell+1)]\, S'_{\ell m} && + [m\cdot\gamma]\, C'_{\ell m} \\
& + [\tfrac{1}{2}(1+\delta_{1m})\beta]\, S'_{\ell,m-1} && - [\tfrac{1}{2}(1+\delta_{1m})\alpha]\, C'_{\ell,m-1} \\
& - [\tfrac{1}{2}(\ell+m+1)(\ell-m)\beta]\, S'_{\ell,m+1} && - [\tfrac{1}{2}(\ell+m+1)(\ell-m)\alpha]\, C'_{\ell,m+1} \\
& - [(\ell-m)\tfrac{tz}{a}]\, S'_{\ell-1,m} && \\
& - [\tfrac{1}{2}(1+\delta_{1m})\tfrac{tx}{a}]\, S'_{\ell-1,m-1} && - [\tfrac{1}{2}(1+\delta_{1m})\tfrac{ty}{a}]\, C'_{\ell-1,m-1} \\
& + [\tfrac{1}{2}(\ell-m-1)(\ell-m)\tfrac{tx}{a}]\, S'_{\ell-1,m-1} && - [\tfrac{1}{2}(\ell-m-1)(\ell-m)\tfrac{ty}{a}]\, C'_{\ell-1,m+1}
\end{aligned}$$

References

Aardom, L.: Some transformation properties for the coefficients in a spherical harmonics expansion of the earth's gravitational potential, Tellus XXI (1969) 572-583

Balmino, G. and N. Borderies: Gravitational Potential of Solid Bodies in the Solar System, Cel. Mech. 17 (1978) 113-119

Giacaglia, G.E.O.: Transformations of Spherical Harmonics and Applications to Geodesy and Satellite Theory, Studia geoph. et geod. 24 (1980) 1-11

Jeffreys, B.: Transformation of Tesseral Harmonics under Rotation, Geophys. J. 10 (1965) 141-145

Kertz, W.: Potentialtheorie in der Geophysik, Institut f. Geophysik und Meteorologie, Braunschweig 1973

Mc Clure, P.: Diurnal Polar Motion, GSFC Rept. X-592-72-259, Greenbelt 1973

Nagel, E.: Bezugssysteme der Satellitengeodäsie, DGK C 223, 1976

Sidlichovsky, M.: The Force Function of two General Bodies, Bull. Astron. Inst. Czechosl. 29 (1978) 90-97

Sidlichovsky, M.: The Force Function of two General Bodies II, Bull. Astron. Inst. Czechosl. 30 (1979) 152-155

Winch, D.E. and R.W. James: Computations with Spherical Harmonics and Fourier Series in Geomagnetism, in: Bolt, B.A. (Editor): Methods in Computational Physics Vol. 13, New York 1973

A Solution for Determination of the Gravity Field from Satellite-to-Satellite Tracking Data

Jan Kryński [1)]

1. Introduction.

In order to use low-low satellite-to-satellite tracking data for investigation of the Earth's gravity field it is necessary to describe mathematically in very detail the measured phenomena. Some solutions of this problem are given by Schwarz /1970/, Kryński /1978/ and Rummel /1978/. The authors use different assumptions and quite different methods in their theories. However, it seems to be difficult to make a choise of the proper solution for practical application. Such a solution should be general, relatively simple and convenient for numerical computations. These requirements have been taken into account in the sequel to derive the observation equations.

Assume that the nongravitational forces do not affect on satellite, so we consider the satellite motion in the Earth's gravity field only. The differential equation of satellite motion in such field W in inertial coordinates system is the following:

$$\ddot{\underline{R}} = \nabla W. \qquad /1/.$$

It is quite natural to describe a motion of celestial body in inertial system of coordinates. But on the other hand in physical geodesy the gravity field of the Earth is usually expressed in the coordinate system which is fixed to the Earth /terrestrial system/. In such a system the equation of motion /1/ has a form

1)Space Research Centre, Polish Academy of Science

$$\ddot{\underline{R}} + \underline{F}_c = \overline{\nabla W} \quad , \qquad /2/$$

where $\underline{F}_c$ is a Coriolis acceleration.

It should be noticed that the integration of the differential equation /2/ is much more complicated then the integration of the defferential equation /1/. What more, the velocity and position vectors obtained from the equation /2/ refer to terrestrial system. They should be transformed to the inertial system in which we determine those vectors from ordinary solution of satellite motion. Therefore we have to formulate such an equation which refers to inertial coordinate system on one hand, and on the other hand which uses the gradient of the potential W expressed in terrestrial system.

Let us notice that the potential W does not explicitly depend on time. Then ∇W is the conservative force, what means that the quantity of the gradient of the potential W is invariant with respect to linear transformation.

Let us consider the inertial coordinate system OXYZ and geocentric terrestrial coordinate system $O'X'Y'Z'$ with the common origin /$O = O'$/ and common Z-axis. Denoting by A the rotational matrix transforming terrestrial system into inertial one

$$\nabla W = A \ \overline{\nabla W} \quad , \qquad /3/$$

we can write the equation of satellite motion in the following form:

$$\ddot{\underline{R}} = A \ \overline{\nabla W} \quad . \qquad /4/$$

The equation /4/ is expressed in inertial system and symultaneously the gradient of potential $\overline{\nabla W}$ refers to the terrestrial system; it is a basic equation used in the sequel.

2. The case of two satellites.

Let us consider the case of two satellites following each other along similar orbits. In appropriate time intervals the relative velocity of two satellites is measured.

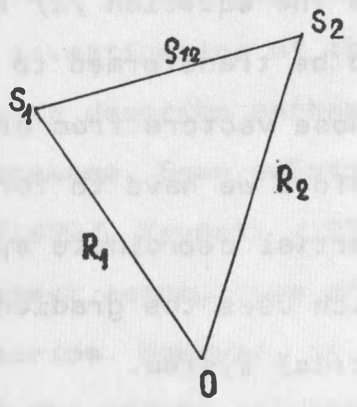

Fig. 1

According to Fig. 1 let S_1 and S_2 denote the real positions of satellites at the epoch t_o. The gravity potential in S_1 and S_2 is $W_{/1/}$ and $W_{/2/}$ respectively. In order to compute the approximate position of satellites we shall use an approximate gravity potential model U which can be regarded as a normal potential. The equations of satellite motion in real gravity field and in the normal gravity field are the following:

$$\ddot{\underline{R}}_{i|w} = A_{/i/} \overline{\nabla W}_{/i/} , \qquad /5/$$

$$/i=1,2/$$

$$\ddot{\underline{R}}_{i|u} = A_{/i/} \overline{\nabla U}_{/i/} , \qquad /6/$$

where $U_{/1/}$ and $U_{/2/}$ are the normal potentials in S_1 and S_2 respectively.

Let us assume that at t_o we know exactly the positions of S_1 and S_2 i.e. the real position is the same as the normal position at t_o. However, at t_o real velocities and accelerations differ on normal ones.

Subtracting /6/ from /5/ we get

$$\underline{\Delta\ddot{R}}_i = \underline{\ddot{R}}_{i|W} - \underline{\ddot{R}}_{i|U} = A_{/i/}\,\overline{\nabla W}_{/i/} - A_{/i/}\,\overline{\nabla U}_{/i/} = A_{/i/}\,/\overline{\nabla W}_{/i/} - \overline{\nabla U}_{/i/}/\,. \qquad /7/$$

If we denote the anomalous potential by T

$$T = W - U, \qquad /8/$$

then the equation /7/ has a form

$$\underline{\Delta\ddot{R}}_i = A_{/i/}\;\overline{\nabla T}_{/i/}\,. \qquad /9/$$

Integrating an equation /9/ we get an increment in the velocity of satellite S_i due to anomalous potential T. We have now

$$\underline{\Delta\dot{R}}_i = \int_{\tau=t_0}^{t} A_{/i/}\,\overline{\nabla T}_{/i/}\,d\tau + \underline{C}_i\,, \qquad /10/$$

where obviously constant $\underline{C}_i$ is determined from the initial condition

$$\underline{C}_i = \underline{\Delta\dot{R}}_i\,/t_o/\,. \qquad /11/$$

Then /10/ can be written in the following form:

$$\underline{\Delta\dot{R}}_{/i/}/t/ = \int_{\tau=t_0}^{t} A_{/i/}\,\overline{\nabla T}_{/i/}\,d\tau + \underline{\Delta\dot{R}}_{/i/}/t_0/\,. \qquad /12/$$

In satellite-to-satellite tracking we shall consider the relative velocity which contain the differential effect of anomalous potential. From Fig. 1 we have

$$\dot{\underline{\varrho}} = \dot{\underline{R}}_2 - \dot{\underline{R}}_1\,. \qquad /13/$$

Differentiating /13/ with respect to time we get

$$\dot{\underline{\varrho}} = \dot{\underline{R}}_2 - \dot{\underline{R}}_1 . \qquad /14/$$

If we denote

$$\Delta\dot{\underline{\varrho}} = \Delta\dot{\underline{R}}_2 - \Delta\dot{\underline{R}}_1 , \qquad /15/$$

where $\Delta\dot{\underline{\varrho}}$ is the increment of the relative velocity vector due to anomalous potential we get from /12/

$$\Delta\dot{\underline{\varrho}}/t/ = \int_{\tau=t_0}^{t} A_{/2/}\,\overline{\nabla T}_{/2/}\,d\tau - \int_{\tau=t_0}^{t} A_{/1/}\,\overline{\nabla T}_{/1/}\,d\tau + \Delta\dot{\underline{R}}_2/t_0/ - \Delta\dot{\underline{R}}_1/t_0/ . \qquad /16/$$

Since

$$\Delta\dot{\underline{R}}_2/t_0/ - \Delta\dot{\underline{R}}_1/t_0/ = \Delta\dot{\underline{\varrho}}/t_0/ , \qquad /17/$$

the equation /16/ will have the form

$$\Delta\dot{\underline{\varrho}}/t/ - \Delta\dot{\underline{\varrho}}/t_r = \int_{\tau=t_0}^{t} \sum_{i=1}^{2} /-1/^{i} A_{/i/}\,\overline{\nabla T}_{/i/}\,d\tau . \qquad /18/$$

The equation /18/ would be an observation equation when the relative velocity vectors are observed quatities. However, in satellite-to-satellite tracking technique we will be able to measure the projection of the relative velocity vector on the direction between two satellites S_1 and S_2. Therefore our observation equation should have a scalar form.

According to Fig. 1 the versor of direction S_1S_2 is

$$\underline{e}_{12} = \frac{\underline{R}_2 - \underline{R}_1}{|\underline{R}_2 - \underline{R}_1|} = \frac{\underline{\varrho}}{|\underline{\varrho}|} . \qquad /19/$$

The projection of the vector $\dot{\underline{\varrho}}$ on the derection $S_1\,S_2$ will be nothing but the scalar product of $\dot{\underline{\varrho}}$ and the versor $\underline{e}_{12}$, i.e.

$$\dot{\varrho} = \dot{\underline{\varrho}}\,\underline{e}_{12} = \frac{\dot{\underline{\varrho}}\,\underline{\varrho}}{|\underline{\varrho}|} \quad . \qquad /20/$$

The component $\dot{\varrho}$ of the relative velocity can be directly measured; it will be considered as a function of time. Let us take the difference

$$\dot{\varrho}/t/-\dot{\varrho}/t_0/=\frac{\dot{\underline{\varrho}}/t/\underline{\varrho}/t/}{\varrho/t/}-\frac{\dot{\underline{\varrho}}/t_0/\underline{\varrho}/t_0/}{\varrho/t_0/}=\frac{1}{\varrho/t/\varrho/t_0/}\left[\dot{\underline{\varrho}}/t/\underline{\varrho}/t/\varrho/t_0/-\dot{\underline{\varrho}}/t_0/\underline{\varrho}/t_0/\varrho/t/\right] . \qquad /21/$$

Using the abbreviation

$$\varrho/t_0/=\varrho/t/-\Delta\varrho_{t_0t} , \qquad /22/$$

where $\Delta\varrho_{t_0t}$ is the increment of the distance ϱ between satellites in the time interval $/t_0, t/$ and substituting /22/ to /21/ we get

$$\dot{\varrho}/t/-\dot{\varrho}/t_0/=\frac{1}{\varrho/t/\left[1-\frac{\Delta\varrho_{t_0t}}{\varrho/t/}\right]}\left\{\dot{\underline{\varrho}}/t/\underline{\varrho}/t/\left[1-\frac{\Delta\varrho_{t_0t}}{\varrho/t/}\right]-\dot{\underline{\varrho}}/t_0/\underline{\varrho}/t_0/\right\} . \qquad /23/$$

After some simple modification in /23/, neglecting terms of second and higher order the formula /23/ has now a form

$$\dot{\varrho}/t/-\dot{\varrho}/t_0/=\frac{1}{\varrho/t/}\left[\dot{\underline{\varrho}}/t/\underline{\varrho}/t/-\dot{\underline{\varrho}}/t_0/\underline{\varrho}/t_0/\right]-\frac{1}{\varrho/t/^2}\dot{\underline{\varrho}}/t_0/\underline{\varrho}/t_0/\Delta\varrho_{t_0t} . \qquad /24/$$

Since in short time intervals a distance ϱ is practically constant we can replace $\varrho/t/$ by $\varrho/t_0/$ in /24/. Now we have

$$\dot{\varrho}/t/-\dot{\varrho}/t_0/=\frac{1}{\varrho/t_0/}\left[\dot{\underline{\varrho}}/t/\underline{\varrho}/t/-\dot{\underline{\varrho}}/t_0/\underline{\varrho}/t_0/\right]-\frac{1}{\varrho/t_0/^2}\dot{\underline{\varrho}}/t_0/\underline{\varrho}/t_0/\Delta\varrho_{t_0t} . \qquad /25/$$

The expression /25/ describes variation of the projection of the relative velocity vector on the direction $S_1\ S_2$ in time

interval $/t_o, t/$. Considering /25/ for the real gravity field we obtain the expression for the observed quantity

$$\Delta\dot{g}_o = [\dot{g}/t/ - \dot{g}/t_o/]_{IW} = \left\{\frac{1}{g/t_o/}\left[\underline{\dot{g}}/t/\underline{g}/t/ - \underline{\dot{g}}/t_o/\underline{g}/t_o/\right] - \frac{1}{g/t_o/^2}\,\underline{\dot{g}}/t_o/\underline{g}/t_o/\Delta g_{t_o t}\right\}_{IW}, \qquad /26/$$

and for the normal gravity field we obtain the expression for the calculated quantity

$$\Delta\dot{g}_c = [\dot{g}/t/ - \dot{g}/t_o/]_{IU} = \left\{\frac{1}{g/t_o/}\left[\underline{\dot{g}}/t/\underline{g}/t/ - \underline{\dot{g}}/t_o/\underline{g}/t_o/\right] - \frac{1}{g/t_o/^2}\,\underline{\dot{g}}/t_o/\underline{g}/t_o/\Delta g_{t_o t}\right\}_{IU}. \qquad /27/$$

In accordance with the previous assumptions

$$g/t_o/_{IW} = g/t_o/_{IU}, \qquad /28/$$

and what more

$$\underline{g}/t_o/_{IW} = \underline{g}/t_o/_{IU}. \qquad /29/$$

Using the abbreviation

$$\underline{g}/t/ = \underline{g}/t_o/ + \underline{\Delta g}_{t_o t} \qquad /30/$$

and subtracting /27/ from /26/ we find

$$\Delta\dot{g}_o - \Delta g_c = \frac{1}{g/t_o/}\left\{\left[\underline{\dot{g}}/t/_{IW} - \underline{\dot{g}}/t/_{IU}\right]\underline{\dot{g}}/t_o/ - \left[\underline{\dot{g}}/t_o/_{IW} - \underline{\dot{g}}/t_o/_{IU}\right]\underline{g}/t_o/ + \left[\underline{\dot{g}}/t_o/\underline{\Delta g}_{t_o t}\right]_{IW} - \right.$$
$$\left. - \left[\underline{\dot{g}}/t/\underline{\Delta g}_{t_o t}\right]_{IU}\right\} - \frac{1}{g/t_o/^2}\,\underline{g}/t_o/\left\{\left[\underline{\dot{g}}/t_o/\Delta g_{t_o t}\right]_{IW} - \left[\underline{\dot{g}}/t_o/\Delta g_{t_o t}\right]_{IU}\right\}. \qquad /31/$$

It is easy to notice that according to the previously used notation

$$\underline{\dot{g}}/t/_{IW} - \underline{\dot{g}}/t/_{IU} = \underline{\Delta\dot{g}}/t/; \qquad \underline{\dot{g}}/t_o/_{IW} - \underline{\dot{g}}/t_o/_{IU} = \underline{\Delta\dot{g}}/t_o/. \qquad /32/$$

Substituting /32/ into /31/ we get

$$\Delta\dot{g}_o - \Delta\dot{g}_c = \frac{1}{g/t_o/}\left[\underline{\Delta\dot{g}}/t/ - \underline{\Delta\dot{g}}/t_o/\right]\underline{g}/t_o/ + \frac{1}{g/t_o/}\left\{\left[\underline{\dot{g}}/t/\underline{\Delta g}_{t_o t}\right]_{IW} - \left[\underline{\dot{g}}/t/\underline{\Delta g}_{t_o t}\right]_{IU}\right\} -$$
$$- \frac{1}{g/t_o/^2}\,\underline{g}/t_o/\left\{\left[\underline{\dot{g}}/t_o/\Delta g_{t_o t}\right]_{IW} - \left[\underline{\dot{g}}/t_o/\Delta g_{t_o t}\right]_{IU}\right\} \qquad /33/$$

and finally using /18/ the equation /33/ will have the following form:

$$\Delta\dot{g}_0 - \Delta\dot{g}_c + C_1 + C_2 = \frac{\underline{g}/t_0/}{g/t_0/} \int_{\tau=t_0}^{t} \sum_{i=1}^{2} /-1/^i A_{/i/} \overline{\nabla T}_{/i/} \, d\tau \quad , \qquad /34/$$

where $$C_1 = \frac{1}{g/t_0/} \left\{ [\underline{\dot{g}}/t/\Delta g_{t_0 t}]_{IW} - [\underline{\dot{g}}/t/\Delta g_{t_0 t}]_{IU} \right\} \quad ,$$

and $$C_2 = \frac{1}{g/t_0/^2} \underline{g}/t_0/ \left\{ [\underline{\dot{g}}/t_0/\Delta g_{t_0 t}]_{IW} - [\underline{\dot{g}}/t_0/\Delta g_{t_0 t}]_{IU} \right\} .$$

Assuming a time interval $/t_0, t/$ as a small one, the expressions C_1 and C_2 can be neglected and the observation equation is now the following:

$$\Delta\dot{g}_0 - \Delta\dot{g}_c = \frac{\underline{g}/t_0/}{g/t_0/} \int_{\tau=t_0}^{t} \sum_{i=1}^{2} /-1/^i A_{/i/} \overline{\nabla T}_{/i/} \, d\tau \quad . \qquad /35/$$

Let us define the rotational matrix A. As it was previously mentioned the matrix A transforms terrestrial system into inertial system. Denoting by Θ - Greenwich siderial time we get

$$A = \begin{pmatrix} \cos\Theta & -\sin\Theta & 0 \\ \sin\Theta & \cos\Theta & 0 \\ 0 & 0 & 1 \end{pmatrix} . \qquad /36/$$

The observation equation /35/ is quite simple and convenient to use when the gradient of anomalous potential is given in the rectangular coordinate system. However, in order to use the COVAX subroutine /Tscherning, 1976/ the gradient of anomalous potential should be expressed in spherical coordinate system.

Denoting by $B_{/i/}$ the matrix transforming spherical coordinate system into rectangular coordinate system we have

$$\overline{\nabla T}_{/i/} = B_{/i/} \quad \nabla T^{s}_{/i/} \ , \qquad /37/$$

where

$$B_{/i/} = \begin{pmatrix} \cos\varphi_{/i/}\cos\lambda_{/i/} & -\sin\varphi_{/i/}\cos\lambda_{/i/} & -\sin\lambda_{/i/} \\ \cos\varphi_{/i/}\sin\lambda_{/i/} & -\sin\varphi_{/i/}\sin\lambda_{/i/} & \cos\lambda_{/i/} \\ \sin\varphi_{/i/} & \cos\varphi_{/i/} & 0 \end{pmatrix}, \qquad /38/$$

and

$$\nabla T^{S}_{/i/} = \begin{pmatrix} T_{R/i/} \\ \frac{1}{R_{/i/}} T_{\varphi/i/} \\ \frac{1}{R_{/i/}\cos\varphi_{/i/}} T_{\lambda/i/} \end{pmatrix} ; \qquad /39/$$

$R_{/i/}$, $\varphi_{/i/}$, $\lambda_{/i/}$ are the spherical coordinates of satellite S_i. Substituting /37/ we can rewrite /35/ in the following form:

$$\Delta\dot{\varrho}_0 - \Delta\dot{\varrho}_c = \frac{\varrho/t_0/}{\varrho/t_0/} \int_{\tau=t_0}^{t} \sum_{i=1}^{2} /-1/^{i} A B_{/i/} \nabla T^{S}_{/i/} \, d\tau \ . \qquad /40/$$

Using the abbreviation

$$P_{/i/} = A \, B_{/i/}, \qquad /41/$$

where

$$P_{/i/} = \begin{pmatrix} \cos\varphi_{/i/}\cos/\lambda_{/i/}+\theta/ & -\sin\varphi_{/i/}\cos/\lambda_{/i/}+\theta/ & -\sin/\lambda_{/i/}+\theta/ \\ \cos\varphi_{/i/}\sin/\lambda_{/i/}+\theta/ & -\sin\varphi_{/i/}\sin/\lambda_{/i/}+\theta/ & \cos/\lambda_{/i/}+\theta/ \\ \sin\varphi_{/i/} & \cos\varphi_{/i/} & 0 \end{pmatrix} \qquad /42/$$

we get from /40/

$$\Delta\dot{\varrho}_0 - \Delta\dot{\varrho}_c = \frac{\varrho/t_0/}{\varrho/t_0/} \int_{\tau=t_0}^{t} \sum_{i=1}^{2} /-1/^{i} P_{/i/} \nabla T^{S}_{/i/} \, d\tau \ ? \qquad /43/$$

In some cases e.g for the computation of covariarces it will be more convenient to describe an observation equation /43/ in another form.

According to /19/

$$\underline{e}/t_0/ = \frac{\underline{\varrho}/t_0/}{\varrho/t_0/} \qquad /44/$$

is the unit vector of the direction between satellites at t_o where

$$\underline{e}/t_0/ = /\overline{\Delta X}_1, \overline{\Delta X}_2, \overline{\Delta X}_3/ . \qquad /45/$$

Let us denote

$$\underline{L}/i/ = P/i/ \quad \nabla T^s/i/, \qquad /46/$$

where

$$\underline{L}/i/ = /L_1/i/ , L_2/i/ , L_3/i/ / , \qquad /47/$$

and

$$L_k/i/ = \sum_{l=1}^{3} P_{kl}/i/ \nabla T^s_l/i/ . \qquad /48/$$

Since

$$\underline{e}/t_0/\underline{L}/i/ = \sum_{K=1}^{3} \overline{\Delta X}_K L_{K/i/} \qquad /49/$$

we can rewrite the equation /43/ in the following form:

$$\Delta\dot{\varrho}_0 - \Delta\dot{\varrho}_c = \int_{\tau=t_0}^{t} \sum_{i=1}^{2} /-1/^i \sum_{K=1}^{3} \overline{\Delta X}_K \sum_{l=1}^{3} P_{Kl/i/} \nabla T^s_{l/i/} d\tau . \qquad /50/$$

Finally, using the low of commutability of summation and replacing constants in front of the integral we obtain the following observation equation:

$$\Delta\dot{\varrho}_0 - \Delta\dot{\varrho}_c = \sum_{K=1}^{3} \overline{\Delta X}_K \sum_{i=1}^{2} /-1/^i \sum_{l=1}^{3} \int_{\tau=t_0}^{t} P_{Kl/i/} \nabla T^s_{l/i/} d\tau . \qquad /51/$$

Now, it is quite easy to derive basic covariances. If we denote by s_A' and s_B' the signals of observations A and B respecively, where

$$S_A' = \sum_{K=1}^{3} \overline{\Delta X}_{K_A} \sum_{i=1}^{2} /-1/^i \sum_{l=1}^{3} \int_{\tau=t_0}^{t} P_{kl/i/_A} \nabla T^s_{l/i/_A} d\tau \,, \qquad /52/$$

and

$$S_B' = \sum_{m=1}^{3} \overline{\Delta X}_{m_B} \sum_{j=1}^{2} /-1/^j \sum_{n=1}^{3} \int_{\sigma=u_0}^{u} P_{mn/j/_B} \nabla T^s_{n/j/_B} d\sigma \,, \qquad /53/$$

then using the low of propagation of covariances /Moritz, 1973/ we obtain the autocovariance

$$cov/S_A', S_B'/ = \sum_{K=1}^{3}\sum_{m=1}^{3} \overline{\Delta X}_{K_A} \overline{\Delta X}_{m_B} \sum_{i=1}^{2}\sum_{j=1}^{2} /-1/^{i+j} \sum_{l=1}^{3}\sum_{n=1}^{3} \int_{\tau=t_0}^{t}\int_{\sigma=u_0}^{u} P_{kl/i/_A} P_{mn/j/_B} cov/\nabla T^s_{l/i/_A}, \nabla T^s_{n/j/_B}/ d\sigma\, d\tau \,, \qquad /54/$$

and the covariance between the signal s_A' and the anomalous potential T at the point Q

$$cov/S_A', T_{/Q/}/ = \sum_{K=1}^{3} \overline{\Delta X}_{K_A} \sum_{i=1}^{2} /-1/^i \sum_{l=1}^{3} \int_{\tau=t_0}^{t} P_{K_l/i/_A} cov/\nabla T^s_{l/i/_A}, T_{/Q/}/ d\tau \,. \qquad /55/$$

It should be noticed that using the low of propagation of covariances all covariances between the signal s' and arbitrary geopotential parameters can be computed from /55/.

3. The case of three satellites.

Let us consider the case when the relative velocity is measured between the "mother" satellite and two subsatellites simultaneously /Zieliński, 1978/. Combination of such two observations gives a simulation of a direct observation between two subsatellites; it allows to minimize the influence of some significant forces on the observed quantity which are in general case rather difficult to eliminate. Geometry of the problem is shown in Fig. 2.

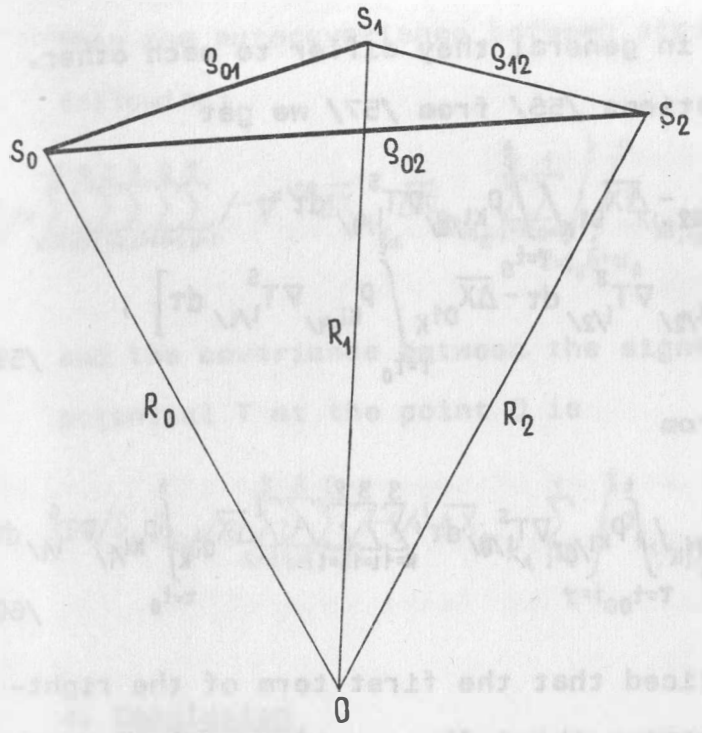

Fig. 2.

For any independent measurement we can use the observation equation /51/. We have now

$$\Delta\dot{\varrho}_{01_0} - \Delta\dot{\varrho}_{01_C} = \sum_{K=1}^{3} \overline{\Delta X}_{01_K} \sum_{l=1}^{3} \left\{ \int_{\tau=t_0}^{t} \rho_{Kl/1/} \nabla T^{s}_{l/1/}\, d\tau - \int_{\tau=t_0}^{t} \rho_{Kl/0/} \nabla T^{s}_{l/0/}\, d\tau \right\}, \qquad /56/$$

and

$$\Delta\dot{\varrho}_{02_0} - \Delta\dot{\varrho}_{02_C} = \sum_{K=1}^{3} \overline{\Delta X}_{02_K} \sum_{l=1}^{3} \left\{ \int_{\tau=t_0}^{t} \rho_{Kl/2/} \nabla T^{s}_{l/2/}\, d\tau - \int_{\tau=t_0}^{t} \rho_{Kl/0/} \nabla T^{s}_{l/0/}\, d\tau \right\}. \qquad /57/$$

Let us denote

$$/\Delta\dot{\varrho}_{02} - \Delta\dot{\varrho}_{01}/_0 - /\Delta\dot{\varrho}_{02} - \Delta\dot{\varrho}_{01}/_C = \overline{\Delta\dot{\varrho}}_{12_0} - \overline{\Delta\dot{\varrho}}_{12_C}, \qquad /58/$$

where the bars used on the right-hand side of /58/ mean that the increment $\overline{\Delta\dot{\varrho}}_{12}$ of the projection of relative velocity between subsatellites S_1 and S_2 on the direction S_1S_2 is very

close to $\overline{\Delta\dot{\varrho}_{12}}$, but in general they differ to each other.

Subtracting equations /56/ from /57/ we get

$$\overline{\Delta\dot{\varrho}_{12}}_0 - \overline{\Delta\dot{\varrho}_{12}}_c = \sum_{K=1}^{3}\sum_{l=1}^{3} /\overline{\Delta X}_{02_K} - \overline{\Delta X}_{01_K}/ \int_{\tau=t_0}^{t} p_{Kl/0/} \nabla T^s_{l/0/}\, d\tau + \sum_{K=1}^{3}\sum_{l=1}^{3} \left[\overline{\Delta X}_{02_K} \int_{\tau=t_0}^{t} p_{Kl/2/} \nabla T^s_{l/2/}\, d\tau - \overline{\Delta X}_{01_K} \int_{\tau=t_0}^{t} p_{Kl/1/} \nabla T^s_{l/1/}\, d\tau \right], \qquad /59/$$

or in more compact from

$$\overline{\Delta\dot{\varrho}_{12}}_0 - \overline{\Delta\dot{\varrho}_{12}}_c = \sum_{K=1}^{3}\sum_{l=1}^{3} /\overline{\Delta X}_{02_K} - \overline{\Delta X}_{01_K}/ \int_{\tau=t_0}^{t} p_{Kl/0/} \nabla T^s_{l/0/}\, d\tau + \sum_{K=1}^{3}\sum_{l=1}^{3}\sum_{i=1}^{2} /-1/^i \overline{\Delta X}_{0i_K} \int_{\tau=t_0}^{t} p_{Kl/i/} \nabla T^s_{l/i/}\, d\tau. \qquad /60/$$

It should be noticed that the first term of the right-hand side of /60/ contains the influence of anomalous potential on the "mother" satellite. This term is very close to zero when the directions $S_o\ S_1$ and $S_o\ S_2$ are close to each other. In fact, if this term is equal to zero then /60/ becomes identical to the observation equation /51/, which is appropriate for the case of two satellites.

The observation equation /60/ can be finally written in the form:

$$\overline{\Delta\dot{\varrho}_{12}}_0 - \overline{\Delta\dot{\varrho}_{12}}_c = \sum_{K=1}^{3}\sum_{l=1}^{3}\sum_{i=1}^{2} /-1/^i \overline{\Delta X}_{0i_K} \sum_{j=0}^{1} \int_{\tau=t_0}^{t} p_{Kl/i-j/} \nabla T^s_{l/i-j/}\, d\tau . \qquad /61/$$

If we denote as previously by s'_A and s'_B the signals of observations A and B respectively, where

$$S'_A = \sum_{K=1}^{3}\sum_{l=1}^{3}\sum_{i=1}^{2} /-1/^i \overline{\Delta X}_{0i_{K_A}} \sum_{j=0}^{1} \int_{\tau=t_0}^{t} p_{Kl/i-j/_A} \nabla T^s_{l/i-j/_A}\, d\tau , \qquad /62/$$

and

$$S'_B = \sum_{m=1}^{3}\sum_{n=1}^{3}\sum_{p=1}^{2} /-1/^p \overline{\Delta X}_{0p_{m_B}} \sum_{q=0}^{1} \int_{\sigma=u_0}^{u} p_{mn/pq/_B} \nabla T^s_{n/pq/_B}\, d\sigma , \qquad /63/$$

then the autocovariance between signals s'_A and s'_B is the following:

$$cov/S'_A,S'_B/=\sum_{K=1}^{3}\sum_{m=1}^{3}\sum_{l=1}^{3}\sum_{n=1}^{3}\sum_{i=1}^{2}\sum_{p=1}^{2}/-1/^{i+p}\overline{\Delta X}_{0i_{K_A}}\overline{\Delta X}_{0p_{m_B}}\sum_{i=0}^{1}\sum_{q=0}^{1}\int_{\tau=t_0}^{t}\int_{\sigma=u_0}^{u}P_{Kl/i\cdot j/_A}P_{mn/p\cdot q/_B}cov/\nabla T^S_{l/i\cdot j/_A},\nabla T^S_{n/p\cdot q/_B}/d\sigma d\tau \qquad /64/$$

and the covariance between the signal s'_A and the anomalous potential T at the point Q is

$$cov/S'_A,T_Q/=\sum_{K=1}^{3}\sum_{l=1}^{3}\sum_{i=1}^{2}/-1/^{i}\overline{\Delta X}_{0i_{K_A}}\sum_{j=0}^{1}\int_{\tau=t_0}^{t}P_{K_{l/i\cdot j/_A}}cov/\nabla T^S_{l/i\cdot j/_A},T_Q/\,d\tau\,. \qquad /65/$$

4. Conclusion

The observation equations derived in the sequel refer to the observations already corrected for the effects of ionospheric refraction and air drag. Another nongravitational effects are relatively small and they can be neglected.

The formulas describing the basic covariances are very convenient for using electronic computer technique. However, it should be noticed that even taking into account a small time interval $/t_o,\ t/$ of about 10 seconds and the simplest algorithm for numerical integration we have to call 10 000 times the subroutine calculating the covariances between the components of the gradient of anomalous potential in order to compute one covariance between the signals. Therefore, if the subroutine for computation of covariances between the components of ∇T works slow in the computer sense, as it is in case of COVAX, then computation of covariance between signals takes a tremendous much computer time. Then the main problem

of practical elaboration of satellite-to-satellite data is to create the covariance function on one hand representing statistical properties of the gravity field as determined from the data and simultaneously having analytical form as simple as possible.

Bibliography

Kryński J. /1978/: Possibilites of Low-Low Satellite Tracking for Local Geoid Improvement, Mitteilungen der geodätischen Institute der Technischen Universität Graz, Folge 31.

Kryński J. /1979/: Observation Equations for Satellite-to-Satellite Tracking, Artificial Satellites, Vol.14, No 2-3.

Moritz H. /1973/: Least-Squares Collocation, Deutsche Geodätische Kommission, Reihe A, No. 75.

Rummel R., Reigber Ch., Ilk K.H. /1978/: The Use of Satellite-to-Satellite Tracking for Gravity Parameter Recovery, European Workshop on Space Techniques for Solid Earth, Oceanography and Geodesy, Schloss Elmau.

Rummel R. /1979/: Determination of Short-Wavelength Components of the Gravity Field from Satellite-to-Satellite Tracking or Satellite Gradiometry. An Attempt to an Identification of Problem Areas, Manuscripta Geodaetica, Vol. 4.

Schwarz Ch.R. /1970/: Gravity Field Refinement by Satellite Doppler Tracking, OSU Report No. 147, Columbus, Ohio

Tscherning C.C. /1976/: Covariance Expressions for Second and Lower Order Derivatives of the Anomalous Potential, OSU Report No. 225, Columbus, Ohio.

Zieliński J.B. /1978/: Investigation of the Earth Gravity Field by Differential Doppler Measurements /satellite-to-satellite tracking/, Artificial Satellites, Vol. 13, No 3.

Abstract:

The concept of measuring the relative velocity of two satellites following each other along similar orbits has been considered. A general form of the observation equation was derived. The main covariances which are necessary for the least-squares solution have been described. The formulas derived can be used for geodetical elaboration of satellite-to-satellite data.

Collocation with analytic (harmonic) splines and stability conditions

by

D. Lelgemann 1/

"The statistical origin of collocation has sometimes overshadowed the fact that this method can also be considered as a purely analytical approximation method" (H. MORITZ).

SUMMARY

Collocation with kernel functions (analytic splines) may yield unstable results if the free parameters R_Q and k_n of the kernel

$$K(P,Q) = \sum_{n=o}^{\infty} k_n \left(\frac{R_Q}{r_P}\right)^{n+1} P_n(\cos\psi)$$

are not chosen properly. As a stability criterion the size of the Euclidian norm of the vector of the interpolation coefficients $\alpha_i(P)$ is used in this study.
Based on this criterion limits $R_{min} < R_Q < R_{max}$ are determined, related to the distance $\delta\psi$ of the (homogeneously distributed) knots on a sphere with radius R:

$$R_{max} = R - (0.5 + 0.5\cdot o_K)\delta\psi \quad , \quad R_{min} = R - (3 + 0.5\cdot o_K)\delta\psi.$$
$$(o_K \neq -1)$$

The order $o_K = O.(k_n)$ is defined as the highest power of n within the explicit expression for k_n. The size of the resulting interpolation coefficients $\alpha_i(P)$ illustrates the usefulness of the stability criterion.

1/ Institut für angewandte Geodäsie, Frankfurt/M.

1. INTRODUCTION

One fundamental method of numerical mathematics is the representation of a function T by the determination of a set of coefficients b_i of a finite series of base functions (Collatz 1968, p.9). For example, the disturbing potential T of the earth is usually approximated by a linear combination t of suitable base functions $\Phi_1, \Phi_2 \ldots \Phi_I$:

$$T(P) \doteq t(P) = \sum_{i=1}^{I} b_i \, \Phi_i(P), \qquad (1 - 1)$$

P denotes a space point in the domain Ω on and outside a sphere ω with radius R (R = 6378140 m).
T should be harmonic in the domain Ω. It may be therefore appropriate to select as base functions Φ_i harmonic functions, satisfying Laplace's equation

$$\Delta \Phi_i = 0 \qquad (1 - 2)$$

at least in the domain Ω. As Φ_i spherical harmonics are frequently chosen but the Φ_i may also be given, for instance, by the potential of point masses suitably distributed inside the sphere ω.

As a special kind of base functions we may also use harmonic functions $K(P,Q_i)$ which depend on space points Q_i on and outside the sphere ω with spherical coordinates $(\Theta_i, \lambda_i, r_i)$:

$$\Phi_i(P) = K(P,Q_i) = \sum_{n=o}^{\infty} k_{ni} \left(\frac{R_i}{r_p} \right)^{n+1} P_n(\cos \psi). \qquad (1 - 3)$$

The points Q_i are frequently called knots and the functions $K(P,Q_i)$ are called analytic (harmonic) splines, harmonic kernel functions, harmonic multiquadric functions etc.
ψ is the spherical distance between P and Q, and R_i and k_{ni} denote free parameters. In general, for each knot Q_i special values k_{ni} and R_i may be chosen with the restriction

$$r_i \cdot R_i = R_o^2 < R^2. \qquad (1 - 4)$$

In this study a homogeneous distribution of the knots on the sphere ω is frequently assumed. As in such cases the parameters R_i and k_{ni} are chosen to be constant they are abbreviated $R_i = R_Q = \text{const}$ and $k_{ni} = k_n = \text{const}$.

The coefficients b_i must be chosen such that they satisfy certain conditions. For example, we may postulate that the approximation t to T, as given by (1-1), exactly reproduces T at a number I of given knots Q_i. On putting

$$t(Q_i) = T(Q_i) = f_i \quad , \quad i = 1, 2, 3 \ldots I \tag{1 - 5}$$

we thus have the equation system

$$\sum_{i=1}^{I} A_{ik}\, b_i = f_k \quad , \quad A_{ik} = K(Q_i, Q_k). \tag{1 - 6}$$

As is well-known we have to distinguish between interpolation, collocation and approximation. A generalisation of the interpolation problem is the case in which I values of linear functionals L_1T, L_2T, ... L_IT of T are to be reproduced in the knots Q_i. On putting

$$L_i f = L_i T = l_i \tag{1 - 7}$$

from (1-1)

$$\sum_{i=1}^{I} B_{ik}\, b_i = l_k \quad , \quad B_{ik} = L_k \phi_i = L_k K(P, Q_i), \tag{1 - 8}$$

$$P = Q_1, Q_2, Q_3 \ldots Q_I.$$

This method of fitting an analytic (harmonic) approximation to I given functionals is called collocation, a generalisation of interpolation (de Boor 1978). The systems of linear equations (1-6) and (1-8), respectively, are in general not symmetric.

It may often be desirable to represent the function T by a number of b_i less than the number of observations - an overdetermined approximation problem instead of a collocation problem. If the number

of observations is greater than the number of knots we may solve the system (1-8) under the condition that the sum of the squares of the residuals

$$v_i = l_i - L_k\, t(Q_i) \qquad (1-9)$$

becomes a minimum (Collatz 1968, p.9, Heitz 1968). In general, an overdetermined problem provides a realistic a-posteriori error estimation.

An essential problem which remains is the choice of the free parameters k_{ni} and R_i, as is easily recognizable in considering the graphs in figure 1. Given the function values

$$f_i = 1 + 0.2(-1)^i \qquad (1-10)$$

in 10 equally spaced knots on a meridian the interpolation has been performed using $k_n = 1$ and four different values R_Q as listed in the figure. If a relatively small value R_Q is used as in graph 1d the interpolating function tends to become unstable at the boundaries, similar to Lagrange interpolation using equally spaced knots. Indeed, in the one-dimensional case interpolation with analytic splines converges to Lagrange interpolation if $R_Q \to 0$. (Golomb 1976, p.104).

The higher order discontinuities of the usual polynomial splines are replaced by the poles of the analytic splines, poles outside the domain Ω, i.e. inside the sphere ω. The poles have a simple geometric relationship to the knots. Considering splines of the form given by (1-3) the sites of the poles of a particular spline form a rotation surface defined by the equation

$$\frac{r_o^2}{R_Q^2} - \frac{2r_o}{R_Q}\cos\psi + 1 = 0; \qquad (1-11)$$

r_o is the radius of the positions of the poles. In case that all knots are situated at the sphere ω all poles can be found therefore on and inside a sphere with radius

$$r_o = R_Q. \qquad (1-12)$$

Figure 1: Analytic spline interpolation using various parameters R_Q

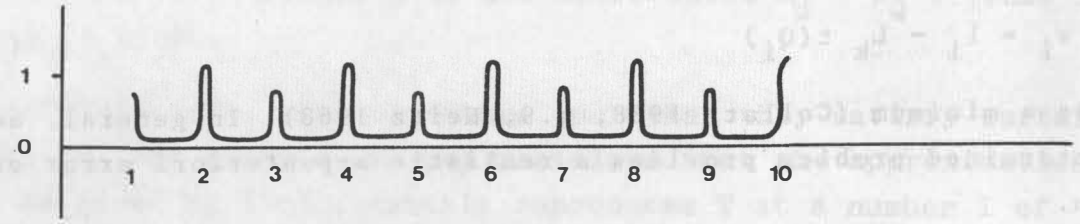

Graph 1a: $R_Q = 6\,378\,000$ m $> R_{max}$

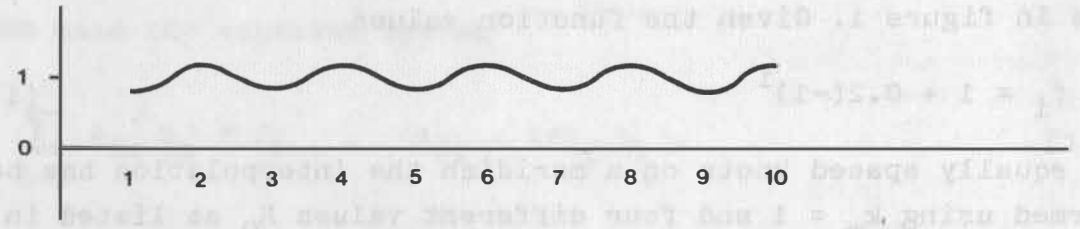

Graph 1b: $R_Q = 6\,367\,008$ m $= R_{max}$

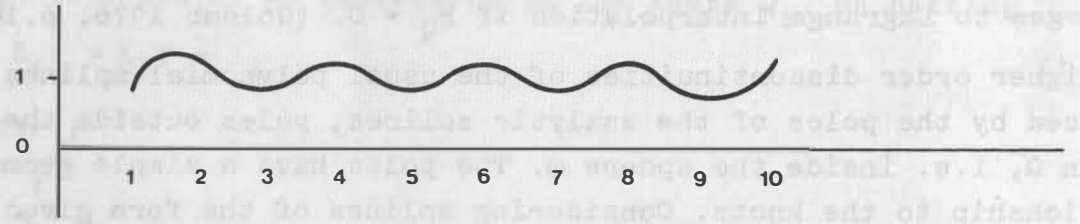

Graph 1c: $R_Q = 6\,311\,348$ m $= R_{min}$

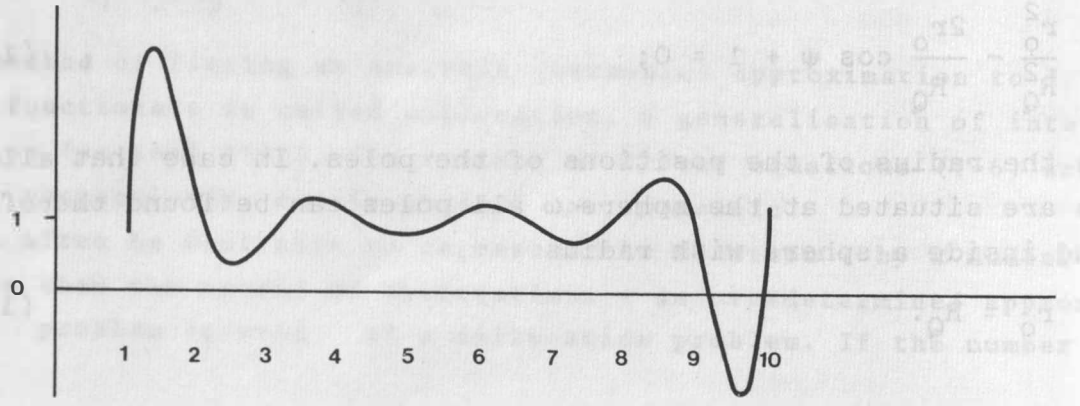

Graph 1d: $R_Q = 6\,000\,000$ m $< R_{min}$

Considering the stability behaviour of an interpolating analytic spline function, attention will be paid to the relation of the distance $\delta\psi$ of homogeneously distributed knots and the position of the poles, i.e. the size of the parameter R_Q.

2. INTERPOLATION AND STABILITY CRITERIA

Analytic splines provide the solution of a linear partial differential equation, namely Laplace's equation. Hadamard has introduced the conception of an ill-posed problem into the theory of linear partial differential equations. A problem is called well-posed if it satisfies three requirements:

- a solution exists and is bounded
- the solution is unique for a given set of initial data
- the solution depends continuously on the size of the initial data.

Otherwise, the problem is called ill-posed.

In the course of the analysis of numerical problems it may be advisable to extend these requirements to the conception of a well-posed algorithm (Isaacson-Keller 1973). An algorithm designed for the solution of a well-posed problem is also called well-posed if

- a solution exists and is bounded
- the solution is unique for the given data
- the solution is stable, i.e. small variations in the initial data effect the result only by small variations.

The series (1-1) is a solution of Laplace's equation if the base functions defined by (1-3) are used. The solution exists and is bounded if condition (1-5) is observed. The solution is unique as long as the equation system (1-6) or (1-8), respectively, remains non-singular. In general, the stability of the solution may depend on the initial data. However, at least the simple interpolation between the knots should be stable. This requirement has to be expressed, of course, by a suitable mathematical formulation.

It is well-known that the stability of interpolation using polynomials depends on the maximal degree n of the polynomial as well as on the distribution of the knots in a given interval [a,b]. The error of polynomial interpolation can be expressed by (Isaacson-Keller 1973)

$$f(x) - P_n(x) = \frac{\omega_n(x)}{(n+1)!} f^{(n+1)}(\xi). \qquad (2 - 1)$$

$f^{(n+1)}(\xi)$ is the (n+1)th derivative in a certain point ξ of the approximation interval [a,b]. The function

$$\omega_n(x) = \prod_{j=o}^{n} (x-x_j) \qquad (2 - 2)$$

is termed the error factor. A graph of the error factor is often used to illustrate the stability properties of polynomial interpolation (Isaacson-Keller 1973, p. 279, Moritz-Sünkel 1978, p.24), especially to illustrate the unfavourable error propagation of polynomial interpolation at points near the boundary of the interval [a,b].
In figure 2 a graph of the error factor $\omega(x)$ is given for equally-spaced knots, in figure 3 a graph of the error factor using the so-called Tschebyschew's interpolation points, which are defined at the zeros of Tschebyschew's polynomials and are given by

$$y_k = \cos\left[\frac{2k+1}{n+1}\frac{\pi}{2}\right] \qquad (2 - 3a)$$

$$k = 0,1 \ldots . n$$

$$x_k = \frac{1}{2}[(b-a)y_k + (a+b)] \qquad (2 - 3b)$$

Since the definition of the error factor is closely related to polynomial interpolation it cannot be used to investigate the stability problems using analytic splines. It is therefore necessary to look for another criterion.

In geodesy the stability property of a functional model is usually described by the size of the standard error, using the law of stochastic error propagation. In the sequel this method will be

Figure 2: Polynomial interpolation: Equidistant knots

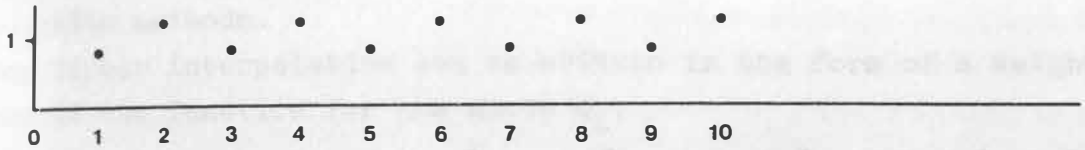

Graph 2a: Distribution of the knots

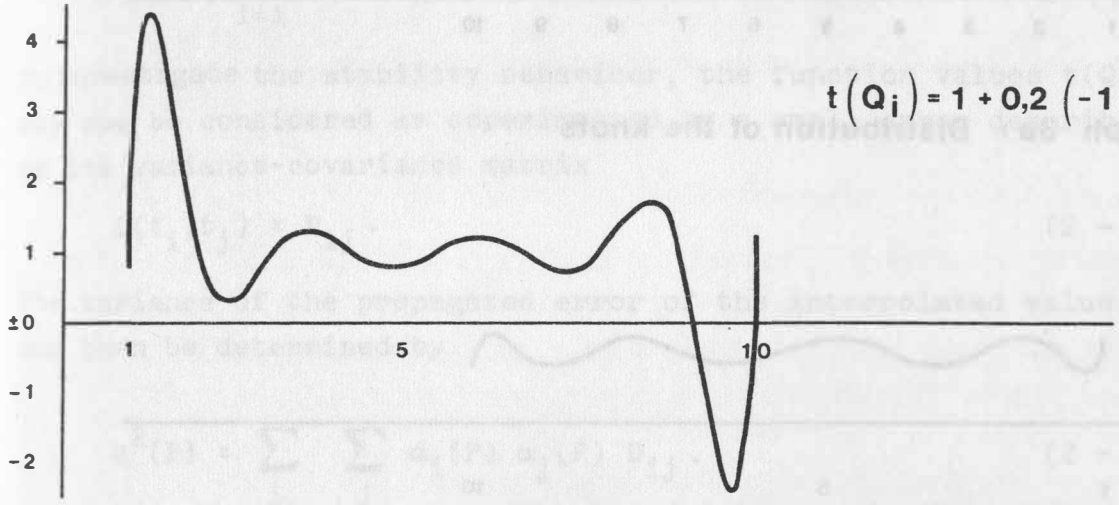

Graph 2b: Graph of the function

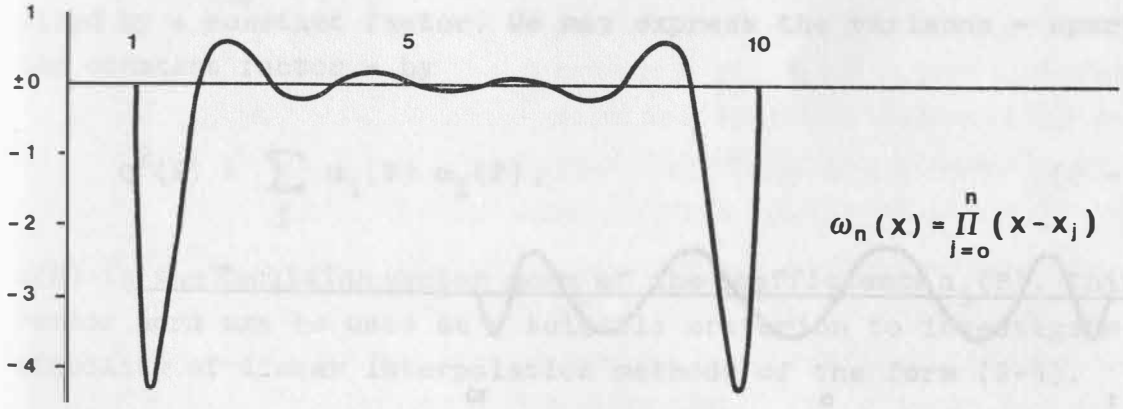

Graph 2c: Graph of the error factor

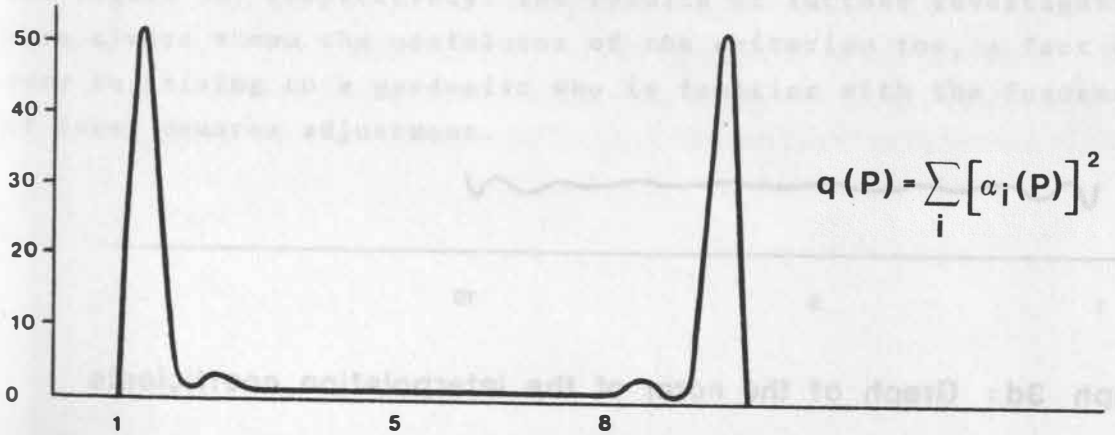

Graph 2d: Graph of the norm of the interpolation coefficients

Figure 3: Polynomial interpolation: Tschebyschew points

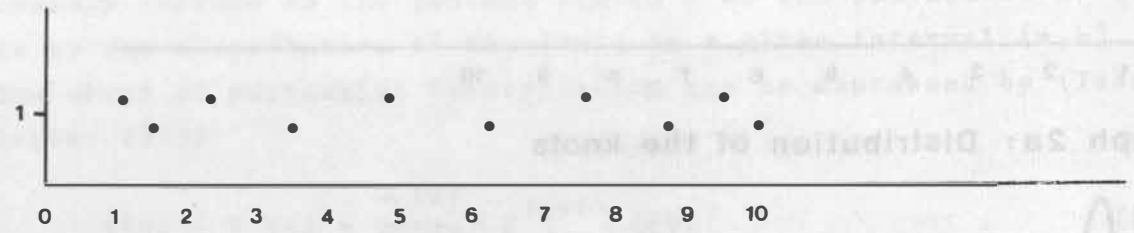

Graph 3a: Distribution of the knots

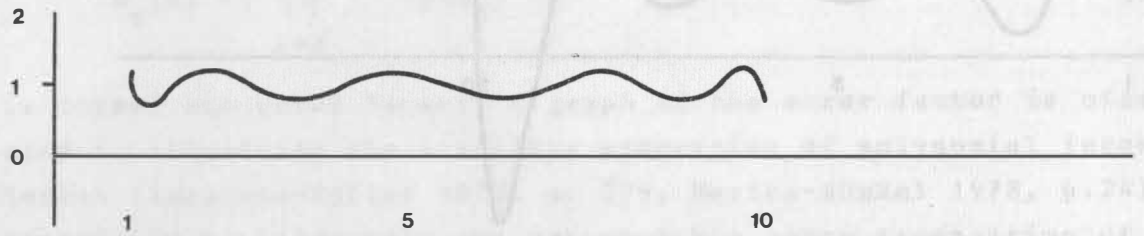

Graph 3b: Graph of the function

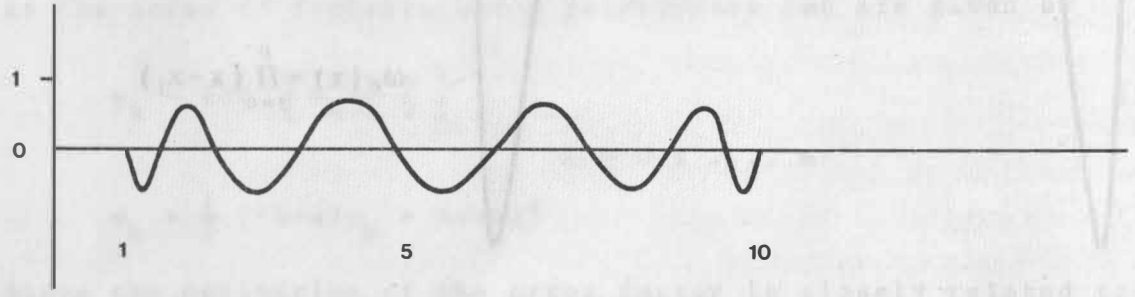

Graph 3c: Graph of the error factor

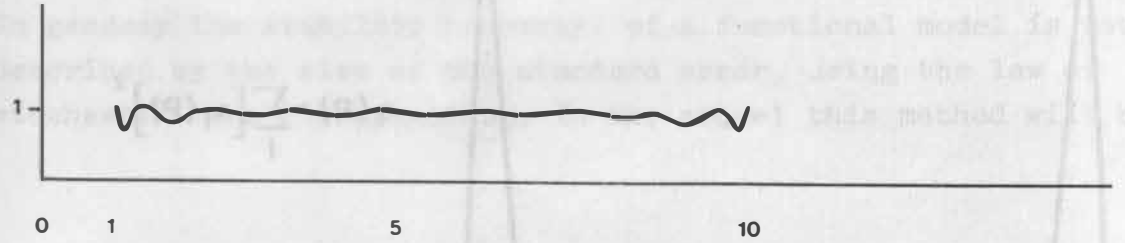

Graph 3d: Graph of the norm of the interpolation coefficients

applied to investigate the stability properties of linear interpolation methods.
Any linear interpolation can be written in the form of a weighted sum of the function for the knots Q_i,

$$t(P) = \sum_{i=1}^{I} \alpha_i(P) \cdot t(Q_i). \qquad (2 - 4)$$

To investigate the stability behaviour, the function values $t(Q_i)$ may now be considered as superimposed by a small error described by its variance-covariance matrix

$$D(t_i,t_j) = D_{ij}. \qquad (2 - 5)$$

The variance of the propagated error of the interpolated value t(P) can then be determined by

$$q^2(P) = \sum_i \sum_j \alpha_i(P)\, \alpha_j(P)\, D_{ij}. \qquad (2 - 6)$$

Assume now the simplest case, namely independent errors of the same size. D_{ij} can be expressed then by the diagonal unit matrix multiplied by a constant factor. We may express the variance - apart from the constant factor - by

$$q^2(P) = \sum_i \alpha_i(P)\, \alpha_i(P). \qquad (2 - 7)$$

q(P) is the Euclidian vector norm of the coefficients $\alpha_i(P)$. This vector norm may be used as a suitable criterion to investigate the stability of linear interpolation methods of the form (2-4).

As an example, a graph of the vector norm q(P) for the results of the polynomial interpolations described above is drawn in figure 2d and figure 3d, respectively. The results of further investigations have always shown the usefulness of the criterion too, a fact not very surprising to a geodesist who is familiar with the fundamentals of least squares adjustment.

Without doubt piecewise linear interpolation or bilinear interpolation (roof functions, bilinear elements) provides very stable results. The norm of the interpolation coefficients attains a value q(P) somewhere between two limits. For the one-dimensional case of piecewise linear interpolation the limits are

$$1 = q_{max}(P) \geq q(P) \geq q_{min}(P) = \sqrt{2 \cdot 0.5^2} = \sqrt{0.5}; \qquad (2 - 8a)$$

for the two-dimensional case of bilinear interpolation the limits are

$$1 = q_{max}(P) \geq q(P) \geq q_{min}(P) = \sqrt{4 \cdot 0.25^2} = 0.5 \qquad (2 - 8b)$$

The maximum is always obtained in the knots and the minimum midway between the knots. Regarding all points P in an interval given by a set of knots an interpolation method may be considered to be stable if these limits are observed, at least approximately.

3. STABLE INTERPOLATION AT A BOUNDARY SPHERE

In the course of investigating a well-posed algorithm it must be ascertained that only well-posed problems are considered. An ill-posed problem is the analytical downward continuation of the potential (Schwarz 1971). To avoid a mishmash of the (natural) instabilities due to downward continuation with (artificial) instabilities due to an ill-posed algorithm all knots have to be placed at the boundary of the domain Ω of harmonicity, i.e. at the sphere ω.

As already pointed out in previous studies (Koch 1973, Lelgemann 1978) the parameters of the kernel function $K(P,Q_i)$ have to be adjusted to the density of the knots in order to obtain satisfactory interpolation results. At least within the course of the investigations of the stability properties of the algorithm a homogeneous distribution of the knots within the region covered by the knots will be advisable. A homogeneous distribution can be obtained by a grid of (nearly) equidistantly chosen knots. The distance between the knots is denoted by $\delta\psi$. The scale of $\delta\psi$ may be degree or km.
By applying analytic splines $K(P,Q_i)$ the vector of the coefficients

$\alpha_i(P)$ has to be computed by the matrix product

$$\alpha_i(P) = K(P,Q_j) \cdot K^{-1}(Q_j,Q_i). \qquad (3 - 1)$$

The coefficients $\alpha_i(P)$ do not depend on the function T but on the size of the free parameters k_n and R_Q. This interrelationship will be investigated in the following two subsections.

3.1 THE CHOICE OF THE FREE PARAMETER R_Q

In the course of this subsection we will always assume $k_n = 1$. The parameter R_Q (or the parameters R_i) is chosen to fall between the limits

$$R_{min} \leq R_Q \leq R_{max}. \qquad (3 - 2)$$

These limits should be chosen such as to observe the limits (2 - 8) of the norm of the interpolation coefficients for any point P within the whole region covered by the knots. Under the two restrictions described above (homogeneous distribution of the knots at the boundary sphere ω) the following relationships have been found by empirical investigations:

$$R_{min} = R - 0.5\ \delta\psi\ [km] \qquad (3 - 3a)$$

$$R_{max} = R - 3 \cdot \delta\psi\ [km] \qquad (3 - 3b)$$

These empirical relations are very rigid with respect to further model modifications. Test computations have shown

- nearly no dependence on the number of the knots (if this number is not to small, say more then 10)
- only little dependence on the dimension of the distribution of the knots (one- and twodimensional)
- nearly no dependence on the size of the distance $\delta\psi$ as long as $\delta\psi \leq 1^o$ (and only little dependence in case of large distances, e.g. $\delta\psi \sim 5^o$)

The size of the extreme values of the parameters R_Q depends, however, strongly on the chosen parameter k_n as will be shown in the next subsection.

If a value R_Q is chosen between the two limits given by (3 - 3) the interpolation result will always behave very stably. If the parameter R_Q is chosen somewhere midway between these limits, e.g.

$$R_Q = R - 2 \cdot \delta\psi_m \qquad (3 - 4)$$

the procedure allows obviously for small inhomogeneities in the distribution of the knots. Therefore, in (3 - 4) $\delta\psi_m$ denotes a mean value of the distances between slightly inhomogeneously distributed knots.

The size of the interpolation coefficients $\alpha_i(P)$ as listed in the tables 1 and 2 in the appendix illustrates the usefulness of criterion (3 - 3). In both cases (one and twodimensional), a (nearly) equidistant point grid of knots was used.

In table 1 the interpolation coefficients (determined with four parameters R_Q, chosen to be the same values as used for the four samples shcwn in graph 1) are listed for two different points P. The points P are marked by dark circles. The parameters R_Q are chosen to demonstrate the behaviour of the coefficients for

$$R_Q > R_{max}$$
$$R_Q = R_{max}$$
$$R_Q = R_{min}$$
$$R_Q < R_{min}$$

Table 2 shows the behaviour of the interpolation coefficients in the twodimensional case. Consider especially the resemblance of the coefficients of example 2d and 2e as compared to the coefficients found in the one-dimensional case 1c. Remarkable is also the very wild behaviour of the coefficients in example 2g and the very regular behaviour of the coefficients in example 2h. Of course, all these coefficients are not related to a special form of the function T. They depend only on the size of the free parameter R_Q and therefore on the position of the poles of the interpolating function.

3.2 THE CHOICE OF THE FREE PARAMETER k_n

It remains to investigate the influence of a modification of the free parameter k_n on the behaviour of the coefficients $\alpha_i(P)$ and in this

connection on the choice of R_Q. As one result of these investigations it turned out that not the individual values of k_n but the order $O.(k_n)$ of k_n is essential for the choice of R_Q. The order $O.(k_n)$, abbreviated in the sequel as o_k, is defined as the highest power of n within the explicit expression for k_n.

The infinite series

$$K(P,Q) = \sum_{n=o}^{\infty} k_n \left(\frac{R_Q}{r_p}\right)^{n+1} P_n(\cos\psi) \qquad (3-5)$$

was summed to form closed expressions for four different parameters k_n. As a common abbreviation

$$L = \frac{r_p^2}{R_Q^2} - 2\frac{r_p}{R_Q}\cos\psi + 1 \qquad (3-6)$$

is used. Test computations have been carried out with six different kernels, including

1. kernel $K_1(P,Q_i)$ (Logarithmic kernel): $k_n = \frac{1}{n+1}$, $o_k = -1$

$$K_1(P,Q) = \ln\left(1 + \frac{2}{(L^{1/2} + \frac{r_p}{R_Q} - 1)}\right) \qquad (3-7)$$

2. kernel $K_2(P,Q_i)$ (Krarups kernel:) $k_n=1$, $o_k=0$

$$K_2(P,Q) = 2\cdot L^{-1/2} \qquad (3-8)$$

3. kernel $K_3(P,Q_i)$ (Szegös kernel:) $k_n = (2n+1)$; $o_k=1$

$$K_3(P,Q) = \frac{r_p^2 - R_Q^2}{R_Q^2 L^{3/2}} \qquad (3-9)$$

4. Kernel $K_4(P,Q_i)$ $k_n = (n+1)(2n+1)$; $o_k=2$

$$K(P,Q) = -2\left(\frac{r_p}{R_Q}\right)^2 L^{-3/2} + 3\left(\frac{r_p}{R_Q}\right)\left(\left(\frac{r_p}{R_Q}\right)^2 - 1\right)\left(\frac{r_p}{R_Q} - \cos\psi\right) L^{-5/2} \qquad (3-10)$$

As a result of the test computations it appeared that the interpolation coefficients undergo negligible change if the extreme values for R_Q are

determined using the following empirical relations:

$$R_{max} = R - (0.5+C\cdot o_k)\,\delta\psi, \qquad C = \begin{cases} 0.25 & \text{if } o_k = -1 \\ 0.5 & \text{if } o_k \neq -1 \end{cases} \qquad (3-11)$$

$$R_{min} = R - (3\ \ +C\cdot o_k)\,\delta\psi. \qquad C = 0.5$$

As an example the coefficients of the one - dimensional test model are listed in table 3 and 4 in the appendix when all four kernels have been used.

The essential effect of a variation of the kernel function by a modification of the parameter k_n is therefore a shifting of the poles of the interpolating function in a radial direction. This fact may be extremely important for such applications of the analytic splines which are directly or indirectly related to analytical downward continuation. A typical problem of that kind is Krarups problem which will be considered in the next section.

4. STABLE INTERPOLATION AT THE SURFACE OF THE EARTH

In (Krarup 1969) a theorem developed by C. Runge was specialised to geodetic problems. According to this theorem the gravity potential outside the earth can be approximated by spherical harmonics converging at least in a domain including the geoid. All poles of the interpolating function must therefore be included inside the geoid. In this way it is ensured that the downward continuation to the geoid fulfils the condition 1 of a well-posed problem.

However, Runge's theorem does not ensure that condition 3 of a well-posed problem is fulfilled too. Since the function of analytical continuation may be very rough inside the earth a development of the potential of analytical continuation at the geoid into a series of spherical harmonics may show undesirable, very unstable numerical properties.

Based on the investigations in the last section we will show how to choose the kernel function $K(P,Q_i)$ for knots Q_i at the earths'surface to get a stable series evaluation of the potential on and outside the earths'surface, but not necessarily stable at the geoid. The geoid is considered to have the form of a sphere (spherical approximation).

The knots Q_i should form for this purpose a grid over the earth surface; the desired resolution of the approximating function is given by the distance $\delta\psi$.

Let us assume that the logarithmic kernel $K_1(P,Q_i)$ is used at the geoid. At height

$$h = R^2_{max} - R^1_{max} = 0.5\ \delta\psi \qquad (4 - 1)$$

we need to use the Krarup kernel $K_2(P,Q_i)$, both K_1 and K_2 should be considered with their corresponding parameter R_{max}. A stable interpolation function is obtained then at the surface of the geoid and e.g. at the top of a mountain of height h. It is important to note that all poles of the interpolating function are inside the geoid as required by Krarup's theorem.

If the mountain is lower than $h = 0.5\ \delta\psi$ or for the knots at the slope of the mountain we may always obtain a suitable kernel by applying a weighted mean,

$$K(P,Q_i) = a(r_i)\cdot K_1(P,Q) + b(r_i)\ K_2(P,Q)\ . \qquad (4 - 2)$$

Since the (empirical) relation between the extreme parameters R_{max} for kernels of various order are linear the coefficients a and b must be chosen according to

$$\frac{r_i - R}{r_h - R} = a \quad \text{and} \quad \frac{r_h - r_i}{r_h - R} = b. \qquad (4 - 2a)$$

If the mountain is higher than $h = 0.5\ \delta\psi$ a third kernel has to be applied with $k^3_n = O.(n)$ or even a fourth kernel with $k^4_n = O.(n^2)$ etc.. In this way a stable interpolation function is obtain at the surface of the earth, at least, if the slope of the terrain is not too large.

5. FINAL REMARKS

The following problems remain:

- downward continuation using analytical splines
- inhomogeneous and anisotropic distributed knots
- the relationship to Least squares collocation.

The problem of downward continuation is one of the most important of modern physical geodesy. A discussion of this very difficult problem is not the objective of this study. On the other hand there seem to be

some remarkable links between the investigation of the range, in which stable or at least nearly stable analytical continuation may be possible and the technique used in the preceding sections.

The problem of inhomogeneously distributed knots may become critical especially if collocation based on all available measurements will be used. Small inhomogeneities in the set of mutual distances of the knots may be caught up by the choice of the parameter R_Q within the limits $R_{max} > R_Q > R_{min}$. If the differences in the distances to neighbouring points are too large, nevertheless, anisotropic kernel functions (i.e. kernel functions depending on the azimuth) have to be used. Investigations by applying anisotropic kernel functions are described e.g. in (Kearsley 1977).

As pointed out e.g. in (Moritz 1978) the advantages of the statistical interpretation of the results of Least squares collocation are the error estimates. Such a statistical interpretation can be preserved by removing global effects from the global covariance function until a local covariance function is obtained which can be approximated by a kernel function of a form in accordance with the stability requirements. In this connection it is an important fact that a critical quantity for the error estimation - the variance at the origin $\psi = 0$ of the covariance function - has no influence on the size of the interpolating function as can be seen from the definition of the coefficients $\alpha_i(P)$ in formula (3 - 1). At any rate the interpretation of the error estimation of Least squares collocation is especially deep as shown by the description of the statistical background of Least squares collocation in (Moritz 1978)

REFERENCES

de Boor, C. (1978) A practical guide to splines. Springer Verlag, Berlin

Collatz, L. (1968) Funktionalanalysis and numerische Mathematik. Springer Verlag, Berlin

Golomb, M. (1976) Interpolation operators as optimal recovery schemes for classes of analytic functions. In "Optimal Estimation in Approximation Theory", ed. by C.A. Micchelli und T.J. Rivlin, Plenum Press, New York

Heitz, S. (1969) Eine astronomisch-geodätische Geoidbestimmung für Westdeutschland. Veröff. der D. Geod. Komm., Reihe B, Nr. 167.

Isaacson, E. and Keller, H.B. (1973) Analyse numerischer Verfahren. Verlag Harri Deutsch, Zürich.

Kearsley, W. (1978) Non-stationary estimation in gravity prediction problems. Rep. of Dep. of Geodetic Sciences, No. 256, Ohio State University.

Koch, K.R. (1973) Höheninterpolation mittels gleitender Schrägebene und Prädiktion. Verm., Phot., Kulturtechnik, Mitteilungsblatt 71, S. 219 - 232.

Krarup, T. (1969) A contribution to the mathematical foundation of physical geodesy. Publ. No. 44, Danish Geod. Inst., Copenhagen.

Lelgemann, D. (1978) Ein Verfahren zur astro-gravimetrischen Geoidbestimmung. Veröff. der D. Geod., Reihe C, No. 247.

Moritz, H. (1978) Least squares collocation. Reviews of Geophysics and Space Physics. Vol. 16, No. 3.

Moritz, H. and Sünkel, H. ed. (1978) Approximation methods in geodesy. Wichmann Verlag, Karlsruhe.

Schwarz, K.P. (1971) Numerische Untersuchungen zur Schwerefortsetzung. Veröff. der D. Geod. Komm., Reihe C, No. 171.

REMARK: This work is a report on the results of the SEASAT-1 North SEA project. It was supported by the Sonderforschungsbereich 78 "Satellitengeodäsie" der TU München and the Sonderforschungsbereich 149 "Vermessungs- und Fernerkundungsverfahren an Küsten und Meeren" der Universität Hannover as part of the SURGE (SeaSat Users Research Group of Europe) SeaSat-A proposal to NASA (National Aeronautics and Space Administration).

APPENDIX: Tables of Interpolation Coefficients for Equidistant Grids of Knots and Various Parameter R_Q

Table 1: Interpolation Coefficients $\alpha_i(P)$ of an Onedimensional Grid (Meridian) (R_Q = variable, k_n = constant=1)

Example 1a: R_Q = 6 378 000 m > R_{max} ;

i	1	2	4	5	6	7	8	9	10	
$\alpha_i(P)$	0.01	● 0.01	0	0	0	0	0	0	0	0
$\alpha_i(P)$	0	0	0	0	0.01	● 0.01	0	0	0	0

Example 1b: R_Q = 6 367 008 m = R_{max} ;

i	1	2	3	4	5	6	7	8	9	10
$\alpha_i(P)$	0.49	● 0.50	-0.03	0.01	0	0	0	0	0	0
$\alpha_i(P)$	0	0	0.01	-0.03	0.50	● 0.50	-0.03	0.01	0	0

Example 1c: R_Q = 6 311 348 m = R_{min}

i	1	2	3	4	5	6	7	8	9	10
$\alpha_i(P)$	0.37	● 0.86	-0.36	0.20	-0.12	0.07	-0.04	0.02	-0.01	0
$\alpha_i(P)$	0.01	-0.04	0.09	-0.19	0.63	● 0.63	-0.19	0.09	-0.04	0.01

Example 1d: R_Q = 6 000 000 m < R_{min}

i	1	2	3	4	5	6	7	8	9	10
$\alpha_i(P)$	0.20	● 1.54	-1.79	2.28	-2.31	1.78	-1.00	0.39	-0.10	0.01
$\alpha_i(P)$	0	-0.01	0.04	-0.14	0.61	● 0.61	-0.14	0.04	-0.01	0

● Interpolation point P

Remark: Regard also the corresponding graph of the interpolating function in figure 1

Table 2: Interpolation Coefficients $\alpha_i(P)$ of a Twodimensional Grid
(R_Q = variable, k_n = constant = 1)

Example 2a: R_Q = 6 367 008 m = R_{max}

i	1	2	3	4	5	6	7	8	9	10
1	0.26	0.27	-0.02	0	0	0	0	0	0	0
2	0.27	0.28	-0.02	0	0	0	0	0	0	0
3	-0.02	-0.02	0	0	0	0	0	0	0	0
4	0	0	0	0	0	0	0	0	0	0
5	0	0	0	0	0	0	0	0	0	0
6	0	0	0	0	0	0	0	0	0	0
7	0	0	0	0	0	0	0	0	0	0
8	0	0	0	0	0	0	0	0	0	0
9	0	0	0	0	0	0	0	0	0	0
10	0	0	0	0	0	0	0	0	0	0

Example 2b: R_Q = 6 367 008 m = R_{max}

i	1	2	3	4	5	6	7	8	9	10
1	0	0	0	0	0	0	0	0	0	0
2	0	0	0	0	0	0	0	0	0	0
3	0	0	0	0	0	0	0	0	0	0
4	0	0	0	0	-0.02	-0.02	0	0	0	0
5	0	0	0	-0.02	0.28	0.28	-0.02	0	0	0
6	0	0	0	-0.02	0.28	0.28	-0.02	0	0	0
7	0	0	0	0	-0.02	-0.02	0	0	0	0
8	0	0	0	0	0	0	0	0	0	0
9	0	0	0	0	0	0	0	0	0	0
10	0	0	0	0	0	0	0	0	0	0

● Interpolation point P

Example 2c: R_Q = 6 311 348 m = R_{min}

i	1	2	3	4	5	6	7	8	9	10
1	0.09	0.41	-0.22	0.12	-0.08	0.04	-0.03	0.01	-0.01	0
2	0.41	0.60	-0.18	0.11	-0.06	0.04	-0.02	0.01	-0.01	0
3	-0.22	-0.18	0	0	0	0	0	0	0	0
4	0.12	0.11	0	0.01	0	0	0	0	0	0
5	-0.08	-0.06	0	0	0	0	0	0	0	0
6	0.04	0.04	0	0	0	0	0	0	0	0
7	-0.03	-0.02	0	0	0	0	0	0	0	0
8	0.01	0.01	0	0	0	0	0	0	0	0
9	-0.01	-0.01	0	0	0	0	0	0	0	0
10	0	0	0	0	0	0	0	0	0	0

Example 2d: R_Q = 6 311 348 m = R_{min}

i	1	2	3	4	5	6	7	8	9	10
1	0.01	0	0	0	0	0	0	0	0	0
2	-0.04	0	0	0	0	0	0	0	0	0
3	0.09	0	0	0	0	0	0	0	0	0
4	-0.19	0	0	0	0	0	0	0	0	0
5	0.63	0	0	0	0	0	0	0	0	0
6	0.63	0	0	0	0	0	0	0	0	0
7	-0.19	0	0	0	0	0	0	0	0	0
8	0.09	0	0	0	0	0	0	0	0	0
9	-0.04	0	0	0	0	0	0	0	0	0
10	0.01	0	0	0	0	0	0	0	0	0

● Interpolation point P

Example 2e: R_Q = 6 311 348 m = R_{min}

i	1	2	3	4	5	6	7	8	9	10
1	0	0	0	0	0	0	0	0	0	0
2	0	0	0	0	0	0	0	0	0	0
3	0	0	0	0	0	0	0	0	0	0
4	0	0	0	0	0	0	0	0	0	0
5	-0.03	0.04	-0.04	0.03	-0.02	0.01	-0.01	0	0	0
6	0.42●	0.79	-0.30	0.16	-0.09	0.05	-0.03	0.02	-0.01	0
7	-0.03	0.04	-0.04	0.03	-0.02	0.01	-0.01	-0.01	0	0
8	0	0	0	0	0	0	0	0	0	0
9	0	0	0	0	0	0	0	0	0	0
10	0	0	0	0	0	0	0	0	0	0

Example 2f: R_Q = 6 311 348 m = R_{min}

i	1	2	3	4	5	6	7	8	9	10
1	0	0	0	0	0.01	0.01	0	0	0	0
2	0	0	0	0.01	-0.02	-0.02	0.01	0	0	0
3	0	0	0.01	-0.02	0.05	0.05	-0.02	0.01	0	0
4	0	0.01	-0.02	0.03	-0.12	-0.12	0.03	-0.02	0.01	0
5	0.01	-0.02	0.05	-0.12	0.39	0.39	-0.12	0.05	-0.02	0.01
6	0.01	-0.02	0.05	-0.12	0.39	0.39	-0.12	0.05	-0.02	0.01
7	0	0.01	-0.02	0.03	-0.12	-0.12	0.03	-0.02	0.01	0
8	0	0	0.01	-0.02	0.05	0.05	-0.02	0.01	0	0
9	0	0	0	0.01	-0.02	-0.02	0.01	0	0	0
10	0	0	0	0	0.01	0.01	0	0	0	0

● Interpolation point P

Example 2g: R_Q = 6 000 000 m < R_{min}

i	1	2	3	4	5	6	7	8	9	10
1	-0.20	1.69	-4.08	6.73	-7.54	5.78	-2.95	0.93	-0.14	0
2	1.69	-5.15	17.24	-29.99	34.41	-26.87	14.07	-4.63	0.81	-0.04
3	-4.11	17.31	-49.66	84.34	-96.79	76.93	-41.97	14.98	-3.14	0.28
4	6.79	-30.18	84.52	-143.46	165.88	-134.06	75.37	-28.36	6.52	-0.70
5	-7.62	34.65	-96.92	165.63	-193.58	158.98	-91.63	35.89	-8.79	1.04
6	5.84	-26.96	76.56	-132.78	157.54	-131.68	77.74	-31.54	8.15	-1.04
7	-2.97	13.94	-41.07	73.15	-88.78	75.92	-46.04	19.38	-5.27	0.72
8	0.91	-4.42	14.08	-26.34	33.19	-29.35	18.46	-8.13	2.34	-0.34
9	-0.13	0.69	-2.68	5.52	-7.44	6.95	-4.61	2.16	-0.66	0.10
10	0	-0.02	0.18	-0.49	0.75	-0.77	0.56	-0.28	0.09	-0.02

Example 2f: R_Q = 6 000 000 m < R_{min}

i	1	2	3	4	5	6	7	8	9	10
1	0	0.01	-0.01	0.01	-0.01	-0.01	0.01	-0.01	0.01	0
2	0.01	-0.03	0.06	-0.07	0.03	0.03	-0.07	0.06	-0.03	0.01
3	-0.01	0.06	-0.13	0.14	-0.04	-0.04	0.15	-0.13	0.06	-0.01
4	0.01	-0.07	0.15	-0.16	-0.01	-0.01	-0.16	0.14	-0.07	0.01
5	-0.01	0.03	-0.04	-0.01	0.33	0.34	-0.01	-0.04	0.03	-0.01
6	-0.01	0.03	-0.04	-0.01	0.34	0.33	-0.01	-0.04	0.03	-0.01
7	0.01	-0.07	0.15	-0.16	-0.01	-0.01	-0.16	0.14	-0.07	0.01
8	-0.01	0.06	-0.13	0.14	-0.04	-0.04	0.15	-0.13	0.06	-0.01
9	0.01	-0.03	0.06	-0.07	0.03	0.03	-0.07	0.06	-0.03	0.01
10	0	0.01	-0.01	0.01	0.01	0.01	0.01	0.01	0.01	0

● Interpolation point P

Table 3: Interpolation Coefficients $\alpha_i(P)$ of an Onedimensional Grid
(k_n = variable, $R_Q = R_{min}$ = variable)

Example 3a: $k_n = \frac{1}{n+1}$, R_Q = 6 322 480 m = R_{min}

i	1	2	3	4	5	6	7	8	9	10
$\alpha_{i(P)}$	0.01	-0.03	0.08	-0.18	0.63●	0.63	-0.18	0.08	-0.03	0.01
$\alpha_i(P)$	0.36●	0.87	-0.36	0.20	-0.11	0.07	-0.04	0.02	-0.01	0

Example 3b: k_n = 1, R_Q = 6 311 348 m = R_{min}

i	1	2	3	4	5	6	7	8	9	10
$\alpha_i(P)$	0.01	-0.04	0.09	-0.19	0.63●	0.63	-0.19	0.09	-0.04	0.01
$\alpha_i(P)$	0.37●	0.86	-0.36	0.20	-0.12	0.07	-0.04	0.02	-0.01	0

Example 3c: $k_n = (2n+1)$, R_Q = 6 300 216 m = R_{min}

i	1	2	3	4	5	6	7	8	9	10
$\alpha_i(P)$	0.01	-0.04	0.09	-0.19	0.63●	0.63	-0.19	0.09	-0.04	0.01
$\alpha_i(P)$	0.38●	0.85	-0.36	0.21	-0.13	0.08	-0.05	0.03	-0.01	0

Example 3d: $k_n = (n+1)(2n+1)$, R_Q = 6 289 084 m = R_{min}

i	1	2	3	4	5	6	7	8	9	10
$\alpha_i(P)$	0.01	-0.04	0.09	-0.19	0.63●	0.63	-0.19	0.09	-0.04	0.01
$\alpha_i(P)$	0.39●	0.85	-0.36	0.22	-0.13	0.08	-0.05	0.03	-0.01	0

● Interpolation point P

Table 4: Interpolation Coefficients $\alpha_i(P)$ of an Onedimensional Grid (k_n = variable, $R_Q = R_{max}$ = variable)

Example 3a: $k_n = \frac{1}{n+1}$, R_Q = 6 372 574 m = R_{max}

i	1	2	3	4	5	6	7	8	9	10
$\alpha_i(P)$	0	0	0.01	-0.02	0.51●	0.51	-0.02	0.01	0	0
$\alpha_i(P)$	0.50●	0.51	-0.02	0.01	0	0	0	0	0	0

Example 3b: k_n = 1, R_Q = 6 367 008 m = R_{max}

i	1	2	3	4	5	6	7	8	9	10
$\alpha_i(P)$	0	0	0.01	-0.03	0.50●	0.50	-0.03	0.01	0	0
$\alpha_i(P)$	0.49●	0.50	-0.03	0.01	0	0	0	0	0	0

Example 3c: k_n = (2n+1), R_Q = 6 355 876 m = R_{max}

i	1	2	3	4	5	6	7	8	9	10
$\alpha_i(P)$	0	0	0.01	-0.08	0.55●	0.55	-0.08	0.01	0	0
$\alpha_i(P)$	0.53●	0.56	-0.08	0.01	0	0	0	0	0	0

Example 3d: k_n = (2n+1) (n+1), R_Q = 6 344 744 m = R_{max}

i	1	2	3	4	5	6	7	8	9	10
$\alpha_i(P)$	0	-0.01	0.02	-0.11	0.58●	0.58	-0.11	0.02	-0.01	0
$\alpha_i(P)$	0.54●	0.59	-0.11	0.03	-0.01	0	0	0	0	0

● Interpolation point P

RESEARCH IN SATELLITE GEODESY IN THE FRAME OF THE INTERCOSMOS PROGRAM

A. G. Massevitch[1], I. Almár[2], N. Georgiev[3], K. Hamal[4], H. Montag[5], S. Tatevian[1], Y. Zielinsky[6]

(Adressen siehe S. 415)

1. INTRODUCTION

At present Bulgaria, Cuba, Czechoslovakia, the GDR, Hungary, Mongolia, Poland, Roumania, the USSR and Vietnam participate in the Intercosmos multilateral cooperation program for space research. In the framework of this program joint experiments are carried out in explorations of the ionosphere and magnetosphere, solar-terrestrial relations, Radio, X-Ray and γ-astronomy, the interplanetary medium, natural resources, and technological experiments in space.

One of the Intercosmos program aspects is scientific cooperation in satellite geodesy and geodynamics. For this purpose a permanent commission - Section 6 of the Working Group "Space Physics" - has been set up which coordinates satellite tracking campaigns, observational data exchange, unification of reduction routines, exchange of observers and experts, modernisation and development of tracking techniques; makes recommendations on participation in other international programs. Four directions of research are currently under way: 1) Satellite Geodesy and Geophysics, 2) Physical Parameters of the Atmosphere, 3) Improvement of Technology and Instrumentation and 4) Balloon Geodesy.

All the four directions are closely connected and are directly or indirectly aimed to solve fundamental problems of Satellite Geodesy and Geodynamics.

As a base for joint observational programs serves a network of satellite tracking stations situated in the collaborating countries and several countries in Asia, Africa and South America having bilateral agreements with the Astronomical Council of the USSR Academy of Sciences who is acting as co-ordinator of the whole problem. All stations are equipped with USSR photographic cameras AFU-75 (several - with the GDR Carl Zeiss, Jena cameras SBG) and Intercosmos laser rangers built in the frame of the co-operation by scientists from Czechoslovakia, the GDR, Hungary, Poland, and the USSR.

The technical parameters of the AFU-75 camera have been several times described in various publications [1,2]. A principal virtue of the camera is its portability and mobility. Satellite directions can be determined up to 2 sec. of arc, positions of geostationary satellites can be obtained with an error of 1 sec of arc.

The Intercosmos laser is a ranging system of the first generation with effective distance ~ 3,000 km, the measurement accuracy 0,6-1,5 m; visual guiding, the impulse energy of the ruby laser is 1 J, puls duration ~ 15 nsec. [2]

The Potsdam laser ranger on the basis of the Zeiss camera SBG has a two-step ruby laser. A unique feature of the SBG-laser is the possibility to carry out alternately photographic and laser-ranging observations during one satellite passage. It is possible to observe all existing satellites with retroreflectors, Lageos including; guiding is automatically, the measurement accuracy is about 1 meter and, with a more sophisticated laser, a 0,2 m accuracy may be achieved.

A SBG-laser will start in 1980 at the Simeiz station as well.

At present 22 photographic and 12 laser ranging stations are operating (Table 1). Building of two new stations in Angola and Vietnam is under way. Former stations in Kuru, Somali and Sudan have been discontinued. Due to civil war conditions observations at the station in Ndzhamena (Republic of Tchad) are interrupted. The last term observations are carried out at the station on the Island New Amsterdam in the Indian Ocean.

2. POSITIONING OF STATIONS

Positioning of new Intercosmos network stations and their geodetic links to global coordinate systems is still one of the major problems in the Intercosmos collaboration.

Geometric methods of satellite geodesy, utilizing simultaneous observations are used for developments of long geodetic traverses (the Arctic-Antarctic, for example [3,4,5]) and for adjustments of regional networks: the European (Fig.1) and the African (Fig.2).

The adjustment is realised by a parametric method [2], which allows to include in the computations both direct measurements of satellite positions and evaluated directions and lengths of geodetical chords between two stations.

Orbital methods allow to utilize observational data more efficiently as usually the number of simultaneous observations does not exceed 10 % of the total amount. In the frame of the Intercosmos cooperation several variations of the short arc method very useful for station positioning in a local coordinate system have been developed and are frequently used [2,6]. A short arc is usually defined as a part of the satellite's orbit observed during a time interval from about ten seconds up to 1-2 whole periods the condition being that the computational error should not exceed the error of the observations itself. Using special

routines developed at the Astronomical Council and the Novosibirsk Geodetic Institute, positions of distant stations: Sant Yago de Cuba, Kerguelen, Helwan and Yuzhno-Sakhalinsk have been determined on base of photographic tracking data of Midas 4 and GEOSA with an accuracy of 15-25 meters. Together with laser range measurements of GEOS A and C the accuracy has been increased up to less than 5 meters (Table 2 and 3).

A more general solution for site positioning was obtained by means of the routine "Potsdam-3", realising a semidynamical method [7] with an accuracy about 10 m. In Table 4 comparison of results obtained by this routine on base of ISAGEX data with SE II, III, IV results is presented. The routine Potsdam 3 is successfully operating also in Hungary and the USSR.

3. ORBITAL COMPUTATIONS

Theoretical investigations in order to improve orbit determinations so they could be utilised for geodynamical purposes are under way in several participating countries. A new improved version of the routine "Potsdam" is being prepared in the GDR. This program is based upon numerical integration and provides a decimetre accuracy of orbital parameters during several days [8] .

Much attention is also paid to analytical methods of orbit determinations based on the theory of an intermediate orbit of two fixed centers [9] .

A new routine "Prognose" is being developed at the Astronomical Council using a new approximation of the geopotential proposed by Marchenko [10] , as a sum of potentials of mass points (sum of potentials of gravitational multipoles). Using, for example, a number of Stokes constants up to the 12th degree, a model of gravitational dipoles consisting of 128 mass-points has been constructed. This method simplifies the whole procedure and requires considerably less computing time for numerical integrations.

The present accuracy of orbit computations requires very accurate atmospheric models. Special investigations allowing to choose the most appropriate atmospheric model for a particular orbital routine are under way [11].

Recently the influence of atmospheric drag on satellites with perigee ~ 700 km has been investigated. Comparison of orbital positions for Explorer 19 (Δ r in meters and Δ t in minutes) computed without and with an atmospheric model (Jaccia 66) is shown in Fig. 3 . In the case when the perigee is in the shadow (Ψ = 123°) the error does not exceed 1-2 m on an interval of 20-30 minutes. For "day time" the same error occurs after 5-7 min. After 3 revolutions "at night" an error of 600 m is obtained, for the"day" - 3-4 km. When choosing an atmospheric model for orbit computations the possibility of its mathematical realisation becomes an important factor. Some precise and rather sophisticated models developed recently cannot be efficiently utilised due to pure mathematical difficulties. A comparison of two atmospheric models, CIRA-72 and the French Drag Temperature Model (DTM) by Barlier [12] has been carried out at the Astronomical Council

recently. Results of numerical integrations of an orbit for a satellite with perigee height 1400 km on a 7 day interval have been compared using both models. The difference Δr of the geocentric radius-vector (the actual difference between the two models) reached a value of $\sim$100 m at the end of the interval for a mean level of solar activity, e.g. a value comparable with the errors of photographic tracking data (Fig. 4). However, an orbit with the DTM requires 6-8 times less computing time than with the model CIRA-72. [13]

Another investigation under way concerns the utilisation of photographic tracking data in order to improve the accuracy of navigation for scientific instrumentation on board of the Intercosmos satellites. The result obtained shows that the errors in timing can be improved 5-10 times along the orbit [9] The influence of non-gravitational forces on the motion of artificial satellites has been investigated at Ondrjeov, Czechoslovakia. A global model of solar radiation reflected by the Earth has been proposed and analysed using spherical harmonics [15] . At present variable components like clouds and seasonal variations of the albedo are being introduced into this model.

4. GEOSTATIONARY SATELLITES

As early as 1972 K. Marek [16] made an estimate of the possible accuracy of direction determinations by means of simultaneous observations of geostationary satellites. He showed that the direction Zvenigorod - Island New Amsterdam (about 10000 km) can be obtained with an accuracy of 0".5 if the position of the satellite is determined with an accuracy of 0".25. However, as experience shows, the most precise photographic cameras provide an accuracy $\sim$ 1 second of arc. Computations, carried out at the Astronomical Council show that such an accuracy may be sufficient for geodetic links at very long distances if the geometric configuration station-satellite-station is optimal and not less than 25 simultaneous pairs are available. Most favourable are directions perpendicular to the Equator [17] .

The first successful photographs of geostationary satellites of the types Intelsat-4 and Molnija have been obtained in 1975 at the Zvenigorod station on the USSR photographic camera VAU (d = 500 mm, f = 700 mm, field of sight 5°x30). At present geostationary satellites are tracked at all the stations of the Intercosmos network. Table 5 shows some results for 1978 and 1979. Outstanding results have been obtained at the station Zvenigorod near Moscow. On one frame of the VAU camera up to 19 geostationary satellites can be found. At Zvenigorod more than 30 different satellites are regularly observed which is remarkable if the latitude of this station (56°) is considered.

Simultaneous photographic tracking data of geostationary satellites can be used as a base for a global triangulation net consisting of triangles (about 100°) around the equator. An example of such a network has been described in [17].

Photographic tracking data of geostationary satellites can be also utilised for theoretical investigations, orbit determination including resonance effects, and determination of the mass centre

of the Earth [18].

5. GEODYNAMICS

Owing to the development of new tracking techniques and an increase in the accuracy, new problems connected with global geodynamical investigations were included in the program of scientific cooperation. In order to recommend an optimal net of stations for geodynamic investigations all Intercosmos stations were analyzed on the base of geological, tectonical, meteorological, instrumental and other conditions [19]. Some of the stations are transferring into special geodynamic observatories, e.g. Potsdam (GDR), Simeiz (USSR), Penc (Hungary), Boroviec (Poland). The number of such stations will be increased in the future.

Into geodynamical stations will be transferred in the nearest future the stations in St. Yago de Cuba and Quito (Equador).

At present investigations are under way to start regular determination of geodynamical components by means of laser range measurements from one or several stations (for example the latitude component of the polar motion on base of laser range measurements of high satellites). Simultaneously with laser range measurements astrometric observations by means of astrolabs or zenith telescopes as well as geophysical measurements are carried out at the geodynamical stations. At the Simeiz station (USSR) systematic determinations of latitude and longitude corrections with a Danjon astrolab are under way. The latitude variation of Simeiz has been determined and for a 3 year period corrected mean values of φ and λ obtained. Starting 1980 Simeiz is included into the International Time and Polar Motion Service.

During 1979 two campaigns of laser range measurements of Geos 1 and Geos 3, aiming the precise determination of distances between geodynamic stations, mentioned above, were organised. Short arc methods are used for data processing. [20,21]

Simultaneously the same stations carry out Doppler measurements for determination of their relative positions by the translocation methods.

In 1980 all laser stations of the Intercosmos network will participate in the preliminary MERIT campaign.

Achievement of the decimeter (and centimeter) accuracy of laser ranging is one of the necessary conditions for progress in space geodynamics. New Laser systems of second and third generations for satellites and the Moon are under development in the Soviet Union, the GDR, CSSR, Poland. At the same time technical improvements of the existing laser systems are carried out. The SBG laser in Potsdam has been already mentioned above. A second generation Czechoslovakian laser is mounted on the Intercosmos ranging system in Cairo (pulse length 4 nsec, resolution of the counter of Polish origin $\sim$ 0,5 nsec, ranging accuracy 20-30 cm

for BEC, Geos 1, Geos 3, Starlette).

6. DOPPLER MEASUREMENTS

Doppler measurements have started in 1978 in Hungary who acts as co-ordinator of this project. Participating are stations in Bulgaria, Hungary, the GDR, Poland, USSR and Czechoslovakia. Observations are carried out by two mobile Doppler receivers (IMR-1 and CMA-751) in Hungary, one CMA-722B receiver in the USSR. A Doppler receiver belonging to the station Graz (Austria) is participating in the campaigns. Polish and Czechoslovakian scientists are constructing their own Doppler installations. Since 1978 the following experiments have been carried out: positioning of the stations Boroviec (Poland), Pentz and Baja (Hungary), a link by translocation of the stations Pentz (Hungary) and Graz (Austria), by multilocation Pentz, Graz and Wetzell (FRG), positioning by simultaneous tracking of the GDR stations Potsdam and Dresden and Potsdam (GDR) and Riga (USSR). In 1980 stations in Hungary, the GDR, the USSR, the CSSR and Poland have participated in the WEDOC campaign. [23-29]

7. NEW PROJECTS

One of the newest projects (Satellite to Satellite tracking) proposed for realisation in the Intercosmos program is the so called DIDEX project (Differential Doppler Experiment): two probes are moving along a circular polar orbit with a distance between them 150-200 km. They are tracked from a satellite moving along a somewhat higher orbit. The tracking will be effectuated by two-way Doppler shift measurements, permitting to obtain an accuracy of 0,05 mm/sec in the radial velocity. The actual data which will be reduced for gravity anomaly deduction is the relative velocity between the two subsatellites. It is expected, that with an assumed accuracy of measurements ~ 0,05 mm/sec the resolution of 3° with an error of 12 mgal in gravity anomalies will be achieved. [30-32]

In 1981 a new Intercosmos satellite "Bulgaria-1300" is planned to be launched. This satellite will have a circular orbit with an inclination > 75° and a perigee height about 950 km. The satellite will be equipped with laser reflecting panels. (Number of prismas 84, reflecting surface ~ 0,05 m^2). A special observation program will be organised, under the general guidance of the Bulgarian Academy of Sciences. [33]

A project of determining latitude and longitude differences in one coordinate system for several geodynamical stations in order to investigate relations and relative shifts of the geocentric coordinate systems will start in 1981. The differences in longitude and latitude for Potsdam, Simeiz and Irkutsk will be determined with the help of a mobile Danjon astrolab with an accuracy ~ 2-3 msec in longitude and 0,05-0,08 in latitude.

8. CONCLUSION

All above mentioned shows that in the participating countries important results have been achieved mainly in improvement of the tracking techniques and theoretical investigations aimed at the

solution of fundamental problems of geodynamics.

REFERENCES

1. Massevitch, A.G., Losinsky, A.M., "Photographic tracking of artificial satellites", Space Sc. Rev., 11, No. 2/3, 308-340.
2. Georgiev, N., Massevitch, A., Klenitsky, B., Tatevjan, S., "Optical Tracking of Satellites for Geodesy" (275 pages), Sofia, 1979 (Russian).
3. Massevitch et al., "The use of satellite tracking data for geodesy and geodynamics" in "Ten years of the Intercosmos co-operation", Moscow, Nauka, 1978 (Russian).
4. Massevitch, A.G., "Results of co-operation in Section 6 of the Intercosmos programme", 3rd Int. Symp. Geodesy a. Phys. of the Earth, vol 1, pp. 31-41, Potsdam, 1977.
5. Massevitch, A., Erpylev, N., Kasimenko, T., 1975: Some Results of the Arctic-Antarctic Project", COSPAR Space Research XV.
6. Tatevian, S., 1968, "A new variation of the orbital routine for station positioning on base of nonsimultaneous tracking data", Nauchn.Inform.Astrosovjata, V. 9, pp. 42-49, Moscow (Russian).
7. Montag, H., Gendt, G., Coordinate determination of stations of the Large Chords Project by the semidynamic method, Veröff. Zentralinst. Phys. d. Erde, Potsdam (1977), No. 52, Teil 1, S. 185-192.
8. Gendt, G., Problems in the numerical integration of satellite orbits with dm accuracy, Bull. "Observations of Satellites", No. 18 (1979), Warsaw, S. 295-312.
9. Aksenov, E.P., 1977, "Theory of motion of a satellite" (240 pages), Nauka, Moscow (Russian).
10. Marchenko, A.N., Meshcherakov, G.A., Maxwell parameters of the gravity field of the Earth, Bull. "Observations of Satellites", No. 18, 1979, Warsaw, pp. 171-188.
11. Buligina, O., Kasimenko, T., Jankovskaja, I., "The Influence of Atmospheric Disturbances on Station Positioning Routines", 1977, Colloquium Atmospheric Physics, Baja, Hungary.
12. Barlier, F. et al., A thermospheric model based on satellite drag data, 1978, Space Research XVIII, p. 169.
13. Sorokin, N., Schmeler, L., Horwath, A., 1980, "Influence of Atmospheric Models on the Accuracy of Determination of the Positions of Satellites", Nauchn. Inform. Astrosovjeta, No. 48.
14. Horwath, A., Kasimenko, T. et al., 1978, "Utilisation of tracking data for the Intercosmos satellites in order to increase the accuracy of navigation", Bull. "Observations of Satellites", No. 18, Warsaw.
15. Lala, P., Sehnal, L., 1969, "The Earth's shadowing effects in the short-periodic perturbations of satellite orbits", Bull. Astr. Inst. of Czechoslovakia, 20, No. 56.
16. Marek, K., 1972, "Possible use of geostationary satellites in satellite geodesy", Nauchn. Inform. Astrosovjeta, v. 25, 103-116, Moscow (Russian).
17. Massevitch, A., Erpylev, N., Losinsky, A., 1978, "Photographic tracking of geostationary satellites for geodetic purposes" - COSPAR Space Research XVIII.
18. Burscha, M., Sima, Z., "Geostationary satellites and the position of the Earth's mass center", Bull. Astron. Inst. Czechosl., 29 (1978), 232-237.
19. Montag, H., Lala, P., Klokocnik, J. On some conditions for complex geodynamic stations (Russian). Zprávy a Pozorováni Geodetcké Observatoře Pecný, VUGTK, Rada 5, Cislo 3, Praha

(1979), pp. 1-11.
20. Stange, L., "Derivation of long terrestrial distances from quasisimultaneous laser observations of artificial satellites", Bull. "Observations of Satellites", No. 18, 1979, Warsaw, 5-16.
21. Tatevian, S.K., Short Arc Method Application Possibility for Determining of Chord Between Two Stations, Nauchn. Inform. Astrosovjeta, No. 44, 1980, Riga, 8-12.
22. Jaks, V., Kasmersky, 1979:"Construction of a Doppler installation in the Space Research Centre of the Polish Ac. Sc.", Trans. KAPG Seminar, Sopron.
23. Dietrich, R. - Fejes, I.: Satellite Doppler observations at Potsdam and Dresden. Paper presented at the 6.8.4. KAPG Seminar, 1979, Sopron.
24. Fejes, I. - Ádám, J. - Czobor, A.: The JMR-1 Doppler receiver application in Hungary, Observations of Artificial Satellites of the Earth, 1978, No. 18, Warszawa.
25. Halmos, F. - Almár, I. - Ádám, J. - Fejes, I.: Application of Radio /Doppler/ observational methods in the geometrical and dynamical satellite geodesy. Acta Geodaet. Geophys. et Montanist. Acad. Sci. Hung. 1976/1-2, Budapest.
26. Mihály, Sz.: Accuracy of the Doppler observational equations. Bull. Observations of Artificial Satellites, 1978, No. 18, Warsaw.
27. Pesec, P. - Jaks, W. - Pachelski, W. - Vorbrich, K.: Determination of the station Borowiec position by means of Doppler observations, Observations of Artificial Satellites, 1978, No. 18, Warsaw.
28. Pesec, P. - Hajos, T.: Doppler translocation measurements Graz-Penc, Paper presented at the 6.8.4. KAPG Seminar, 1979, Sopron.
29. Gergov, C., Georgiev, N., 1979, "Optimisation of Doppler measurements in the East European network", Transactions KAPG Seminar, Sopron.
30. Kryński, J., "Possibilities of Low-Low Satellite Tracking for Local Geoid Improvement", Mitt. der Geodätischen Institut der Technische Univ. Graz, 1978, No. 31.
31. Kryński, J., "A solution for Determination of the Gravity Field from Satellite-to-Satellite Tracking Data", 1980 (this issue).
32. Zielinski, J.B., "Investigation of the Earth Gravity Field by Differential Doppler Measurements", Geodezia i Kartografia, 1977, No. 4.
33. Georgiev, N., Dikov, V., Hadzhijsky, A., Testing of the optical-mechanical properties of the laser retroreflector, Sofia, 1980, Bull. Inst. for Archit. a. Construct.

Table 1. Intercosmos Tracking Network

CODE No.	STATION	LAND	COORDINATES		CAMERA	LASER-SYSTEM
1156	Borowiec	Poland	17°05'	52°17'	SBG	
1856	Borowiec	- " -	- " -	- " -		Intercosmos
1141	Ondrejov	CSSR	14 47	49 55	SBG,AFU-75	
1841	- " -	- " -	- " -	- " -		Intercosmos
1115	Penc	Hungary	19 17	47 47	SBG,AFY-75	
1815	Penc	- " -	- " -	- " -		Intercosmos JMR-Doppler
1113	Baja	- " -	18 58	46 11	AFU-75	
1107	Plana	Bulgaria	23 27	42 28	AFU-75	
1131	Bucharest	Roumania	26 06	44 25	AFU-75	
1660	Ulan-Bator	Mongolia	107 03	47 52	AFU-75	
1661	Dalan Dzadagad	- " -	104 24	43 34	AFU-75	
1753	Santiago de Cuba	Cuba	284 14	20 01	AFU-75	
1853	Santiago de Cuba	- " -	- " -	- " -		Intercosmos
1690	Phenian	Korea	124 00	39 04	AFU-75	
1901	Helwan	Egypt	31 20	29 52	AFU-75	
1801	Helwan	- " -	- " -	- " -		Intercosmos
1911	N'Djamena	Chad	15 02	12 07	AFU-75	
1924	Bamaco	Mali	352 02	12 40	AFU-75	
1692	Kavalur	India	78 49	12 54	AFU-75	
1892	Kavalur	- " -	- " -	- " -		Intercosmos
1767	Quito	Equador	281 31	-0 12	AFU-75	
1867	Quito	- " -	- " -	- " -		Intercosmos
1762	Pataca-maya	Bolivia	292 06	-17 15	AFU-75	
1862	Pataca-maya	- " -	- " -	- " -		Intercosmos
1072	Zveni-gorod	USSR	36 46	55 42	SBG,AFU-75 VAU	
1872	Zveni-gorod	- " -	- " -	- " -		Intercosmos
1073	Simeis	USSR	34 00	44 24	SBG,AFU-75	
1873	Simeis	- " -	- " -	- " -		Intercosmos SBG
1084	Riga	- " -	56 57	24 04	SBG,AFU-75	
1884	Riga	- " -	- " -	- " -		Intercosmos

Table 1. (continued)

1181	Potsdam	GDR	52 23	13 04	SBG-laser
1056	Uzhgorod	USSR	22 16	48 36	SBG,AFU-75
1265	Yuzhno-Sakhalinsk	- " -	142 42	46 57	AFU-75
1650	New Amsterdam	Indian ocean France	77 32	-37 42	AFU-75

Table 2. Mean-Square Errors for Rectangular Coordinates (m_x, m_y, m_z) of Intercosmos Tracking Stations Determined by the Potsdam-3 Routine (in Meters). Photographic tracking data only have been used.

Station(number)	m_x M	m_y M	m_z M	M
Uzhgorod(1055)	4	4	5	7
Zvenigorod(1072)	7	6	6	11
Riga(1084)	8	5	9	13
Kerguelen(1108)	10	11	13	20
Ondrejov(1147)	9	6	7	13
Potsdam(1181)	6	5	5	10
Ulan-Bator(1660)	5	6	7	10
Helwan(1901)	5	3	4	7

Table 3. Positioning of the Simeis station on base of photographic and laser tracking data by the short arc method. (Basic stations are Helwan and Potsdam.)

X	Y	Z	Date MID	Satellite
3783927± 1.4	2551505± 2.7	4441053± 1.6	-	GEOS-1 GEOS-2
3783917± 4.8	2551490± 2.5	4441067± 2.2	43795-43797	GEOS-1
3783961± 3.6	2551487± 7.5	4441124± 5.7	43790-43792	GEOS-1
3783967± 0.6	2551435± 0.5	4440994± 0.7	43831-43835	GEOS-1
3783920± 2.1	2551513± 1.5	4441112± 2.0	43770-43775	GEOS-3
3783922± 1.4	2551531±10.5	4441107± 7.5	43784-43786	GEOS-3
mean values				
3783935	2551493	4441076		

Table 4. Comparison with SE II, III, IV of positioning results obtained by means of the "Potsdam-3" routine (differences in meters).

Station(number)		SE II 1976	SE III 1975	SE IV 1976
			±5	±8
Uzhgorod	X		-1	+26
(1055)	Y		-4	-22
	Z		-2	-40
		±27	±10	±24
Zvenigorod	X	-67	+ 7	-35
(1072)	Y	+66	+22	+23
	Z	-10	+22	-74
		±24	±5	±8
Riga	X	+ 2	+7	+16
(1084)	Y	+26	+29	- 4
	Z	-20	-15	-22
		±32	±44	
Kerguelen	X	-201	-73	
(1108)	Y	+141	-35	
	Z	+ 41	-30	
Ondrejov			±5	±10
	X		-10	- 3
(1147)	Y		-13	-53
	Z		+11	+20
			±9	±31
Potsdam	X		±3	-26
(1181)	Y		+13	+23
	Z		-10	-13
			±9	
Ulan-Bator	X		-15	
(1660)	Y		+6	
	Z		+25	
		±44	±5	±16
Helwan	X	+211	+10	+27
(1901)	Y	-28	+3	-56
	Z	-396	-8	+54

Table 5. Observations of geostationary satellites at the Intercosmos tracking stations during 1978 and 1979.

Station	Number of observations (tot/sim)	
	1978	1979
Santiago	2/-	20
N'Djamena	212/24	470/97
Kavalur	171/21	363/35
Uzhgorod	108/9	127/21
Zvenigorod	116/18	201/60
Ulan-Bator	113/13	36/8
New Amsterdam	29/10	56/16
Quito	-	95/-
Yuzhno-Sakhalinsk		17/3
Phenian	5/-	12/1
Patacamaya	25/-	-

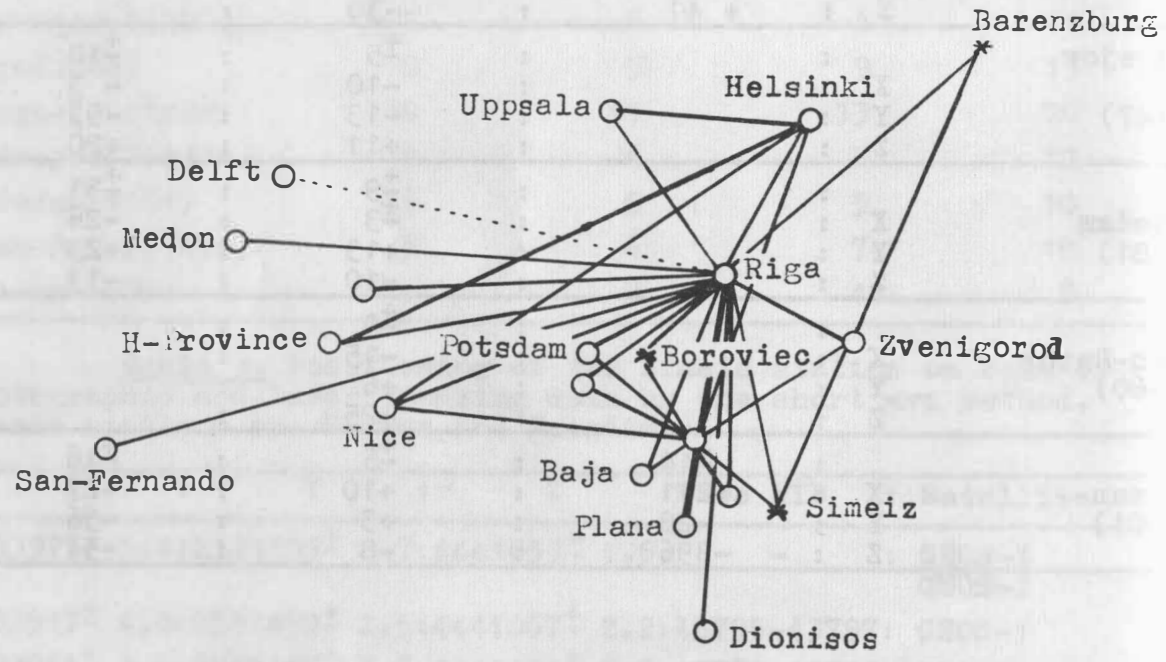

Fig. 1. Adjustment of a regional European network based on Intercosmos tracking stations.

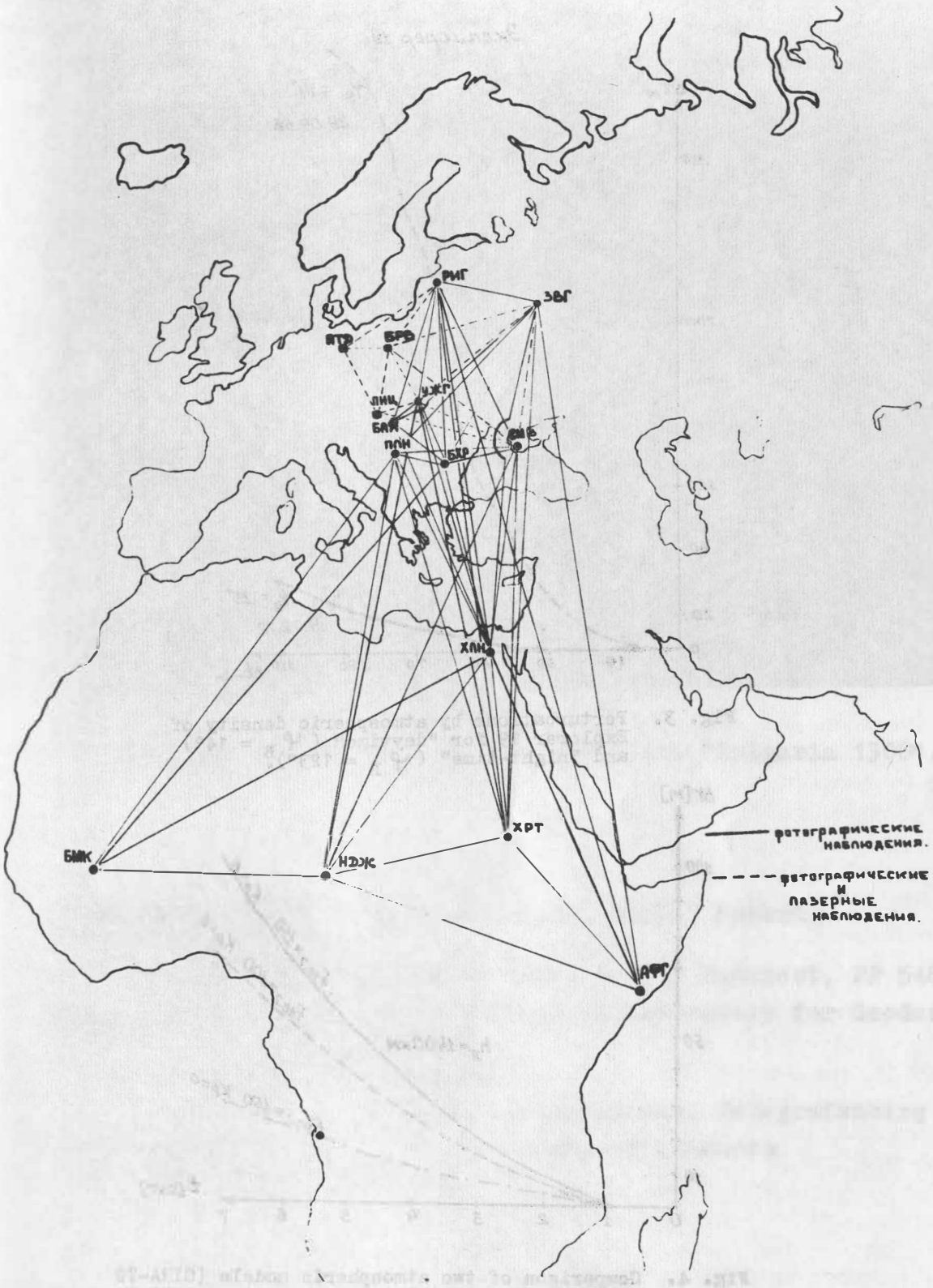

Fig. 2. Adjustment of a regional Europa-Africa network based on Intercosmos tracking stations
——— links by photographic tracking data
– – – photographic and laser data.

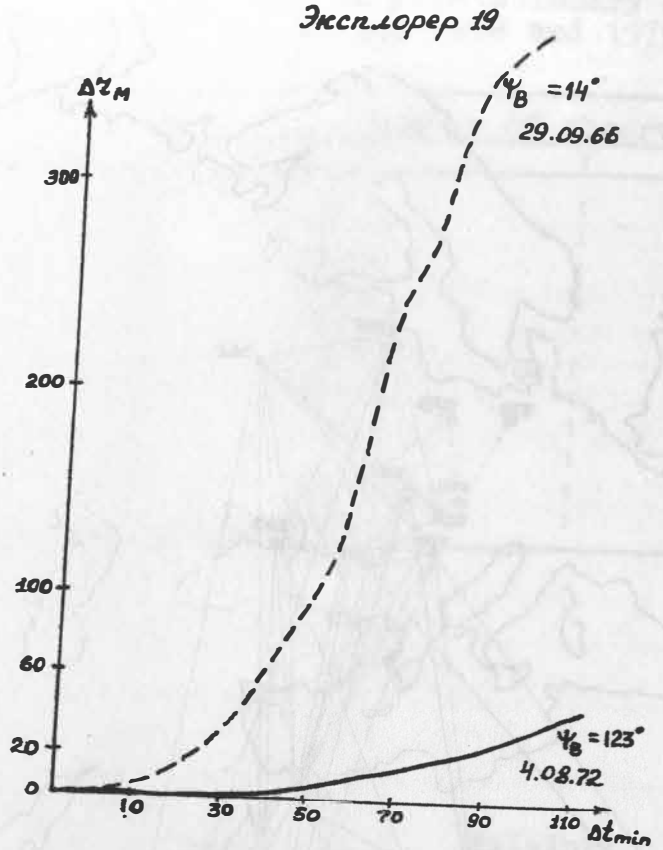

Fig. 3. Perturbations by atmospheric density of Explorer 19 for "daytime" ($\varphi_B = 14°$) and "night-time" ($\varphi_B = 123°$).

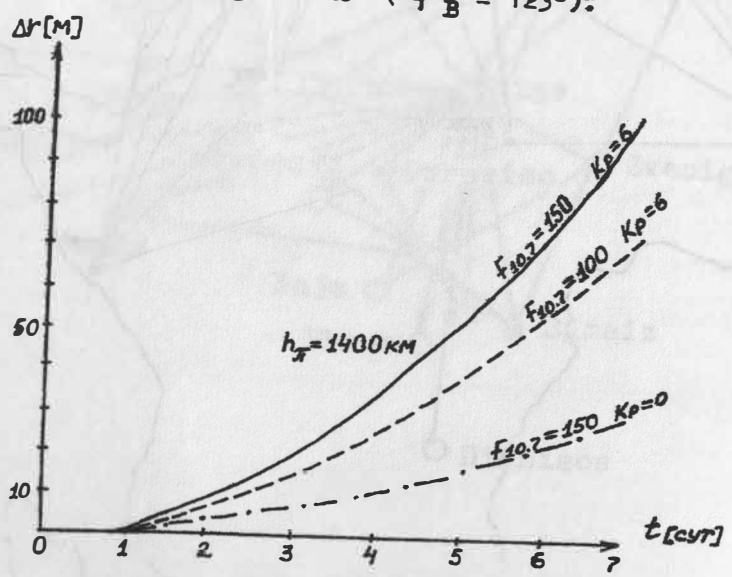

Fig. 4. Comparison of two atmospheric models (CIRA-72 and DTM) for a satellite with perigee 1400 km. Different lines correspond to different degrees of solar activity. Δ r is given in meters, Δ t - in days.

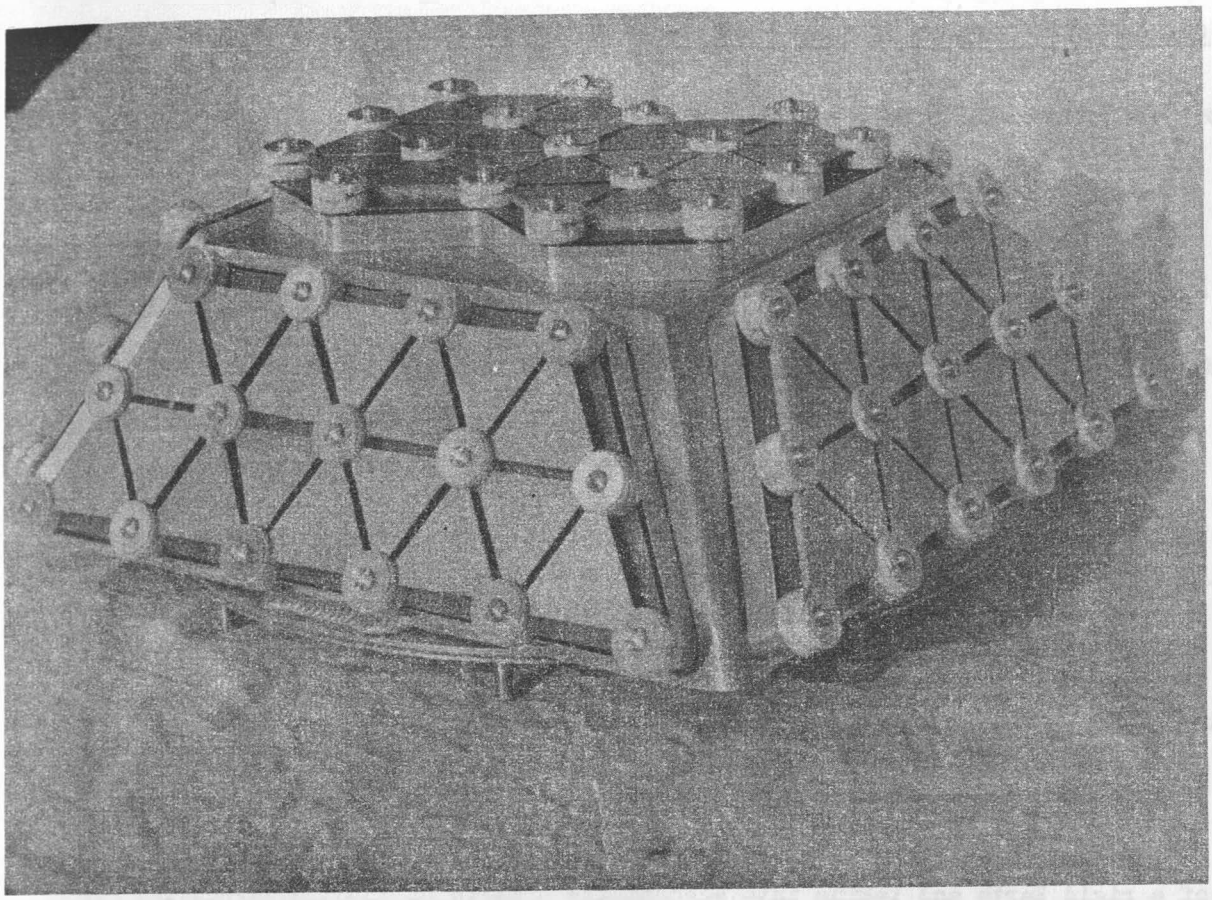

Fig. 5. Laser retroreflector for the satellite "Bulgaria 1300".

---

1) Astronomischer Rat der AdW der UdSSR, 109017 Moskau
Pjatritzkaja ul. 48

2) Satellite Geodetic Observatory Penc, H-1373 Budapest, PF 546

3) Bulgarian Academy of Sciences, Central Laboratory for Geodesy
1000 Sofia, 7. Novemberstr. 1

4) TU Prag, 11519 Prag 1, Břehová 7

5) Zentralinstitut für Physik der Erde, Potsdam, Telegrafenberg

6) Space Research Centre, Polish Academy of Sciences
00-716 Warszawa, Bartycka 18

ON THE INVESTIGATION OF GEODYNAMIC PARAMETERS BY MEANS OF LASER MEASUREMENTS

by

H. Montag[1)]

Summary

The general behaviour of the geodynamic parameters is discussed, especially the spectrum of changes of the Earth's rotation vector.

The determination of polar motions by the aid of dynamic methods of satellite geodesy is treated more in detail. It is shown that the use of laser measurements to artificial Earth's satellites is one of the most accurate methods of studying polar motions and other parameters. By means of the observation equation for the determination of improved polar coordinates from the orbit computation residuals the influences of station coordinates and the orbital inclination are discussed. Some conclusions are derived.

1. Spectrum of changes of the Earth rotation vektor and other parameters

Taking as a starting point the fundamental theory of the gyratory motion in space of a rigid Earth and taking into account the effects of the tide-producing forces of the Sun, Moon, and planets and the influence of a real model of the Earth with an elastic mantle, a liquid outer core, and a hydrosphere and atmosphere, there is obtained the spectrum of the Earth rotation vektor given in Table I A, B and C [3, 5, 7, 8, 10]. This divides into movements of the axis of rotation in space (precession and nutation), movements of the axis of rotation within the terrestrial body (polar motions), and variations in angular velocity of the Earth (length of day). The periods and amplitudes of the movements have been determined not only from theories but from observations as well. The causes of these movements have been derived from model concepts that require to be studied in detail.

The individual components of polar motion, Earth's rotation, and terrestrial tides are superimposed one on the other, and the main problem is to separate the individual effects from the measurement results.

According to the causes of the phenomena (with the exception of luni-solar forces) dealt with here it can be said that they are to be found primarily in the parameters of the solid mantle of the Earth. Superimposed on them are influences exerted by the non rigid part of the Earth (liquid outer core, ocean, atmosphere) and its interaction with the solid mantle. Today, the latter effects are of major importance to a better understanding of the entire process.

1) Akademie der Wissenschaften der DDR, Zentralinstitut für Physik der Erde, DDR-1500 Potsdam, Telegrafenberg A 17

As discussed by LAMBECK [7] some causes for the different phenomena (Tab. I) are still very much in doubt, especially

- the relative magnitudes of atmospheric, earthquake and aseismic effects on the free polar wobble
- the amount of non-tidal rotational acceleration
- the nature of dissipation of both polar wobble and tides and
- the dominating mechanism of core-mantle coupling.

For demonstration by measurement techniques all that involves the need for as high a degree of resolution and accuracy as possible.

Additionally superimposed on the geodynamic processes referred to previously are tectonic movements of the Earth's crust, which are local to global in nature. Therefore, it is necessary to determine the tectonic movements and separate them from the other effects. So far as local movements are concerned, this is relatively easily done with the help of local or regional control networks and simultaneous gravimetric and inclination measurements. Today, interest is also focussed on the influences of global tectonics. The amounts of relative plate movements are between a few cm/a and 2 dm/a. The refinement of this particular model of global tectonics also is an important task of the interpretation of measurement results obtained at geodynamic observatories.

2. Possibilities of measuring geodynamic effects

Major progress in the study of geodynamic effects can be made if detection by means of special measurement techniques is possible with an accuracy of 10^{-8} of the Earth's radius ($<$ 1 dm). This means that it is also necessary for a reference system to be realized with at least the same degree of accuracy. To satisfy these accuracy requirements it is essential that the observations be made continuously or quasicontinuously with the use of methods with as high a degree of complexity as possible. These include astronomic-geodetic methods, gravimetric measurements and cosmic-geodetic methods of measurements [9].

Although the low accuracy of astronomic-geodetic methods of measurement does not, in general, allow a fine resolution of the different phenomena to be obtained, they will continue to be of interest because of the long series of measurements. On the other hand, cosmic-geodetic methods of measurement will become increasingly more important for these tasks. In this connection the proposed international observation programm MERIT(Monitoring of Earth Rotation and Intercomparison of the Techniques of observations and analyses) is very important. The aim of this international project is to compare these different classical and modern observation techniques and to estimate the possibilities of the different measurements in determining the geodynamic parameters, especially polar motion and Earth rotation.

3. Analysis of satellite orbits for determining polar motions

Realization of a suitable inertial reference system is a primary prerequisite for high-accuracy analysis of satellite orbits to detect geodynamic parameters. For this, the constants of precession and nutation required to determine the axis of rotation of the Earth in space are needed. All the changes in the axis of rotation relative to the terrestrial body (polar motion) and the variations in rotation will then manifest themselves as variations in station coordinates or as residuals in the orbit determination.

The investigation of polar motions and variations of rotation by the use of such analyses of satellite orbits is referred to as the kinematic method. The dynamic method may still be used for determining polar motions. This method needs variations in spherical harmonic coefficients C_{21} and S_{21} to be studied. These coefficients are known to give the difference between the axis of rotation and the principal axis of inertia (which is equal to 0 if the two axis are coincident), and variations may thus be interpreted as reflecting polar motions. However, orbital disturbances caused by C_{21} and S_{21} are usually of a rather low degree, and determination of polar motions by this method is quite difficult. Estimates showed minimum requirements for the determination of orbits to be $\pm$ 3 cm [5].

Therefore, the major focus is on using the kinematic method which is of a more general nature. Because of inadequate knowledge of the parameters of the perturbation model, an accuracy better than $\pm$ 1 to several meters cannot be expected to be obtained in the analyis of laser measurements made from globally distributed stations to geodetic satellites. Consequently, it is necessary that special methods be available by which it is possible to analyze, for example, only the transverse component. Therefore, for the orbit determination it is useful to adjust the measurements in a rectangular coordinate system accompanying the orbital motion, with the u-axis pointing in the direction of the velocity vector of the satellite, v vertically to the orbital plane, and w vertically outward in the plane of the orbit. This gives as low a degree of correlation between the components as possible, and interpretation of residuals for individual components is greatly facilitated.

If satellites are observed whose orbital inclination agree with the terrestrial latitude of the observing station, the transverse component, v, will correspond to the orbital inclination, i. The disturbances of inclination are smallest from an orbital mechanics aspect, and they are reduced still further near the greatest latitude of the satellite ($\omega + v \approx 90^{\circ}$) [13]. On the other hand, the orbital inclination may be particularly easily determined by laser measurements near the greatest latitude, it being also possible there to observe the satellite from one station during four to five consecutive passages (the period of time being about six hours) [6]. By means of an orbital computer programme we have simulated how the principal components of polar motion are reflected in the variations of the orbital components u, v, and w [4]. But this single-station approach of laser ranging to appropriate artificial satellites has several limitations [1]: of polar motion the meridional component can be measured only; it is difficult to separate this component from dynamic perturbations of inclination i and from precession and nutation; it is an big influ-

ence of systematical error effects.

Avoiding these disadvantages it is necessary to use more than one station and to analyse the results in such a way that the more accurate components have the greatest influence on the determination of polar motions. This can be done on the basis of the knowledge of the relations between the polar motions and the residuals in the used coordinate system. Obtaining the influence of polar motions on the residuals in the u, v, w-coordinate system accompanying the satellite orbit we transform the station vektor $\underline{r_E}$ of the Earth fixed system into the coordinate system accompanying the orbit $\underline{r_B}$:

$$\underline{r_B} = R_x(\tfrac{\pi}{2})\, R_z(\tfrac{\pi}{2})\, R_z(\omega + v)\, R_x(i)\, R_z(\Omega - \theta)\, R_y(\xi)\, R_x(\eta)\, \underline{r_E}$$

with R - rotation matrizes, ω - argument of perigee of the satellite orbit, v - true anomaly, i - inclination, Ω - longitude of the ascending node, θ - sideral time, ξ, η - polar coordinates. Variations of the vector $\underline{r_B}$ due to polar motions we get by partial derivatives

$$\begin{pmatrix} du \\ dv \\ dw \end{pmatrix} = \frac{\partial \underline{r_B}}{\partial \xi}\, d\xi + \frac{\partial \underline{r_B}}{\partial \eta}\, d\eta \ .$$

From this follows in detail

$$\begin{pmatrix} du \\ dv \\ dw \end{pmatrix} = \left[\begin{pmatrix} \cos L & \sin i \\ & \cos i \\ \sin L & \sin i \end{pmatrix} x_E + \begin{pmatrix} \sin L & \cos M + \cos L & \sin M & \cos i \\ & -\sin M & \sin i & \\ -\cos L & \cos M + \sin L & \sin M & \cos i \end{pmatrix} z_E \right] d\xi$$

$$+ \left[\begin{pmatrix} -\cos L & \sin i \\ & -\cos i \\ -\sin L & \sin i \end{pmatrix} y_E + \begin{pmatrix} -\sin L & \sin M + \cos L & \cos M & \cos i \\ & -\cos M & \sin i & \\ \cos L & \sin M + \sin L & \cos M & \cos i \end{pmatrix} z_E \right] d\eta$$

with $L = \omega + v$; $M = \Omega - \theta$ and x_E, y_E, z_E - station coordinates in the Earth fixed system.

This is the "observation equation" for the determination of improvements to polar motions ξ and η from the orbit computation residuals du, dv, dw. The discussion of this equation shows several dependences. The periods one can see from the parameter L (orbital period) and M (diurnal period). That means the components du and dw show in general periods which are mainly equivalent to the satellite revolution, whereas dv has mainly an diurnal period.

Further one can see from the last equation the well known matter, that one need for determining of both ξ and η at least two stations with a difference in longitude of about 90°. Additionally z_E should be not so small; that means the stations should be situated away from the equator. On the other hand x_E and y_E desire to be not so small for determining $d\xi$ and $d\eta$, respectively; that means one should have two stations in the nearness of the equator with a difference in longitude of 90 degrees. Analogously is the influence of the orbital inclination. An increasing inclination raises the

contribution of the z - coordinate of the station position and an decreasing inclination raises the influence of the x- and y-coordinates.

4. Laser measurements to artificial Earth's satellites and some conclusions

The use of laser rangings to artificial Earth's satellites is one of the most accurate methods of studying geodynamic parameters.

Using the single-station method, Kolenkiewicz et. al [6] obtained in 1973 first results on polar motion and Earth's tides from laser measurements at the station Greenbelt ($\varphi = 39^{\circ}$) to the satellite BE-C ($i = 41^{\circ}$). The analysis of all short arcs of about six hours each, in which the four to five passages had been observed, showed an accuracy of the latitude variations to be about $\pm$ 1 m for a total period of seventeen months. The accuracy of laser ranging has been considerably improved ($< \pm$ 10 cm for the third generation and $\pm$ 10 to $\pm$ 30 cm for the second generation) since these experiments were performed, and the accuracy of orbit modeling also could be improved substantially. However, of particular importance in this connection is the launching of special geodynamic satellites such as Starlette (H_A=1100 km, H_P = 810 km, $i = 50^{\circ}$, 24 cm diam., 47 kg weight) and LAGEOS (H = 6000 km, $i = 110^{\circ}$, 60 cm diam., 411 kg weight). For the LAGEOS satellite the orbital perturbations may be relatively easily modeled to an accuracy of $\pm$ 10 cm because of the high altitude and the large weight-to-cross section ratio. By using this orbital accuracy and by second and third generation laser ranging techniques it is possible to obtain accuracies of $\pm$ 10 cm and better for polar coordinates.

An analysis of the orbital perturbations of the LAGEOS satellite also allows other phenomena to be studied, and these include distances between remote terrestrial stations from short-arc solutions, tidal effects, constancy of the gravitational constant (from semi-major axis a), and variation of the harmonic coefficient J_2 (from change in the longitude of perigee).

Consequently, within the Intercosmos-cooperation on several satellite tracking stations being set up improved or new laser ranging instruments with a higher accuracy and the capability to observe LAGEOS too. In addition to a number of globally distributed stations (e.g. Cuba), they will be centered especially on Europe and Asia. This distribution (difference in longitude about 180°) makes it possible greatly to contribute to a better determination of polar motions and other parameters (tidal models, variations in rotation and global tectonics). In order to avoid systematical errors and to separate the individual components of geodynamic effects the laser ranging results will be combined with other measurements.

References

[1] AARDOOM, L.: Earth Rotation and Polar Motion from Laser Ranging to the Moon and Artificial Satellites.
Reports Department Geodetic Sc. No. 280 (1978). Columbus, Ohio, pp. 19-28

[2] BENDER, P.L.; GOAD, C.C.: Probable Lageos Contribution to Worldwide Geodynamic Control Network.
The Use of Artificial Satellites for Geodesy and Geodynamics Vol. II (Proceedings of the Symposium in Athens 1978), Athens (1979), pp. 145-161

[3] KAUTZLEBEN, H.: Some Actual Problems in the Interpretation of Geodynamic Processes.
Veröff. Zentralinstitut Physik der Erde Potsdam Nr. 52, Teil 1 (1977), pp. 17-29

[4] KAUTZLEBEN, H.; HEMMLEB, G.; ELSTNER, C.; MONTAG, H.: Complex Studies in Planetary Dynamics of the Earth.
Nabljudenija iskusstvennych nebesnych tel No. 15 (1975), Moskva 1976, pp. 63-84

[5] KOLACZEK, B.; JAKS, W.: Polar Motion Determinations by the Use of New Observational Techniques.
Artificial Satellites 13 (1978) 3, Warszawa - Lodz, pp. 31-48

[6] KOLENKIEWICZ, R.; SMITH, D.E.; DUNN, P.H.: Polar Motion and Earth Tides from Beacon Explorer C.
Proceedings Symposium on Use of Artificial Satellites for Geodesy and Geodynamics, Athens 1973

[7] LAMBECK, K.: Progress in Geophysical Aspects of the Rotation of the Earth.
Rep. Dep. Geodetic Sc. No. 280 (1978), Columbus, Ohio, pp. 1-11

[8] LEICK, A.: The Observability of the Celestial Pole and its Nutation.
Rep. Dep. Geodetic Sc. No. 262 (1978) , Columbus (Ohio)

[9] MONTAG, H.; LALA, P.; KLOKOCNIK, J.: O nekotorych trebovanijach dlja kompleksnych stancii geodinamiceskich issledovanij.
Zprávy a pozorováni Geodeticke Observatore Pecný (VUGTK), Rada 5, Cislo 3, Praha (1979), pp. 1-11

[10] ROCHESTER, M.G.: The Earth's Rotation
Transact. Amer. Geophys. Union 54 (1973) pp. 769-780

[11] SHAPIRO, I.I.: Principles of Very Long Baseline Interferometry.
Rep. Dep. Geodetic Sc. No. 280 (1978), Columbus, Ohio, pp. 29-33

[12] SMITH, D.E.; DUNN, P.H.: Determination of Station Coordinates from Lageos.
The Use of Artificial Satellites for Geodesy and Geodynamics Vol. II (Proceedings of the Symp. Athens 1978), Athens (1979) pp. 162-172

[13] STANGE, L.; MONTAG, H.: On the Determination of Coordinates and their Temporal Variations Using the Orbital Method.
Veröff. Zentralinstitut Physik der Erde, Potsdam (1974) 30, Teil 2, pp. 435-439

Table 1. Spectrum of Changes in Earth's Rotation and Polar Motion

A. Inertial orientation of spin axis

Phenomena	Period	Amplitude	detected by	probable origin/causes
Precession	25 700 yr	23,5°	theory, astr.obs.	Lunisolar perturbations, mass distribution in the Earth
Principal Nutation	18,6 yr	9,2"	theory, astr.obs.	lunar perturbations, mass distribution in the Earth
Other periodic nutation terms	9,3/1/0,5 yr 183/122/27/14 d	} < 1"	theory, astr.obs.	lunisolar, planetar perturbations, mass distribution in the Earth
Free principal core nutation	associated to nearly diurnal free nutation	?	theory	interaction between liquid core and mantle
Secul.decrease in obliquity ε	-	-0,01"/yr	astr.obs. theory	perturbations by planets

B. Orientation of the rotation axis inside the Earth (polar motion)

Secular motion of the pole	-	0,002 to 0,003"/yr (7-10 cm /yr)	astr.obs. (IPMS, ILS)	melting of Greenland ice (?)
Force free nutation				
- chandler nutation	425 d to 440 d (changable)	0,1"-0,2" (3m-7m)	astr.obs. theory, satellite obs.	- elastic model of the Earth (mantle and core) - seismic excitation hypothesis (core-mantle interface) - atmospheric and hydrologigal mass distribution - influences of pole tide in ocean and of actions in Earth mantle
- nearly diurnal nutation	sideral day ± several minutes	<0,02" (≤0,7 m)	theory	interactions between liquid core and mantle
- long period. nutation	20 yr - 40 yr	≤0,02" (0,7 m)	astr.obs.	possibly observing effect and not real (difference BIH and ILS)
Forced nutation				
- Seasonal nutation	1 yr; 0,5 yr	0,09"(2,9m) 0,01"(0,3m)	astr.obs. satellite obs.	meteorological (?)
- other periodical (Oppolzer) terms	as diurnal nutation	≤0,02" (0,7 m)	theory	lunisolar attraction

C. Changes in the length of day (LOD)

continued Table 1

Phenomena	Period	Amplitude	detected by	probable origin / causes
Secular acceleration $\dot{\omega}/\omega$	-	$-5 \cdot 10^{-10}$/yr (-2ms/100yr)	- astron. obs. (- satellite Obs.) [1] - Lunar Laser rang. - estimates from tidal parameters	- tidal friction - slow changes in mass distribution in the Earth - non-tidal torques acting on the mantle
Long-periodic fluctuations and irregular changes	10-300yr	$\pm 5 \cdot 10^{-10}$/yr	astr. obs.	- electromagnetic coupling of core motions to mantle - topographic coupling core-mantle - variations in atmospheric and oceanic mass distri-
	1- 10yr	$\pm 80 \cdot 10^{-10}$/yr		
	months, weeks, "abrupt"	$\pm 500 \cdot 10^{-10}$/yr		
Short-periodic variations	2 yr	9 ms	astr. obs.	meteorological
	1 yr	20 - 25 ms	Lunar laser	
	0,5 yr	9 ms	ranging	meteorological, especially zonal wind circulations, tides
	month	1 ms		global wind circulation
	fortnight	1 ms		

1) - only indirect via acceleration of mean motion of the moon

L.P.Pellinen [1)]

REFERENCE SYSTEMS IN SOLVING MOLODENSKY'S PROBLEM FOR THE SEA SURFACE

1. The progress of satellite altimetry opens possibilities to determine the sea topographic surface (STS) with potential accuracy of about 0.1 m. The departures of the STS from the geoid become essential at this level of accuracy. The best way to derive these departures is given by the combination of gravity and altimetry data. We may obtain the STS-heights h above the geoid by the formula (Fig. 1):

$$h = H - \bar{\zeta} + \delta H \quad , \qquad (1)$$

where H is the STS-height above the reference ellipsoid ($H=0$) which is used in processing altimetry data; $\bar{\zeta}$ is the gravimetric geoid height with reference to some conventional level ellipsoid; δH is the correction for non-coincidence of the reference ellipsoid ($H=0$) and the level ellipsoid.

Let us assume that the regular tide component of the h-heights is already known from special harmonic analysis of gravity and altimeter data and we have to determine the quasi-stationary, long-period and non-regular components of these heights. It should be stressed that the existence of quasistationary departures of the sea topography from any level surface causes difficulties in defining such terms as the geoid and the level ellipsoid. The analogy of the known classical definition of the geoid as the level surface best fitting to the mean sea surface may be strictly realised only after the complete and detailed determination of the figure of the STS. Moreover, we should rigorously define the STS (for instance, we may include internal sea surfaces in it?). We should also fix the epoch of the geoid taking in consideration sea level variations in time.

Thus, there are some advantages to assume as the geoid some level surface of the real gravity field which may be defined before the STS-determination.

2. It is sufficient to assume four fundamental geodetic constants, i.e. the geocentric gravitational constant GM, the second zonal harmonic (geopotential coefficient) J_2, the Earth equatorial radius a_e and the angular velocity of the Earth's rotation ω, for deriving all parameters of the Normal Earth and its gravity field. The surface of the Normal Earth assumed

1) ZNIIGAiK Labor Geodäsie und Gravimetrie, Moskva 125413 Onezškaja ul. 26

to be the level (or normal) ellipsoid. The constants GM, J_2 and ω are independent from the definition of the Normal Earth. We have another situation be defining the constants representing the Normal Earth directly. If we do not define the term "geoid" we are not able to choose the Normal Earth as the best approximation of the geoid. Thus it is sufficient to choose some value of the a_e with the $1m$ - accuracy which is within the range of the STS-departures from the geoid. Then we derive the value of the normal gravity potential U_o at the normal ellipsoid surface.

Let us define the normal geoid as the real level surface on which the gravity potential W is equal to U_o. The departure of the normal geoid from the corresponding quasigeoid is approximately [1] equal to

$$\delta\zeta = \frac{\Delta g}{\gamma} h \quad , \qquad (2)$$

where Δg is the free-air "mixed" anomaly on the STS; γ is the mean normal gravity value. Because $|h| < 2$ m; $|\Delta g| < 400$mGal, we have $|\delta\zeta| < 0{,}8$ mm. Thus, we need not distinguish on seas and oceans the definitions of the geoid and the quasigeoid. It is also possible to use other terms applied in solving Molodensky's problem. The normal geoid departure from the normal ellipsoid may be interpreted as the height anomaly

$$\bar{\zeta} = \frac{T}{\gamma} \quad , \qquad (3)$$

where T is the disturbing potential at the STS. The height $H = H_o$ may be interpreted as the geodetic height and the height h as the normal height (see Fig. 1).

The definition of the normal geoid may be realised if we determine the STS-figure in a geocentric coordinate system with the required accuracy by means of the geometric satellite altimetry technique without any geoid figure data. In this case it is possible to assume that the reference surface for the H-heights coincides with the normal ellipsoid. Thus, the δH - term is excluded from (1) and we have

$$h = H_o - \bar{\zeta} \quad . \qquad (4)$$

Because we are not able to know the h - heights before studying of the geoid figure it is not reasonable to obtain mixed gravity anomalies Δg from gravity measurements at sea. It is more logical to obtain and use "proper" gravity anomalies or gravity

disturbances δg . The related problems are considered by V.V.Brovar [2]. H.Moritz [3] has considered these problems for the geoid (quasigeoid) figure to be determined with the 0.1 m-accuracy.

3. The errors of realization of the geocentric coordinate system from geodetic satellite observations are actually essential and cause a shift of the reference ellipsoid which is used for obtaining the H - values. There are also a scale error of the coordinate system and an error of altimeter bias correction.

The δH - correction in the formula (1) may be represented when taking into account the systematic errors of the H - heights as

$$\delta H = x\cos B\cos L + y\cos B\sin L + z\sin B + \delta H_o \ , \qquad (5)$$

where x , y , z are geocentric coordinates of the reference ellipsoid center; B and L are geodetic latitude and longitude; δH_o is a constant component. The equation (6) is similar to the well known height equation of grade measurements.

Let us assume that departures of the STS from the geoid do not include zero- and first-degree spherical harmonics. The second assumption is probably justified from the physical point of view. The first assumption corresponds to transition from the normal geoid to another "mean sea" geoid fitting to the STS within ocean area covered with altimeter measurements.

Let us put in (1) instead of δH the expression (5) and consider the obtained formula as "observation equation":

$$h + v_h = x\cos B\cos L + y\cos B\sin L + z\sin B + \delta H_o + (H - \bar{\zeta}) \ . \qquad (6)$$

Let us obtain the parameters x , y , z , δH_o from the least-square solution of equations (6) for a uniform grid of points on ocean area, where altimeter data are available. Further, we find

$$\bar{H} = H + \delta H \ , \qquad (7)$$

where $\bar{H}$ is the STS height with reference to mean sea ellipsoid which is fitted to the mean sea geoid, and

$$\bar{h} = \bar{H} - \bar{\zeta} \qquad (8)$$

where $\bar{h}$ is the STS height with reference to the mean sea geoid (Fig. 1).

As before (section 3) it is logical to use proper gravity

anomalies δg for determining the $\bar{\zeta}$ - values. The geodetic heights $\bar{H}$ are obtained from (7).

The similar procedure was used widely by R.Rapp [4] in processing altimeter data. The H -values obtained for each orbital arc were fitted to the planetary geoid heights according to the gravity model GEM-10. Such radical transformation of these heights by future studying departures the STS from the geoid will have as a consequence that a local part of the h - heights will be determined only. However, it is possible to use planetary geoid heights based on some gravity models instead of the detailed values of $\bar{\zeta}$ in solving observation equation (6) systems.

4. It is an important peculiarity of the above results that we impose no requirements on the determination of the zero harmonic of the $\bar{\zeta}$ - heights, though these requirements are often stressed. This conclusion refers to the determination of normal geoid heights above the normal ellipsoid as well as to mean sea geoid heights above the mean sea ellipsoid. It is easy to prove that the $\bar{\zeta}$ - values will be practically the same for both cases. Consequently, we have to choose formulae for computing geoid heights from gravity anomalies.

As may be seen the equatorial radius $\bar{a}$ of the mean sea ellipsoid remains unknown. Its determination is a special problem which may be solved if we know for some points the heights above some fixed reference ellipsoid in addition to the heights above the mean sea ellipsoid.

5. Let us compare national height systems with those based on normal geoid or mean sea geoid. Geopotential numbers C obtained after processing spirit levelling data are referred to the level surface $W = W_0 = \text{const}$ in the initial levelling point O (Fig. 1). Let us assume that we have obtained the h -height with reference to the normal geoid for a coastal point M of spirit levelling from gravity and altimeter data. Taking to account that the h is small we may write the potential W at point M as

$$W = U_0 - hg = W_0 - C \quad .$$

Hence, we have

$$W_0 = U_0 - hg + C \quad . \qquad (9)$$

The correction to normal heights for a shift of reference level-

ling surface is equal to

$$\Delta H_o^{\gamma} = \frac{U_o - W_o}{\gamma_m} = h\frac{g}{\gamma_m} - \frac{C}{\gamma_m} \quad . \tag{10}$$

Here g is the gravity value at point M, γ_m is the mean value of normal gravity between the normal ellipsoid and the telluroid for the same point.

We have similar formulae for transition to the mean sea geoid putting instead of h and U_o, respectively, $\bar{h}$ and

$$\bar{W} = U_o + (a_e - \bar{a})\gamma$$

We see that the precise determination of h - or $\bar{h}$ - values and gravimetric geoid heights ξ in coastal areas is important for the effective application of satellite altimeter data. Spirit levelling, mareographic, detailed gravity and altimeter data should be combined. Additional independent results may be obtained from determining geodetic heights by means of doppler and other satellite methods as well as of astrogeodetic (astrogravimetric) levelling.

Let us consider some questions related to the solution of Molodensky's problem for coastal areas. We have two different sets of information there :

a) Mixed gravity anomalies on land [5]

$$\Delta g = -\frac{\partial T}{\partial H} + \frac{T}{\gamma}\frac{d\gamma}{dH} - \frac{U_o - W_o}{\gamma}\frac{d\gamma}{dH} \quad , \tag{11}$$

b) Proper gravity anomalies at sea

$$\delta g = -\frac{\partial T}{\partial H} \quad . \tag{12}$$

As O.M.Ostach has shown [6], the term with $(U_o - W_o)$ in (11) may be excluded by solving the geodetic boundary problem for a level ellipsoid $U = W_o$ = const. The boundary values become unchanged after transition to another geoid W' = const and ellipsoid U' = const if $U' = W' = W_o + \delta W$, where δW is a small quantity. Thus we may assume that the boundary values are referred to the normal geoid and ellipsoid or to the mean sea geoid and ellipsoid.

It is reasonable to consider Molodensky's problem in coastal area as a problem of approximation and, for instance, to find numerically some anomaly mass model fitting to observed Δg and δg - anomalies.

References

1. Heiskanen W., Moritz H. Physical geodesy. W.H.Freeman and Co., San Francisco, 1967, 364 p.
2. Бровар В.В. О возможном повышении точности гравиметрических выводов в геодезии. "Астрон. ж.", 1971, 48, № 6, 1327-1332.
3. Moritz H. Precise gravimetric geodesy. Repts. Dep. Geod. Sci. Ohio State Univ., 1974, N 219.
4. Rapp R.H. Geos 3 data processing for the recovery of geoid undulations and gravity anomalies. "J.Geophys. Res.", 1979, 84, N B8, 3784-3794.
5. Молоденский М.С., Еремеев В.Ф., Юркина М.Н. Методы изучения внешнего гравитационного поля и фигуры земли. "Труды ЦНИИГАиК, 1960, вып. 131, 251 с.
6. Остач О.М. О выборе нормального эллипсоида. "Геод., картогр. и аэрофотосъемка", Львов, 1969, вып. 9, 47-49.

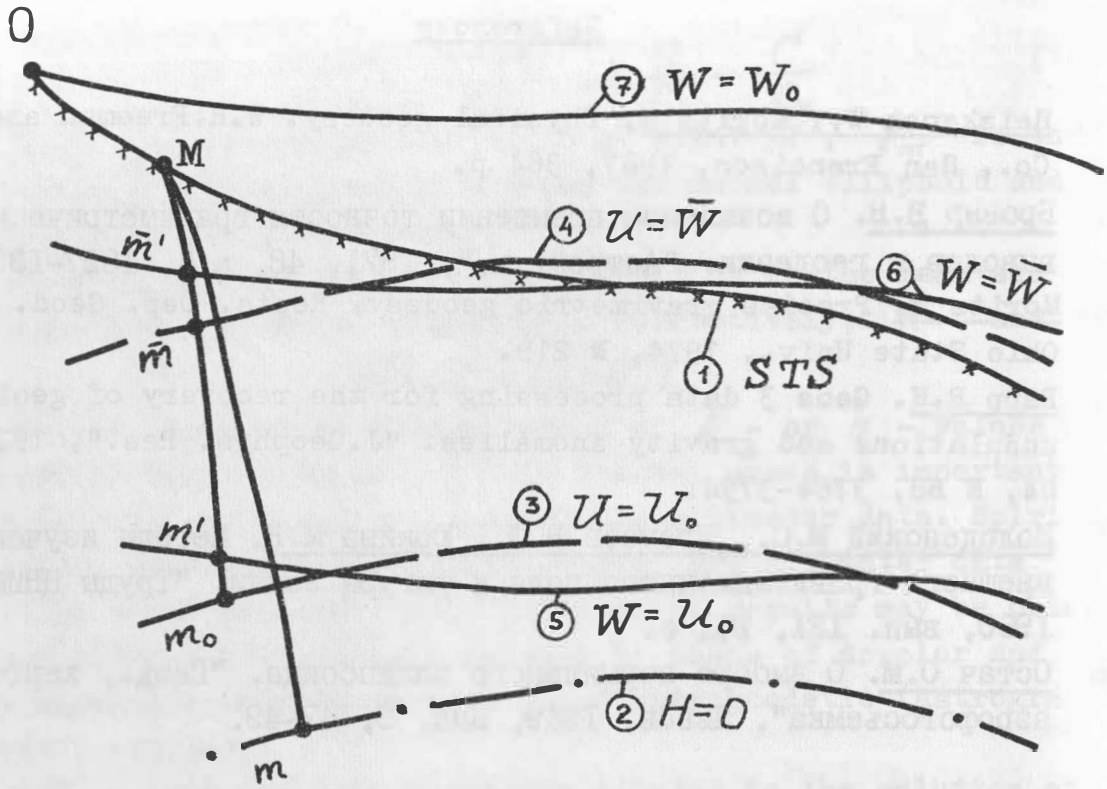

Fig. 1. Reference systems for the STS.
1 - Sea topographic surface (STS);
2 - Reference ellipsoid used in processing altimetry data (H = 0);
3 - Normal ellipsoid (U = U_0);
4 - Mean sea ellipsoid (U = $\bar{W}$);
5 - Normal geoid ($W = U_0$);
6 - Mean sea geoid ($W = \bar{W}$);
7 - Level surface in the initial levelling point O ($W = W_0$).

STS - heights :

$Mm = H$ - above reference ellipsoid ($H = 0$);
$Mm_0 = H_0$ - above normal ellipsoid;
$M\bar{m} = \bar{H}$ - above mean sea ellipsoid;
$Mm = h$ - above normal geoid;
$Mm = \bar{h}$ - above mean sea geoid.

$m'm_0 = \bar{m}'\bar{m} = \zeta$ - gravimetric geoid height.

The 1° x 1° Mean Anomaly Field of the Earth and Prospects for Its Improvement

by

Richard H. Rapp [1)]

Summary

Currently we have estimates for 41973 1° x 1° anomalies based on terrestrial gravity data. Of these, 721 are highly uncertain estimates (σ > 30 mgals) and 6912 may be geophysically predicted. When combined with anomalies derived from Geos-3 altimeter data, there is total field of 52917 of which 6943 have $\sigma \leq 5$ mgals.

Attempts to improve this field in the ocean areas using altimeter data will be hampered by the effects of sea surface topography. Consequently, new techniques such as satellite to satellite tracking (SST) and gradiometry need to be developed if an improved field is to be found. Error analyses are described that estimate the accuracy to which anomalies and undulations can be found using the new methods. A typical result is the following: Given a low-low SST mission of six month duration at an altitude of 180 km with a data noise of ± 1 μm/sec, and one data point every eight seconds, a 1° x 1° anomaly can be determined to ± 3 mgals, and the corresponding undulation to 7 cm. Similar results are found for a radial component gradiometer with an accuracy of ± 0.01 E. These estimates ignore systematic error and assume orbit error can be filtered out.

Introduction

Many studies of the gravitational field of the earth have used estimates of mean gravity anomalies at the surface of the earth. These mean anomalies have been used for the determination of geoid undulations, deflections of the vertical, gravity disturbances in space, and potential coefficients (in combination with satellite information) among other items. In addition, extensive studies have been made for geophysical implications of the gravity field using mean anomalies.

Such mean anomalies can be estimated in various sizes. Traditional sizes have included 5° anomalies and 1° anomalies. In some applications approximately equal area blocks are used and in others, equi-angular blocks. In certain types of calcu-

[1)] Department of Geodetic Science, The Ohio State University, 1958 Neil Avenue, Columbus, Ohio 43210, USA

lations smaller block dimensions such as 30'x 30', 15'x 15', 5'x 5', 6'x 10' in size are used. Such mean anomaly estimates have primarily been made in local areas whereas the 5° and 1° values have been estimated on a global or near global basis.

For the past several years we, at The Ohio State University, have prepared 1°x 1° anomaly data tapes based on terrestrial gravity measurements incorporating data from various sources. In addition, we have now estimated 1°x 1° gravity anomalies from Geos-3 satellite altimeter data. In this paper we will discuss these anomaly fields and show where they are lacking. In addition, we will discuss how this field may be improved in the future.

The Terrestrial 1°x 1° Mean Anomaly Field

The collection of gravity material for a 1°x 1° data file was started in 1971. The extensive data file provided by the Defense Mapping Agency Aerospace Center formed the initial basis for our work. This organization has continued to provide our base data files at periodic intervals. Our procedures are to update the Aerospace Center data with revised data, and new data that we have collected. The new data we have primarily used consists of 1°x 1° mean anomalies estimated from gravity anomaly maps. In all cases we try to use the latest data in our updating process. In addition, we try to be sure, where we can, that the anomaly accuracy estimates are reasonable. This is done by comparing anomaly estimates from various sources including altimeter estimates of the anomalies where available. Since we started this analysis we have produced six 1°x 1° anomaly data tapes. The number of anomalies in each tape is given in Table 1.

Table 1. Number of 1°x 1° Anomalies in Various Data Sets

Date	Number
June 72	23355
Sept 73	29789
July 75	36149
Aug 76	38406
June 78	39405
Oct 79	41973

Our latest tape was created in October 1979. The information on this tape will now be discussed in more detail.

The development of the anomalies on the October 1979 data set started from a base file provided by the DMA Aerospace Center. This file was updated and checked against our June 78 data tape. We then compared new data sources with the existing data and selected data to be merged. In doing this we would modify accuracy estimates if a difference of greater than 20 mgals existed between two anomaly estimates. Then the new standard deviation was taken as half of the absolute difference, not to exceed 97 mgals, unless it is smaller than the standard deviation on the tape when the tape value would be retained. A file containing 41973 anomalies was generated that contained data from 45 data sources. Of these anomalies 721 values had standard deviations greater than 30 mgals and 16209 anomalies were anomalies not from the Aerospace Center. The location of these anomalies is shown in Figure 1.

A number of anomalies on our original data file were based on estimates made through geophysical prediction techniques. In such cases it is important for us to identify these anomalies. This has been tentatively done based on published accounts (e.g. Wilcox, 1973) of where such predictions have taken place. For the October 1979 update we have identified 6912 possible anomalies which are shown in Figure 2.

A statistical analysis has been carried out with the anomalies of the Oct 79 data set with some typical results shown in Table 2. All values are with respect to the gravity formula of the Geodetic Reference System 1967.

Table 2. Statistics on the Oct 79 1°x 1° Data Set

Quantity	Value
Mean Value	-0.3 mgals
Minimum Anomaly	-282 "
Maximum Anomaly	365 "
Weighted RMS Average	±30.1 "
Minimum Std. Dev.	± 1. "
Maximum Std. Dev.	97 "
Weighted RMS Std. Dev.	16.3 "

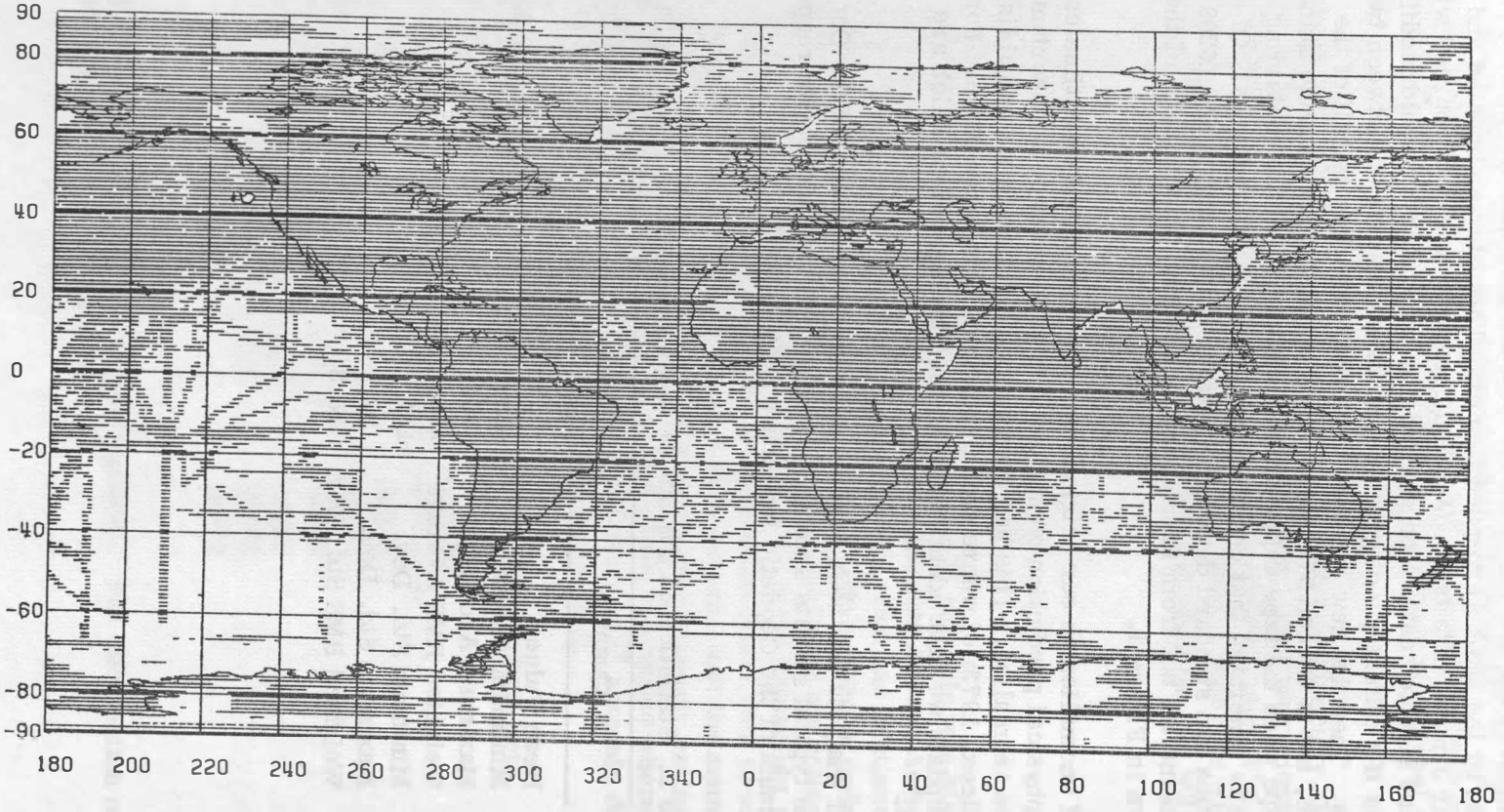

Figure 1. Location of 41973 1° x 1° Anomalies in the October 1979 Terrestrial Data Set

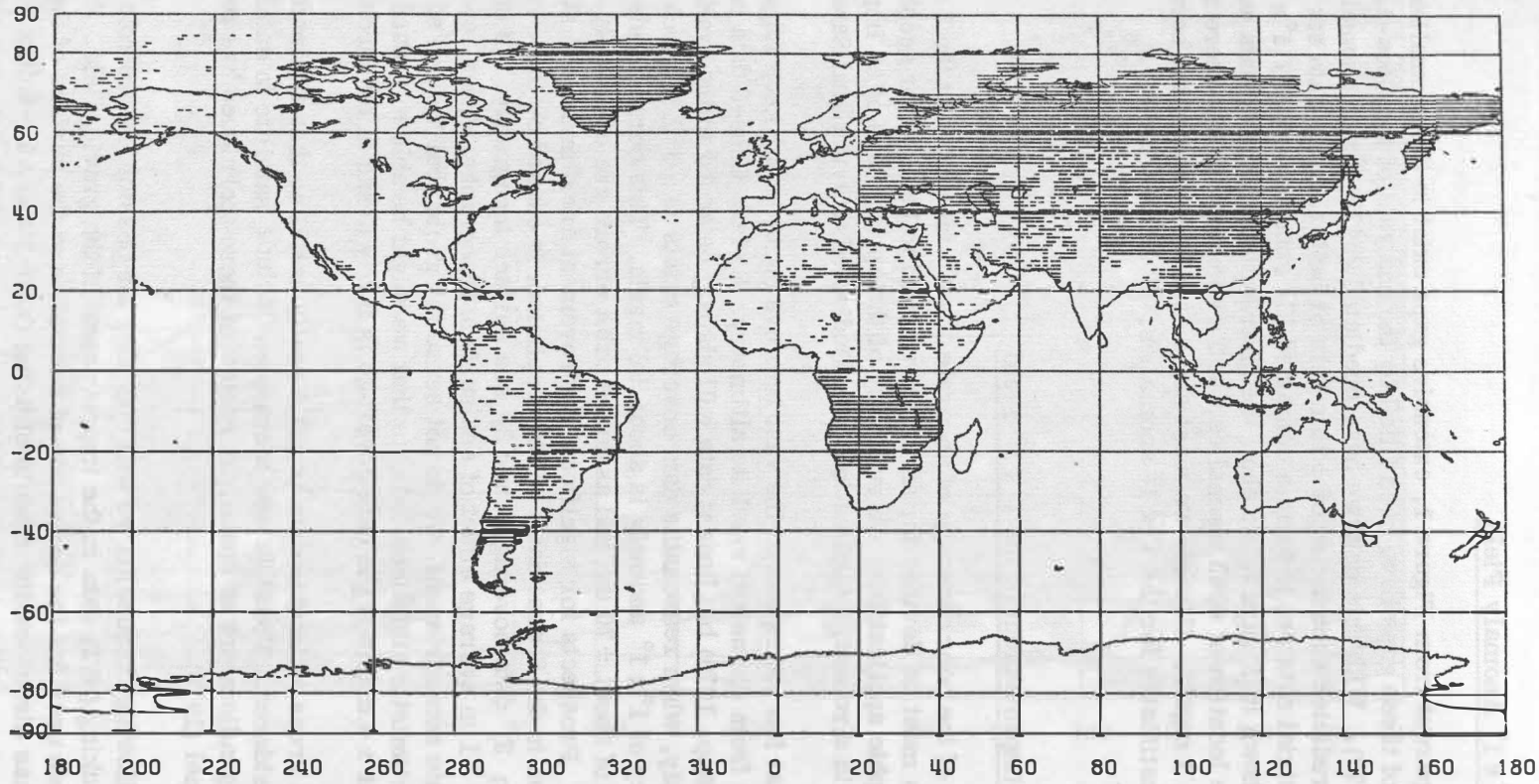

Figure 2. Location of 6912 1°x 1° Anomalies Thought to be Geophysically Predicted

A Combined 1°x 1° Anomaly Field

As is apparent from Figure 1, extensive gaps exist in the anomalies in ocean areas. Many of these gaps have been filled by the analysis of the Geos-3 altimeter data (Rapp, 1979). With this data we have predicted 29479 1°x 1° anomalies, 27488 of which had predicted accuracies of ± 15 mgals or better. This data set was merged with the terrestrial data set to form a combined file containing 52917 1°x 1° anomalies. This field is shown in Figure 3. To show the distribution of "good" data we have plotted in Figure 4 the location of 6943 anomalies, in the combined field, where the standard deviation is ≤ 5 mgals. Clearly we must say that major parts of the earth do not have reliable estimates for the 1°x 1° anomalies.

Prospects for Improvement of the 1°x 1° Field

Because of the poor coverage of accurate 1°x 1° anomalies at the 5 mgal level, new techniques must be devised for an improved field to be used for geophysical and oceanographic applications. A summary of the applications of an improved field are discussed in a report, "Applications of a Dedicated Gravitational Satellite Mission."

In the past few years one of the vast improvements in our knowledge of the 1°x 1° field has come from the use of satellite altimetry. So far, Geos-3 data has been widely used (Rapp, 1979) but Seasat data will shortly be added to the available data base. Currently, when reasonable data coverage exists in a 1°x 1° block, the expected accuracy of 1°x 1° anomaly is about ± 6 mgals. This corresponds to a measurement noise of about ± 70 cm and assumes orbit errors are effectively removed from the data. Prospects for significant improvement are dim despite significant noise reduction in the Seasat data. This pessimism is caused by three concerns: 1) orbit error; 2) data coverage; and 3) sea surface topography. Of special concern is the ± 1 m average effect of sea surface topography. Thus, even if we have an accurate measurement, we do not sense the geoid, but the sea surface. Tests under optimistic situations indicate that we might be able to reduce our 1°x 1° errors to about ± 4 mgals if the data coverage is fairly dense in the block.

For land areas altimeter data is not directly useful so that alternate techniques need to be considered. Possible new techniques include satellite to satellite tracking and the use of gradiometry in space. A review of these techniques has recently been given by Rummel (1979).

In the following discussion we will consider the possible future role of satellite to satellite tracking (SST) data in the improvement of the gravity field. Such data has already been used for the derivation of anomalies at the surface of the earth. Hajela (1979) has discussed the results of using Geos-3 and ATS-6 data which was a high-low mission. Vonbun et al. (1980) have discussed the determination of 5° anomalies using ATS-6 and Apollo data taken in July 1975. Results showed that the techniques used were promising although limited by a too high satellite (Geos-3) or very noisy data (Apollo).

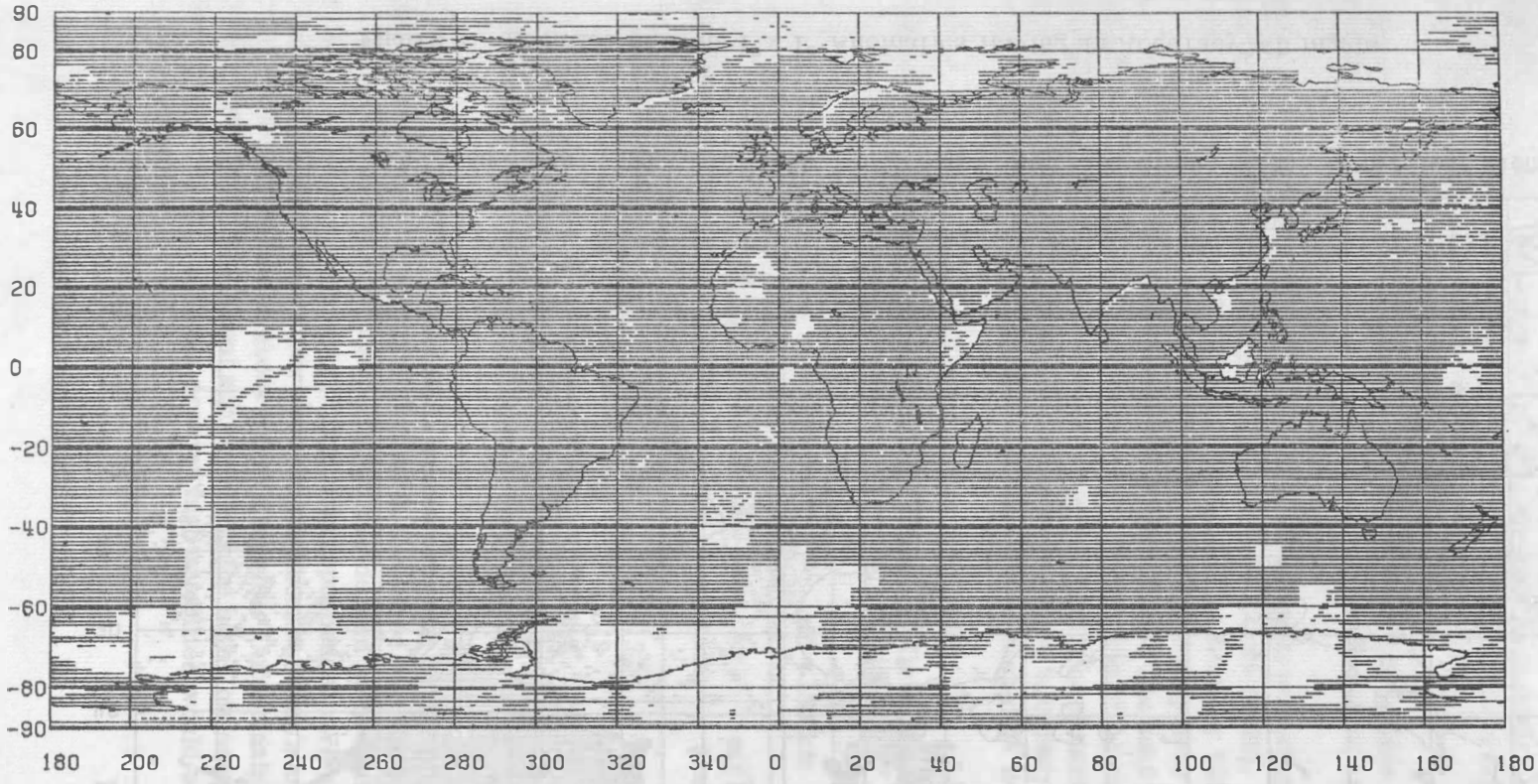

Figure 3. Location of 52917 1°x 1° Anomalies Based on a Combined Terrestrial-Altimeter Data Set

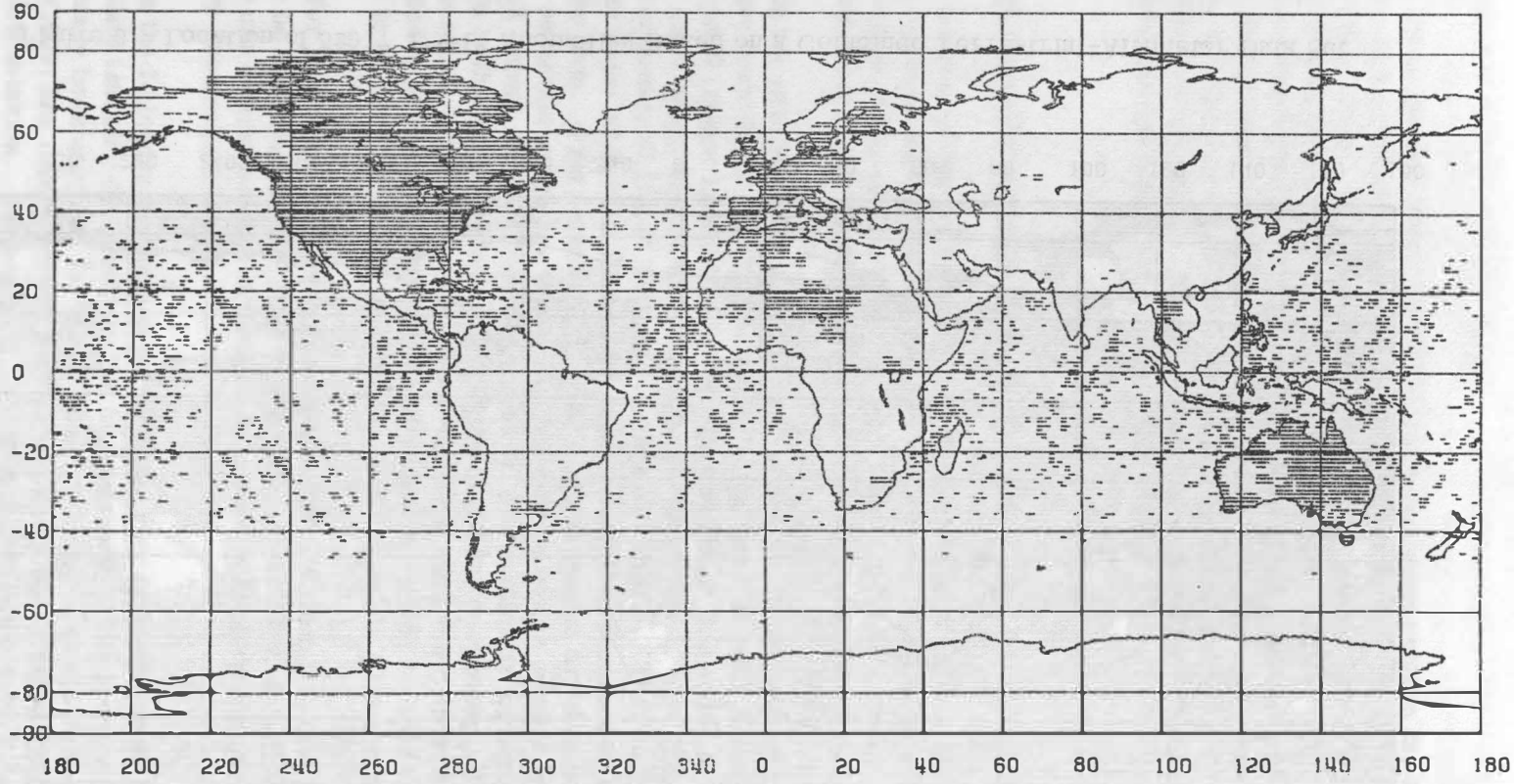

Figure 4. Location of 6943 1° x 1° Anomalies Having an Accuracy ≤5 mgals

Considerable interest has been expressed in using SST data with at least one satellite at a low altitude. A number of investigations have recently been carried out that try to estimate what could be expected from such a mission. Discussion can be found in Breakwell (1979), Rapp and Hajela (1979), Douglas et al. (1980) and Rummel (1980).

An extensive review of the methods used will not be done here. Instead, I propose to discuss some recent results obtained at The Ohio State University.

We first examine the results for a high-low SST mission using the procedures of least squares collocation as described in Rapp and Hajela (1979). We consider the observed quantity to be an acceleration which can be found by fitting the range rate data to a function and then differentiating. For simplicity here we assume only the vertical component of the acceleration is determined. The data we have assumed consists of 163 data points located at 0.25 intervals over the 1° block and at 0°.5 intervals outside the block (to 3° from the center). Using the covariances of Tscherning/Rapp with respect to a 12th degree reference field the accuracy of the 1°x 1° anomalies and undulations that would be recovered from such data is shown in Table 3.

Table 3. 1°x 1° Anomaly and Undulation Accuracies Using Least Squares Collocation for a High-Low SST Mission

		H = 150 km		H = 180 km	
$\dot{\rho}$ (μm/sec)	$\ddot{\rho}$ (mgals)	m(Δg) (mgals)	m($\overline{N}$) (cm)	m(Δg) (mgals)	m($\overline{N}$) (cm)
22	0.50	7.0	49	8.7	47
3.3	0.10	4.4	43	5.9	38
1.3	0.08	4.1	42	5.6	37
0.2	0.01	2.6	39	3.3	33

The range rate ($\dot{\rho}$) values were computed from a program kindly provided by Rummel. This $\dot{\rho}$ value corresponds to the acceleration in the sense that the signal to noise ratio for both $\ddot{\rho}$ and $\dot{\rho}$ are the same. The values depend somewhat on the height (H) so the values given represent an average correspondence. We see from Table 3 that if we obtain range rate data whose accuracy is about ± 1 μm/sec we could expect to derive 1°x 1° anomalies to about ± 3 to 4 mgals. Unfortunately, this high accuracy in the range rate data is not achievable in the high-low case because of the effect of the ionosphere. In addition, several high satellites would be needed to obtain the global coverage needed.

We now turn to the use of a low-low SST mission. Such a mission is discussed by Rummel (1980) using the methods of least squares collocation. We will therefore discuss it using an alternate approach motivated by the discussion of Rummel (1979). This procedure considers the spectrum of the signal and noise to arrive at accuracy estimates for the quantities of interest.

The velocity spectra associated with a satellite has been described by Kaula (1969), Rummel (1979) and others. For the velocity difference spectra of two satellites separated in a radial direction we have (Rummel, private communication)

$$\sigma^2(\dot{X}_{12R})_\ell = \frac{1}{|\dot{X}|^2}\left(1 - \left(\frac{r_P}{r_Q}\right)^{\ell+1}\right)^2 \frac{\sigma_T^2(r_P)_\ell}{2\ell+1} \tag{1}$$

where $\sigma(\dot{X}_{12R})_\ell$ is the information, by coefficient in degree ℓ, in the velocity difference of two satellites located at a distance r_P (low satellite) and r_Q (far satellite) from the center of the earth. σ_T^2 are the potential degree variances which are related to anomaly degree variances by:

$$\sigma_T^2(r_P)_\ell = \left(\frac{R^2}{r_P^2}\right)^{\ell+1} \frac{R^2}{(\ell-1)^2} c_\ell \tag{2}$$

where R is usually considered to be the radius of the Bjerhammer sphere imbedded in the earth. $|\dot{X}|$ is the average velocity of the satellites.

For two satellites at the same altitude, but separated horizontally by a central angle ψ, the corresponding spectra is:

$$\sigma^2(\dot{X}_{12H})_\ell = \frac{2\sigma_T^2(r_P)_\ell}{|\dot{X}|^2(2\ell+1)}\left(1 - P_\ell(\cos\psi)\right) \tag{3}$$

For the case of 150 km high satellite we have plotted in Figure 5 the radial and horizontal difference spectra when the two satellites are separated by 300 km. In addition, the radial velocity difference spectra is shown for an altitude of 180 km. The c_ℓ model used is that of Tscherning/Rapp. The difference between the horizontal and vertical spectra is small, being on the order of $\sqrt{2}$.

We are now interested in the error spectrum of the velocity difference $\sigma^2(\rho_{n\ell})$ given a certain measurement accuracy, $\sigma(\dot{\rho})$. One approach to the error spectrum determination is given by Rummel (1979). An alternate approach has been developed by Jekeli (1980, private communication). Assuming the data noise is uncorrelated Jekeli shows that:

$$\sigma^2(\dot{\rho}_{\ell n}) = \frac{\Delta\sigma}{4\pi R^2}\sigma^2(\dot{\rho}) \tag{4}$$

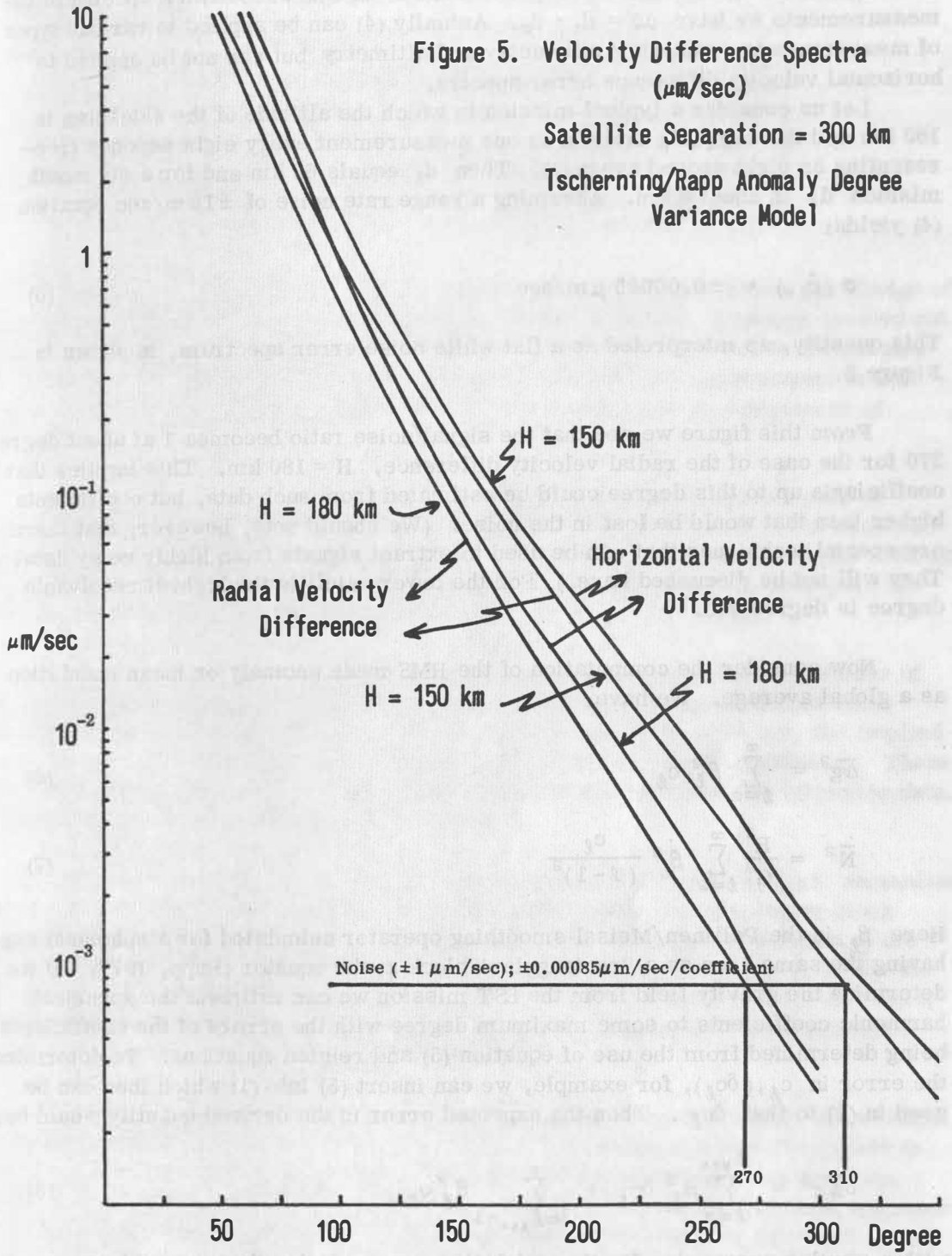

Figure 5. Velocity Difference Spectra (μm/sec)

Satellite Separation = 300 km

Tscherning/Rapp Anomaly Degree Variance Model

Here $\Delta\sigma$ is the area of a block whose side length is the distance between successive measurements. If d_1 and d_2 represent the along and cross track spacing of the measurements we have $\Delta\sigma = d_1 \cdot d_2$. Actually (4) can be applied to various types of measurements, such as gradiometry and altimetry but can not be applied to horizontal velocity difference error spectra.

Let us consider a typical mission in which the altitude of the satellites is 180 km and the sampling interval is one measurement every eight seconds (representing an eight second average). Then d_1 equals 62 km and for a six month mission d_2 is about 6 km. Assuming a range rate noise of $\pm 1\mu$m/sec equation (4) yields:

$$\sigma(\dot{\rho}_{\ell m}) = \pm 0.00085\ \mu\text{m/sec} \tag{5}$$

This quantity, as interpreted as a flat white noise error spectrum, is shown in Figure 5.

From this figure we see that the signal/noise ratio becomes 1 at about degree 270 for the case of the radial velocity difference, H = 180 km. This implies that coefficients up to this degree could be estimated from such data, but coefficients higher than that would be lost in the noise. (We should note, however, that there are special techniques that can be used to extract signals from highly noisy data. They will not be discussed here.) For the lower satellite the highest resolvable degree is degree 310.

Now consider the computation of the RMS mean anomaly or mean undulation as a global average. We have:

$$\overline{\Delta g}^2 = \sum_{\ell=2}^{\infty} \beta_\ell^2\, c_\ell \tag{6}$$

$$\overline{N}^2 = \frac{R^2}{G^2} \sum_{\ell=2}^{\infty} \beta_\ell^2\, \frac{c_\ell}{(\ell-1)^2} \tag{7}$$

Here β_ℓ is the Pellinen/Meissl smoothing operator calculated for a spherical cap having the same area as a "rectangular" block at the equator (Rapp, 1977). If we determine the gravity field from the SST mission we can estimate the spherical harmonic coefficients to some maximum degree with the errors of the coefficients being determined from the use of equation (5) and related equations. To determine the error in c_ℓ, (δc_ℓ), for example, we can insert (5) into (1) which then can be used in (2) to find δc_ℓ. Then the expected error in the derived quantity would be:

$$\delta\overline{\Delta g}^2 = \sum_{\ell=2}^{\ell_{max}} \beta_\ell^2\, \delta c_\ell + \sum_{\ell=\ell_{max}+1}^{\infty} \beta_\ell^2\, c_\ell \tag{8}$$

with a similar expression for the undulation error. Using these procedures accuracy estimates for mean anomalies and undulations can be obtained. Such results are shown in Table 4 where the c_ℓ model of Tscherning/Rapp was used in the calculation of the truncation effect.

Table 4. Accuracy of Mean Anomaly and Mean Geoid Undulation From SST Tracking (Noise = ±1 μm/sec, Radial Separation = 300 km)

Block Size	H = 150 km		H = 180 km	
	Anomaly	Undulation	Anomaly	Undulation
2°	—	—	1.2 mgal	3 cm
1°	2.2 mgal	4 cm	3.2 mgal	7 cm
30'	—	—	10.6 mgal	21 cm

These computations show that a significant improvement in our knowledge of the earth's gravity field can be found using the SST mission. Although carried out for radial separations which are not feasible in practice, the results should also hold closely for the horizontal type of mission. Significant improvement in the anomaly field does rely on having an accurate range rate measurement of ±1 μm/sec.

The results from Table 3 and Table 4 may be compared for the case of H = 180 km and 1° x 1° blocks. For the 1 μm/sec data noise both collocation and the harmonic analysis approach gives a 1° x 1° accuracy of about ±4 mgals although the collocation solution is for a high-low case. The agreement is quite good for the anomaly but the undulation agreement is poor (35 cm vs 7 cm).

To further test this harmonic analysis approach we considered the case of satellite altimetry used to derive mean anomalies based on geoid undulations. Assuming 10 measurements in a 1° block, with an accuracy of 70 cm, the implied accuracy of a 1° anomaly is ±5.4 mgals and ±22 cm for the 1° undulation. These numbers agree quite well with thousands of values derived from the altimeter data. This gives us some confidence in this method.

We have also considered the correlation of the 1° x 1° and 30' x 30' anomalies by propagating the error estimated for the smaller block into the larger block error solving for an average correlation coefficient. For the correlation of the 1° blocks we found $\rho = -0.13$ and for 30' blocks $\rho = -0.21$. The value of ρ for the 1° blocks agrees with that found by Rummel (1980) for a similar case. However, it disagrees with the general expectation that 1° x 1° anomalies recovered from such low satellites should be highly correlated.

We have also applied this analysis assuming we have determined the vertical gravity gradient with an accuracy of ±0.01 E. The highest degree resolvable is very close to that found in the case of the low-low SST mission. For example, with H = 180 km, n_{max} is 280. The error propagation using the previous approach yielded essentially the same accuracy for anomaly and undulation recovery as did the SST mission. For example, with H = 180 km, the 1° x 1° anomaly accuracy was ±3.0 mgals and the corresponding undulation accuracy was 6 cm. Thus a gradiometer mission with 0.01 E accuracy and a low-low mission of 1 μm/sec will yield about the same final gravity field improvement.

We have also considered the sensitivity of the analysis to the model used for the anomaly degree variances, or in effect the potential coefficient decay. This was done by using Kaula's $10^{-5}/\ell^2$ rule and a new model described in Rapp (1979). Our results do not show any significant change when different models are used. (For example, at H = 180 km, a 1° accuracy is ±3.8 mgals and 8 cm when using the best two component model described in Rapp (1979))

Conclusions

In this paper we have discussed the status and improvement of the 1°x 1° anomaly field of the earth. The current situation is a considerable improvement over what existed ten years ago. However, the coverage is still poor in some land areas and the information at sea is primarily available from Geos-3 data. The average accuracy of the terrestrial data set (excluding altimeter derived anomalies) is ±16 mgals. In the combined data set only 6943 values have standard deviations ≤ 5 mgals. If we are to improve our gravity field, significant strides must be taken. We cannot expect that such strides will be taken through ground base measurement systems. Instead we need to look towards space techniques.

In examining such methods we found there is a possibility of significant improvement of our field from a low-low SST mission with an accuracy of ±1 μm/sec for the range rate data, or through gradiometry with a vertical gradient device of ±0.01 E accuracy. Then we expect to be able to obtain 1° anomalies and undulations to an accuracy of about ±3-4 mgals and 7 cm,respectively,. These accuracies make a number of assumptions that will need careful consideration in the future.

The primary analysis method used here is an error propagation procedure. To gain confidence in our results, a simulation study should be performed to carry out a typical real world solution. Such simulations are complex and costly. In addition, we need to understand better orbit error problems, and problems in the downward continuation area. What, for example, is the best way to obtain and define anomalies and undulations in rugged topographic areas? What are optimum reduction procedures to be used? How can we overcome the apparent instability in least squares collocation solutions when very dense data is used? What are the orbit computation problems for this highly precise computation? Are global solutions required?

First steps have been taken to assess the feasibility of a gravity mapping mission. Current prospects appear to say that highly accurate data can be obtained. Such information will be extremely valuable to geophysicists and to oceanographers, as well as geodesists. For example, the precise geoid that will be available from such a mission will help solve a number of problems in ocean circulation, if combined with precise altimeter measurement. Clearly we are ready for the next significant advance in the improvement in our knowledge of the earth's gravity field.

Acknowledgement

The research described in this report is supported by the National Aeronautics and Space Administration, Goddard Space Flight Center, Greenbelt, Maryland, under Grant NGR 36-008-161.

Christopher Jekeli significantly contributed to this work through the derivation of a number of important equations and the computer implementation of the algorithms described. Very helpful discussions were held with Oscar Colombo and Reiner Rummel.

References

Breakwell, John, Satellite Determination of Short Wavelength Gravity Variations, The Journal of the Astronautical Sciences, Vol. XXVII, No. 4, Sept-Dec, 1979.

Douglas, B. C., et al., Determination of the Geopotential from Satellite-to-Satellite Tracking Data, NOAA Technical Memorandum, NOS NGS 24, Rockvill, Maryland, January, 1980.

Hajela, D. P., Tests for the Recovery of 5° Mean Gravity Anomalies in Local Areas from ATS-6/Geos-3 Satellite to Satellite Range-Rate Observations, J. Geophys. Res., 84, 6884-6890, 1979.

Kaula, W., The Appropriate Representation of the Gravity Field for Satellite Geodesy, in Proceedings of the IV Symposium on Mathematical Geodesy, Triest, 1969.

Rapp, R. H., The Relationship Between Mean Anomaly Block Sizes and Spherical Harmonic Representations, J. Geophys. Res., Vol. 82, No. 33, 5360-5364, 1977.

Rapp, R. H., Global Anomaly and Undulation Recovery using Geos-3 Altimeter Data, Dept. of Geodetic Science Report No. 285, The Ohio State University, Columbus, 54 p., 1979.

Rapp, R. H., Applications of a Dedicated Gravitational Satellite Mission, publication of the National Academy of Science, Washington, D.C. (Available from: NASA, Applications Directorate, (Code 900), Goddard Space Flight Center, Greenbelt, Maryland 20771.

Rapp, R. H., Potential Coefficient and Anomaly Degree Variance Modelling Revisited, Dept. of Geodetic Science Report No. 293, The Ohio State University, Columbus, 1979.

Rapp, R., and D. P. Hajela, Accuracy Estimates of 1°x 1° Mean Anomaly Determinations from a High-Low SST Mission, Dept. of Geodetic Science Report No. 295, The Ohio State University, Columbus, 1979.

Rummel, R., Determination of Short-Wavelength Components of the Gravity Field from Satellite-to-Satellite Tracking or Satellite Gradiometry, manuscripta geodaetica, Vol. 4, No. 2, 197-148, 1979.

Rummel, R., Geoid Heights and Mean Gravity Anomalies from "Low-Low" Satellite-to-Satellite Tracking - An Error Analysis, Dept. of Geodetic Science Report, The Ohio State University, Columbus, 1980.

Vonbun, F., et al., Determination of 5°x 5° Gravity Anomalies Using Satellite-to-Satellite Tracking Between ATS-6 and Apollo, Geophys. J. R. astr. Soc., 61, 1980.

Wilcox, L., Bouguer Gravity Anomaly Map of South America, DMAAC Technical Paper No. 73-2, St. Louis AFB, Missouri 63118, 1973.

RESULTS OF AN EXPERIMENT ON BALLOON - TRIANGULATION BETWEEN POTSDAM AND DRESDEN

by

H. Rehse [x]

Summary

In September 1979 we carried out a balloon-triangulation between Potsdam and Dresden. On this occasion obtained observations have been analysed. The results have been compared with other methods.

Zusammenfassung

Im September 1979 wurde zwischen Potsdam und Dresden eine Ballontriangulation durchgeführt. Die hierbei erzielten Beobachtungen wurden ausgewertet und die Ergebnisse wurden mit anderen Auswertungen verglichen.

Balloon-triangulation is a stellar triangulation, basing on the fact, that high aims (balloon borne flashes) can be observed photographically by two observation stations against the fixed star sky. These simultaneous observations define together with the observation stations the so-called simultaneous planes. If two of these planes come to a section (see fig. 1), the direktion to the 2nd station (B) can be deduced in an equatorial coordinate system /1/. Our task was to determine the direction Potsdam - Dresden by means of balloon-triangulation. Besides, Doppler-measurements were carried out to compare results of both methods.

In the Central Earth Physics Institute a mobile balloon ascent station and flash probes have been developed. The meteorological balloons with flash probes were started at adequate places, and these probes had to produce flashes of light. For light generation, magnesium flash powder /2/ were used which was released radio electrically by means of electric bridge igniters. The field works on determination of the direction between Potsdam and Dresden were carried out in september 1979. Herzberg was the central station, and from here the places for starting the meteorological balloons according to the corresponding altitude winds could be reached in a short time (see fig.2). The field station of the Technical University of Dresden in Dresden-Gönnsdorf and the Helmert Tower of the Central Earth Physics Institute in Potsdam served as observation stations. For the observations an astrograph were used in Dresden and the Automatic Camera for Astrogeodesy (SBG) in Potsdam.

x Akademie der Wissenschaften der DDR, Zentralinstitut für Physik der Erde, DDR-1500 Potsdam, Telegraphenberg A 17

Kartengenehmigungsnummer P 326/80

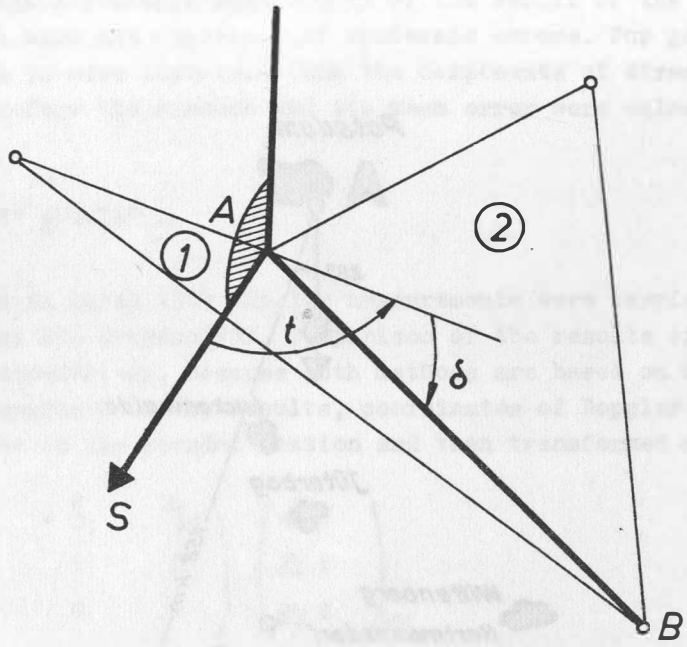

Fig. 1: Principle of balloon-triangulation

During the observation period 10 balloon ascents were carried out. 8 simultaneous plates with 14 simultaneous planes were gained. Photographs were measured by the Ascorecord, and by means of fixed points the flash positions were determined by compensation with 6 unknowns. The flash positions were corrected by rocket refraction, polar motion, daily aberration and centring data. Using the corrected observations the hour angle t and declination δ were computed by means of the method of least squares:

$$t = 26^{\circ}\ 0'\ 27{,}89'' \pm 3{,}16'', \qquad \text{with } m_o = \pm 2{,}06'' ,$$
$$\delta = -35^{\circ}\ 21'\ 41{,}32'' \pm 1{,}95''. \tag{1}$$

The result cannot be considered statisfactory because of the big mean error. The reasons for the big errors can be seen in the fact that on the one hand too little and on the other hand only one-sided observations were made. For confirmation of the result we used therefore the little number of observations received for the determination of the direction between Potsdam and Dresden, in 1968 (see fig. 2). Because they had been carried out on excentric points, they had to be centred. Including these observations the 18 observations totally gave the following results:

$$t = 26^{\circ}\ 0'\ 24{,}60'' \pm 0{,}89'' , \qquad \text{with } m_o = \pm 2{,}13'' ,$$
$$\delta = -35^{\circ}\ 21'\ 39{,}30'' \pm 0{,}58'' . \tag{2}$$

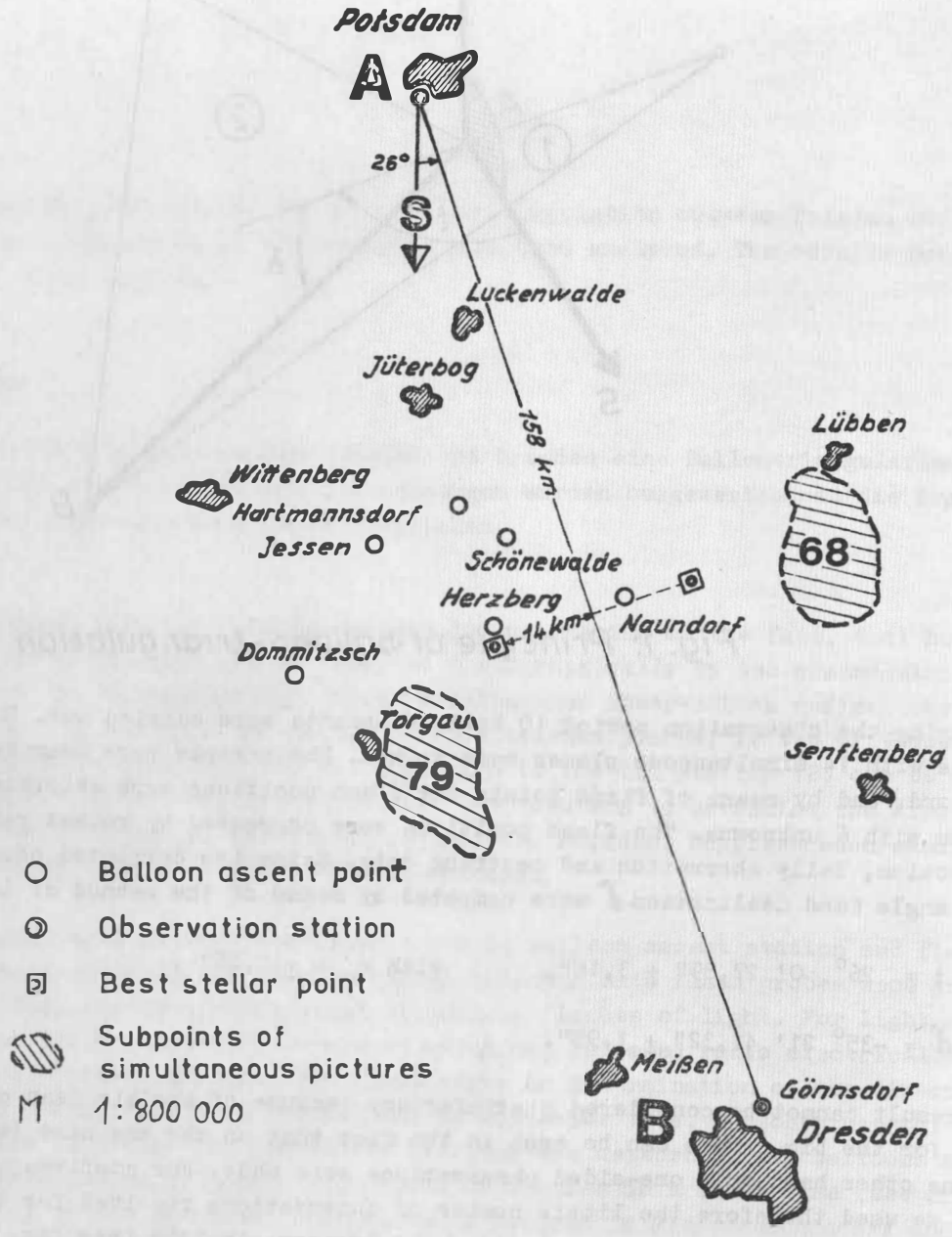

Fig. 2: Triangulation area

These results are satisfactory in geodetic respect. The existing deviations between both solutions are within the simple mean errors of the result of the observations made in 1979 and do not have the character of systemaic errors. For geodesy the azimuth between two points is more important than the components of direction in the equatorial system. Therefore the azimuth and its mean error were calculated from the direction angles:

(3) $A_Z = 20^o\ 57'\ 12{,}91'' \pm 0{,}72''$.

In November 1978 and in March 1979 Doppler measurements were carried out at the same stations in Potsdam and Dresden /3/. Comparison of the results of both methods cannot be carried out immediately, because both methods are based on different coordinate systems. For comparison of the results, coordinates of Doppler measurements were used with reference to the Potsdam station and then transformed according to

$$(4)\quad \begin{pmatrix} \Delta X \\ \Delta Y \\ \Delta Z \end{pmatrix} = \begin{pmatrix} 1 & -\xi_1 & \xi_2 \\ \xi_1 & 1 & 0 \\ -\xi_2 & 0 & 1 \end{pmatrix} \begin{pmatrix} \Delta X \\ \Delta Y \\ \Delta Z \end{pmatrix}_{BE}$$

into the astronomic system of Potsdam (where $\Delta X - \Delta Y - \Delta Z_{BE}$ are the differences of coordinates between Potsdam and Dresden in the broadcasting system). ξ_1, ξ_2 are differences between astronomic coordinates and geographic Doppler coordinates. From the $\Delta X - \Delta Y - \Delta Z$ - data, the direction angles in the equatorial system were calculated and from that the azimuth inclusively its error. The result of these calculations is

(5) $A_{ZD} = 20^o\ 57'\ 14{,}83'' \pm 4{,}23''$

Comparision of calculated azimuths according to balloon-triangulation and to the Doppler measurement and their mean errors shows that the azimuth determined by balloon - triangulation was determined for nearly an order of magnitude more accurate and that the difference of the azimuths which is 1,92" is within the simple mean error of the Doppler azimuth.

Literature

/1/ VÄISÄLÄ, Y.: An astronomical method of triangulation.
Sitzungsberichte der Finnischen Akademie der Wissenschaften 1946, S. 99-107
Helsinki 1947.

/2/ REHSE, H.: Fehlertheorie zur Stellartriangulation und die Bestimmung der Richtung Potsdam - Dresden/Gönnsdorf.
Dissertation, TU Dresden 1970.

/3/ FEJES, I.; DIETRICH, R.: Satelliten-Dopplermessungen in Potsdam und Dresden.
Vermessungstechnik, Berlin 28 (1980), Heft 3

Error Analysis of "Low-Low" Satellite-to-Satellite Tracking

Reiner Rummel

Bayerische Kommission für die Internationale Erdmessung,
Bayerische Akademie der Wissenschaften
München

A b s t r a c t :

An error analysis for the estimation of surface geoid heights, geoid height differences, and $1^o \times 1^o$ mean gravity anomalies from an SST experiment in the low-low mode is presented. The employed method is least squares collocation. The error estimates are analyzed in their dependence of the measurement precision, the spatial configuration of the two satellites, the intersatellite distance, and the experiment altitude. In an optimal situation - range rate precision $\pm 10^{-6}$ m s^{-1}, intersatellite distance 250 km, experiment altitude 200 km - an a posteriori std.dev. of ± 0.9 m for geoid heights, ± 0.7 m for geoid height differences (distance 150 km), and ± 6 to 7 mgal for $1^o \times 1^o$ mean gravity anomalies is feasible. Thereby short wavelength uncertainties in the orbit have to be controlled down to 1 cm in radial direction, whereas for long wavelength effects 10 m should not be exceeded.

Further improvement could be obtained if the solution of the large and unstable system of linear equations could be avoided. Since in SST a globally very dense pattern of observations is available it is proposed to construct a stabilized operator valid for globally and continuously given data with variance σ_δ^2 on which a discrete approximation by numerical integration could be based.

Z u s a m m e n f a s s u n g :

Unter Anwendung von Least-Squares Kollokation wurde eine Fehleranalyse für die Schätzung von Geoidhöhen, Geoidhöhenunterschieden und $1^{o} \times 1^{o}$ mittlere Schwereanomalien aus Satellite-to-Satellite Tracking (SST) im "low-low" Modus durchgeführt. Untersucht wurde die Abhängigkeit der Schätzungen von der Beobachtungsgenauigkeit, der räumlichen Anordnung der beiden Satelliten, vom Abstand zwischen den Satelliten und von der Höhe, in der das Experiment durchgeführt wird. Unter optimalen Bedingungen - Beobachtungsgenauigkeit $\pm 10^{-6}$ m s^{-1} , Satellitenabstand 250 km, Höhe des erdnahen Satelliten 200 km - wäre eine a posteriori Standardabweichung von ± 0.9 m für Punktgeoidhöhen, ± 0.7 m für Geoidhöhenunterschiede und von ± 6 bis 7 mgal für $1^{o} \times 1^{o}$ Schwereanomalien erreichbar. Der Einfluß hochfrequenter Bahnstörungen muß dabei unter 1 cm in Radialrichtung bleiben, während für langwellige Störungen 10 m nicht überschritten werden dürfen.

Eine weitere Verbesserung der Schätzergebnisse wäre möglich, gelänge es die notwendige Auflösung des großen und instabilen, linearen Gleichungssystems zu umgehen. Da SST Beobachtungen global und in sehr dichter Anordnung liefert, könnte man einen für eine globale, kontinuierliche Beobachtungsbelegung mit Varianz σ_0^2 gültigen stabilisierten Operator ableiten, der die Grundlage für eine Näherunglösung über numerische Integration aus diskretem Beobachtungsmaterial liefert.

In the near future a considerable improvement of our current knowledge about the detailed structure of the earth's gravity field is expected from satellite-to-satellite tracking (SST) in the low-low mode, as expressed e.g. in *(Geodesy: Trends & Prospects, 1978)* or *(Hieber & Guyenne, 1978)*. Possible candidate missions with very different characteristics are for instance the GRAVSAT project *(Applications of a Dedicated Gravitational Satellite Mission, 1979)*, the SLALOM experiment *(ESA, 1978)*, or the DIDEX experiment *(Drożyner, 1978)*.

Existing simulation studies or error analyses produced results that were partly in disagreement with each other or not comparable at all, mainly due to the employment of different error measures or different mathematical models, e.g. flat earth approximation, finite models restricted to a limited area. As a result the panel on gravity field & sea level requirements of the committee on geodesy, National Academy of Sciences, U.S.A., *(Applications of a Dedicated Gravitational Satellite Mission, 1979)*, compiled a catalogue of open questions to be answered in future studies and tried to define the user requirements for geodetic, geophysical, and oceanographic applications.

The goal of this paper is to summarize the results of an error analysis for an application of low-low SST for the estimation of surface $1^{\circ} \times 1^{\circ}$ mean gravity anomalies, geoid heights, and geoid height differences. Details are described in *(Rummel, 1980)*.

Mathematical Model and Error Analysis Results

The applied mathematical model for the range rate $\dot{\rho}$ between two satellites at S_1 and S_2 is:

$$\dot{\rho}(S_1, S_2) = \dot{\underline{X}}_{12} \cdot \underline{e}_{12} \qquad (1)$$

where $\dot{\underline{X}}_{12} = \dot{\underline{X}}(S_2) - \dot{\underline{X}}(S_1)$, is the velocity difference between the two satellites and $\underline{e}_{12} = \rho^{-1}\underline{X}_{12}$, the unit vector pointing

from S_1 (with position vector $\underline{X}_1$) to S_2, and ρ is the inter-satellite distance. When using the least-squares collocation method for the gravity parameter estimation the underlying model of the gravity field comes because of its global and continuous character closest to physical reality. Uniqueness of the estimates is thereby achieved by a least squares solution with minimum norm in a Hilbert space with reproducing kernel. But, as shown in the study by *(Krynski, 1978)*, the incorporation of time dependent quantities such as the position or velocity of satellites into the collocation model is a rather complex problem. Thus, instead of working with range rates we will analyze range rate changes, $\ddot{\rho}$, (line of sight accelerations) which are assumed to be derived from the observed range rates by numerical differentiation:

$$\ddot{\rho}(S_1, S_2) = \ddot{\underline{X}}_{12} \cdot \underline{e}_{12} + \dot{\underline{X}}_{12} \cdot \dot{\underline{e}}_{12} . \qquad (2)$$

An evaluation of the average magnitude of the second term on the right hand side from degree 2 to ∞ gives approximately $0.24 \cdot 10^{-10}$ m s^{-2} = $0.24 \cdot 10^{-5}$ mgal (for ℓ = 19 to ∞ : $0.02 \cdot 10^{-5}$ mgal) as compared to $\doteq$ 1.50 mgal (1.08 mgal) for the first term. For a range rate change precision 0.2 mgal, or a range rate precision of 10^{-5} m s^{-1}, respectively, the second term can therefore easily be neglected. For a moment the true orbit is assumed to be known. Then the observation model for gravity parameter estimation becomes

$$\underline{\ell} = \ddot{\underline{\rho}}^{c}(S_1, S_2) + \underline{e}_{12} \cdot \frac{\partial \operatorname{grad} T_{12}}{\partial \underline{\beta}} \Bigg|_{S_1^c, S_2^c} \underline{\delta\beta} + \underline{\epsilon} , \qquad (3)$$

where $\underline{\ell}$ ... vector of "observed" range rate changes,

$\ddot{\underline{\rho}}^{c}$ ... range rate changes, computed from a chosen reference field,

$\operatorname{grad} T_{12} = \operatorname{grad} T(S_2) - \operatorname{grad} T(S_1) = \underline{\delta\ddot{X}}_{12}$ ... difference of the gradient of the disturbing potential at S_1 and S_2 ($\underline{\delta\ddot{X}}_{12}$ ... residual acceleration difference)

$\underline{\delta\beta}$ ... parameters of the residual gravity field (e.g. geoid heights, gravity anomalies referring to the chosen reference field).

$\underline{\epsilon}$ ... vector containing the measurement noise and the terms of second and higher order of the series expansion.

With $\underline{r} = \underline{\ell} - \ddot{\underline{\rho}}^c(S_1, S_2)$ and $\underline{e}_{12} \cdot \left.\frac{\partial \text{ grad } T_{12}}{\partial \underline{\beta}}\right|_{S_1^c, S_2^c} = \underline{A}$

the estimation model becomes:

$$\underline{r} = \underline{A}\,\underline{\delta\beta} + \underline{\epsilon} \,. \tag{4}$$

A separate sensitivity study for the orbit requirement shows that unmodelled short-wavelength orbit uncertainties, especially due to drag effects, have to be controlled down to 1 cm in radial and to 1.5 m in along and cross track direction, whereas unmodelled long-wavelength effects, e.g. due to tracking station uncertainties should only not exceed 10 m, independent of the direction.

With the a priori model for the variance-covariance matrix of the observations $\underline{D} = \sigma_o^2\underline{I}$ (σ_o^2 ... variance of the observations, $\underline{I}$ ... identity matrix), and $\underline{C}_\beta$ the second-order moment ("covariance matrix", reproducing kernel model) the best linear estimate of

$$\min(\|\underline{r} - \underline{A}\underline{\delta\beta}\|^2_{\underline{D}^{-1}} + \|\underline{\delta\beta}\|^2_{\underline{C}_\beta^{-1}})$$

becomes:

$$\underline{\hat{\delta\beta}} = \underline{C}_\beta \underline{A}^T(\underline{A}\underline{C}_\beta\underline{A}^T + \sigma_o^2\underline{I})^{-1}\underline{r}$$

or with $\underline{C}_\beta\underline{A}^T = \underline{C}_{\beta\ddot{\rho}}$ and $\underline{A}\underline{C}_\beta\underline{A}^T = \underline{C}_{\ddot{\rho}}$ in a more familiar form:

$$\underline{\hat{\delta\beta}} = \underline{C}_{\beta\ddot{\rho}}(\underline{C}_{\ddot{\rho}} + \sigma_o^2\underline{I})^{-1}\underline{r} \,. \tag{5}$$

Finally we denote

$$\underline{L} = \underline{C}_{\beta\ddot{\rho}}(\underline{C}_{\ddot{\rho}} + \sigma_o^2\underline{I})^{-1} \tag{6}$$

the linear estimator.

In our error analysis the a posteriori variance-covariance matrix $\underline{E}_\beta$ of the gravity parameters is computed from the a priori model for $\underline{D}$ and $\underline{C}_\beta$. The results represent the error situation to be expected from a real world experiment. $\underline{E}_\beta$ is computed for a variety of observation noise levels σ_o and arrangements of the sample points.

It is

$$\underline{E}_\beta = E\{[\hat{\underline{\delta\beta}} - \underline{\delta\beta}][\hat{\underline{\delta\beta}} - \underline{\delta\beta}]^T\} = \underline{C}_\beta - \underline{C}_{\beta\ddot{\rho}}(\underline{C}_{\ddot{\rho}} + \sigma_o^2\underline{I})^{-1}\underline{C}_{\beta\ddot{\rho}}^T \quad . \quad (7)$$

This form can be rewritten to

$$\underline{E}_\beta = \underline{B}\underline{C}_\beta\underline{B}^T + \underline{L}\underline{D}\underline{L}^T \quad (8)$$

where $\underline{B} = (\underline{L}\underline{A} - \underline{I})$.

In equation (8), the first term represents the configuration inadequacy, the second term more or less the pure error propagation. Thus, the two terms provide information on what could be gained from an improved configuration of the sampling points and, separately, from an improved instrumentation.

The error analysis was performed for surface $1^o \times 1^o$ *mean gravity anomalies, point geoid heights,* and *geoid height differences*. The covariance elements needed in equation (7) were supplied by the subroutine COVAX with degree variance model 2, *(Tscherning, 1976)*. The 74 sample points, covering an area of $[\lambda | 0^o \leq \lambda \leq 5^o]$ and $[\varphi | 1^o \leq \varphi \leq 9^o]$, were located along a circular orbit with inclination 68^o and period 5301 s at an altitude of 200 km (and 150 km, 250 km, 300 km) with a sample rate of 20 s for a mission period of 50 days. All computations refer to a reference field up to degree $\ell = 12$, assumed to be known perfectly. Analyzed was the variation of the a posteriori std.dev. as a function of the a priori range rate change (or range rate) precision for

- radial, along and cross track variation of the two satellites,
- changing intersatellite distance,
- different experiment altitudes, and

- a variation of the location of the gravity parameters with respect to the pattern of sample points.

Table 1 summarizes the results for the estimation of $1^{\circ} \times 1^{\circ}$ mean gravity anomalies. The assumed a priori range rate change or range rate precisions correspond to the envisaged instrumentation precisions for SLALOM ($\sigma(\dot{\rho}) = 10^{-5}\ m\,s^{-1}$) and GRAVSAT ($\sigma(\dot{\rho}) = 10^{-6}\ m\,s^{-1}$). From Table 1 one concludes, that

- a radial separation of the two satellites yields better results than a along or cross track separation,
- the intersatellite distance should be comparably large,
- the experiment altitude should be as low as possible (but: experiment life time; necessity of a drag free system).

$\sigma(\hat{\Delta g})$	$\sigma(\ddot{\rho}) = \pm$ 0.22 mgal ($\sigma(\dot{\rho}) = \pm 10^{-5}\ m\,s^{-1}$) mgal	$\sigma(\ddot{\rho}) = \pm$ 0.031 mgal ($\sigma(\dot{\rho}) = \pm 10^{-6}\ m\,s^{-1}$) mgal
spatial arrangement (altitude: 200 km; separation: 250 km)		
cross track	14.5	13.0
along track	11.7	9.9
radial	9.1	6.8
intersatellite distance (altitude: 200 km; radial separation)		
10 km	13.7	8.3
50 km	9.7	7.0
250 km	9.1	6.8
experiment altitude (radial separation: 50 km)		
300 km	14.0	10.5
250 km	12.2	8.8
150 km	7.4	5.4
location of the anomaly (altitude: 200 km; radial separation: 250 km)		
arbitrary	10.2	8.6
optimal	9.1	6.8

Table 1: Estimated $1^{\circ} \times 1^{\circ}$ mean gravity anomaly standard deviation

In an optimal case it seems to be possible to derive $1^{\circ} \times 1^{\circ}$ mean gravity anomalies with a std.dev. of $\pm$ 6 to 7 mgal from a SST low-low experiment at 200 km altitude. The better result obtained for a radial separation, as compared to a along or cross track separation is only due to the shorter correlation length for radial separation. The difference would disappear when using sample points for the along and cross track study covering a sufficiently large area. In all cases the correlation between the estimates of different blocks was almost negligible.

The a posteriori variance for a geoid height difference δN between two points P_1 and P_2 is derived from the variances and covariances of the point estimates by:

$$\sigma^2\{\delta\hat{N}(P_2 - P_1)\} = \sigma^2\{\hat{N}(P_2)\} - 2\,\mathrm{cov}\{N(P_2)\hat{;}N(P_1)\} + \sigma^2\{\hat{N}(P_1)\} \quad . \quad (9)$$

Equation (9) shows that only for high correlations between the point estimates low variances for the geoid height differences are to be expected. This is the reason that for points located along the direction of the separation of the two satellites, either along or cross track, especially good geoid height difference estimates are obtained. Otherwise the results for geoid heights but also for geoid height differences follow the same pattern as those for mean gravity anomalies. An exception is the variation with experiment altitude, where the picture looks rather heterogeneous. Again the comparably small area ($5^{\circ} \times 8^{\circ}$) covered with sample points is responsible. The coverage with data has to be considerably larger for the estimation of geoid heights than for gravity anomalies.

Some results for the a posteriori std.dev. of a point geoid height (point no. 1) and for geoid height differences between points no. 1 and 2 (distance: 151 km) and points no. 1 and 3 (distance: 302 km) for two different intersatellite distances are given in Table 2. The a priori measurement std.dev. are identical to those in Table 1.

altitude 200 km radial separation	$\sigma(\ddot{\rho}) = \pm 0.22$ mgal ($\sigma(\dot{\rho}) = \pm 10^{-5}$ m s^{-1}) m	$\sigma(\ddot{\rho}) = \pm 0.031$ mgal ($\sigma(\dot{\rho}) = \pm 10^{-6}$ m s^{-1}) m
	$\sigma\{N(P_1)\}$	
10 km	1.73	1.33
250 km	0.97	0.87
	$\sigma\{\delta N(P_2 - P_1)\}$	
10 km	1.44	0.93
250 km	0.89	0.72
	$\sigma\{\delta N(P_3 - P_1)\}$	
10 km	1.77	1.28
250 km	1.08	0.93

Table 2: Estimated geoid height and geoid height difference standard deviations

From the derived numbers we conclude that for point geoid heights a std.dev. of $\pm$ 0.9 m, for geoid height differences over 150 km $\pm$ 0.7 m are attainable. Thus, SST low-low with a range rate precision of about 10^{-6} m s^{-1} at 200 km altitude and with the above described configuration should be capable of providing results for geoid heights and mean gravity anomalies comparable in accuracy and resolution with those obtained for the sea-surface topography from the GEOS-3 satellite.

Alternative Estimation Procedure

Figure 1 shows the variation of the estimated a posteriori std.dev. of a $1^{\circ} \times 1^{\circ}$ mean gravity anomaly with changing experiment altitude as a function of the a priori measurement std.dev.. Also contained is the contribution of $\underline{L}\underline{D}\underline{L}^{T}$, equation (8), and the optimum lower bound, which is derived analytically for an assumed global and continuous coverage

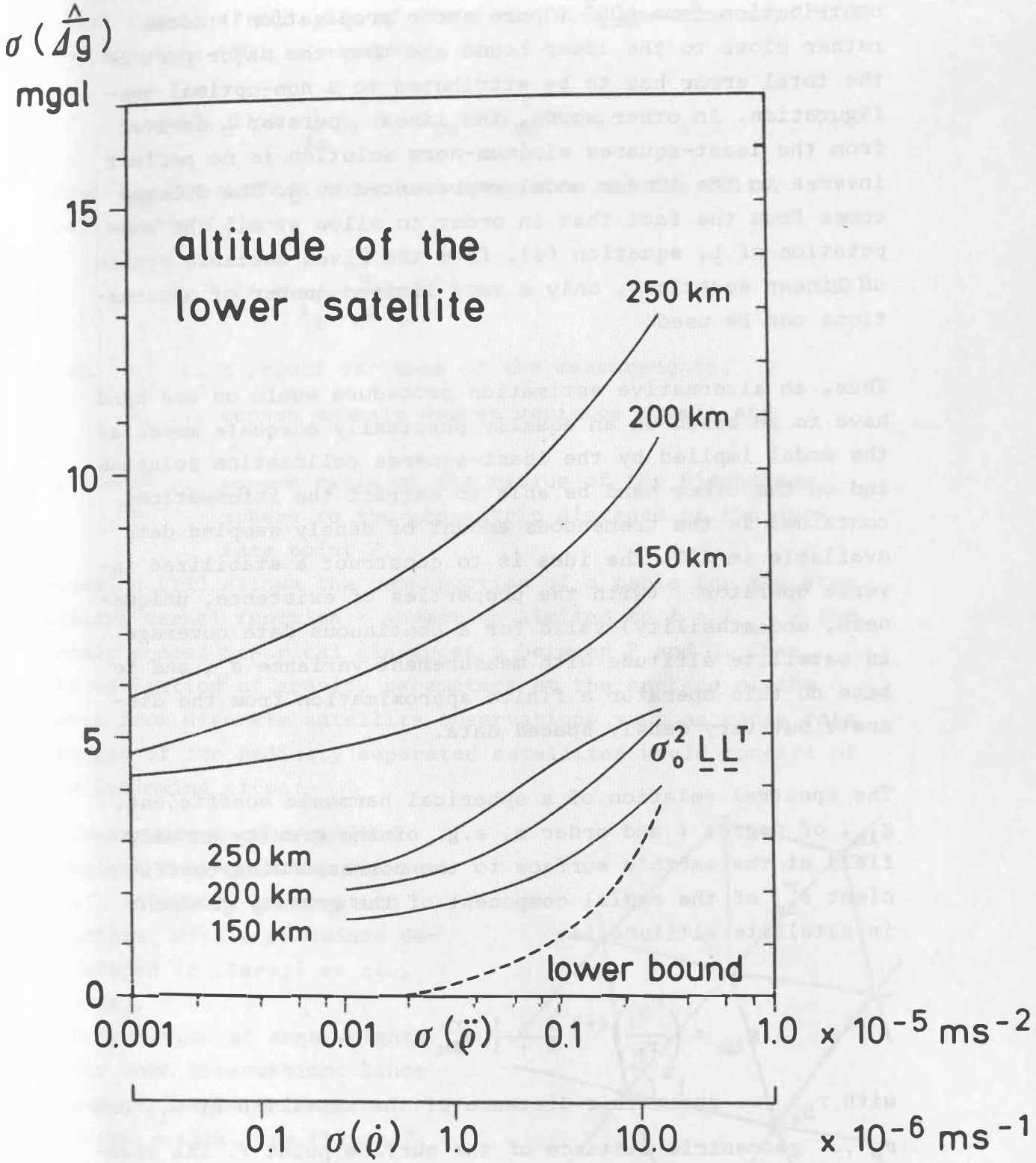

Figure 1: Variation of the estimated a posteriori std.dev. of a 1° × 1° mean gravity anomaly with changing experiment altitude (radial separation 50 km), contribution of $\sigma_0^2 \underline{L}\underline{L}^T$ and theoretical lower bound (for 200 km).

with measurements at an altitude of 200 km. We see that the contribution from $\underline{L}\underline{D}\underline{L}^T$ ("pure error propagation") comes rather close to the lower bound and that the major part of the total error has to be attributed to a non-optimal configuration. In other words, the linear operator $\underline{L}$ derived from the least-squares minimum-norm solution is no perfect inverse to the linear model represented by $\underline{A}$. The dilemma comes from the fact that in order to allow at all the computation of $\underline{L}$, equation (6), from the given unstable system of linear equations, only a very limited number of observations can be used.

Thus, an alternative estimation procedure would on one hand have to be based on an equally physically adequate model as the model implied by the least-squares collocation solution and on the other hand be able to extract the information contained in the tremendous amount of densly sampled data available in SST. The idea is to construct a stabilized inverse operator (with the properties of existence, uniqueness, and stability) valid for a continuous data coverage in satellite altitude with measurement variance σ_o^2, and to base on this operator a finite approximation from the discrete but very densly spaced data.

The spectral relation of a spherical harmonic coefficient, $g_{\ell m}$, of degree ℓ and order m, e.g. of the gravity anomaly field at the earth's surface to the corresponding coefficient $\delta^r_{\ell m}$ of the radial component of the gravity gradient in satellite altitude is:

$$g_{\ell m} = \left(\frac{r_{S_1}}{r_P}\right)^{\ell+2} \frac{\ell - 1}{\ell + 1}\, \delta^r_{\ell m} ,$$

with r_{S_1} ... geocentric distance of the satellite at S_1, and r_P ... geocentric distance of the surface point P. The spectral relation to an acceleration difference coefficient, $\Delta\delta^r_{\ell m}$, of two radially separated satellites is then:

$$g_{\ell m} = \left(1 - \left(\frac{r_{S_2}}{r_{S_1}}\right)^{\ell+2}\right)^{-1}\left(\frac{r_{S_1}}{r_P}\right)^{\ell+2} \frac{\ell - 1}{\ell + 1}\, \Delta\delta^r_{\ell m}$$

$$= \lambda_\ell \Delta\delta^r_{\ell m} . \qquad (10)$$

According to the derivations in *(Gerstl & Rummel, 1979)* the kernel function, K(P, S), of the stabilized operator may with equation (10) be expressed as:

$$K(P, S) = \sum_{\ell m} f_\ell \lambda_\ell Y_{\ell m}(P) Y^*_{\ell m}(S) , \qquad (11)$$

where $Y_{\ell m}$ are surface spherical harmonics and the filter coefficients f_ℓ are

$$f_\ell = (1 + \frac{\sigma_o^2}{\lambda_\ell^{-2} c_\ell s^{\ell+2}})^{-1} \qquad (12)$$

with σ_o^2 ... a priori variance of the measurements,

c_ℓ ... chosen anomaly degree variance model, and

$s = \frac{r_{Bje}^2}{r_P^2}$ ... square ratio of the radius of the Bjerhammar sphere to the geocentric distance of the surface point P.

Equation (11) allows the construction of a table for the stabilized kernel function - summation limited to $\ell = \ell_{max}$ - for densly spaced spherical distances ψ between P and Q. Thus, the estimation of gravity parameters at the surface of the earth from discrete satellite observations such as range rate changes of two radially separated satellites would consist of the following steps:

- Construction of a minimum weight triangulation between all satellite observation points, with a procedure developed in *(Gerstl et al., 1979)*.
- Computation of area weights for each observation: Since each triangle belongs to three points, see Figure 2, the area, f_i, for an arbitrary point S_i is derived from

$$f_i = \frac{1}{3} r_{S_i}^2 \text{ arc tan } \sum_j \kappa_j$$

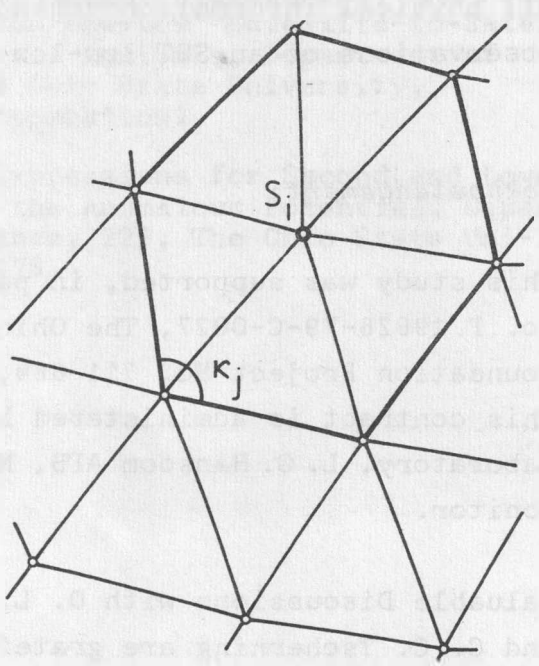

Figure 2

where κ_j are the angles of the polygon around S_i.

- Evaluation of the kernel function K(P, S) for the estimation point P_k and observation point S_i, multiplication with f_i and, finally, summation over all observation points:

$$\hat{\delta\beta}_k = \sum_i f_i \, K(P_k, S_i) r_i \qquad (13)$$
$$= \tilde{\mathcal{L}} \, \underline{r}$$

The a posteriori variance-covariance matrix, equations (7) and (8), is modified to

$$\underline{E}_\beta = \underline{C}_\beta - \tilde{\mathcal{L}} \, (\underline{C}_{\ell\ell} + \sigma_o^2 \underline{I}) \, \tilde{\mathcal{L}}^T, \text{ or} \qquad (14)$$

$$\underline{E}_\beta = \underline{B}\underline{C}_\beta\underline{B}^T + \sigma_o^2 \, \tilde{\mathcal{L}} \, \tilde{\mathcal{L}}^T, \qquad (15)$$

with $\underline{B} = (\tilde{\mathcal{L}} \, \underline{A} - I)$. Now, the first term on the right hand side of equation (15) gives the contribution of the finite approximation of $\mathcal{L}$ by $\tilde{\mathcal{L}}$. Equation (14) shows that no problematic solution of a large system of linear equations is required anymore for the evaluation of $\underline{E}_\beta$. Of course, one has to pay a price: The possibility of combining different types of observed quantities is not easily possible anymore. Nevertheless, the alternative procedure should be capable to circumvent the major numerical obstacles which prevent to extract all physical information contained in the large amount of observations of an SST low-low experiment.

Acknowledgement:

This study was supported, in part, through Air Force Contract No. F 19626-79-C-0027, The Ohio State University Research Foundation Project No. 711 664, Project Supervisor R. H. Rapp. This contract is administered by the Air Force Geophysics Laboratory, L. G. Hanscom AFB, Mass., Mr. Bela Szabo, Contract Monitor.

Valuable Discussions with O. L. Colombo, R. H. Rapp, H. Sünkel, and C. C. Tscherning are gratefully acknowledged.

References

Applications of a Dedicated Gravitational Satellite Mission, prepared by Panel on Gravity Field & Sea Level Requirements, National Academy of Sciences, Washington, D.C., 1979.

Drożyner, A.: Construction of Orbital System for DIDEX Experiment, Artificial Satellites, 13, 2, 21-35, 1978.

European Space Agency: SLALOM Mission/System Definition Study Contract No. 3483/78/F/DK(SC), Final Report, prepared by Messerschmitt-Bölkow-Blohm, München, 1978.

Geodesy: Trends & Prospects, prepared by Committee on Geodesy, National Research Council, National Academy of Sciences, Washington, D.C., 1978.

Gerstl, M., G. Heindl, E. Reinhart: Interpolation and Approximation by Piecewise Quadratic Smooth Functions of Two Variables, paper pres. at the 17th IUGG General Assembly, Canberra, 1979.

Gerstl, M., R. Rummel: Stability Investigations of Various Representations of the Gravity Field, paper pres. at the 17th IUGG General Assembly, Canberra, 1979.

Hieber, S. & T. D. Guyenne (eds.): Space Oceanography, Navigation, and Geodynamics, ESA SP-137, Schloß Elmau, 1978.

Kryński, J.: Possibilities of Low-Low Satellite Tracking for Local Geoid Improvement, Mitteilungen der geodätischen Institute der Technischen Universität Graz, 31, Graz, 1978.

Rummel, R.: Geoid Heights, Geoid Height Differences, and Mean Gravity Anomalies from "Low-Low" Satellite-to-Satellite Tracking - An Error Analysis, Department of Geodetic Science, The Ohio State University, Columbus, 1980 (in preparation).

Tscherning, C. C.: Covariance Expressions for Second and Lower Order Derivatives of the Anomalous Potential, Department of Geodetic Science, 225, The Ohio State University, Columbus, 1976.

THE INVERSE GRAVIMETRIC PROBLEM FOR THE EARTH

Matej Škorvanek

Introduction

In the work [1] we were interested in inverse gravimetric problem for the density distribution in the Earth by the help of some functional of the density. We demanded, that the density $\rho(\bar{r})$ in sphere V, which is bounded by surface S_0, minimized the functional

$$K = \frac{1}{2}\iiint_V [\nabla\rho(\bar{r})]^2 d^3r \qquad /1/$$

at determined value of potential on the surface

$$U(\bar{s}) = \varkappa \iiint_V \frac{\rho(\bar{r})}{|\bar{r}-\bar{s}|} d^3r \ , \quad \bar{s} \in S_0 \qquad /2/$$

and boundary conditions

$$U(\bar{r}) = U_0(\bar{r}) \ , \quad \bar{r} \in S_0 \ , \qquad /3/$$

$$\rho(\bar{r}) = \rho_0(\bar{r}) \ , \quad \bar{r} \in S_0 \ . \qquad /4/$$

Then for the variation of functional /1/ must be

$$\delta K = 0 \ , \qquad /5/$$

for potential

$$\delta U(\bar{r}) = 0 \ , \quad \bar{r} \in S_0 \qquad /6/$$

and for density

$$\delta\rho(\bar{r}) = 0 \ , \quad \bar{r} \in S_0 \ . \qquad /7/$$

The equation for the density $\rho(\bar{r})$ is

Geophysical Institute of Slovak Academy of Sciences, Dúbravská cesta, 899 30 Bratislava

$$\iiint_V \left[\frac{\delta K}{\delta \rho(\bar{r})} + \varkappa \iint_{S_0} \frac{\lambda(\bar{s})}{|\bar{r}-\bar{s}|} d^2 s \right] \delta\rho(\bar{r})\, d^3 r = 0, \qquad /8/$$

where $\lambda(\bar{s})$ is Lagrange's multiplicator.

The solution of equation /8/ is

$$\Delta\Delta\rho(\bar{r}) = 0, \quad \bar{r} \in V, \qquad /9/$$

i. e. biharmonical equation. When we define operator G in form

$$Gf(\bar{r}) = -\frac{1}{4\pi} \iiint_V \frac{f(\bar{r}')}{|\bar{r}-\bar{r}'|} d^3 r' \qquad /10/$$

where $f(\bar{r})$ is arbitrary function which is sufficiently differentiable in sphere V, we can the solution of equation /9/ writte in form

$$\rho(\bar{r}) = -\frac{1}{4\pi} \left[H_1(\bar{r}) + G H_2(\bar{r}) \right], \quad \bar{r} \in V, \qquad /11/$$

where $H_1(\bar{r}), H_2(\bar{r})$ are arbitrary harmonical functions in V, which we determine from boundary conditions /3/ and /4/.

The solution of inverse gravimetric problem for spherical body

In this case we used the equation /11/. The harmonical functions $H_1(\bar{r})$ and $H_2(\bar{r})$ are given in the form

$$H_i(\bar{r}) = \sum_{\ell=0}^{\infty} \sum_{m=-\ell}^{\ell} A_i^{\ell,m} \left(\frac{r}{R}\right)^{\ell} P_{\ell}^{|m|}(\cos\vartheta)\, e^{im\varphi}, \qquad /12/$$

where $A_i^{\ell,m}$, $i = 1,2$ are unknown coefficients, which will be determined from boundary conditions /3/, /4/. After calculations, tne solution of inverse gravimetric problem for spherical body with radius R in case that we know its density on the surface and its gravitational field has the form

$$\rho(\bar{r}) = -\frac{1}{2}\sum_{l=0}^{\infty}\sum_{m=0}^{l} x^{l}(l_3 - l_5 x^2)(\sigma_{l,m}\cos m\varphi + \tau_{l,m}\sin m\varphi) P_l^m(\cos\vartheta) -$$

$$+ \frac{1}{6}\rho_s \sum_{l=0}^{\infty}\sum_{m=0}^{l} l_1 l_3 l_5 x^{l}(1-x^2)(C_{l,m}\cos m\varphi + S_{l,m}\sin m\varphi) N_{l,m} P_l^m(\cos\vartheta), \qquad /13/$$

where $x = \frac{r}{R}$, $l_i = 2l + i$, $N_{l,m} = \left[\varepsilon_m l_1 \frac{(l-m)!}{(l+m)!}\right]^{1/2}$, $\varepsilon_m = 2 - \delta_{m,0}$,

ρ_s is the mean density of spherical body,

$\sigma_{l,m}$, $\tau_{l,m}$ - coefficients in expansion of the density on the surface,

$C_{l,m}$, $S_{l,m}$ - coefficients in expansion of the gravitational field.

The solution /13/ was applied for the calculation of the density distribution in the Earth. The values of the density on the Earth's surface were for the continental crust ρ = 2700 kgm^{-3} and for the oceanical crust ρ = 3000 kgm^{-3}. The data of Earth gravitational field were taken from [3] . The results for selected distances from centre of the Earth are in table 1. /where λ - geographical longitude, φ - geographical latitude and ρ is given in kgm^{-3}/.

When we assume, that we do not know the density of spherical body on the surface, we cannot apply the boundary condition /4/. Therefore in this case we applied the condition for the minimum of functional [1,2]

$$J = \frac{1}{2}\iiint_V [r\rho(\bar{r})]^2 d^3r . \qquad /14/$$

The variation refers to the coefficients $A_1^{l,m}$, $A_2^{l,m}$ in harmonical functions /12/ in equation /11/. The solution in the case, that

Table 1.

r [km]	φ \ λ	-150°	-120°	-90°	-60°	-30°	0°	30°	60°	90°	120°	150°	180°
300	90°	9407	9407	9407	9407	9407	9407	9407	9407	9407	9407	9407	9407
	60°	9401	9401	9403	9405	9408	9410	9410	9410	9408	9406	9403	9401
	30°	9394	9395	9398	9402	9406	9409	9410	9409	9407	9403	9398	9395
	0°	9388	9390	9393	9398	9402	9405	9406	9405	9402	9398	9393	9389
	-30°	9385	9386	9389	9393	9396	9399	9400	9399	9396	9393	9389	9386
	-60°	9384	9385	9386	9388	9391	9392	9392	9392	9390	9388	9386	9385
	-90°	9387	9387	9387	9387	9387	9387	9387	9387	9387	9387	9387	9387
3300	90°	7665	7665	7665	7665	7665	7665	7665	7665	7665	7665	7665	7665
	60°	7640	7680	7705	7686	7669	7700	7738	7754	7752	7726	7676	7637
	30°	7601	7664	7728	7690	7671	7761	7808	7791	7780	7744	7648	7597
	0°	7596	7618	7686	7738	7688	7735	7784	7705	7697	7742	7671	7605
	-30°	7575	7581	7626	7688	7639	7637	7670	7617	7611	7664	7650	7592
	-60°	7562	7566	7583	7594	7584	7579	7580	7575	7575	7581	7580	7569
	-90°	7603	7603	7603	7603	7603	7603	7603	7603	7603	7603	7603	7603
6300	90°	3104	3104	3104	3104	3104	3104	3104	3104	3104	3104	3104	3104
	60°	3017	2855	2878	2895	3109	2950	2881	2876	2872	2877	2900	3018
	30°	3142	3079	2893	3116	3138	2886	2880	2888	2887	2951	3134	3142
	0°	3143	3164	3137	2887	3095	3012	2892	3142	3131	2904	3079	3134
	-30°	3144	3156	3148	2901	3145	3139	2965	3143	3142	3019	3025	3138
	-60°	3139	3136	3129	3079	3136	3133	3134	3132	3134	3136	3134	3133
	-90°	2897	2897	2897	2897	2897	2897	2897	2897	2897	2897	2897	2897

we know only the gravitational field of spherical body, has the form

$$\rho(\bar{r}) = \frac{1}{3}\rho_s \sum_{l=0}^{\infty}\sum_{m=0}^{l} \frac{l_1 l_3 l_5}{l_3 l_5 + 8} x^l (2l_5 - l_3 x^2)(C_{l,m}\cos m\varphi + S_{l,m}\sin m\varphi) N_{l,m} P_l^m(\cos\vartheta), \qquad /15/$$

where $x = \frac{r}{R}$.

The results for selected distances from centre of the Earth are in table 2.

The solution of inverse gravimetric problem for rotation ellipsoid

By analogical method which we applied in the case of spherical body, we proceeded for rotation ellipsoid. Because the value of the Earth's flattening ε = 1/298.256 [3] is very small, we took only the first approximation with respect to ε . But in this case instead of operator G in /10/ we must take operator G_1 , which has the form

$$G_1 = G - G_0, \qquad /16/$$

where

$$Gf(\bar{r}) = -\frac{1}{4\pi}\iiint_V \frac{f(\bar{r}')}{|\bar{r} - \bar{r}'|} d^3r',$$

$$G_0 f(\bar{r}) = -\frac{1}{4\pi}\iiint_{V_0} \frac{f(\bar{r}')}{|\bar{r} - \bar{r}'|} d^3r',$$

V - sphere which is bounded by spherical surface with radius R ,

V_0 - sphere which is bounded by spherical surface with radius R and by the surface of rotation ellipsoid with equator ra-

Table 2.

r [km]	φ \ λ	-150°	-120°	-90°	-60°	-30°	0°	30°	60°	90°	120°	150°	180°
300	90°	11923	11923	11923	11923	11923	11923	11923	11923	11923	11923	11923	11923
	60°	11923	11923	11923	11923	11923	11923	11923	11923	11923	11923	11923	11923
	30°	11924	11924	11924	11924	11924	11924	11924	11924	11924	11924	11924	11924
	0°	11924	11924	11924	11924	11924	11924	11924	11924	11924	11924	11924	11924
	-30°	11924	11924	11924	11924	11924	11924	11924	11924	11924	11924	11924	11924
	-60°	11923	11923	11923	11923	11923	11923	11923	11923	11923	11923	11923	11923
	-90°	11923	11923	11923	11923	11923	11923	11923	11923	11923	11923	11923	11923
3300	90°	9035	9035	9035	9035	9035	9035	9035	9035	9035	9035	9035	9035
	60°	9048	9048	9048	9048	9048	9048	9048	9048	9048	9048	9048	9048
	30°	9073	9073	9073	9073	9073	9073	9073	9073	9073	9073	9073	9073
	0°	9086	9086	9086	9086	9086	9086	9086	9086	9086	9086	9086	9086
	-30°	9073	9073	9073	9073	9073	9073	9073	9073	9073	9073	9073	9073
	-60°	9048	9048	9048	9048	9048	9048	9048	9048	9048	9048	9048	9048
	-90°	9035	9035	9035	9035	9035	9035	9035	9035	9035	9035	9035	9035
6300	90°	1412	1412	1412	1412	1412	1412	1412	1412	1412	1412	1412	1412
	60°	1429	1429	1426	1427	1430	1427	1429	1428	1426	1427	1429	1429
	30°	1452	1472	1466	1445	1468	1461	1465	1470	1464	1469	1456	1453
	0°	1457	1508	1499	1457	1503	1480	1482	1496	1476	1487	1472	1446
	-30°	1450	1477	1475	1453	1477	1465	1461	1463	1456	1462	1468	1451
	-60°	1429	1429	1427	1428	1431	1427	1430	1423	1428	1431	1427	1426
	-90°	1411	1411	1411	1411	1411	1411	1411	1411	1411	1411	1411	1411

dius R and polar radius $(1-\varepsilon)R$. The function $f(\bar{r})$ is defined as in /10/.

We assumed in this case, that we did not know the density on the surface of rotation ellipsoid. Therefore we used the condition /14/ and by analogical way we obtained the solution of inverse gravimetric problem for the rotation ellipsoid in the case, that we know only its gravitational field

$$\rho(\bar{r}) = \frac{1}{3}\rho_s \sum_{l=0}^{\infty}\sum_{m=0}^{l} x^l \left(\alpha_{l,m}(r)\cos m\varphi + \beta_{l,m}(r)\sin m\varphi\right) P_l^m(\cos\vartheta), \quad /17/$$

where

$$\begin{vmatrix}\alpha_{l,m}(r)\\ \beta_{l,m}(r)\end{vmatrix} = \frac{l_1 l_3 l_5}{M_l}(2l_5 - l_9 x^2) N_{l,m} \begin{vmatrix} C_{l,m}\\ S_{l,m}\end{vmatrix} +$$

$$+ \frac{\varepsilon l_5}{M_l}\left\{\frac{l_7 l_9}{l_3 l_{11} M_{l+2}}(2l_3 A_l - l_5 B_l x^2)(l+m+2)(l+m+1) N_{l+2,m} \begin{vmatrix} C_{l+2,m}\\ S_{l+2,m}\end{vmatrix} +\right.$$

$$+ \frac{l_1}{l_3 M_{l-2}}(2l_3 D_l - l_9 E_l x^2)(l-m)(l-m-1) N_{l-2,m} \begin{vmatrix} C_{l-2,m}\\ S_{l-2,m}\end{vmatrix} +$$

$$\left. + \frac{l_1 l_5}{l_{-1}}(2l_3 - l_9 x^2)[2l(l+1) - 2m^2 - 1] N_{l,m} \begin{vmatrix} C_{l,m}\\ S_{l,m}\end{vmatrix}\right\},$$

$A_l = l_1^3 - 19l_1^2 + 106l_1 + 152$, $\quad B_l = l_1^3 + 22l_1^2 + 136l_1 + 144$,

$D_l = l_1^3 + 5l_1^2 + 22l_1 + 80$, $\quad E_l = l_1^3 + 6l_1^2 + 40l_1 + 96$,

$M_l = l_3 l_5 + 8$, $\quad x = \frac{r}{R}$.

Table 3.

r [km]	φ \ λ	-150°	-120°	-90°	-60°	-30°	0°	30°	60°	90°	120°	150°	180°
300	90°	11963	11963	11963	11963	11963	11963	11963	11963	11963	11963	11963	11963
	60°	11963	11963	11963	11963	11963	11963	11963	11963	11963	11963	11963	11963
	30°	11964	11964	11964	11964	11964	11964	11964	11964	11964	11964	11964	11964
	0°	11964	11964	11964	11964	11964	11964	11964	11964	11964	11964	11964	11964
	-30°	11964	11964	11964	11964	11964	11964	11964	11964	11964	11964	11964	11964
	-60°	11963	11963	11963	11963	11963	11963	11963	11963	11963	11963	11963	11963
	-90°	11963	11963	11963	11963	11963	11963	11963	11963	11963	11963	11963	11963
3300	90°	9069	9069	9069	9069	9069	9069	9069	9069	9069	9069	9069	9069
	60°	9079	9079	9079	9079	9079	9079	9079	9079	9079	9079	9079	9079
	30°	9100	9100	9100	9100	9100	9100	9100	9100	9100	9100	9100	9100
	0°	9110	9110	9110	9110	9110	9110	9110	9110	9110	9110	9110	9110
	-30°	9100	9100	9100	9100	9100	9100	9100	9100	9100	9100	9100	9100
	-60°	9079	9079	9079	9079	9079	9079	9079	9079	9079	9079	9079	9079
	-90°	9068	9068	9068	9068	9068	9068	9068	9068	9068	9068	9068	9068
6300	90°	1465	1465	1465	1465	1465	1465	1465	1465	1465	1465	1465	1465
	60°	1462	1462	1459	1461	1463	1460	1462	1462	1459	1460	1462	1463
	30°	1450	1472	1465	1443	1467	1460	1464	1469	1463	1468	1454	1452
	0°	1436	1492	1482	1436	1486	1462	1463	1478	1458	1469	1453	1425
	-30°	1448	1476	1475	1451	1477	1464	1460	1462	1455	1461	1468	1469
	-60°	1463	1463	1460	1462	1465	1461	1464	1457	1462	1464	1460	1459
	-90°	1459	1459	1459	1459	1459	1459	1459	1459	1459	1459	1459	1459

The results in this case for selected distances from centre of the Earth are in table 3.

Conclusion

The results of the density distribution in the Earth in our three cases we can consider as satisfactory, especially when we compare the mean values of the density with the Bullen-Haddon's model /HBl [4] / of the Earth /table 4., figure 1./. From this follows, that the differences between our models and model HBl are due to abov all, that we did not consider the discontinuities of the density in the Earth. The discontinuities we did not take into consideration, as we did not know sufficiently exactly their space distribution and their values. But if we realize the fact, that we did not use at the calculation any equations for the description of the structure of the Earth, the results are very interesting from point of view of used method.

References

[1] Škorvanek,M.: Obrátená úloha gravimetrie pre zemské teleso a guľovú vrstvu. Kandidátska dizertačná práca, Geofyzikálny ústav SAV, Bratislava,1978. /Theses for the degree of CSc./

[2] Pohánka,V.,Škorvanek,M.: Určenie rozloženia hustoty v zemskom telese z údajov o vonkajšom gravitačnom poli Zeme. Geologické práce - Správy 68, Bratislava, 1977.

[3] Gaposchkin,E.M.: 1973 Smithsonian standard Earth /III/. SAO Special report N°353, Cambridge, Massachusetts, 1973.

[4] Stacey,F.D.: Fizika Zemli,.Izd. Mir, Moskva, 1972.

Table 4.

r [km]	ρ_1 [kgm^{-3}]	ρ_2 [kgm^{-3}]	ρ_3 [kgm^{-3}]	ρ_{PREM} [kgm^{-3}]
0	9412	11947	11987	12460
171	9407	11940	11980	12455
371	9390	11911	11951	12437
571	9359	11861	11901	12405
771	9316	11790	11829	12360
971	9260	11698	11737	12301
1171	9192	11585	11623	12229
1250	9161	11534	11572	12197
1371	9110	11451	11488	12130
1389	9102	11438	11475	12121
1571	9016	11295	11332	12017
1771	8909	11118	11154	11887
1971	8788	10921	10956	11737
2171	8656	10702	10736	11570
2371	8510	10462	10494	11383
2571	8351	10200	10232	11176
2771	8180	9918	9948	10948
2971	7996	9614	9644	10697
3171	7799	9290	9318	10421
3371	7589	8944	8971	10121
3493	7454	8722	8748	9927
3493	7454	8722	8748	5527
3571	7366	8577	8602	5487
3771	7130	8189	8213	5387
3971	6882	7779	7802	5288
4171	6621	7349	7370	5188
4371	6347	6897	6917	5087
4571	6060	6425	6443	4983
4771	5760	5931	5947	4877
4971	5447	5416	5431	4768
5171	5122	4880	4893	4655

Table 4. /continued/

r [km]	ρ_1 [kgm^{-3}]	ρ_2 [kgm^{-3}]	ρ_3 [kgm^{-3}]	ρ_{HB1} [kgm^{-3}]
5371	4784	4322	4334	4538
5387	4756	4277	4289	4529
5571	4433	3744	3754	4380
5721	4161	3296	3305	4200
5721	4161	3296	3305	4150
5771	4069	3144	3153	4075
5871	3882	2837	2845	3925
5958	3717	2565	2572	3795
5971	3692	2524	2531	3775
6021	3596	2365	2372	3700
6021	3596	2365	2372	3441
6071	3499	2205	2212	3424
6171	3302	1882	1887	3387
6271	3103	1553	1558	3348
6311	3022	1420	1424	3332
6356	2931	1269	1273	3313
6356	2931	1269	1273	2840
6371	2900	1219	1223	2840

ρ_1 - the mean density in the Earth, which is approximated by spherical body, when we know the density on the surface and gravitational field,

ρ_2 - the mean density in the Earth, which is approximated by spherical body, when we know only the gravitational field,

ρ_3 - the mean density in the Earth, which is approximated by rotation ellipsoid, when we know only the gravitational field,

ρ_{HB1} - the density in the Earth from model HB1.

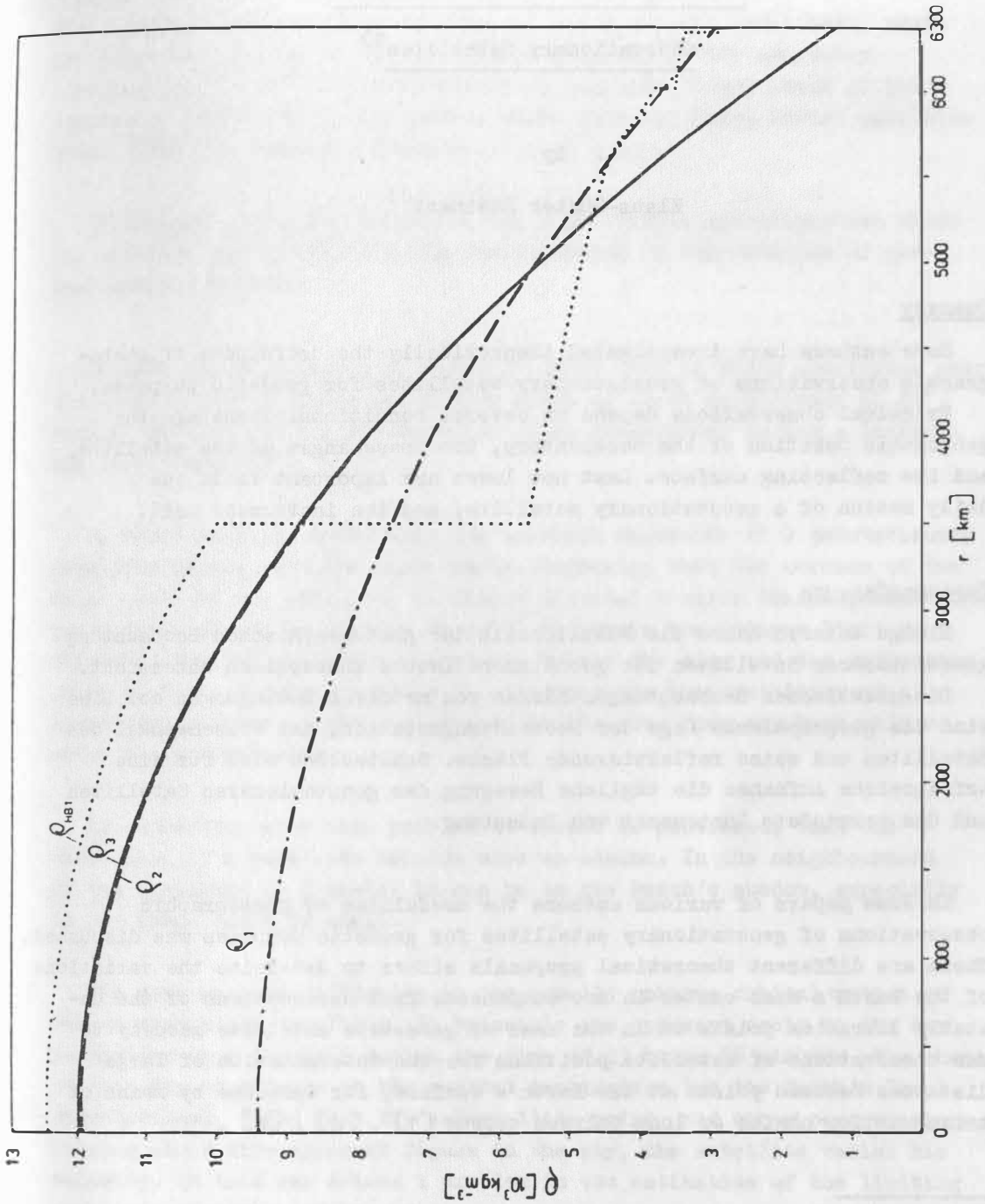
ρ [10³ kg m⁻³]
r [km]
ρ_HB1
ρ_3
ρ_2
ρ_1
0
1000
2000
3000
4000
5000
6000
6300
1
2
3
4
5
6
7
8
9
10
11
12
13

Fig. 1

Requirements for Observations of Geostationary Satellites[1)]

by

Klaus-Günter Steinert[2)]

Summary

Some authors have investigated theoretically the usefulness of photographic observations of geostationary satellites for geodetic purposes.

Practical observations depend on several conditions. These are the geographic position of the observatory, the phase angle of the satellite, and its reflecting surface. Last not least are important facts the daily motion of a geostationary satellite, and the instrument used.

Zusammenfassung

Einige Autoren haben die Nützlichkeit der photographischen Beobachtung geostationärer Satelliten für geodätische Zwecke theoretisch untersucht.

Die praktischen Beobachtungen hängen von mehreren Bedingungen ab. Dies sind die geographische Lage der Beobachtungsstation, der Phasenwinkel des Satelliten und seine reflektierende Fläche. Schließlich sind für eine erfolgreiche Aufnahme die tägliche Bewegung des geostationären Satelliten und das verwendete Instrument von Bedeutung.

In some papers of various authors the usefulness of photographic observations of geostationary satellites for geodetic purposes was discussed. There are different theoretical proposals either to determine the variations of the Earth's mass center in two components from observations of the unstable libration points or in the case of geometric satellite geodesy to use observations of satellite positions for the determination of large distances between points at the Earth's surface, for instance by means of triangulation chains or long polygon chords [1] , [2] , [6] .

---

1) Mitteilung des Lohrmann-Observatoriums der Technischen Universität Dresden Nr. 44

2) Technische Universität Dresden, Sektion Geodäsie und Kartographie DDR-8027 Dresden, Mommsenstr. 13

However there is not in all cases agreement in the theoretical results obtained.
What concerns practical observations of geostationary satellites, there are manyfold experiences and successful results in USSR and other countries [3], [4]. For instance it is possible to get about 20 geostationary satellites at one photo, taken with the large Soviet satellite camera VAU [7], having a field of 5° x 30° [5].

Besides this it seems useful to add some further investigations about the practical conditions for the possibilities of observations of geostationary satellites.

Because of the parallax of about 7° under good darkness conditions near the horizon geostationary satellites reach at least an altitude of 28° during passing through the meridian of an observatory having a latitude not larger than 55°.

An other problem, concerning the apparent magnitude of a geostationary satellite arises from its phase angle. Supposing that the surface of the solar cells of the satellite is always directed towards the sun, the phase angle should be smaller than 30° to obtain the optimum light reflection from the satellite. Of course mainly the size and the reflecting power of the reflecting surface is important for the visibility of a satellite. However in the most cases the observer does not know values about these quantities.

In connection with this problem it should be mentioned, that the visibility of a satellite depends also on season. In the neighbourhood of the equinoxes ($\pm$ 3 weeks) it can be in the Earth's shadow, especially if the phase angle is small.

The most serious difficulty is the usually unknown orbital motion of the geostationary satellite. In principle its apparent orbit in the sky is similar to a figure 8 during the time of 23 hours 56 minutes. The shape of this figure depends on the orbital inclination, on the Earth's local gravitational field near the subsatellite point, and other perturbations. Running along this apparent figure in the sky, the satellite varies his velocity. In this way arises a problem in the estimation of the limiting magnitude of the telescope used.

There are very different dates in the literature about the expected magnitude of geostationary satellites. From theoretical calculations MAREK [6] found a mean value of 15 magnitudes. DIXIT and others [3] get from observations $10,5^m$ to $12,5^m$. In the second case the results are theoretically better about $0,5^m$ because of the smaller extinction (the latitude of the observatory is $12,5^o$).

In the following table there are estimated some dates for an orbital inclination $i = 0,1^o$ under the approximative assumption of a constant velocity of the periodic daily motion of a geostationary satellite. The given time of exposition depends on the focal distance of each instrument mentioned. This time is limited in such a way, that the star's trail is not larger than 35 μm. Under these conditions the limiting magnitude for the given exposure time was calculated. The quotient D^2/F is a characteristic value for the qualification of a telescope for observations of geostationary satellites. The weight p of the position of a geostationary satellite is proportional to the focal length of the telescope.

Telescope	Time of exposition	Limiting magnitude	D^2/F (cm^2/cm)	p
2-m-Schmidt Tautenburg (GDR)	2 min	$16,0^m$	45	5,7
Baker-Nunn (USA)	14	15,2	51	0,7
VAU (USSR)	10	15,0	36	1,0
SBG (GDR)	9	14,4	23	1,1
400/2000 x)	4	14,0	8	2,8
300/1500 x)	5	13,5	6	2,1
AFU (USSR)	10	13,0	6	1,0

x) Astrographs VEB Carl Zeiss Jena, Sonnefeld type

First experimental photographs at Tautenburg Schmidt (a geostationary satellite of $14,7^m$ yielded a strong blackening after an exposition of 5 minutes) and Dresden Astrograph Zeiss 300/1500 confirmed the dates of the table above. Beyond this was found out:

1. There are geostationary satellites (or quasistationary ones), which may reach the magnitude 6^m (an object at two plates of Dresden astrograph)

2. The apparent velocity of a geostationary satellite depends on its position in the orbit, and may vary quickly, so that the limiting magnitude for a given exposure time varies very much too.

The problem of timing is not yet solved for telescopes, which are no satellite telescopes.

Determination of positions of geostationary satellites may be done by Schlesinger's method of dependences or Turner's method using plate constants.

The accuracy of determined positions of a geostationary satellite depends on the focal distance of the telescope used, on the precision of timing, and on the positions of the reference stars used. Because there is not yet a timing device at 2-m-Schmidt-telescope and at astrographs, the position accuracy attainable is not investigated till now.

The author thanks Dr. Börngen and Dr. Kirsch from Tautenburg observatory (ZIAP) for taking a series photographs at 2-m-Schmidt, and Dr. Losinskij from Astronomical council (Moscow) for some valuable advice. Some results of the present paper were taken from the diploma thesis of M. Schmidt, TU Dresden 1980.

References

[1] Bursa, M., Šíma, Z.: Geostationary satellites and the position of the Earth's mass center. Bull. Astron. Inst. of Czechoslovakia, Vol. 29 (1978) No. 4, pp 232-237.

[2] Bursa, M., Šíma, Z.: Motion of geostationary satellites due to first-degree harmonics. Bull. Astron. Inst. of Czechoslovakia, Vol. 30 (1979), No. 4, pp 193 - 198.

[3] Dixit, P. S. et al.: Optical observations of geostationary satellites from Satellite Tracking and Ranging Station, Kavalur/India, 1978.

[4] Massevitch, A. G. et al.: Photographic tracking of geostationary satellites for geodetic purposes. Paper at the 20 th Annual COSPAR meeting, Tel Aviv 1977.

[5] Massevitch, A. G. et al.: Results of the Intercosmos programme in the field of satellite geodesy. Paper at the 4 th International Symposium "Geodesy and Physics of the Earth" GDR/DDR Karl-Marx-Stadt, May 12 th - 17 th, 1980.

[6] Marek, K.-H.: O vozmožnosti ispol'zovanija nabljudenij stacionarnych sputnikov v geometričeskoj sputnikovoj geodezii. Akad. nauk SSSR, Naučnye informacii 25, Moskva 1972, pp 103 - 116.

[7] Osipenko, V. P., Yurevič, V.A.: Zvenigorodskaja eksperimental'naja stancija. Zemlja i Vselennaja (Moskva), 1972, No. 6, pp 54 - 57.

A Method for the Construction of spheroidal Mass Distributions consistent with the harmonic Part of the Earth's Gravity Potential.

by

C.C. Tscherning[1)] and Hans Sünkel[2)]

Abstract

Approximations to the harmonic part of the gravity potential of the Earth may be expressed as a series in external spheroidal harmonics,

$$V(u, \beta, \lambda) = \Sigma_{n=o}^{N} \Sigma_{m=-n}^{n} A_{nm} V_{nm}^{e}(u, \beta, \lambda).$$

where u, β, λ are "ellipsoidal" coordinates.

Models for the mass distribution (ρ) of a spheroidal approximation to the Earth may be expressed as a series in internal spheroidal harmonics, contingently multiplied by a function $F(u, \beta, \lambda)$, i.e.

$$\rho(u, \beta, \lambda) = F(u, \beta, \lambda) \Sigma_{n=o}^{N} \Sigma_{m=-n}^{n} a_{nm} V_{nm}^{i}(u, \beta, \lambda).$$

It is shown, that for suitable choice of $F(u, \beta, \lambda)$, simple relations between the coefficients a_{nm} and A_{nm} can be established. This permits the construction of spheroidal mass distribution models consistent with the known low-degree harmonic expansions of the Earths gravity potential.

In order to construct geophysically realistic mass distributions a generalisation of a procedure due to Moritz has been used. First the coefficients A_{nm}^{o} of a spheroidal harmonic expansion of the potential of a geophysically realistic (discontinuous) approximation ρ_o to the mass distribution of the Earth are computed. A mass distribution ρ_1 is then computed based on the residual coefficients $A_{nm}^{1} = A_{nm} - A_{nm}^{o}$, using $F(u,\beta,\lambda) = u^2/(u^2 + E^2\cos^2\beta)$. (This is one of the functions, which gives a simple relation between the coefficients A_{nm}^{1} and the coefficients a_{nm}^{1} of ρ_1). E is the excentric anomaly. The harmonic part of the potential of the density distribution $\rho = \rho_o + \rho_1$ will then be equal to V.

1) Geodaetisk Institut, DK-2920 Charlottenlund, Gamlehave Alle 22.

2) Institute of Physical Geodesy, Technical University at Graz, Steyrergasse 17, A-8010 Graz, Austria.

Presented 4'th International Symposium "Geodesy and Physics of the Earth", Karl-Marx-Stadt, DDR, May, 12-17, 1980.

Results of a numerical example showing the density variations within the Earth implied by a set of potential coefficients (GEM10B) are given.

1. Introduction

Models for the density distribution of the Earth (or another planet) are useful in geophysical research e.g. when comparing observed data with the values derived from a model with known physical properties. In geodesy such models are needed, when constructing approximations to the gravitational potential of the Earth, $W=V+\Phi$, (where V is the potential due to the mass distribution of the Earth and Φ is the rotational potential). The reason for this is the following.

In order to linearize the functionals relating observed quantities (such as gravity values and astronomical latitude and longitude) to W, a certain normal or reference potential U is adopted. Approximations to the anomalous potential, $T = W-U$ can then be constructed using the linearised functionals and the observation anomalies (gravity anomalies, deflections of the vertical). If information about the mass distribution is to be used, U or a reference mass distribution producing U must be defined inside the Earth. Also when using statistical models, not the absolute density values, but the residuals with respect to a reference model are the basic quantities, cf. Tscherning (1977).

Up to now only harmonic functions U have been used, for which the mass distribution is a multipole distribution at or near the origin, (the Earths gravity center). Therefore we must now construct reference mass functions, which are geophysically realistic volume distributions, and which outside the masses produce the adopted U-function. Hence, the main purpose of this paper is to describe techniques for the construction of such mass models.

When working with density anomalies (d) it is permitted to work in spherical approximation, i.e. so that the Earth is regarded as a sphere with radius R = 6371.0 km. The anomalous potential T, produced by these density anomalies,

$$T(P) = G \int_{\Omega} d(Q)/\|P - Q\| \, dQ \qquad (1.1)$$

may in spherical approximation be expressed as a series in solid spherical harmonics outside the surface of the Earth. (Ω is the set in $\mathbb{R}^3$ inside the surface of the Earth, P and Q are points in $\mathbb{R}^3$ and G is the gravitational constant).

Let the point P outside Ω have spherical coordinates φ = latitude, λ = longitude and r = distance from the origin. Then

$$T(P) = \sum_{i=2}^{\infty} \frac{GM}{r} \left(\frac{R}{r}\right)^i \sum_{j=0}^{i} \bar{P}_{ij}(\sin\varphi) \left[\bar{C}^*_{ij} \cos j\lambda + \bar{S}_{ij} \sin j\lambda\right], \qquad (1.2)$$

where M is the mass of the Earth, $\bar{P}_{ij}$ are the fully normalized solid spherical harmonics and $\bar{C}^*_{ij}$ and $\bar{S}_{ij}$ are constants.

When the density anomaly function d is required to fulfil a simple condition like

$$\Delta(r^m d) = 0, \qquad (1.3)$$

where Δ is the Laplace-operator, then d can be expressed as a series in internal solid spherical harmonics multiplied by r^{-m},

$$d(P) = r^{-m} \sum_{i=0}^{\infty} \left(\frac{r}{R}\right)^i \sum_{j=0}^{i} \bar{P}_{ij}(\sin\varphi) \left[c_{ij} \cos j\lambda + s_{ij} \sin j\lambda\right]. \qquad (1.4)$$

In this case there is a simple relationship between the coofficients of the two series, cf. Tscherning (1974),

$$\left.\begin{matrix} c_{ij} \\ s_{ij} \end{matrix}\right\} = \frac{(2i-m+3)(2i+1)}{R^{3-m} \cdot 4\pi G} \left\{\begin{matrix} C^*_{ij} \\ S_{ij} \end{matrix}\right. \qquad (1.5)$$

for $i > -m$, i.e. i generally ≥ 0.

When working with the density distribution ρ itself, it is no longer permitted to work in spherical approximation, but we must work with a spheroidal (or ellipsoidal) reference model. Let the Earth be approximated by a spheroid with semi-major axis a, semi - minor axis b, and hence half focal distance $E = (a^2 - b^2)^{1/2}$. We will also introduce spheroidal coordinates, i.e. the point

P will have the coordinates (u,β,λ) where u = the semi-minor axis of the spheroid confocal with the reference spheroid and passing through P, β = the reduced latitude and λ = the longitude, cf. Heiskanen and Moritz (1967, section 1-19). The gravity potential of the Earth, V, can then be approximated by an abbreviated series in spheroidal harmonics.

We will in the following work with both internal and external spheroidal harmonics, which we will denote $V^i_{nm}(P)$ and $V^e_{nm}(P)$, respectively. Then

$$V^i_{nm}(P) = P^m_n(i\tfrac{u}{E})P^m_n(\sin\beta)\begin{cases}\cos m\lambda & 0 \leq m \leq n\\ \sin|m|\lambda & -n \leq m < 0\end{cases} \tag{1.6}$$

$$V^e_{nm}(P) = Q^m_n(i\tfrac{u}{E})P^m_n(\sin\beta)\begin{cases}\cos m\lambda & 0 \leq m \leq n\\ \sin|m|\lambda & -n \leq m < 0\end{cases} \tag{1.7}$$

Here we put $P^m_n = P^{-m}_n$, $Q^m_n = Q^{-m}_n$, where Q^m_n are the associated Legendre polynomials of the second kind. The "i" appearing within the argument of P^m_n and Q^m_n is the imaginary unit.

We then have

$$V(P) \simeq GM \sum_{h=o}^{N} \sum_{m=-n}^{n} A_{nm} V^e_{nm}(P) , \tag{1.8}$$

where the coefficients A_{nm} can be determined from one of the standard earth models like the Smithsonian or Goddard Earth models. These models are expressed as series in solid spherical harmonics with coefficients C_{ij} and S_{ij} like in eq. (1.2). The coefficients A_{nm} may be computed from these coefficients using e.g. Hotine (1969, eq. (22.59)).

The summation limit N becomes in reality infinite, but the coefficients of degree 4, 6 larger than the maximal degree of the sperical harmonic coefficients are very small and can be put equal to zero.

If we require

$$\Delta(f(u,\beta,\lambda) \cdot \rho) = 0 \tag{1.9}$$

where $f(u,\beta,\lambda) \neq 0$, we may express ρ as a modified series in solid spheroidal harmonics,

$$\rho(P) = \sum_{n=0}^{\infty} \frac{1}{f(u,\beta,\lambda)} \sum_{m=-n}^{n} a_{nm} V_{nm}^{i}(P). \qquad (1.10)$$

Selecting $f(u,\beta,\lambda)$ in a suitable way, we then can hope to obtain relationships between the coefficients A_{nm} and a_{nm} similar to these given in eq. (1.5).

In the following sections 2-3 we will determine such relationships, by simply computing the potential of a mass distribution $F(u,\beta,\lambda) \cdot V_{nm}^{i}(P)$, $F(u,\beta,\lambda) = 1/f(u,\beta,\lambda)$ being a simple function. In section 4 we will describe how these relations can be used for the construction of geophysically realistic mass distributions, the potential of which will agree with a given set of coefficients A_{nm}. Finally in section 5, we point out some future research problems.

2. The potential of $V_{nm}^{i}(u,\beta,\lambda)$

We will in this section regard the simplest case where F = constant. In this case we must compute the potential of a harmonic mass distribution in a point Q with coordinates (u',β',λ'),

$$Y_{nm}(u',\beta',\lambda') = \int_{u=o}^{u=b} \int_{\lambda=o}^{2\pi} \int_{\beta=-\pi/2}^{\pi/2} V_{nm}^{i}(u,\beta,\lambda)(u^2+E^2\sin^2\beta)/L \qquad (2.1)$$
$$\cdot \cos\beta \, d\beta \, d\lambda \, du$$

where $L = \| P - Q \|$ and $(u^2 + E^2\sin^2\beta)\cos\beta \, d\beta \, d\lambda \, du$ is the volume element.

According to Hotine (1969, eq. (22.55)) we have

$$\frac{E}{L} = i \sum_{n=o}^{\infty} (2n+1)\Big[Q_n(i\tfrac{u'}{E}) P_n(i\tfrac{u}{E}) P_n(\sin\beta') P_n(\sin\beta)$$

$$+ 2\sum_{m=1}^{n} (-1)^m \left(\frac{(n-m)!}{(n+m)!}\right)^2 Q_n^m(i\tfrac{u'}{E}) P_n^m(i\tfrac{u}{E}) P_n^m(\sin\beta') P_n^m(\sin\beta) \qquad (2.2)$$
$$\cdot \cos m(\lambda' - \lambda)\Big].$$

When evaluating eq. (2.1) we can then take advantage of the known orthogonality properties of the Legendre polynomials. We also have

$$\frac{1}{2\pi}\int_0^{2\pi}\int_{-\pi/2}^{\pi/2}(P_n(\sin\beta))^2\cos\beta d\beta d\lambda = \frac{2}{2n+1} \tag{2.3}$$

$$\frac{1}{2\pi}\int_0^{2\pi}\int_{-\pi/2}^{\pi/2}(P_n^m(\sin\beta))^2\begin{Bmatrix}\cos^2 m\lambda\\ \sin^2 m\lambda\end{Bmatrix}\cos\beta d\beta d\lambda = \frac{1}{2n+1}\,\frac{(n+m)!}{(n-m)!} \tag{2.4}$$

here $m \neq 0$ in the last equation.

Let us regard the part of the integrand equal to

$$I = -E^2 P_n^m(i\tfrac{u}{E})P_n^m(\sin\beta)\begin{Bmatrix}\cos m\lambda\\ \sin m\lambda\end{Bmatrix}((i\tfrac{u}{E})^2-\sin^2\beta)$$

$$= -E^2 P_n^m(q)P_n^m(t)\begin{Bmatrix}\cos m\lambda\\ \sin m\lambda\end{Bmatrix}(q^2-t^2)\ , \tag{2.5}$$

where $q = i\frac{u}{E}$ and $t = \sin\beta$. We will express I only using Legendre-polynomials.

Using the well-known recursion formulae

$$(n-m+1)P_{n+1}^m(t) = (2n+1)t\,P_n^m(t)-(n+m)P_{n-1}^m(t) \tag{2.6}$$

we have

$$t\,P_n^m(t) = \frac{n-m+1}{2n+1}\,P_{n+1}^m(t)+\frac{n+m}{2n-1}\,P_{n-1}^m(t) \tag{2.7a}$$

$$t\,P_{n-1}^m(t) = \frac{n-m}{2n-1}\,P_n^m(t) + \frac{n+m-1}{2n-1}\,P_{n-2}^m(t) \tag{2.7b}$$

$$t\,P_{n+1}^m(t) = \frac{n-m+2}{2n+3}\,P_{n+2}^m(t) + \frac{n+m+1}{2n+3}\,P_n^m(t) \tag{2.7c}$$

and

$$t^2P_n^m(t) = \frac{(n-m+1)(n-m+2)}{(2n+1)(2n+3)}\,P_{n+2}^m(t) + \frac{(n-m+1)(n+m+1)}{(2n+1)(2n+3)}\,P_n^m(t)$$

$$+\frac{(n+m)(n-m)}{(2n+1)(2n-1)}\,P_n^m(t) + \frac{(n+m)(n+m-1)}{(2n+1)(2n-1)}\,P_{n-2}^m(t)\ , \tag{2.8}$$

which we will write

$$= A\, P^m_{n+2}(t) + (B+C)P^m_n(t) + D\, P^m_{n-2}(t)\ , \tag{2.9}$$

hereby defining the quantities A,B,C and D.

Hence

$$I = -E^2\Big[(AP^m_{n+2}(q)+(B+C)P^m_n(q)+D\, P^m_{n-2}(q))P^m_n(t)\begin{Bmatrix}\cos m\lambda\\ \sin m\lambda\end{Bmatrix}$$

$$-P^m_n(q)(A\, P^m_{n+2}(t)+(B+C)P^m_n(t)+D\, P^m_{n-2}(t))\begin{Bmatrix}\cos m\lambda\\ \sin m\lambda\end{Bmatrix}\Big]$$

$$= E^2\Big[A\, P^m_n(q)P^m_{n+2}(t) - (A\, P^m_{n+2}(q) + D\, P^m_{n-2}(q))P^m_n(t) + D\, P^m_n(q)P^m_{n-2}(t)\Big]$$

$$\begin{Bmatrix}\cos m\lambda\\ \sin m\lambda\end{Bmatrix} \tag{2.10}$$

Using the orthogonality property and eq. (2.3) and (2.4) we get

$$Y_{nm} = -E^2 4\pi\Big[\int_{q=0}^{ib/E}(AP^m_{n+2}(q) + DP^m_{n-2}(q))P^m_n(q)dq \cdot Q^m_n(q')P^m_n(t')\cdot B'$$

$$-\int_{q=0}^{ib/E} A\, P^m_n(q)P^m_{n+2}(q)dq \cdot Q^m_{n+2}(q')P^m_n(t')\cdot A'$$

$$-\int_{q=0}^{ib/E} D\, P^m_n(q)P^m_{n-2}(q)dq \cdot Q^m_{n-2}(q')P^m_{n-2}(t')\cdot D'\Big]$$

with A'=B'=D'=1 for m=0,

$$B' = \frac{(n-m)!}{(n+m)!}(-1)^m\begin{Bmatrix}\cos m\lambda'\\ \sin m\lambda'\end{Bmatrix},\quad A' = \frac{(n-m+2)!}{(n+m+2)!}(-1)^m\begin{Bmatrix}\cos m\lambda'\\ \sin m\lambda'\end{Bmatrix}$$

and

$$D' = \frac{(n-m-2)!}{(n+m-2)!}(-1)^m \begin{Bmatrix} \cos m\lambda' \\ \sin m\lambda' \end{Bmatrix} \qquad \text{for } m \neq 0$$

Then

$$Y_{nm} = -E^2 \cdot 4\pi \Big[\int_{q=o}^{ib/E} A\, P^m_{n+2}(q) P^m_n(q)\, dq \,(B' Q^m_n(q') P^m_n(t') - A' Q^m_{n+2}(q') P^m_{n+2}(t'))$$

$$+ \int_{q=o}^{ib/E} D \cdot P^m_n(q) P^m_{n-2}(q)\, dq \cdot (B' \cdot Q^m_n(q') P^m_n(t') - D' \cdot Q^m_{n-2}(q') P^m_{n-2}(t'))\Big]$$

Using eq. (A.1.3) we have

$$Y_{nm} = E^2 \cdot 4\pi \Big[\frac{b^2/E^2+1}{-2(2n+3)} \Big(P^m_{n+2}(i\tfrac{b}{E}) \frac{d}{dq} P^m_n(i\tfrac{b}{E}) - P^m_n(i\tfrac{b}{E}) \frac{d}{dq} P^m_{n+2}(i\tfrac{b}{E})\Big) \cdot A$$

$$\cdot (B' \cdot Q^m_n(i\tfrac{u'}{E}) P^m_n(\sin\beta') - A' \cdot Q^m_{n+2}(i\tfrac{u'}{E}) P^m_{n+2}(\sin\beta'))$$

$$+ \frac{b^2/E^2+1}{2(2n-1)} \Big(P^m_{n-2}(i\tfrac{b}{E}) \frac{d}{dq} P^m_n(i\tfrac{b}{E}) - P^m_n(i\tfrac{b}{E}) \frac{d}{dq} P^m_{n-2}(i\tfrac{b}{E})\Big) \cdot D$$

$$\cdot (B' \cdot Q^m_n(i\tfrac{u'}{E}) P^m_n(\sin\beta) - D \cdot Q^m_{n-2}(i\tfrac{u'}{E}) P^m_{n-2}(\sin\beta'))\Big], \qquad (2.11)$$

which may be stightly simplified by factorizing out $\frac{1}{2}(b^2/E^2+1) = a^2/(2E^2)$.

Example 1, m=0.

Here $A = \frac{(n+1)(n+2)}{(2n+1)(2n+3)}$, $D = \frac{n(n-1)}{(2n+1)(2n-1)}$, $A' = B' = D' = 1$,

so

$$Y_{no} = \frac{-2\pi a^2}{2n+1} \Big[\frac{(n+1)(n+2)}{(2n+3)^2} \Big(P_{n+2}(i\tfrac{b}{E}) \frac{d}{dq} P_n(i\tfrac{b}{E}) - P_n(i\tfrac{b}{E}) \frac{d}{dq} P_{n+2}(i\tfrac{b}{E})\Big)$$

$$* (V^e_{no}(u',\beta',\lambda') - V^e_{n+2,o}(u',\beta',\lambda'))$$

$$- \frac{n(n-1)}{(2n-1)^2} \Big(P_{n-2}(i\tfrac{b}{E}) \frac{d}{dz} P_n(i\tfrac{b}{E}) - P_n(i\tfrac{b}{E}) \frac{d}{dz} P_{n-2}(i\tfrac{b}{E})\Big) (V^e_{no}(u',\beta',\lambda') - V_{n-2,o}(u',\beta',\lambda'))\Big]$$

Example 2, n=0.

Here $A=\frac{2}{3}$, $D=0$, $A'=B'=D'=1$, so

$$Y_{oo}=\frac{-2\pi a^2}{3}\left(-P_o(i\tfrac{b}{E})\frac{d}{dq}P_2(i\tfrac{b}{E})\right)\frac{2}{3}\left(Q_o(i\tfrac{u'}{E})P_o(\sin\beta')-Q_2(i\tfrac{u'}{E})P_2(\sin\beta')\right)$$

$$=\frac{4\pi a^2 b\,i}{3E}\left(V^e_{oo}(u',\beta',\lambda')-V^e_{2o}(u',\beta',\lambda')\right)$$

This agrees with MacMillan (1958, eq. (39.2)).

Example 3, m=0, n=1.

$$Y_{1,o}=-\frac{2\pi a^2}{3}\left[\frac{2\cdot 3}{25}\left(\frac{5}{2}(i\tfrac{b}{E})^3-\frac{3}{2}i\tfrac{b}{E}\right)-(i\tfrac{b}{E})\left(\frac{15}{2}(i\tfrac{b}{E})^2-\frac{3}{2}\right)\right)$$

$$\cdot(V^e_{1o}-V^e_{3o})$$

$$=-\frac{2\pi a^2 b\,i}{25E}\left(-5\frac{b^2}{E^2}-3+15\frac{b^2}{E^2}+3\right)(V^e_{1,o}-V^e_{3,o})$$

$$=-\frac{4\pi a^2 b^3 i}{5E^3}(V^e_{1o}-V^e_{3o})$$

3. The potential of some simple non-harmonic mass-distributions.

In section 2 we found that the (harmonic part of the) potential of an internal spheroidal harmonic V^i_{nm} was equal to a linear combination of generally three external spheroidal harmonics $V^e_{n+2,m}$, V^e_{nm} and $V^e_{n-2,m}$. The reason for this was the occurrence of the factor $t^2=\sin^2\beta$ in eq.(2.5). This factor will disappear when we compute the potential of functions

$$F(u,\beta,\lambda)\,V^i_{nm}(u,\beta,\lambda)=\frac{F_1(q)}{(q^2-t^2)}V^i_{nm}(q,t,\lambda), \qquad (3.1)$$

where we again have put $q = i\frac{u}{E}$.

If we choose $F_1(q)$ to be equal to a polynomial in q, then we may without difficulty carry out the needed integrations. We may even choose $F_1(q)$ to be equal to different polynomials in different intervals of q, i.e. $F_1(q)$ may be a discontinuous function.

In order to carry out the integrations we must first convert the quantities $q^k P_n^m(q)$ into a linear combination of associated Legendre polynomials:

$$q^k P_n^m(q) = \sum_{j=-k}^{k} C_n^m(k,j) P_{n+j}^m(q) \tag{3.2}$$

From eq. (2.7a) we have $C_n^m(0,0) = 1$,

$$C_n^m(1,-1) = \frac{n+m}{2n-1}, \quad C_n^m(1,0) = 0 \text{ and } C_n^m(1,1) = \frac{n-m+1}{2n+1}. \tag{3.3}$$

Then we get the following recursion formulae for the determination of the coefficients

$$C_n^m(k,j) = C_n^m(k-1,j-1)\, C_{n+j-1}^m(1,1) + C_n^m(k-1,j+1) C_{n+j+1}^m(1,-1)$$

$$= C_n^m(k-1,j-1)\, \frac{n+j-m}{2(n+j)-1} + C_n^m(k-1,j+1)\, \frac{n+j+m+1}{2(n+j)+3} \tag{3.4}$$

(We must put $C_n^m(k,j) = 0$ for $|j| > k$).

For $F_1(q) = \sum_{i=0}^{I} c_i q^i$ we then have

$$F_1(q) P_n^m(q) = \sum_{i=0}^{I} c_i q^i P_n^m(q)$$

$$= \sum_{i=0}^{I} c_i \sum_{j=-i}^{i} C_n^m(i,j) P_{n+j}^m(q), \tag{3.5}$$

which we will write as

$$= \sum_{j=-I}^{I} c_j^* P_{n+j}^m(q) ,$$

which also will define the constants c_j^* .

We then have

$$Y_{nm}(u',\beta',\lambda') = \int_{u=o}^{b} \int_{\lambda=o}^{2\pi} \int_{\beta=-\pi/2}^{\pi/2} F_1(q) V_{nm}^i(u,\beta,\lambda)/L \cos\beta d\beta d\lambda du$$

$$= -E^2 4\pi \Big[\int_{q=o}^{q=ib/E} \sum_{j=-I}^{I} c_j^* P_{n+j}^m(q) P_n^m(q) dq \Big] Q_n^m(q') P_n^m(t') \cdot B'$$

$$= -E^2 4\pi \Big[\sum_{j=-I}^{I} c_j^* \int_{q=o}^{iu/b} P_{n+j}^m(q) P_n^m(q) dq \Big] Q_n^m(q') P_n^m(t') B'$$

$$= B_{nm} V_{nm}^e(u',\beta',\lambda') \qquad (3.6)$$

where $B_{nm} = -4\pi E^2 \frac{(n-m)!}{(n+m)!} (-1)^m \sum_{j=-I}^{I} c_j^* \int_{q=o}^{ib/E} P_{n+j}^m(q) P_n^m(q) dq \qquad (3.7)$

In a similar way we can handle functions $F(u,\beta,\lambda)$, which are polynomials in q and t. (Or in $r^2 = u^2 - E^2 \sin^2\beta$).

The potential Y_{nm} of a function $F(u,\beta,\lambda) V_{nm}^i(u,\beta,\lambda)$ will be a linear combination of external solid harmonics

$$Y_{nm}(u',\beta',\lambda') = \sum_{k \in J} B_{nm}^k V_{km}^e(u',\beta',\lambda') \qquad (3.8)$$

where J is a suitable index-set (equal to n+2, n and n-2 when F is equal to a constant as used in section 2).

4. Construction of mass distributions.

Let us suppose that the external potential is given by eq.(1.8) or equivalently by a set of coefficients GMA_{nm}, $n \leq N$.

If we require the density distribution to fulfil the condition (1.9) with $F(u,\beta,\lambda)$ equal to a polynomial in $q = i\frac{u}{E}$ and $t = \sin\beta$ in each interval $u_j < u < u_{j+1}$, $j = 0,..,M$, $u_j \leq u_{j+1}$, $u_o = 0$ and $u_M = b$ then eq. (3.8) is valid. For the density distribution given by

$$\rho(u,\beta,\lambda) = \sum_{n=o}^{N} \sum_{m=-n}^{n} a_{nm} F(u,\beta,\lambda) V_{nm}^{i}(u,\beta,\lambda) , \tag{4.1}$$

we must then have the relationship

$$\sum_{n \in J} B_{nm}^{j} a_{nm} = GM \circ A_{jm} \tag{4.2}$$

For a given set of coefficients it will only in a few cases be possible to solve the set of linear equations (4.2).

If the coefficients, B_{nm}^{j}, which can not be solved for, are very large, one may artificially adopt some very small potential coefficients A_{nm}, and then solve the equations. Or, using an elimination method, one may start with the high order and degree terms, ending up with a mass distribution ρ_1 and some residuals A_{nm}^{o} for the low degree terms. These residuals can then be used for the computation of a mass distribution ρ_o, using one of the functions F, which gives a one to one correspondance between A_{nm}^{o} and the coefficients a_{nm}^{o} of a mass distribution ρ_o. We will then have $\rho = \rho_o + \rho_1$.

Due to lack of time, we have, however, only tried the simple situation, described in section 3, where $F(u,\beta,\lambda) = F_1(q)/(q^2-t^2)$. Then we simply have

$$a_{nm} = GM \cdot A_{nm}/B_{nm}^{o} \tag{4.3}$$

In Figure 1 are shown the radial variation of the mass distributions obtained using the set of coefficients GEM10B and $F_1(q) = 1, q, q^2$ and q^3, respectively. Note, that for $F_1(q) = q^2$, we will get a mass distribution, which is approximately harmonic. None of these results are geophysically meaningful .

A more meaningful result was obtained using $F_1(q)$ equal to q^2 times a

polynomial expression ρ_o for the radial variation of the mass distribution, (with u/b substituted for r/R as a parameter), see Moritz (1968, eq. 88). The reason for this is obviously, that the condition (1.9) in this case is equivalent to requiring ρ to be equal to the constant function 1, - which for sure is harmonic. We expect, that the use of a discontineous function, $F_1(q) = \rho_o \cdot q^2$, will give a mass distribution, which is geophysically meaningful and we are still investigating this possibility.

Numerical experiments with an alternative method (inspired by methods discussed in Moritz (1968, 1973)), resulted in the following procedure, which will produce a geophysically meaningful mass distribution. Instead of starting by trying to solve the equations (4,2), the idea is to use a parametric earth (mass) model, ρ_o, and then determine a small pertubation to this model, using eq. (4,3).

We have carried out this procedure for one specific parametric earth model (PEM), given by (Dziewonski et.al., 1975, Table 1), and one set of potential coefficients, GEM10B, given in (Lerch et.al., 1978).

We choosed the PEM describing an average structure (with respect to the continents and the oceans). This model is given in spherical approximation, by 8 polynomials in different continuity intervals with r/R as a parameter. We modified the polynomials, so that they each were defined from 0 to R_i, where R_i is the radius of the i'th surface of discontinuity.

Instead of using r/R as a parameter, we then used u_i/b_i, where b_i is the semiminor axis of an ellipsoid having the same volume as the sphere with radius R_i. u_i is the ellipsoidal u-coordinate, so that $u_i = b_i$ on the ellipsoid. We fixed b_8, so that it was equal to b, but varied all the others, so that the potential produced by the mass distribution agreed with GM and $C_{2,o}$ of the used set of potential coefficients (GEM10B). We parameterized the b_i by putting

$$\frac{a_i^2 - b_i^2}{a_i^2} = \frac{a^2 - b^2}{a^2} \left(\frac{R_i}{R}\right)^c , \qquad (4.4)$$

which through an iterative procedure gave the correct $C_{2,o}$ value for $c \approx 11.2$ Let us denote this mass distribution for ρ_o, and the potential coefficients for A^o_{nm}. (Only the even zonal harmonics are different from zero because of the rotational and equatorial symmetry).

The set of potential coefficients GEM10B were slightly modified by subtraching the potential coefficients of the isostatically compensated topography, computed as described in (Lachapelle, 1975). We then had the potential coefficients of an ellipsoidal Earth, without topography, which were converted into coefficient A_{nm} of an ellipsoidal harmonics series.

The residual coefficients $A^1_{nm} = A_{nm} - A^o_{nm}$, where then converted using eq. (4.3), with $F_1(u, \lambda, \beta) = u^2$, resulting in a (residual) mass distribution ρ_1. The total mass distribution $\rho = \rho_o + \rho_1$ will produce an external potential, with the ellipsoidal harmonic coefficients, A_{nm}. Figure 2 show the variation of ρ_1 in various depths. We see, that the maximal values numerically are below 0.01 g/cm^3, i.e. ρ is only a slight perturbation af ρ_o, and hence also a geophysically realistic PEM. The main deficiency is the behavior near the Earth center, enforced by using ellipsoidal coordinates. However, this is, seen from a geodetic standpoint, of minor importance, because we mainly are concerned with the variations in the crust and mantle.

5. Conclusion

We have in this paper given examples of possible methods of constructing mass density distributions, which will produce an approximation to the external gravity potential given by a set of low degree potential coefficients. We also have carried through a computation which gave a fairly realistic mass distribution as a result, or more correctly: the perturbations of the used PEM were insignificant.

There are, however, some problems, which need to be solved, primarily related to the use of the PEM. Which excentricities should be adopted for the different discontinuity surfaces, which mean density should be used at the surface of the Earth and how do we get rid of the problems originating from the use of ellipsoidal coordinate systems ? We have thoughout used the condition eq. (1.9). However, this condition is just one which makes the construction of density distributions possible in a unique way. The ideal situation would be to have a condition which corresponded to the minimalization of an integral formula like the one discussed in Moritz (1968, section 12), see also Rubincam (1979).

Acknowledgement: The cooperation of the authors was initiated in june 1979, when the first author, supported by a NATO Grant, visited the Ohio State University, where the second author worked at that time. The support of NATO Grant No. 1378 is therefore gratefully acknowledged.

Appendix Integrals of products of associated Legendrepolynomials of the same order.

The associated Legendrepolynomials fulfil the well known differential-equation

$$(1-t^2)\frac{d^2}{dt^2}P_n^m(t)-2t\frac{d}{dt}P_n^m(t)+\left[n(n+1)-\frac{m^2}{1-t^2}\right]P_n^m(t)=0 \qquad \text{(A 1.1)}$$

which we will use in order to evaluate the following integral for $n \neq k$,

$$I=\int_o^t P_n^m(z)P_k^m(z)dz \qquad \text{(A 1.2)}$$

We have

$$(n-k)(n+k+1) = n^2+nk+n-nk-k^2-k$$

$$= n^2-n-k^2-k = n(n+1)-k(k+1)$$

and

$$n(n+1)P_n^m(z) = (z^2-1)\frac{d^2}{dz^2}P_n^m(z)+2z\frac{d}{dz}P_n^m(z)+\frac{m^2}{1-z^2}P_n^m(z),$$

hence

$$(n(n+1)-k(k+1))P_n^m(z)P_k^m(z) =$$

$$= P_k^m(z)(n(n+1)P_n^m(z))-P_n^m(z)(k(k+1)P_k^m(z))$$

$$= P_k^m(z)\left[(z^2-1)\frac{d^2}{dz^2}P_n^m(z)+2z\frac{d}{dz}P_n^m(z)\right]-P_n^m(z)\left[(z^2-1)\frac{d^2}{dz^2}P_k^m(z)\right.$$

$$\left.+2z\frac{d}{dz}P_k^m(z)\right]$$

$$= (z^2-1)\left[\frac{d^2}{dz^2} P_n^m(z)P_k^m(z) - \frac{d^2}{dz^2} P_k^m(z).P_n^m(z)\right]$$

$$+ 2z\left[P_k^m(z)\frac{d}{dz} P_n^m(z) - P_n^m(z)\frac{d}{dz} P_k^m(z)\right]$$

$$= \frac{d}{dz}\left[(z^2-1)\left(P_k^m(z)\frac{d}{dz} P_n^m(z) - P_n^m(z)\frac{d}{dz}P_k^m(z)\right)\right]$$

$$= \frac{d}{dz}\left[P_k^m(z)\left(\frac{n(n-m+1)}{2n+1} P_{n+1}^m(z) - \frac{(n+1)(n+m)}{2n+1} P_{n-1}^m(z)\right)\right.$$

$$\left. - P_n^m(z)\left(\frac{k(k-m+1)}{2k+1} P_{k+1}^m(z) - \frac{(k+1)(k+m)}{2k+1} P_{k-1}^m(z)\right)\right]$$

For $z = 0$ we know that either $P_n^m(z) = 0$ or $\frac{d}{dz} P_n^m(z) = 0$, so

for $k-n$ even and $\neq 0$ we have

$$\int_0^t P_n^m(z)P_k^m(z)\,dz$$

$$= \frac{t^2-1}{(n-k)(n+k+1)}\left[P_k^m(t)\frac{d}{dz} P_n^m(t) - P_n^m(t)\frac{d}{dz}P_k^m(t)\right] \qquad \text{(A 1.3)}$$

$$= \frac{1}{(n-k)(n+k+1)}\left[P_k^m(t)\left(\frac{n(n-m+1)}{2n+1} P_{n+1}^m(t) - \frac{(n+1)(n+m)}{2n+1} P_{n-1}^m(t)\right)\right.$$

$$\left. -P_n^m(t)\left(\frac{k(k-m+1)}{2k+1} P_{k+1}(t) - \frac{(k+1)(k+m)}{2k+1} P_{k-1}^m(t)\right)\right]$$

For $k-n$ odd, terms with $P_n^m(0)$ or $P_k^m(0)$ must be added.

Literature

Dziewonski, A.M., A.L. Hales and E.R. Lapwood: Parametrically simple earth models consistent with geophysical data. Physics of the Earth and Planetary Interiors, Vol. 10, pp. 12-48, 1975.

Heiskanen, W.A. and H. Moritz: Physical Geodesy, W.H. Freeman. San Francisco, 1967.

Hotine, Martin: Mathematical Geodesy, ESSA Monograph no. 2, Washington, D.C., 1969.

Lerch, F.J., C.A. Wagner, S.M. Klosko, R.P. Belott, R.E. Laubscher, and W.A. Taylor: Gravity Model Improvement using GEOS-3 Altimetry (GEM10A and 10B), presented AGU Spring Meeting, April 1978.

Lachapelle, G.: Determination of the Geoid using Meterogeneous Data, Mitteilungen der geodätischen Institute der Technische Universität Graz, Folge 19, 1975.

MacMillan, W.D.: The theory of the potential, Dover reprint, New York, 1958.

Moritz, Helmut: Density Distributions for the Equipotential Ellipsoid, Reports of the Department of Geodetic Science, No. 115, The Ohio State University, 1968.

Moritz, Helmut: Ellipsoidal Mass Distributions, Reports of the Department of Geodetic Science, No. 206, The Ohio State University, 1973.

Rubincam, David Parry: Gravitational Potential Energy of the Earth: A Spherical Harmonic Approach, Journal of Geophysical Research, Vol. 84, No. B11, pp. 6219-6225, 1979.

Tscherning, C.C.: Some simple methods for the unique Assignment of a Density Distribution to a Harmonic Function, Reports of the Department of Geodetic Science No. 313, The Ohio State University, 1974.

Tscherning, C.C.: Models for the Auto- and Cross Covariances between Mass Density Anomalies and First and Second Order Derivatives of the Anomalous Potential of the Earth, Proceedings 3rd International Symposium Geodesy and Physics of the Earth, Part 2, pp. 261-268, 1977.

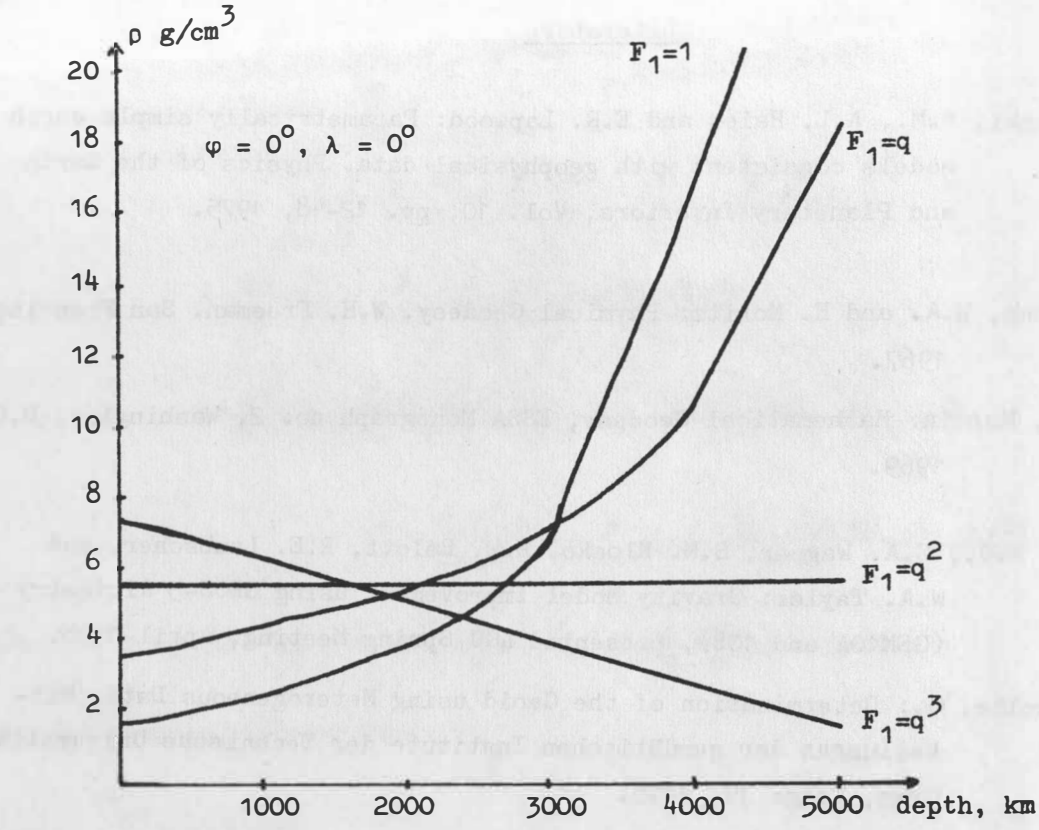

Figure 1. Density variation for varying depths corresponding to different weight-functions, F_1. GEM10B with n = 12 used.

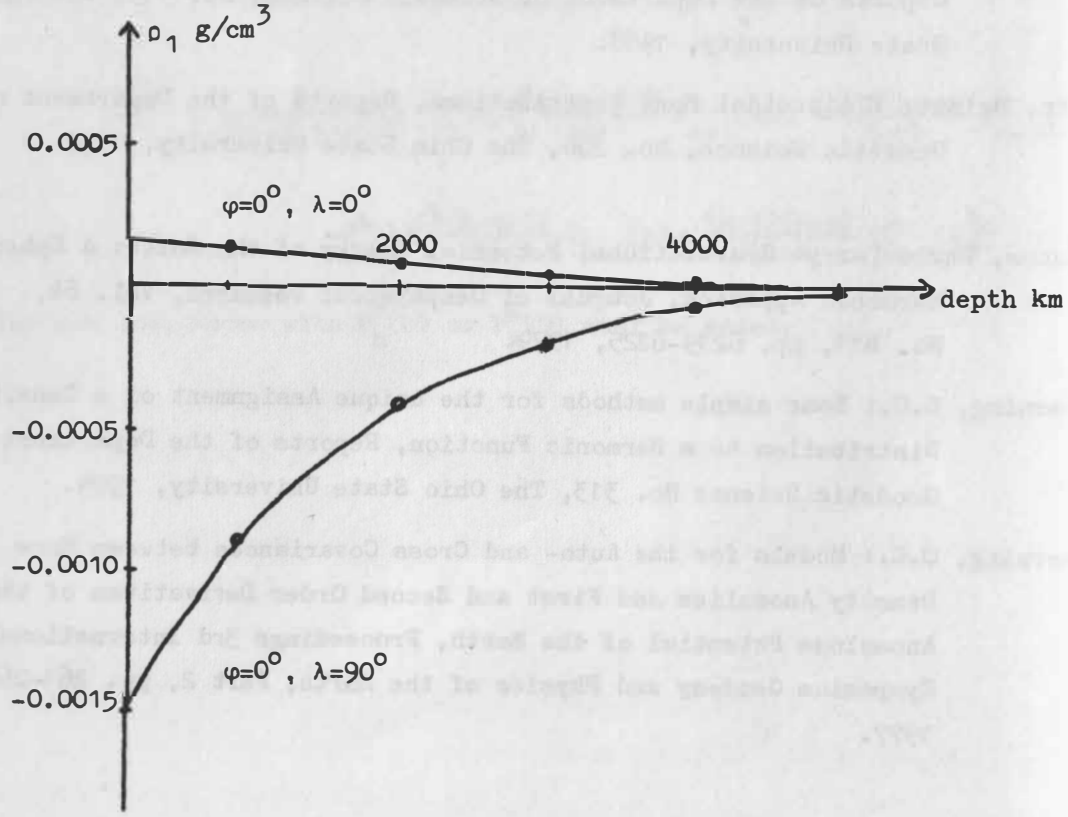

Figure 2. Density anomaly variation with depth. GEM10B with n=12 and $F = q^2$ used.

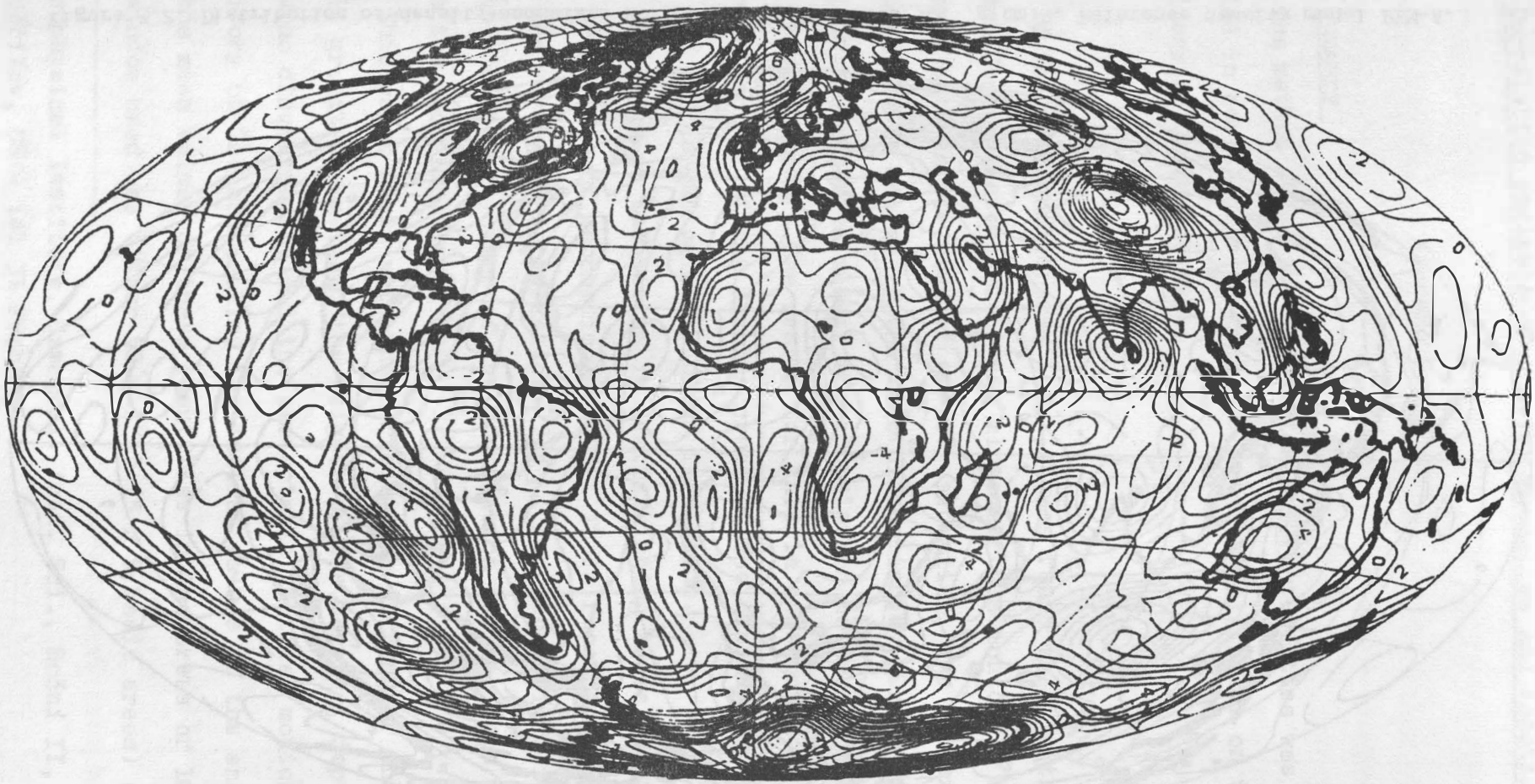

Figure 3.1. Distribution of density anomalies at the Earth's surface. Units 10^{-3} g cm^{-3}. Reference density model: PEM-A. Potential coefficients GEM10B, N = 36, topographic-isostatic effects removed.

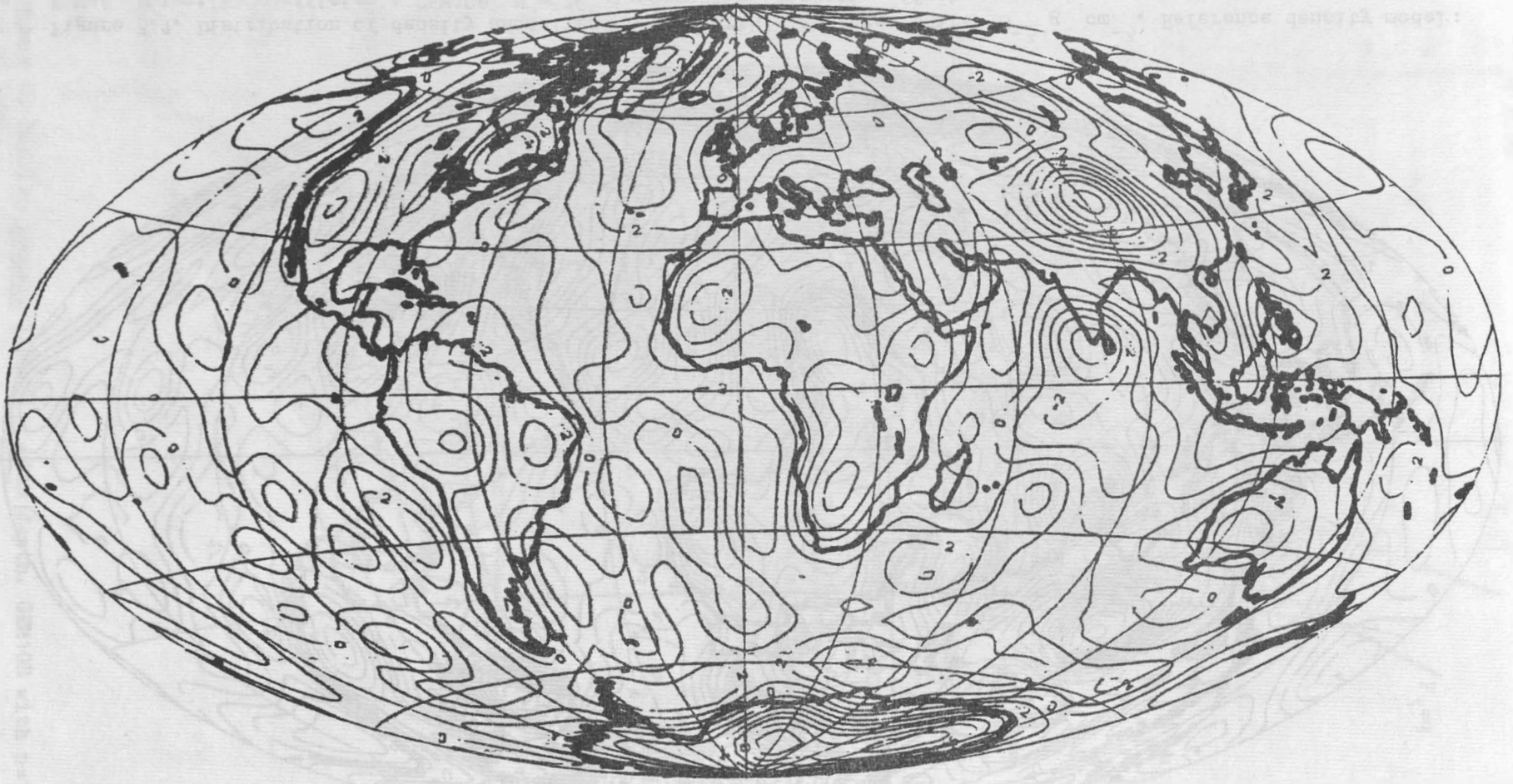

Figure 3.2. Distribution of density anomalies at 300 km depth. Units 10^{-3} g cm^{-3}. Reference density model PEM-A. Potential coefficients GEM10B, N = 36, topographic-isostatic effects removed.

Correlation analysis of gravity anomalies and isostasy

by

Vincenc Vyskočil [1)]

Summary

The method of moving statistical characteristics was applied in correlation analysis of geophysical fields on the territory of Czechoslovakia.

In the previous papers [1,2] it was found that in the Western Carpathians a relatively close correlation could be observed between the Bouguer gravity anomalies, the heights of the terrain and the depths of the Moho discontinuity. On the other hand, in the Bohemian massif the correlation between these quantities is much weaker. The reason for this is apparently in the different structure of the earth's crust of the Alpine-Carpathian zone and of the geologically older formations.

Since we are interested in distinguishing areas with differing properties of geophysical fields, it is recommended to compute the moving characteristics [3,4]. For geophysical interpretation the moving values of the correlation coefficients seem to be the most important.

This paper deals with the correlations of Bouguer and isostatic gravity anomalies, the heights of the terrain, depths of the Moho discontinuity and the neotectonic vertical motions on the territory of Czechoslovakia. The initial values of the analyses are the mean values of these quantities in the areas of 10'x 15'. The window used was either 50'x 1°15'(5 x 5 basic areas) or

1) Geophysical Institute, Czechosl. Acad. Sci., Boční II, Spořilov, CS - 141 31 Praha 4

$1^{\circ}10' \times 1^{\circ}45'$ (7 x 7 basic areas). The values of correlation coefficients calculated for the 5 x 5 windows are shown and discussed in [4]. Here, only a brief review of the results can be presented.

The obtained values of the moving correlation coefficients indicate that there are some differencies in the geophysical properties of the Carpathians and the Bohemian massif. The Carpathians appear as a relatively homogeneous block from the point of view of the investigated correlations. On the other hand, the Bohemian massif presents itself as an inhomogeneous block. This is expressed by the observed variability of the values of the correlation coefficients. Their anomalous signs occur mostly in the Southern and Eastern part of the Bohemian massif. Consequently, in some cases a relatively weak correlation is observed if the input data from the whole region of the Bohemian massif are included in one set, although it is quite significant in some of its parts.

The results prove the partial justification of the Airy's isostatic model in the Carpathians. The isostatic conditions of the Bohemian massif are more complicated and indicate the necessity of a more general approach to isostasy, which cannot be associated only with the compensation of topografic masses. According to the present experience, all the irregularities in the distribution of the masses inside the lithosphere must be considered in studying the isostatic conditions [5,6].

References

[1] Vyskočil V.: Comments on the manifestation of the deep structure of Czechoslovakia in the anomalous gravity field. Travaux Inst. Géophys. Acad. Sci. Tchécosl. No. 365, Geofysikální sborník 1972, Academia, Praha 1974.

[2] Kubáčková L., Vyskočil V.: Nekotorye rezultaty statisticheskogo analiza geofizicheskikh dannykh. Anwendung numerischer Methoden in Geophysik, Liblice 1972, GFÚ ČSAV, Praha 1973, 163.

[3] Vyskočil V.: Zur Ausgangsbedingungen der Korrelationsanalyse der geophysikalischen Felder. Geophysikalische Interpretationsmethoden, Veda, Bratislava 1978, 237.

[4] Vyskočil V., Burda M.: Some results of the correlation analysis of geophysical fields on the territory of the ČSSR. Geofysikální sborník 1978, Academia, Praha (in print).

[5] Vyskočil V.: Isostatic properties of the territory of Czechoslovakia and their assotiation with the motions of the earth's crust. Travaux Inst. Géophys. Acad. Tchécosl. Sci. No. 432, Geofysikální sborník 1975, Academia, Praha 1977.

[6] Kvitkovič J., Plančár J., Vyskočil V.: The isostatic conditions in relation to the recent vertical movements of the earth's crust in the West Carpathians. Geografický časopis, 28 (1976), 122.

Determination of the Earth's Figure by Solving an Inverse Astro-Gravi-Magnetic-Geodesic Problem

by

Dimiter Zidarov[1)]

Summary

An inverse astro-gravi-magneto-geodesical problem on the base of all available astronomical, gravimetrical, magnetical and geodesical data is formulated. The Earth gravimetric and magnetic fields are represented by the fields of simple gravimetric and magnetic layers on the Earth surface. The problem is solved by minimization of the sum of the differences between the corresponding empirically and theoretically determined values. The uniqueness of the solution of the inverse astro-geogesical and the inverse gravi-geodesical problems is proved.

Zusammenfassung

Eine umgekehrte astro-gravi-magneto-geodäsische Aufgabe auf die Grundlage von allen vorhandeln astrronomischen, gravimetrischen, magnetischen und geodäsischen Daten wird formuliert. Das gravimetrische und das magnetische Feld werden durch das Feld einer einfachen gravimetrischen Schicht und einer einfachen magnetischen Schicht dargestelt. Die Aufgabe wird durch die Minimisierung einer Summe der Differenzen zwischen den entsprechenden empirisch und theoretisch bestimmten Werten gelöst. Die Eindeutigkeit der Lösung der gravi-gedesischen und astro-geodesischen umgekehrten Aufgabe wird bewiesen.

1. Introduction

We will examine the simultaneous use of astronomic, magnetic, gravimetric and geodesic measurements in determing the Earth's figure, see Stokes G.G. [15,16], Laplace P.S. [8], Helmert W. [6], Molodensky M.S. [9-12], Moritz H. [13,14]. This paper represent a continuation of the investigations aimed at determing the Earth's figure through solving the inverse gravi-geodesic problem, as proposed by Zidarov D.P. [19,21,22,25,29,30,32]. Astronomic and magnetic measurements have been added here to the gravimetric and geodesic data.

2. Inverse Astro-Gravi-Magneto-Geodesic Problem

Let us assume that we have at our disposal the following data:

1. Known are the astronomic coordinates $\vartheta^*(Q_{0i})$, $\varphi^*(Q_{0i})$ of the Earth's surface in a certain number of points Q_{0i}, $i=0,1,\ldots, M_0$. The approximite values of the coordinates r_{0i}, ϑ_{0i}, φ_{0i} of the points Q_{0i} are denoted by r^0_{0i}, ϑ_{0i}, φ_{0i}. The angle $\vartheta^*(Q_{0i})$ is closed between the unit vector $\vec{N}(Q_{0i})$ of the vertical in point Q_{0i} and the unit vector $\vec{P}$ of the Earth's rotation axis; $\varphi^*(Q_{0i})$ represents the angle between the plane determined by the vectors $\vec{N}(Q_{00})$ and $\vec{P}$, where Q_{00} is a fixed point on the Earth's surface (Greenwish Observatory) and the plane determined by the vectors $\vec{N}(Q_{0i})$ and $\vec{P}$,

2. Known are the values of the geopotential

$$\Delta W(Q_{1i}) = W(Q_{1i}) - W(Q_{10}) = \int_L g\,dh$$

1) Bulgarian Academy of Sciences, Geophysical Institute, Sofia 1113, 13 Acad. G.Boncev Str., Bulgaria

in a certain number of points Q_{1i}, $i=0,1,\ldots M_1$, on the Earth's surface S, $\Delta W(Q_{1i})$ representing the difference between the gravity potential W in point Q_{1i} and the gravity potential W in the basic point Q_{10} ; L is an arbitrary line on S, connecting points Q_{1i} and Q_0 , g is the gravity field intensity in the points of L ; dh is the distance between the corresponding equipotential surfaces W=const. and r^0_{1i} , ϑ^0_{1i} , φ^0_{1i} are the approximate values of the coordinates r_{1i} , ϑ_{1i} , φ_{1i} of the points Q_{1i} ,

3.Known are the values $g(Q_{2i})$ of the gravity field intensity in the points Q_{2i} (r^0_{2i} , ϑ^0_{2i} , φ^0_{2i}), $i=0,1,\ldots M_2$, where r^0_{2i} , ϑ^0_{2i} , φ^0_{2i} are the approximate values of the coordinates r_{2i} , ϑ_{2i} , φ_{2i} of the points $Q_{2i} \in S$,

4.Known are the geodesically determined distances r_{ij} between every two "neighbouring" points Q_{3i} and Q_{3j} of the triangulation network and the approximate values $r^0_{3\ell}$, $\vartheta^0_{3\ell}$, $\varphi^0_{3\ell}$ of the coordinates $r_{3\ell}$, $\vartheta_{3\ell}$, $\varphi_{3\ell}$ of the points $Q_{3\ell}$, $\ell=0,1,\ldots,M_3$,

5.Known are the northen $X(Q_{0i})$, the eastern $Y(Q_{0i})$ and the vertical $Z(Q_{0i})$ components of the Earth's magnetic field intensity in the points Q_{0i} ,

6.Known are the absolute values $T(Q_{4i})$ of the Earth's magnetic field intensity in the points $Q_{4i} \equiv (r^0_{4i}, \vartheta^0_{4i}, \varphi^0_{4i})$, $i=0,1,\ldots,M_4$, where r^0_{4i} , ϑ^0_{4i} , φ^0_{4i} are the approximite values of the coordinates r_{4i} , ϑ_{4i} , φ_{4i} of the points Q_{4i} .

7.Known is an approximates expression $r(\vartheta,\varphi)$ of the Earth's surface S (assumed to be sttelliform with respect to the Earth's centre of gravity), which will be used in the regions where there are no points of type Q_{Ki} , k=0,=,2,3,4.

Given these data, the Earth's figure will be determined by solving an inverse astrogravi-magnetic-geodesic problem, consisting in the determination of the Earth's figure, (coordinates of the points Q_{Ki} , k=0,1,2,3,4) and a simple layer (of a density $\mu(\vartheta,\varphi)$), at which the difference between the observed elements of the Earth's gravitational field and the corresponding elements of the field of the introduced simple gravitational layer is the smallest in the sense of the least sqares, and in the determing a simple magnetic layer (of a density $\mu_m(\vartheta,\varphi)$), at which the difference between the observed elements of the Earth's magnetic field and the corresponding elements of the field of the introduced simple magnetic layer is the smallest in the same sence.This problem is solved by seeking the conditional minimum of the sum

$$U_{gm} = \sum_{i=0}^{M_1} p_{1i}\left[\Delta W(Q_{1i}) - \Delta\widetilde{W}(Q_{1i})\right]^2 \Delta S_{1i} + \sum_{i=0}^{M_2} q_{2i}\left[g(Q_{2i}) - \widetilde{g}(Q_{2i})\right]^2 \Delta S_{2i} + \sum_{i=0}^{M_4} t_{4i}\left[T(Q_{4i}) - \widetilde{T}(Q_{4i})\right]^2 \Delta S_{4i} ,$$

where $W(Q_{1i})$, $g(Q_{2i})$ and $T(Q_{4i})$ are the corresponding measured magnitudes,

$$\widetilde{W}(Q_{1i}) = \frac{\omega^2}{2}(x_{1i}^2 + y_{1i}^2) + \int_S \frac{\mu(Q)\,dS_Q}{R(Q_{1i},Q)}$$

is a trial gravity potential, $\frac{\omega^2}{2}(x_{1i}^2 + y_{1i}^2)$ is the potential of the centrifugal force, and $\int_S \frac{\mu(Q)\,dS_Q}{R(Q_{1i},Q)}$ is the Newtonian potential of the simple layer with density $\mu(Q)$, located on the Earth's surface (see Zidarov D.P. [19,20,21,22,28,29,30,34], Weightam J.A. [17], Dempney G.N.G. [3], Holota P. [5]),

$$\Delta\widetilde{W}(Q_{1i}) = \widetilde{W}(Q_{1i}) - \widetilde{W}(Q_{10});$$

$$\widetilde{g}(Q_{2i}) = \left| -\operatorname{grad}_{Q_{2i}} \widetilde{W} \right| =$$

$$\left\{\left[\omega^2 x_{2i} + 2\pi\mu(Q_{2i})\cos\hat{xn}_{2i} + \int_S \frac{\mu(Q)\cos\hat{xR}(Q_{2i},Q)\,dS_Q}{R^2(Q_{2i},Q)}\right]^2 + \left[\omega^2 y_{2i} + 2\pi\mu(Q_{2i})\cos\hat{yn}_{2i} + \int_S \frac{\mu(Q)\cos\hat{yR}(Q_{2i},Q)\,dS_Q}{R^2(Q_{2i},Q)}\right]^2 + \left[2\pi\mu(Q_{2i})\cos\hat{zn}_{2i} + \int_S \frac{\mu(Q)\cos\hat{zR}(Q_{2i},Q)\,dS_Q}{R^2(Q_{2i},Q)}\right]^2\right\}^{1/2},$$

$T=-\mathrm{grad}\,\varphi$ is the magnetic field intensity of the trial simple magnetic layer with a density $\mu_m(Q)$, located on S,

$$T(Q_{4i}) = \left\{\left[2\pi\mu_m(Q_{4i})\cos\hat{xn}_{4i} + \int_S \frac{\mu_m(Q)\cos\hat{xR}(Q_{4i},Q)\,dS_Q}{R^2(Q_{4i},Q)}\right]^2 + \left[2\pi\mu_m(Q_{4i})\cos\hat{yn}_{4i} + \int_S \frac{\mu_m(Q)\cos\hat{yR}(Q_{4i},Q)\,dS_Q}{R^2(Q_{4i},Q)}\right]^2 + \left[2\pi\mu_m(Q_{4i})\cos\hat{zn}_{4i} + \int_S \frac{\mu(Q)\cos\hat{zR}(Q_{4i},Q)\,dS_Q}{R^2(Q_{4i},Q)}\right]^2\right\}^{1/2},$$

ω is the Earth's angular velocity, $R(Q_{ki},Q)$ is the distance from point Q_{ki} to an arbitrary point $Q\equiv(x,y,z)\equiv(r,\vartheta,\varphi)$ on S, $\hat{n_{2i}x}$, $\hat{n_{2i}y}$, $\hat{n_{2i}z}$ and $\hat{n_{4i}x}$, $\hat{n_{4i}y}$, $\hat{n_{4i}z}$ are the respective angles between the normals to the surface S in the points Q_{2i} and Q_{4i} and the axes x,y,z (approximite values are put for these angles at first and after the first approximation they are replaced by the corresponding newly obtained more exact values), $\hat{xR}(Q_{ki},Q)$, $\hat{yR}(Q_{ki},Q)$, $\hat{zR}(Q_{ki},Q)$ are the angles between the axes x,y,z and the radius-vectors $R(Q_{ki},Q)$, $k=1,2,4$, dS_{ki} are the areas of "squarelets" in the middle of which are the points Q_{ki}, $k=1,2,4$ and p_{ki}, q_{ki}, t_{ki} are the weights of the respective measurements.

The sum U_{gm} is a function of the densities $\mu(Q)$ and $\mu_m(Q)$ and of the coordinates of the points Q_{ki}, $k=0,1,2,3,4$. Let us express $\mu(Q)$ and $\mu_m(Q)$ by series of Legendre polynomials

$$\mu(\vartheta,\varphi) = \sum_{n=0}^{n_0}\sum_{m=0}^{n}\left[\alpha_n^m\cos m\varphi + \beta_n^m\sin m\varphi\right]P_n^m(\cos\vartheta),$$

$$\mu_m(\vartheta,\varphi) = \sum_{n=0}^{n_0}\sum_{m=0}^{n}\left[\gamma_n^m\cos m\varphi + \delta_n^m\sin m\varphi\right]P_n^m(\cos\vartheta),$$

where α_n^m, β_n^m and γ_n^m, δ_n^m are coefficients which we have to determine.

Let us represent the coordinates r_{ki}, ϑ_{ki}, φ_{ki} of the points Q_{ki} by binomials $r_{ki}^0+\Delta r_{ki}$, $\vartheta_{ki}^0+\Delta\vartheta_{ki}$, $\varphi_{ki}^0+\Delta\varphi_{ki}$ and the very corrections Δr_{ki}, $\Delta\vartheta_{ki}$, $\Delta\varphi_{ki}$ - by the series

$$\Delta r_{ki} = \sum_{n=0}^{n_0}\sum_{m=0}^{n}\left[A_n^m\cos m\varphi_{ki} + B_n^m\sin m\varphi_{ki}\right]P_n^m(\cos\vartheta_{ki}),$$

$$\Delta\vartheta_{ki} = \sum_{n=0}^{n_0}\sum_{m=0}^{n}\left[C_n^m\cos m\varphi_{ki} + D_n^m\sin m\varphi_{ki}\right]P_n^m(\cos\vartheta_{ki}),$$

$$\Delta\varphi_{ki} = \sum_{n=0}^{n_0}\sum_{m=0}^{n}\left[E_n^m\cos m\varphi_{ki} + F_n^m\sin m\varphi_{ki}\right]P_n^m(\cos\vartheta_{ki}),$$

where $A_n^m, B_n^m, \ldots, F_n^m$ are coefficients which we have to determine.

Replacing these expressions for r_{ki}, ϑ_{ki}, φ_{ki} and for $\mu(\vartheta,\varphi)$, $\mu_m(\vartheta,\varphi)$ in U_{gm}, this sum turn into a function of the coefficients α_n^m, β_n^m, γ_n^m, δ_n^m, $A_n^m,\ldots,F_n^m$, which we have to determine by its minimizing.

The conditional minimum of U_{gm} must be attained on the following four limiting conditions:

(1) $$r_{ij} = \tilde{r}_{ij},$$

where r_{ij} are the triangularly determined distances between the points Q_{3i} and Q_{3j}, while $\tilde{r}_{ij}$ are the distances between the same points, expressed by the corresponding coordinates,

(2) $$\gamma_{ij} = \tilde{\gamma}_{ij},$$

where γ_{ij} are the astronomically determined angular "distances" between the zeniths $Z(Q_{0i})$ and $Z(Q_{0j})$ in the points Q_{0i} and Q_{0j}, while $\tilde{\gamma}_{ij}$ are the angular "distances" between the normals to the respective equipotential surfaces W=const., determined by means of the relations $\cos\tilde{\gamma}_{ij} = \operatorname{grad}_{Q_{0i}} \tilde{W} \cdot \operatorname{grad}_{Q_{0i}} \tilde{W} / |\operatorname{grad}_{Q_{0i}} \tilde{W}| \cdot |\operatorname{grad}_{Q_{0j}} \tilde{W}|$,

$$\gamma_{mij} = \tilde{\gamma}_{mij}, \tag{3}$$

where γ_{mij} are the determined on the basis of the components X,Y,Z and the astronomic coordinates ϑ^*, φ^* in the points Q_{0i} and Q_{0j} angles between the unit vectors $\vec{T}^e(Q_{0i})$ and $\vec{T}^e(Q_{0j})$ of the vectors $\vec{T}(Q_{0i})$ and $\vec{T}(Q_{0j})$, while $\tilde{\gamma}_{mij}$ are determined by means of the relations $\cos\tilde{\gamma}_{mij} = \operatorname{grad}_{Q_{0i}} \tilde{\varphi} \cdot \operatorname{grad}_{Q_{0i}} \tilde{\varphi} / |\operatorname{grad}_{Q_{0i}} \tilde{\varphi}| \cdot |\operatorname{grad}_{Q_{0j}}|$,

$$\int_S \mu(Q)\, x\, dS_Q = \int_S \mu(Q)\, y\, dS_Q = \int_S \mu(Q)\, z\, dS_Q = 0, \tag{4}$$

which express the condition that the Earth's centre of dravity coincides with the origin O(0,0,0) of the coordinate system $Or\vartheta\varphi$.

After minimizing U_{gm} with respect to α_n^m, β_n^m, γ_n^m, δ_n^m, and $A_n^m, \ldots, F_n^m$, while satisfying the limiting conditions (1)-(4), we shall minimaze this function again with respect to the same unknowns, after having accepted the values newly obtained for r_{ki}, ϑ_{ki}, φ_{ki}, k=0, 1,2,3,4 and for $n_{ki}^{\wedge}x$, $n_{ki}^{\wedge}y$, $n_{ki}^{\wedge}z$, k=2,4, as initial values and with a new and more exact expression $r(\vartheta,\varphi)$ for the Earth's surface (valid in the regions where there are no points of the type Q_{ki}, k=0,1,2,3,4) and so on and so forth, until the respective differences become negligible. The set astro-gravi-magnetic-geodesic problem thus has been solved: we have determined the exact values of the coordinates of the points Q_{ki}, k =0, 1,2,3,4, i=0,1,...,M_k, as well as a more exact expression $r(\vartheta,\varphi)$ for the Earth's surface (valid in the regions in which there are no points of the type Q_{ki}, k=0,1,2,3,4) and as a side result of our calculations- the simple gravimetric and magnetic layers, which have fields with elements differing but little from the respective observed magnitudes.

Remark I.The same problem may be solved minimizing an other sum $U'_{gm} = U_{gm} + \sum_i \sum_j \lambda_{ij} (r_{ij} - \tilde{r}_{ij})^2 + \sum_i \sum_j \mu_{ij} (\gamma_{ij} - \tilde{\gamma}_{ij})^2 + \sum_i \sum_j \nu_{ij} (\gamma_{mij} - \tilde{\gamma}_{mij})^2 + \lambda_1 \left[\int_S \mu(Q)\, x\, dS_Q\right]^2 + \lambda_2 \left[\int_S \mu(Q)\, y\, dS_Q\right]^2 + \lambda_3 \left[\int_S \mu(Q)\, z\, dS_Q\right]^2$,

where λ_{ij}, μ_{ij}, ν_{ij} and $\lambda_1, \lambda_2, \lambda_3$ are suitable positive numbers.

Remark II.Satelit data may be used anologously.

3.Uniquness of the Solution of the Inverse Astro-Geodesical Problem

Theorem 1.There do not exist two twofold smooth closed surfaces S^I and S^{II}, except those differing only in there position in space, between the points of which mutual and univocal correspondance has been established, so that every point (u,v) of S^I a point of S^{II} with the same coordinates u,v is juxtaposed, when on the surfaces S^I and S^{II} two one-parameter families of lines u=const and v=const are plotted, if

1.1.the coefficients of the first square forms after Gauss C.F[4] of the surfaces S^I and S^{II} in an arbitrary point $(u,v)\in S^I$ and $(u,v)\in S^{II}$ are equal and

1.2.the projections of the unit vectors $\vec{n}^I(u_1,v_1)$ and $\vec{n}^{II}(u_1,v_1)$ of the normals to S^I and S^{II} in their arbitrary point (u_1,v_1) on the unit vectors $\vec{t}_u^{\,I}(u,v)$, $\vec{t}_v^{\,I}(u,v)$ and $\vec{t}_u^{\,II}(u,v)$, $\vec{t}_v^{\,II}(u,v)$ of the tangents of the curves u=const and v=const, passing through onother arbitrary point $(u,v)\in S^I$ and $(u,v)\in S^{II}$, and the projections of the same vectors on the unit vectors $\vec{n}^I(u,v)$ and $\vec{n}^{II}(u,v)$ of the normals to S^I and S^{II} in the same points $(u,v)\in S^I$ and $(u,v)\in S^{II}$ are equal:

$$\vec{n}^I(u_1,v_1) \cdot \vec{t}_u^{\,I}(u,v) = \vec{n}^{II}(u_1,v_1) \cdot \vec{t}_u^{\,II}(u,v), \tag{5.1}$$

$$n^I(u_1,v_1)\cdot t_v^I(u,v) = n^{II}(u_1,v_1)\cdot t_v^{II}(u,v), \tag{5.2}$$

$$n^I(u_1,v_1)\cdot n^I(u,v) = n^{II}(u_1,v_1)\cdot n^{II}(u,v). \tag{5.3}$$

Proof theorem 1. Let us have two corresponding points $(u,v)\in S^I$ and $(u,v)\in S^{II}$ coincide. Let also the tangential planes to S^I and S^{II} coincides in the points $(u,v)\in S^I$ and $(u,v)\in S^{II}$, as well as the vectors $t_u^{II}(u,v)$ and $t_v^{II}(u,v)$ coincide respectively with the vectors $t_u^I(u,v)$ and $t_v^I(u,v)$. We cosider points $(u_1,v_1)\in S^I$ and $(u_1,v_1)\in S^{II}$, located at infinitely small distance from points $(u,v)\in S^I$ and $(u,v)\in S^{II}$. From condition 1.1 of theorem 1 it follows that the radius vector $d\vec{r}^I$ connecting point $(u,v)\in S$ with point $(u_1,v_1)\in S^I$ can be equalized with radius vector $d\vec{r}^{II}$, connecting point $(u,v)\in S^{II}$ with point $(u_1,v_1)\in S^{II}$. Moreover, on the basis of eq. (5.1)-(5.3) we can assert that the change $d\vec{n}^I = \vec{n}^I(u_1,v_1) - \vec{n}^I(u,v)$ of the unit vector $\vec{n}^I$ of the normal to S^I, when passing from point $(u,v)\in S^I$ to point $(u_1,v_1)\in S^I$, is equal to the change $d\vec{n}^{II} = \vec{n}^{II}(u_1,v_1) - \vec{n}^{II}(u,v)$ of the unit vector $\vec{n}^{II}$ of the normal to S^{II}, when passing from $(u,v)\in S^{II}$ to $(u_1,v_1)\in S^{II}$. But since (u_1,v_1) is an arbitrary point of S^I and S^{II} in the region of $(u,v)\in S^I$ and $(u,v)\in S^{II}$, it follows that the second square forms $\varphi_2^I = -d\vec{n}^I\cdot d\vec{r}^I$ and $\varphi_2^{II} = -d\vec{n}^{II}\cdot d\vec{r}^{II}$ after Gauss G.F.[4] of the surfases S^I and S^{II} in point $(u,v)\in S^I$ and $(u,v)\in S^{II}$ are equal. From this and from the equality of the first square forms of S^I and S^{II} it follows after Gauss that the surfases S^I and S^{II} can differ only in their position in space. Thereby theorem 1 is proved.

From theorem 1 it follows that when a surface S is a level surface of the potential W of the gravity ($S\equiv W=\text{const}$), this surface is determined univocally on the basis of geodesic measurements (of the distances r_{ij} between every two "neighbouring" and sufficiently close points Q_i and Q_j on S) and - of astronomical measurements (determination of angles closing the normal to S in an arbitrary its point with the normal to S in another arbitrary its point). No gravimetric measurements are necessary in this case.

Theorem 2. There do not exist two twofold smooth closed surfaces S^I and S^{II}, except those differing only in their position in space, between the points of which mutual and univocal correspondance has been established, so that every point (u,v) of S^I a point of S^{II} with the the same coordinates u,v is juxtaposed, when on the surfaces S^I and S^{II} two one-parameter families of lines u=const and v=const are plotted, if

2.1. the coefficients of the first basic square forms after Gauss C.F.[4] of S^I and S^{II} in their respective points $(u,v)\in S^I$ and $(u,v)\in S$ are equal,

2.2. the components of certain unit vectors $\vec{N}^I(u,v)$ and $\vec{N}^{II}(u,v)$ determined in a common Cartesian coordinate system Oxyz are equal,

2.3. the components of the same vectors are equal, when they are determined in the local coordinates systems, defined by triplet of vectors $\vec{t}_u^I(u,v)$, $\vec{t}_v^I(u,v)$, $\vec{n}^I(u,v)$ and $\vec{t}_u^{II}(u,v)$, $\vec{t}_v^{II}(u,v)$, $n^{II}(u,v)$, where $t^I(u,v)$, $t^I(u,v)$, $n^I(u,v)$ and $t^{II}(u,v)$, $t^{II}(u,v)$, $n^{II}(u,v)$ are the unit vectors of the tangents to the curves u=const and v=const and of the normals to S^I and S^{II} in the points $(u,v)\in S^I$ and $(u,v)\in S^{II}$ respectively and

2.4. the unit vector $\vec{P}$ of the axis Oz is located in the same plane as the vectors $\vec{t}_v^I(u,v)$ and $\vec{N}^I(u,v)$ and in the same plane as the vectors $\vec{t}_v^{II}(u,v)$ and $\vec{N}^{II}(u,v)$.

Theorem 2 can be proved by demonstrating that, on the basis of the unit vector $\vec{N}(u,v)$ located in the "meridional" plane v=const, which passes through the point (u,v), the unit vector $\vec{n}(u,v)$ of the normal to the examined surface S can be determined, when $\vec{N}(u,v)$ is subordinated to the respective conditions of theorem 2. Let us denote by $\vec{M}$ the unit vector of the tangent to the curve v=const, which passes through a given point (u,v). The end points M,N,n and P of the unit vectors $\vec{M},\vec{N},\vec{n}$ and $\vec{P}$ will form on the unit

sphere spherical triangles ΔNMn, ΔPMn and ΔNPn shown in Fig. 1. By condition N is located on the arc $\overset{\frown}{MP}$, while the arc $\overset{\frown}{Mn}$ is equal to $\pi/2$. Let us examine the triangle ΔNMn in which $\overset{\frown}{Mn}$, $\overset{\frown}{NM}$ and $\overset{\frown}{Nn}$ (this arc is determined by us on the basis of the components of the vector $\vec{N}(u,v)$ on the lines u=const and v=const passing through point (u,v)) are known. From this triangle we determine the angle $N\overset{\frown}{M}n$ by means of the respective formulas of the spherical trigonometry. We then consider the triangle ΔPMn and from it determine the sought arc $\overset{\frown}{Pn}$. Finally we consider the triangle ΔNPn, in which by condition the arc $\overset{\frown}{PN}$ is also known and from it determine the sought angle $N\overset{\frown}{P}n$. The position of the vector $\vec{n}(u,v)$ in the basic Cartesian coordinate system has thereby been determined.

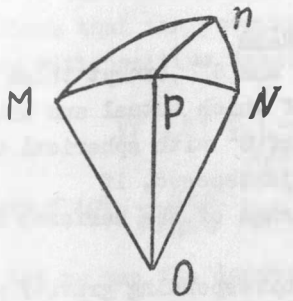

Fig. 1

From the above it follows that, if the vectors $\vec{N}^I(u,v)$ and $\vec{N}^{II}(u,v)$ and their projections on the tangents to the curves u=const and v=const passing through the points $(u,v)\in S^I$ and $(u,v)\in S^{II}$ are known, the unit vectors $\vec{n}^I(u,v)$ and $\vec{n}^{II}(u,v)$ of the normals to the surfaces S^I and S^{II} can be determined in the points $(u,v)\in S^I$ and $(u,v)\in S^{II}$ and thus the theorem 2 can be reduced to the case examined in theorem 1. Thereby theorem 2 is proved.

Note. Let the surfaces S^{I*} and S^{II*} be twofold smooth and let they encompass gravitational masses (index * has been added in connection with the use of astronomical coordinates in section 1). Let a mutual univocal correspondance exists between the points of S^I and S^{II}, established by plotting on S^{I*} and S^{II*} two families of one-parameter lines θ=const and φ=const and juxtaposing to every point of S^{I*} with coordinates θ,φ a point of S^{II*} with the same coordinates. Let the angles θ^* and φ^* represent the astronomical coordinates of the corresponding points of S^{I*} and S^{II*}; θ^* be the angle encllused between the unit vectors $\vec{N}^I(\theta,\varphi)$ and $\vec{N}^{II}(\theta,\varphi)$ of the gravity intensity of the masses encompassed by S^{I*} and S^{II*} with the unit vector of the rotational axis $\vec{P}$ of the surfaces S^{I*} and S^{II*} and the masses encompassed by them (vector $\vec{P}$ is oriented along axis Oz of the coordinate system), while angle φ^* be enclosed between the plane determined by the vectors $\vec{N}^I(\theta,\varphi)$ and $\vec{P}$ or $\vec{N}^{II}(\theta,\varphi)$ and $\vec{P}$, and the plane determined by the vectors $\vec{N}^I(\theta_0,\varphi_0)$ and $\vec{P}$ or by the vectors $\vec{N}^{II}(\theta_0,\varphi_0)$ and $\vec{P}$, (θ_0,φ_0) is a certain point of S^{I*} or S^{II*}. Let the lines φ=const be plotted so, that the tangents to them in the point (θ,φ) lie in a plane determined by the vectors $\vec{N}^I(\theta,\varphi)$ and $\vec{P}$ or the vectors $\vec{N}^{II}(\theta,\varphi)$ and $\vec{P}$. Let assume that $\vec{N}^I(\theta,\varphi)=\vec{N}^{II}(\theta,\varphi)$ and that the projections of the vectors $\vec{N}^I(\theta,\varphi)$ and $\vec{N}^{II}(\theta,\varphi)$ on the tangents to the lines θ=const and φ=const, which pass through the point (θ,φ) are respectively equal. Let us futher assume that the coefficients of the first basic equare forms after Gauss of the surfaces S^{I*} and S^{II*} are equal in their corresponding points (or that the distances between every two "neighbouring" points of S^{I*} are equal to the distances between their corresponding points of S^{II*}). On these assumption on the basis of theorem 2 we shall conclude that the surfaces S^{I*} and S^{II*} coincide.

From the above it follows that the figure of the Earth S can be univocally determined by solving the inverse astro-geodesic problem (when the unit vectors $\vec{N}(\theta,\varphi)$ of the gravity intensity and the distances r_{ij} between every two "neighbourning" points on the Earth's surface are known) only, if S represents a level surface of the potential W of the gravity. Otherwise we must also know the projections of the vectors $\vec{N}(\theta,\varphi)$ on the tangents to the corresponding lines θ=const and φ=const, while the determination of these projections calls for gravimetric data.

After determing the coordinates of the points Q_{ki}, $k=0,1,2,3,4$, $i=0,1,\dots,M_k$, we may determine the final expression $r(\theta,\varphi)$ of the Earth's surface. Futher on we may introduce other coordinate systems on the base of the expression $r(\theta,\varphi)$.

4. Uniquness of the Solution of the Inverse Gravi-Geodesical Problem

Theorem 3. There are no two twofold smooth closed surfaces S^I and S^{II}, except those differing only in their position in space, between the points of which mutual and univocal correspondance has been established, so that every point of S^I with spherical coordinates θ,φ a point of S^{II} with the same coordinates θ,φ is jaxtaposed, if

3.1. the coefficients of the first basic square forms after Gauss of the surfaces S^I and S^{II} in arbitrary point $(\theta,\varphi)\in S^I$ and $(\theta,\varphi)\in S^{II}$ are equal,

3.2. the surfaces S^I and S^{II} represent level surfaces of the corresponding gravity potentials W^I and W^{II} ($S^I \equiv W^I = \text{const}$, $S^{II} \equiv W^{II} = \text{const}$),

3.3. the surfaces S^I and S^{II} are stelliform with respect to the gravity centers of the regions $\check{\tau}_1$ and $\check{\tau}_2$ enveloped by S^I and S^{II}; these centers coincide with the origines $O(o,o,o)$ of the corresponding coordinates systems,

3.4. the vectors $\operatorname{grad}_{Q^I} W^I$ and $\operatorname{grad}_{Q^{II}} W^{II}$ are directed (like to the normal ν to S^I and S^{II}) into $\check{\tau}_1$ and $\check{\tau}_2$ respectively, $Q^I\in S^I$ and $Q^{II}\in S^{II}$,

3.5. $\left|\operatorname{grad}_{Q^I} W^I\right| = \left|\operatorname{grad}_{Q^{II}} W^{II}\right|$ at $Q^I(\theta,\varphi)\in S^I$ and $Q^{II}(\theta,\varphi)\in S^{II}$.

At first we will prove the following

Lemma 1. Let the partially smooth surfaces S^I and S^{II} envelop the regions (or sets of regions) $\check{\tau}_1$ and $\check{\tau}_2$ possessing an intersection $\check{\tau} = \check{\tau}_1 . \check{\tau}_2$ with positive three dimentional measure. Let denote with S^i the surface of $\check{\tau}$, with ΔS_1 and ΔS_2 the surfaces of $\check{\tau}_1 - \check{\tau}_2$ and $\check{\tau}_2 - \check{\tau}_1$, with ΔS_2^i and ΔS_1^i the surfaces delimiting $\check{\tau}$ from $\check{\tau}_1 - \check{\tau}_2$ and $\check{\tau}_2 - \check{\tau}_1$ respectively. Let suppose that all points of the parts $\Delta S_1^e = \Delta S_1 - \Delta S_2^i$ and $\Delta S_2^e = \Delta S_2 - \Delta S_1^i$ of the surfaces ΔS_1 and ΔS_2 are external to $\check{\tau}$ i.e. they may be shifted to infinity without crossing the points of $\check{\tau}$. If the potentials of two simple layers with positive densities σ_1 and σ_2, situated on S^I and S^{II} respectively, are equal in the points of $\check{\tau} = \check{\tau}_1 . \check{\tau}_2$, then the inequalities will be in force:

$$(6.1)\qquad \int_{\Delta S_2^e} \sigma_2\, dS > \int_{\Delta S_1^i} \sigma_1\, dS \qquad \text{at } \Delta S_2^e > 0,$$

$$(6.2)\qquad \int_{\Delta S_1^e} \sigma_1\, dS > \int_{\Delta S_2^i} \sigma_2\, dS \qquad \text{at } \Delta S_1^e > 0.$$

Proof of lemma 1. Let $\Delta S_2^e > 0$ (i.e. let ΔS_2^e has a positive two dimentional measure). Let us sweep out (using the Poincare balayage method) the masses situadet on S^{II}, which are outside of $\check{\tau}$, see Fig 2. These masses are the masses of S^{II} situated on ΔS_2^e while all other masses of S^{II} are situated on the surface S^i of $\check{\tau}$. Thus we receive on S^i a simple layer with density $\widetilde{\sigma_2} > 0$. Analogously we sweep out the masses situated on S^I (on ΔS_1^e), which are outside of $\check{\tau}$, and obtain on S^i a simple layer with density $\widetilde{\sigma_1} > 0$. The thus obtained simple layers possess equal densities $\widetilde{\sigma_1}(Q) = \widetilde{\sigma_2}(Q)$, $Q\in S^i$, and equal potentials in the points of $\check{\tau}$. The masses $m_2 = \int_{\Delta S_2^i} \sigma_2\, dS$ are more than the masses $m_1 = \int_{\Delta S_1^i} \widetilde{\sigma_1}\, dS = \int_{\Delta S_2^i} \widetilde{\sigma_2}\, dS$, because during the sweeping out of the masses a part of the masses m_2 has been going in infinity. On the other hand the initial masses $\int_{\Delta S_1^i} \sigma_1\, dS$ located on ΔS_1^i are less (or equal -when $\Delta S_1^e = 0$) than the final masses $\int_{\Delta S_1^i} \widetilde{\sigma_1}\, dS$ which will be obtained on ΔS_1^i as result of the corresponding sweeping out of the masses located on ΔS_1^e. Combining these two inequalities we obtain exactly (6.1). Inequality (6.2) is

obtained analogously.Thsreby lemma 1 has been proved.

Proof of theorem 3.Let us suppose that there are two surfaces S^{I} and S^{II} subordinated to the coditions of theorem 3.From the conditions 3.2 and 3.4. of theorem 3. it follows that the potentials W^{I} and W^{II} may be represented as potentials of simple layears with positive densities σ_1 and σ_2 (see Fig 3):

$$W^{I}(A) = \int_{S^{I}} \frac{\sigma_1(Q^{I})\, dS_{Q^{I}}}{R(A,Q^{I})}, \quad W^{II}(A) = \int_{S^{II}} \frac{\sigma_2(Q^{II})\, dS_{Q^{II}}}{R(A,Q^{II})}, \quad Q^{I}(\theta,\varphi)\in S^{I}, Q^{II}(\theta,\varphi)\in S^{II},$$

where $\sigma_1(Q^{I}) = \frac{1}{4\pi}\left(\frac{dW^{I}}{d\nu}\right)_{Q^{I}}$, $\sigma_2(Q^{II}) = \frac{1}{4\pi}\left(\frac{dW^{II}}{d\nu}\right)_{Q^{II}}$, while (by condition) $\sigma_1(Q^{I}(\theta,\varphi)) = \sigma_2(Q^{II}(\theta,\varphi))$.

Let us use the denotations introduced at the proof of lemma 1.Then from the conditions 3.1,3.3 and 3.5 of theorem 3 it follows that

$$(7.1) \qquad \int_{\Delta S_2^{e}} \sigma_2\, dS = \int_{\Delta S_1^{i}} \sigma_1\, dS \qquad at \quad \Delta S_2^{e} > 0,$$

$$(7.2) \qquad \int_{\Delta S_1^{e}} \sigma_1\, dS = \int_{\Delta S_2^{i}} \sigma_2\, dS \qquad at \quad \Delta S_1^{e} > 0.$$

These equations contradict to the inequalities (6.1) and (6,2)The contradiction is removed when we accept that $S^{I} \equiv S^{II}$ .Thereby theorem 3. is proved.

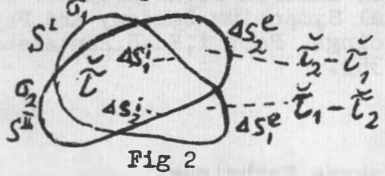

Fig 2

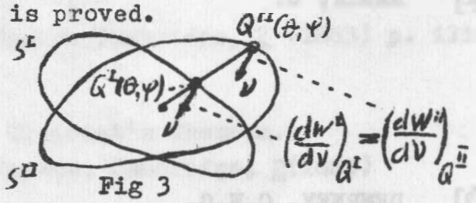

Fig 3

5.Conclusions

The proposed solution of the problem concerning the determination of the Earth's surface help us to use simultaneously all given astronomical,gravimetrical, magnetical and geodesical measurements.At the formulated common inverse astro-gravi-magneto-geodesical problem one has to find simultaneously such a surface S of the Earth and such simple gravimetric and "magnetic" layers on S, at which the unit vectors of the corresponding gravimetric and magnetic field intensities coincide (by condition) with the unit vectors of the intesities of the respective gravimetric and magnetic fields, determined experimentally in certain points of the Earth's surface.In other points of the Earth's surface the absolute values of the mentioned field intensities differ but little in the sence of the least squares from the corresponding experimentally determined absolute values of the field intensities.The distances $r_{i,j}$ between each two "neighbouring" points Q_i and Q_j on the Earth's surface S are equal (by condition) to the corresponding geodesically measured distances.Thus we have determined the corrections of the initial coordinates of certain points on the Earth's surface, in which there are astronomical, gravimetrical, magnetical and geodesical measurements without using incorrect operation (reduction of the gravimetric and magnetic data on oceanic level, see Lambert W. [7],Zidarov D. [18,26,31].Such incorrect operations we are forced to use when Stoks G. G. [15,16] or Molodensky M.S. [9.-12] methods are applied.

The obtained analytical expressio $r(\theta,\varphi)$ for the Earth's surface and- for the gravimetric and "magnetic" simple layers, corresponding to the observed (measured) gravimetric and magnetic field intensities, may be used as basic point for further investigation of the distribution of the gravimetric and magnetic masses in the Earth. Using

the mass -compression method after Zidarov D.P. [25,26,29,31,32,34] we can determine univocally the "most concentrated" masses, corresponding to the given gravimetric field data. Thus we determine the so called comressed geoid, the surface of which coincides with the undisturbed oceanic surface (W=const); under the continents the compressed geoid coincides with the lewel surface W=const. Further on we can determine other mass-distributions possessing the same gravimetric field, using the sweeping out method after Zidarov D.P. [22,34] and Zidarov D.P. and Zh.Zhelev [23]. Thus the determination of the Earth's figure and mass-distribution in the Earth will help us to solve the problem of the Earth's structure and evolution, see Barta G. [2] and Zidarov D.P. [24,27,33].

References

[1] BALMINO, G. A New Point Masses Model for the Earth Gravity Models. In: International Symposium on Earth Gravity Model and Related Problems, St. Louis, Missuri 1972

[2] BARTA, G. Anvendungsmöglichkeiten der Satellitengeodäsie bei der Erforshung der inneren Strukturen der Erde. In: 2 nd International Symposium Geodesy and Physics of the Earth, Proceedings, Part 1, Ed. H. Kautzleben and E. Buschmann, p. 351-353. Potsdam 1974

[3] DEMPNEY, C.N.G. The Equivalent Sourse Technique. Geophysics 34 (1969), p. 39-53

[4] GAUSS, C.F. Disquisitiones generales circa superficies curvas. Götingen 1828

[5] HALOTA, P. Representation of the Earth Gravimetric Field through the Potential of Point Masses (in Rassian). Observacje sztucznich satelitov 18 (1978), p. 159-169

[6] HELMERT, W. Die mathematischen und physikalischen Theorien der höheren Geodäsie, Band II. Leipzig 1884

[7] LAMBERT, W. The Reduction of Observed Values Gravity to See Level. Bulletin Geodesique 26 (1930)

[8] LAPLACE, P.S. Theorie des attractions des spheroids et de la figure des planetes. Mec. col. 3 (1785), Chap III

[9] MOLODENSKY, M.S. Fundamental Problems of the Geodesical Gravimetry (in Rassian). Тр. ЦНИИГА и К 42 (1945)

[10] MOLODENSKY, M.S. — External Gravitational Field and Physical Earth's Figure (in Rassian). Bull.Acad.USSR,Geograph. and Geoph. Series 12 (1948)

[11] MOLODENSKY, M.S.; EREMEEV, V.F.; JURKINA, M.I. — Method for External Gravitational Field and Earth's Figure Studing (in Rassian). Тр.ЦНИИГА и К 131 (1960)

[12] MOLODENSKI, M.S. — Approximative Method for Solving of Equation Determing the Quasigeoid Figure (in Rassian). Тр.ЦНИИГА и К 68 (1969)

[13] MORITZ, H. — The boundary Value Problem of Physical Geodesy. Suomalais tiedeakao toitaks, Ser. A III, 83 (1965) 48 p.

[14] MORITZ, H. — Eine neue Rechenlösung des Problems von Molodenski. Vermessungstechnik 18 (1970) p.445-446

[15] STOKES, G.G. — On the variation of Gravity on the Surfaces of the Earth. Mathem. and Phys. Papers,Cambridge, 2 (1883) p. 131-171

[16] STOKES, G.G. — On Attractions and Clairaut's Theorem. Mathem. and Phys. Papers, Cambridge, 2(1883)

[17] WEIGHTMAN,E.H. — An Unified Analytical Approach.In:The Use of Artefi-cial Satelites for Geodesy,vol 2,Ed.G.Veis,p. 467-486. Net.Tech.Univ.Athens 1967

[18] ZIDAROV,D.P. — Sur les corrections gravimetrique et magnetometrique. Compt.rend.Acad.bulg.Sci. 11 (1958) p. 351-354

[19] ZIDAROV, D.P. — A Solution of the Inverse Gravimetric (and Magnetic) Problem and Its Application to the Study of the Earth Structure. Compt.rend.Acad. bulg.Sci. 17 (1964) p.817-820

[20] ZIDAROV, D.P. — On the Solution and the Uniqueness of the Solution of the Inverse Gravimetric Problem. Bulletin of the Bulgarian Geophysical Institute 5 (1964)

[21] ZIDAROV, D.P. — Solution of Some Inverse Problems of Applied Geophys sics. Geophysical Prospecting 13 (1965) p.240-246

[22] ZIDAROV, D.P. — On the Solution of Some Inverse Potential Fields Problems and Its Application in Geophysical Problems (in Rassian with english summary). Sofia 1968

[23] ZIDAROV, D.P.; ZHELEV, ZH. — On Obtaining a Family of Bodies with Identical Exterior Fields-Method of Bobling. Geophysical Prospecting 18 (1970) p.14-33

[24] ZIDAROV, D. — Palaeomagnetic Data Analysis and Continental Drift. Comt.rend.Acad.bulg.Sci. 24 (1971) p. 1637-1640

[25] ZIDAROV, D. — Point (Dipole) Solution of Inverse Potential Field Problem-Mass-Pressing-Method. Comt. rend. Acad. bulg. Sci. 25 (1972) p. 1347-1350

[26] ZIDAROV, D.P. — Method of Finding Point (Dipole) Solution of the Potential Field Problem. Pageoph.110 (1973) p.1918-1926

[27] ZIDAROV, D.P. — Theory of the Evolution of the Earth and Earth's Crust. Pageoph. 105 (1973) p. 655-668

[28] ZIDAROV, D.P. — On the construction of Bodies with Equal Potentials and Uniqueness of Solution of Inverse Problem of Potential Fields. Compt. rend. Acad. bulg. Sci. 26 (1973) p.179-181

[29] ZIDAROV, D.P. — Characteristic Solution of the Inverse Gravimetric and Magnetic Problem. Compt. rend. Acad. bulg. Sci. 25 (1974) p. 643-646

[30] ZIDAROV, D.P. — Application of the Solution of the Inverse Gravimetric and Magnetic Problem for Studing the Earth's Figure, Structure and Evolution.In:International Symposium Geodesy and Physics of the Earth,Proceedings, Part 2,Ed.H. Kautzleben and E. Buschmann, p.423-429. Potsdam 1974

[31] ZIDAROV, D.P. — Reduction of Gravimetric Data with Accounting Nonhomogeneities of the Intermediary Layer. Compt. rend. Acad. bulg. Sci. 28 (1975) p.1027-1030

[32] ZIDAROV, D.P. — Application of the Solution of the inverse Gravimetric Problem for the Earth's Figure Determination (in Bulgarian). Bulgarian Geophysical Magazine 1 (1975) p.78-95

[33] ZIDAROV, D.P. — Theory of the Evolution of the Earth and Earth's Crust Based on the Mobile Earth Core Concept. Geologica Balcanica 7 (1977) p.3-26

[34] ZIDAROV, D. — New Approach to the Solution of the Integral Equation of First Kind.In: Inverse and Impropely Posed Problem in Differential Equations.Ed. G.Anger ,vol 1. Berlin 1979

Janusz B. Zieliński
Department of Planetary Geodesy
Space Research Centre
Polish Academy of Sciences
Warsaw

Project DIDEX
/Differential Doppler Experiment/

1. Scientific objective of the project

The present state of technology allows to use in principle three methods enabling determination of the gravity field of the Earth in a global scale: ground gravimetric meausrements, analysis of perturbations of satellite orbits and altimetry. Each of them has specific advantages as well as limitations.

Ground gravimetric measurements is rather slow method. At present covering of the Earth surface with gravimetric measurements is estimated at about 50% /Groten 1978/ and we cannot expect that before the end of this century this value will increase at least to 90%, Besides, it is extremely difficult to maintain equal precision and avoid systematic errors not to mention that some areas are so difficult of access that we cannot look forward to data acquisition.

As far as the satellite method is concerned, its great advantage is obtention of a global result. It was the crucial feature at the moment of introduction of this method. The limitation concerns possibility of obtaining of details of an obtained image, that is the resolution power. It is difficult to define precisely what is the limit of this resolution but it is estimated as near to the 40th order of spherical harmonics

/4°.5 x 4°.5/, therefore to models published at present.

Altimetry has vast possibilities of data collecting with two limitations: they refer to ocean areas only and to the physical surface of water which can differ from the equipotential surface which the geoid is.

As each of these methods has the limited efficiency, it is necessary to search for new ways. Gradiometry and two variants of satellite-to-satellite tracking are taken into account. The variant low-low is the most promising at the present moment.

Taking this into account and considering the results of newest determinations of the Earth's gravity field Space Research Centre of the Polish Academy of Sciences has proposed the project of experimental measurements with the method of satellite-to-satellite tracking called DIDEX /Differential Doppler Experiment/ to be realized in the frame of the programme INTERKOSMOS. Aims of this project are the following:

1/ resolution of gravimetric anomalies on the earth $3^{\circ} \times 3^{\circ}$;
2/ precision of the mean value of the geoid undulation in a segment $\pm$ 2 m;
3/ obtention of a global image of the geopotential;
4/ securing possibilities of more precise analysis of selected regions.

2. General idea of the method.

The low-low satellite-to-satellite tracking method has been already presented and discussed by many authors /Wolf /1969/, Balmino /1974/, Rummel at al. /1978/, Krynski /1978/ /. In the present paper we will mention only some of its more important

characteristics.

Let us imagine two objects moving on the same circular orbit, a short way one from another. It is possible to measure continuosely a relative velocity between these objects. If we exclude the atmospheric drag, anomalies of the gravitational potential along the trajectory will be the source of changes of this velocity. It results from the energy conservation law fulfilled for each of these objects:

$$U + \frac{1}{2} v^2 = h \qquad /1/$$

U - potential of gravitation

v - velocity of motion

A change of the potential value along the orbit will thus influence a change of the velocity:

$$U + \Delta U = h - \frac{1}{2} (v + \Delta v)^2$$

from that

$$\Delta U = - v \Delta v + \frac{\Delta v^2}{2} \qquad /2/$$

Because the ratio $\Delta v / v$ is of the order of 10^{-5}, the square term is negligible, thus

$$\Delta U \cong - v \Delta v \qquad /3/$$

For two objects we obtain

$$\Delta v_1 = - \frac{\Delta U_1}{v_1} ; \qquad \Delta v_2 = - \frac{\Delta U_2}{v_2} ; \qquad /4/$$

$$\dot{\varrho} = \Delta v_2 - \Delta v_1 = \frac{\Delta U_1}{v_1} - \frac{\Delta U_2}{v_2}$$

where $\dot{\varrho}$ - the relative velocity between the two objects.

Let us decompose the Earth potential into the normal potential and perturbing potential

$$U = V + T \qquad /5/$$

and

$$\Delta U = \Delta V + T \qquad /6/$$

However, the observed value can be decomposed too, namely into the part depending on the normal and perturbing potential

$$\dot{\varrho} = \dot{\varrho}_V + \dot{\varrho}_T \qquad /7/$$

and so

$$\dot{\varrho}_V + \dot{\varrho}_T = \frac{\Delta V_1 + T_1}{v_1} - \frac{\Delta V_2 + T_2}{v_2} = \left(\frac{\Delta V_1}{v_1} - \frac{\Delta V_2}{v_2}\right) + \left(\frac{T_1}{v_1} - \frac{T_2}{v_2}\right) \qquad /8/$$

This equation divides into two and we are interested in

$$\dot{\varrho}_T = \frac{T_1}{v_1} - \frac{T_2}{v_2} \qquad /9/$$

It is one of possible shapes of the observational equation but it contains a substantial simplification.

The accurate expression will be obtained starting from /1/ and remebering that velocity is the vector value as well as resigning from the assumption of circularity and identity of orbits of the two objects. In such a case

$$v_1 \neq \bar{v}_2 \; ; \quad \bar{\dot{\varrho}} = \bar{v}_2 - \bar{v}_1 \qquad /10/$$

$$\dot{\varrho}^2 = v_1^2 + v_2^2 - 2 v_1 v_2 \cos \alpha \qquad /11/$$

where α - angle between vectors v_1 and v_2. Replacing /1/ we get

$$\dot{\varrho} = 2\left[(h_1 - U_1) + (h_2 - U_2) - 2\sqrt{(h_1 - U_1)(h_2 - U_2)}\cos\alpha\right]^{1/2} \qquad /12/$$

This equation is a non-linear expression indeed but it has the virtue of connecting the measured value with values in request, that is with the potential U, and, at the same time, it shows the role of orbital elements occuring in the form of constants h.

3. Accuracy estimation

For the simplified accuracy estimation it is enough to use the equation /9/

$$\dot{\varrho}_T = \frac{T_1}{v_1} - \frac{T_2}{v_2}$$

We assume that $v_1 = v_2$

$$\dot{\varrho}_T = \frac{\Delta T}{v}$$

so

$$d\dot{\varrho} = \frac{d\Delta T}{v}$$

Putting $d\Delta T = 1m \cdot \gamma$

$$\gamma = 878\,cm/s^2$$

$$v = 7{\cdot}8\,km/s$$

we get $d\varrho = 1{\cdot}12\,mm/s$

This value corresponds to 1 m difference of the equipotential surfaces at the 300 km hight.

In order to obtain the corresponding figures for the see-level /geoid/ we have to divide it by the factor

$$k = \left(\frac{r}{R}\right)^{n+1}$$

wher n is the degree of the spherical harmonics development

conforming to assumed resolution. In our case n = 60
So, for getting ± 1 m accuracy in the geoid determination we have to measure the relative velocity in space on the altitude of 300 km with precision ± 0.07 mm/s.

This estimation is supported by results published by other autors, e.g. by Schwartz /1970/ who accomplished rather detailed simulation of the experiment. Analysis of Rummel /1979/ though made for quite different measurement precision and orbit is also conforming to our results.
Kryński /1978/ gives similar figures: for $n > 60$,
$d\dot{\varrho} = 0{,}1\,mm/s$, $m_N \cong 1\,m$
It shows that for $d\dot{\varrho} = 0{,}07 - 0{,}1\,mm/s$ we can find
1-2 m differences in the geoid undulation with resolution 3°.

4. Concept of realization

The atmospheric drag is the main reason of difficulty in realization of the SST method. In this connexion we have developed the idea /Zielinski 1977/ allowing to eliminate this effect in a great part. The use of three, instead of two objects has been proposed, two of which would be similar and the most favourable in respect of aerodynamics, the third being different. Such a system - the satellite "mother" SM and two subsatellites SS would have many other technological advantages facilitating carrying out the experiment /Fig 1/.

Aboard SM a proper measuring system would be placed measuring the relative velocity by means of the doppler effect. A signal is emitted from SM and retransmitted from SS by means of the transponder. Doppler measurement is taken aboard SM again.

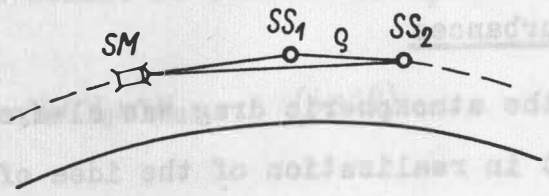

Fig. 1

To cover all the globe with measurements, the polar orbit 320 km above the earth is suggested. Separation of the subsatellites will be 200 km, distance between the pair of the subsatellites and the main spaceship will increase from 0 to 600 km.

During 120 hours of the experiment we will obtain distribution of orbits $4^{\circ}5$ at the equator. It is less than required resolution 3°, but for latitudes greater than 45°, that means for most interesting regions coverage by orbits will be more dense.

The measurement will be taken in two frequencies, in the band 3.8 GHz and 5 GHz with appropriate offsets for the first and second subsatellite to avoid interferences. Time of integration is 10 sec. The budget of errors of the measuring system gives, according to theoretical estimates, cumulative error 0.03 mm/sec. Taking notice of other sources of errors still unknown we can admit that accuracy of the measurement on the line SM-SS will be $\pm$ 0.05 mm/sec. It secures the accuracy of

the relative velocity between the subsatellites not worse than 0.08 mm/sec conforming to the requirements.

5. Elimination of disturbances

The influence of the atmospheric drag was always considered as the basic impediment in realization of the idea of satellite--to-satellite tracking. The drag can influence motion of objects so significantly that influences of gravitational anomalies will be distorted strongly. The way proposed in DIDEX allows to reduce this influence to the highest degree without recource to a drag-free device.

Let us take our system of three objects in which the two subsatellites SS_1 and SS_2 are proper gravitational probes, the third - we call it the satellite mother SM - contains a greater part of measuring and board systems. The aerodynamic characteristics of the third object is different from the two others. In that case influence of the atmospheric drag on the satellite mother will be different from that on the subsatellites. Acceleration affecting each of these objects can be resolved into the gravitational and atmospheric components, and velocities in a similar manner. We measure, however, relative velocities, denoted $\dot{\varrho}$

$$\dot{\varrho}_{Mi} = V_i - V_M \qquad (i = 1,2) \qquad /13/$$

from that

$$\dot{\varrho}_{12} = \dot{\varrho}_{M2} - \dot{\varrho}_{M1} = v_2 - v_1 \qquad /14/$$

Let us denote as v_a this component of velocity which is caused by the atmospheric drag along the orbital arc which

corresponds with one observation. The other part being the function of the gravity field and parameters of the orbit at the previous moment is denoted by v_g

Thus

$$v_i = v_{gi} + v_{ai} \qquad (i = 1,2) \qquad /15/$$

The following values are measured

$$\dot{\varrho}_{Mi} = v_i - v_M = v_{gi} - v_{gM} + (v_{ai} - v_{aM}) \qquad (i = 1,2) \qquad /16/$$

from which we calculate

$$\dot{\varrho}_{12} = \dot{\varrho}_{M2} - \dot{\varrho}_{M1} = v_{g2} - v_{g1} + (v_{a2} - v_{a1}) \qquad /17/$$

The difference in the brackets if different from 0 will burden the result of the measurement thus it should be determined. It can be in such a case if the atmosphere density will change along the orbit /Fig. 2/.

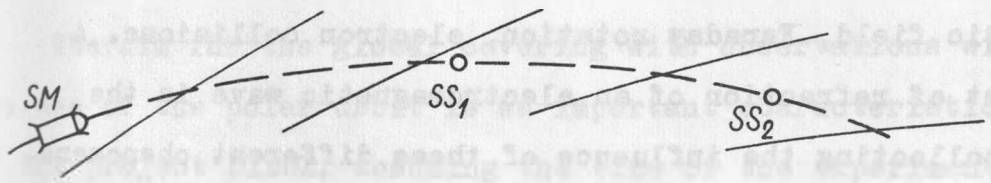

Fig. 2

However, because all the system moves along the orbit, after several seconds SM will be at the point where SS_1, was before that, whereas SS_1 passes through the point in which SS_2 was,

and so on. Thus we can write

$$v_{a1}^{t+\Delta t} = v_{a2}^{t} \qquad /18/$$
$$v_{aM}^{t+\Delta t} = k\, v_{a1}^{t}$$

where k- ratio of ballistic coefficients of SM and SS. Combining properly equations /16/ we obtain a system of 2n equations /n a number of observations/ allowing to determine successive terms v_{ai}

Such the method allows to avoid practically the influence of the atmospheric drag. The only limiting assumption is that the atmosphere density in a given place will not change in time necessary for the shift of the whole system on the orbit by the section equal to the distance between the first and the last object. The other assumption, this one of the technological nature, is that the orbits of all three objects are very similar.

The other, not less important source of errors, is the influence of the ionosphere on radio signal propagation and the measurement of doppler effect. This influence is the resultant of many phenomena, that is of electron density in the ionosphere, the magnetic field, Faraday rotation, electron collisions. A coefficient of refraction of an electromagnetic wave is the parameter collecting the influence of these different phenomena.

$$n = \sqrt{1 - \frac{F_n}{A}}$$

where F_n and A are functions connected with the above mentioned phenomena.

The analysis by Łatka /1980/ has proved that the influence of the ionosphere on the measurement of doppler effect can be of the order of 0.2 Hz, frequency being 3 GHz, and 0.15 at 5 GHz. At the same time the accuracy of this measurement requested to obtain the velocity accuracy under 0.05 mm/sec should be of the order of 5.10^{-4} Hz. Thus the introduction of corrections is necessary, determination of which is possible if using three frequencies, that is two high ones given above: 3.8 GHz and 5 GHz as well as one low about 150 MHz. It allows to arrange the system of equations determining all corrections in demand with the accuracy necessary in the experiment.

Motion of antenna in relation to the centre of mass both aboard the main satellite and the subsatellites is another source of errors. The elimination of these disturbances consists first in a technological solution assuming gravitational stabilization of all the three objects and monitoring their orientation in relation to stars in the second place.

6. Data processing

The aim for the global covering with observations with the use of the polar orbit is an important characteristics of the project DIDEX. Assuming the time of the experiment as 120 hours, permanent observations with integration time equal to 10 sec, we will obtain 43 200 observations. Their density along the orbit will be about 80 km, intervals between particular orbits at the equator 500 km condensing toward the poles. Thus regions from mean latitudes to the poles will be covered best of all.

Kryński /1980/ has discused the mathematical aspects of the problem giving the relation between the observed value and gradient of the perturbing potential T. The method proposed by Kryński provides for the solution of a system of observational equations by means ofleast squares collocation. It assumes also starting from a sufficiently good model of the gravitational field as the first approximation as well as indpendent determination of initial orbital elements. The use of collocation will allow to make local determination and to use other kinds of data at the same time, ground gravimetric measurements especialy.

References

1. Balmino G. "Determination of the Earth potential by means of space methods" La Geodynamique Spatiale, CNES, L'ecole d'eté Lanion,1974
2. Groten E."The present /1977/ state of the art in gravimetry" Proc. of the European Workshop on Space Oceanography, Navigation and Geodynamics /SONG/, Schloss Elmau, 1978
3. Kryński J. "Possibilities of low-low satellite tracking for local geoid improvement" Mitteilungen der Geodätischen Institute der TU Gratz No 31, 1978
4. Kryński J. "Solution for determination of the Gravity Field from satellite -to- satellite tracking data"Pres. at 4th Int. Symp. "Geodesy and Physics of the Earth", Karl-Marx-Stadt 1980.
5. Łatka J. "Ionospheric refraction in DIDEX experiment" Internal Report 1980
6. Rummel R. "Determination of Short - Wavelenght Components of the Gravity Field from Satellite to Satellite Tracking or Satellite Gradiometry" Manuscripta Geodaetica Vol.4 1979
7. Rummel R.,Reigber Ch., K-H. Ilk "The use of satellite to satellite tracking for gravity parameter recovery" Proc. of the SONG, ESA Sp-137,1978
8. Schwartz C.R. "Gravity field refinement by satellite to satellite doppler tracking" Report of Repartment of Geodetic Sciences, OSV. No 147 1970

9. Wolf M. "Direct measurement of the Earth's gravitational potential using the satellite pair" Journal of Geophys. Res.Vol.74 No 22, 1969

10, Zieliński J.B. "Investigation of the Earth Gravity Field by Differantial Doppler Measurements" Geodezja i Kartografia No 4, 1977.

Abstract:

For improving the Earth gravitational potential the low-low satellite tracking experiment has been proposed.

The paper presents the general idea of the experiment, scientific objectives, accuracy analysis, outlines of technical realization. With an assumed measurement accuracy $\pm$ 0.05mm/sec the significant improvement of the geopotential model is expected.